Structure and reactivity of organometallic aqua complexes of ruthenium(II)

Hargreaves, Matthew David

Award date:
2002

Awarding institution:
University of Bath

Structure and Reactivity of Organometallic Aqua Complexes of Ruthenium(II)

Submitted by Matthew David Hargreaves

For the degree of Ph.D.

Of the University of Bath

2002-12-05

ProQuest LLC
789 East Eisenhower Parkway
P.O. Box 1346
Ann Arbor, MI 48106-1346

Acknowledgements

I would like to thank my supervisor at the University of Bath, Dr. Michael K. Whittlesey for his help, support and guidance throughout my Ph.D, and to EPSRC for the funding of this project. I would also like to thank Johnson Matthey Plc. for their kind loan of ruthenium starting materials, Dr. Mary F. Mahon of the University of Bath for collecting X-ray data and Dr. Steve Black of the University of Bath for his help with ^{19}F-^{19}F NOESY experiments (Chapter 4).

I would also like to thank Samuel Kirkham, Jose Goicoechea and especially Rodolphe Jazzar for help and support in the laboratory.

Most of all I would to thank my Mum and Dad for all their support and Caroline for being there when I needed her the most.

Structure and Reactivity of Organometallic Aqua Complexes of Ruthenium(II)

Matthew David Hargreaves

Abstract

The aqua complexes Ru(dppe)(CO)(H_2O)(OTf) (**3**) and [Ru(dppe)(CO)(H_2O)$_3$][OTf]$_2$ (**4a**) have been prepared from all-*cis*-Ru(dppe)(CO)$_2$(OTf)$_2$ (**2**). The water soluble compounds, [Ru(dppe)(CO)(H_2O)$_3$][BF_4]$_2$ (**4b**) and [Ru(dppe)(CO)(H_2O)$_3$][SbF_6]$_2$ (**4c**), were prepared by the reaction of all-*cis*-Ru(dppe)(CO)$_2$(Cl)$_2$ (**1**) with the respective silver (I) salts and 10 equivalents of H_2O.

The labile nature of the coordinated water ligands in [Ru(dppe)(CO)(H_2O)$_3$][OTf]$_2$ has been investigated through substitution reactions with a range of incoming ligands. Dissolution of **4a** in CH_3CN or $(CH_3)_2SO$ results in the facile displacement of all three waters to give [Ru(dppe)(CO)(CH_3CN)$_3$][OTf]$_2$ (**5a**) and [Ru(dppe)(CO)(($CH_3)_2SO$)$_3$][OTf]$_2$ (**6a**), respectively. Similarly, **4a** reacts with Me_3CNC to afford [Ru(dppe)(CO)($CNCMe_3$)$_3$][OTf]$_2$ (**7a**). **4a** also reacts with pyridine to yield the mono aqua species [Ru(dppe)(CO)(H_2O)(C_5H_5N)$_2$][OTf]$_2$ (**8a**). Addition of 1 equiv of 2,2'-bipyridyl (bpy) or 4,4'-dimethyl-2,2'-bipyridyl (Me_2bpy) to acetone/water solutions of **4a** initially yields [Ru(dppe)(CO)(H_2O)(bpy)][OTf]$_2$ (**9a**) and [Ru(dppe)(CO)(H_2O)(Me_2bpy)][OTf]$_2$ (**10a**), in which the coordinated water lies *trans* to CO. Compounds **9a** and **10a** rapidly rearrange to isomeric species (**9a'**, **10a'**) in which the ligated water is *trans* to dppe. Further reactivity has been demonstrated for **10a'**, which, upon dissolution in $CDCl_3$, loses water and coordinates a triflate anion to afford [Ru(dppe)(CO)(OTf)(Me_2bpy)][OTf] (**11a**). Reaction of **4a** with $CH_3CH_2CH_2SH$ gives the dinuclear bridging thiolate complex [{(dppe)Ru(CO)}$_2$(-$SCH_2CH_2CH_3$)$_3$][OTf] (**12a**). The reaction of **4a** with CO in acetone/water is

slow and yields the cationic hydride complex [Ru(dppe)$(CO)_3$][OTf] (**13a**) via a water gas shift reaction. Moreover, the same mechanism can also be used to account for the synthesis of **4a** upon reaction of Ru(dppe)$(CO)_2(OTf)_2$ with water. Most of the above reactions have been repeated using **4b** and the same reactivity patterns are observed.

Attempts were made to synthesise analogues of $[Ru(dppe)(CO)(H_2O)_3]^{2+}$ (**4**) with different substituents placed on the dppe to alter the electronic effects and hence to probe the possible effects on solubility, reactivity, examples being (p-F-$C_6H_4)_2PCH_2CH_2P$(p-F-$C_6H_4)_2$ and (p-OMe-$C_6H_4)_2PCH_2CH_2P$(p-OMe-$C_6H_4)_2$. The synthesis of an aqua complex containing Me_2bpy was also investigated. It was not possible to make a tris aqua species but the mono aqua complex [Ru(Me_2bpy)$(CO)_2(H_2O)$(Cl)][OTf] (**14**) was prepared and characterised.

Abbreviations

Bpy	2,2'-bipyridyl
Me_2bpy	4,4'-dimethyl-2, 2'-bipyridyl
AgOTf	Silver (I) Trifluoromethanesulfonate
HOTf	Triflic acid
OTf	Triflate
Phen	1,10-Phenanthroline
dppe	1,2-bis(diphenylphosphino)ethane
dppe-Me	1,2-bis{di(4-methylphenyl)phosphino}ethane
dppe-OMe	1,2-bis{di(4-methoxyphenyl)phosphino}ethane
dppe-F	1,2-bis{di(4-fluorophenyl)phosphino}ethane
dppe-CF_3	1,2-bis{di(4-trifluoromethylphenyl)phosphino}ethane
triphos	$(PCH_2)_3CH$
bipim	2,2'-bipyrimidine
H_2im	Imidazolium salt
TPPTS	Triphenylphosphinetrisulfonate
Tos	*p*-toluenesulfonate
Ph	Phenyl
Cp	Cyclopentadienyl
Cp^*	Pentamethylcyclopentadienyl
ROMP	Ring Openiing Metathesis Polymerisation
WGSR	Water Gas Shift Reaction
KTE	Kinetic Trans Effect
NMR	Nuclear Magnetic Resonance
δ	Chemical Shift
ppm	Parts per million
J	Coupling constant
Hz	Hertz
IR	Infra-Red
υ	Frequency
cm^{-1}	Wavenumbers
h	hours
min	minutes
mol	moles
mmol	millimoles
g	grams
mg	milligrams
mL	millilitres
μL	microlitres
Å	Angstroms

NB: Field strengths on $^{31}P\{^1H\}$ and ^{19}F NMR spectra refer to ^1H frequencies. e.g. for $^{31}P\{^1H\}$, 400 MHz corresponds to 162 MHz, ^{19}F 376 MHz.

Table of Contents

Chapter 1

Introduction

1.1 Preface

Organometallic aqua complexes represent an exceptionally interesting but underdeveloped class of compounds. For a long time organometallic chemistry was dominantly restricted to non-aqueous media, due to the vulnerability of many organometallic compounds to either oxidation or hydrolytic decomposition. As a result many chemists exclude both air and water from their reactions thus adding to the rarity of these compounds.

In recent years aqueous organometallic chemistry has been widely studied due to the significant ecological advantages of water as a solvent in industrial processes. Industrial organic chemists regard water as a low cost solvent, which is environmentally compatible and also allows for low cost recovery of the water soluble catalyst in those processes which result in catalysis in the water phase and the substrate and the product are in the organic phase.

1.2 Water soluble transition metal complexes

One method to impart water solubility upon transition metal complexes is through the use of ancillary ligands that are functionalised to be hydrophilic, typically phosphines. This class of water soluble catalytic precursors has received much attention of late on the grounds that many catalytically active species contain phosphines.[1-3] Functionalised phosphines are a most attractive class of ligand due to their versatile coordination chemistry and their ability to stabilise specific oxidation states of transition metals. A notable example is the Rh^{I} complex with sulfonated triphenyl phosphine, an example being $[HRh(CO)_2(TPPTS)_2]$. This water soluble catalyst was developed by Kuntz at

Rhône-Poulenc industries for the hydroformylation process of alkenes to aldehydes in the presence of H_2, CO and a catalyst (***Figure 1.1***).[4,5]

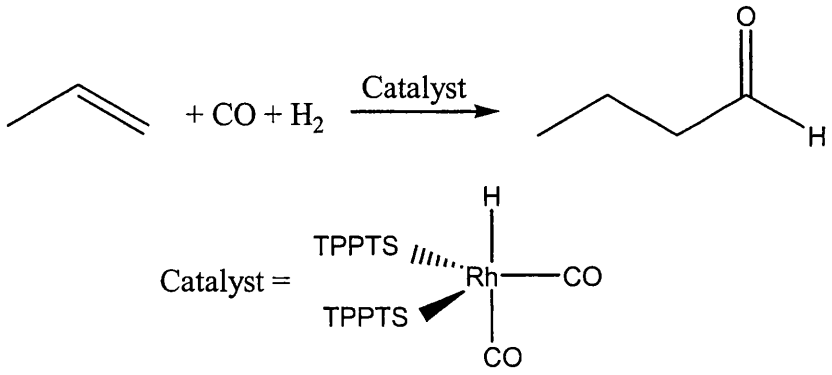

Figure 1.1: *Rhône-Poulenc hydroformylation process of propene to propanal using* $[HRh(CO)_2(TPPTS)_2]$ *as the catalyst.*

Sulfonated triphenyl phosphines were the first commercially successful and widely published water soluble phosphine ligands.

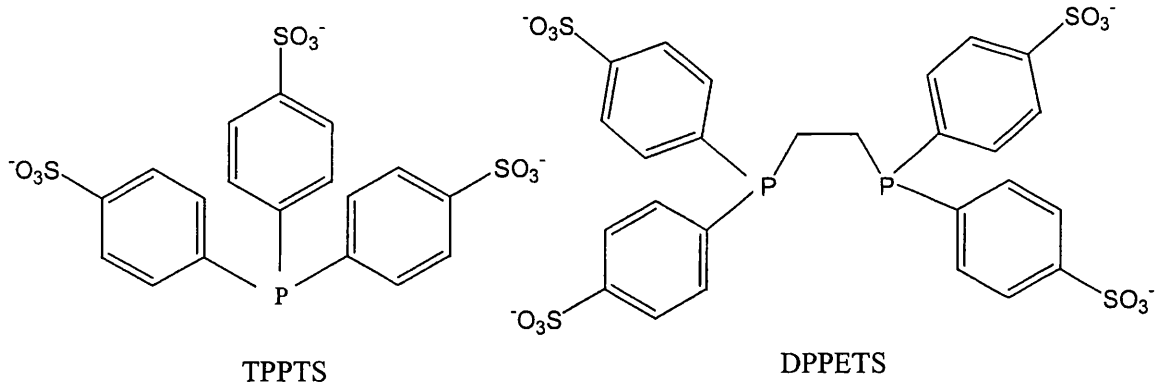

Figure 1.2: *Some commonly used water soluble phosphine ligands.*[6]

Due to the attention given to sulfonated phenyl phosphines, relatively few water soluble alkyl phosphines have been developed. Baxley et al[7,8] have synthesised Rh^I

complexes containing such ligands as 1,2-bis(hydroxymethylphosphino)ethane (DHMPE) as depicted in ***Figure 1.3***.

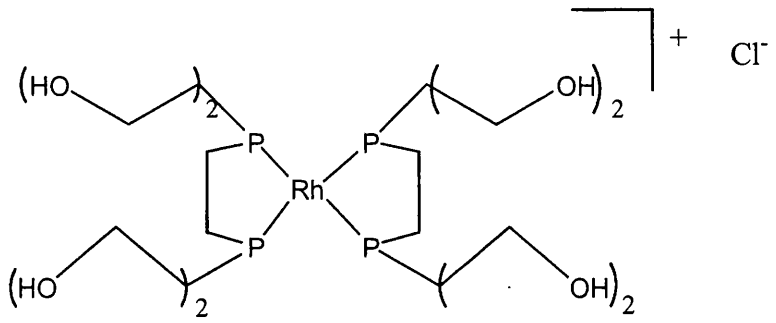

Figure 1.3: *The structure of the water soluble [Rh(DHMPE)$_2$][Cl] complex.*

Another example can be found for the selective two phase hydrogenation of sorbic acid, using the water soluble Ru(Cp*)(CO)(PR$_3$)(Cl) and [Ru(Cp*)(CO)(PR$_3$)][OTf] complexes (where R = CH_2OH or $(CH_2)_3OH$).[9] The hydrogenation of sorbic acid can lead to many different products as depicted in ***Figure 1.4***. However it was found possible to hydrogenate selectively sorbic acid (**1**) to **2**, **3**, **4**, **5** or **6** depending upon the catalyst employed. The cationic Ru complex was found to be 4-7 times more active than the neutral adduct due to the increased Lewis acidity and a vacant coordination site.

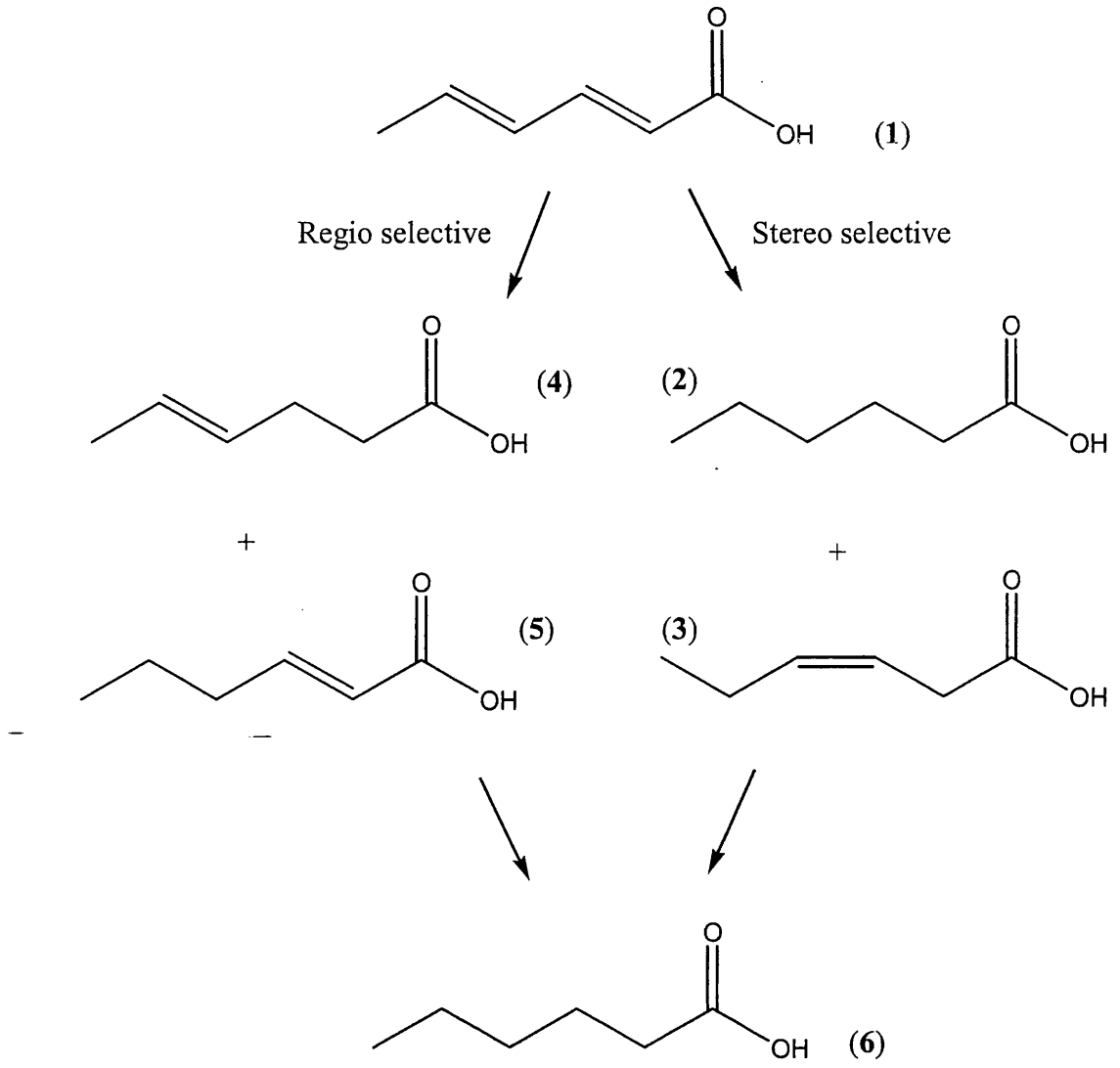

Figure 1.4: *The possible hydrogenated products obtained from sorbic acid.*[9]

1.3 Organometallic reactions of water

There have been many reactions reported in the past where water played an important role in organometallic reactions. This is due to the ease of which metal-carbon (M-C) bonds can be hydrolysed to form more thermodynamically stable products. Water can attack M-C bonds either by proton transfer (H^+, electrophilic reaction) or via the oxygen (OH^- or OH_2, nucleophilic reaction)(***Figure 1.5***).[3]

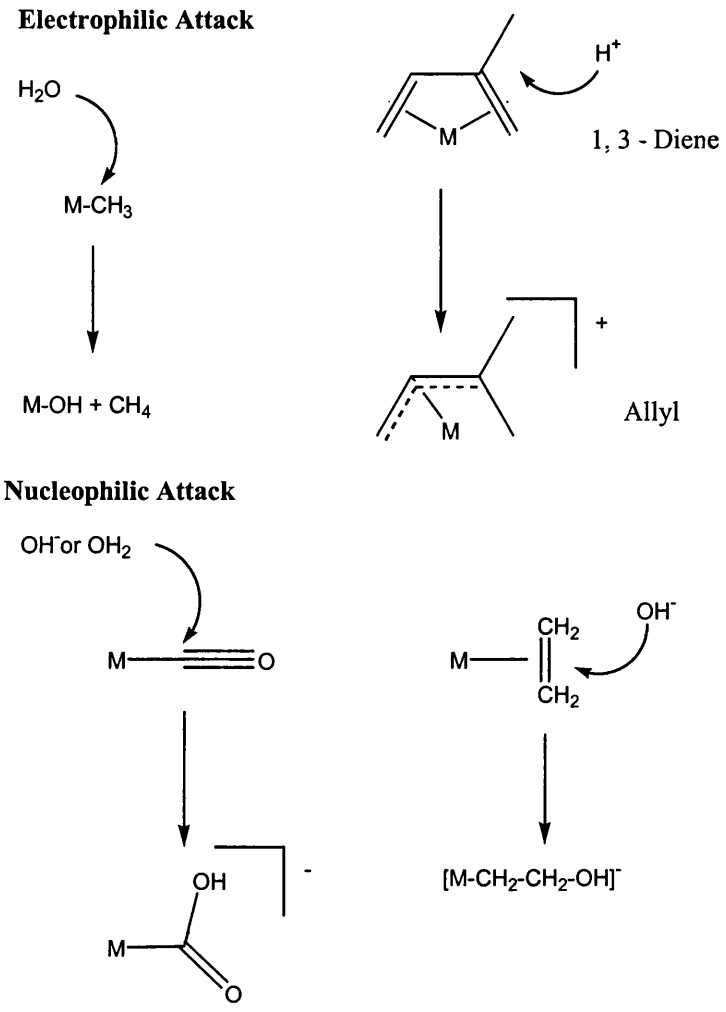

Figure 1.5: *Mechanisms of attack.*[3]

There have been many organometallic catalytic reactions with water reported as the attacking substrate. Such notable examples being the water-gas shift reaction (WGSR) and the selective oxidation of ethene in the Wacker-Hoeschst Acetaldehyde process.[10]

The WGSR was first reported over 60 years ago[11] and it derives its importance from its role to produce H_2 on an industrial scale and, in the presence of CO, can be used to hydrogenate substrates such as olefins. Extensive studies have been conducted to obtain H_2 from CO and H_2O especially since the 1973 petroleum crisis. Efficient catalysts for the WGSR are late transition metals such as Fe and Ru[1,12] as the metal centre needs to

accommodate several oxidation states in such a way that the two main reactions involved can produce CO_2 and then H_2 (***Equation 1.1***).

$$CO_{(g)} + H_2O_{(g)} \rightarrow CO_{2(g)} + H_{2(g)}$$

$\Delta H^{\theta} = -41.2$ KJ/mol

$\Delta G^{\theta} = -28.5$ KJ/mol

Equation 1.1: *The net equation for the WGSR. ΔH^{θ} and ΔG^{θ} are for the net uncatalysed reaction.*

The mechanism of the WGSR has been studied in detail and is depicted below using $Fe(CO)_5$ (***Scheme 1.1***) and the key step is the nucleophilic attack of H_2O (or OH^-) on a coordinated CO ligand (step marked *).

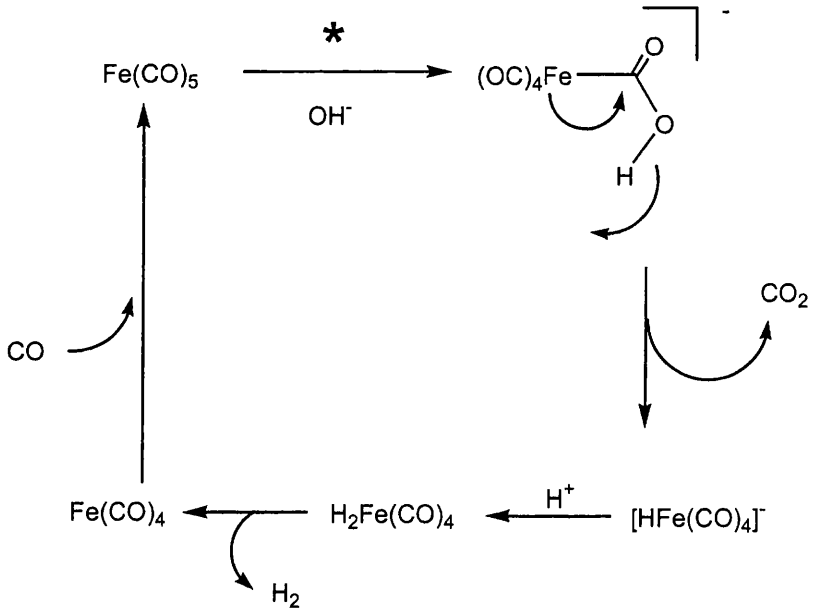

Scheme 1.1: *WGSR Mechanistic scheme for $Fe(CO)_5$ in Methanol. Reaction conditions, 180 °C and P_{CO}~34 bar, the key step that marked as * is the nucleophilic attack of H_2O on a coordinated CO ligand.*[10]

An important factor to consider is the thermodynamics of the WGSR. It is important to find catalytic systems which are active at low temperatures as a high temperature would disfavour the exothermic WGSR reaction. Therefore a room temperature active catalyst would result in large cost savings as water rather than steam could be used. As a result studies have been conducted into potential photochemical WGSR by Tanaka et al,[13] using $[Ru(bpy)_2(CO)(Cl)]^+$. Although all of the intermediates were isolated and characterised, and the complex was highly active, the complex did not show any significant difference in activity in light or dark conditions. However, Ziessel[14] found a family of cationic polypyridine complexes, $[Ir^{III}(Cp^*)(bpy)(Cl)][Cl]$ which catalyse homogeneous photoactivated WGSR at room temperature, ambient pressure, visible light and neutral pH. The photochemical step of the reaction was found to be the protonation of the hydride, generating H_2 and the starting material.

The Wacker-Hoechst Acetaldehyde process involves the oxidation of ethene to ethanal and has an annual turnover of around 4 million tonnes. The process is based on three well known reactions;

1. the oxidation of ethene by aqueous Pd^{2+} (known since 1894);
2. the copper catalysed oxidation of Pd^0 to Pd^{2+};
3. the air oxidation of Cu^+ to Cu^{2+}.

These three reactions combine to hydrate and oxidise ethene to ethanal and to regenerate the palladium(II) catalyst.

1. $C_2H_4 + PdCl_2 + H_2O \rightarrow CH_3CHO + Pd^0 + 2\ HCl$
2. $Pd^0 + 2\ CuCl_2 \rightarrow PdCl_2 + 2\ CuCl$
3. $2\ CuCl + 2\ HCl + \frac{1}{2}\ O_2 \rightarrow 2\ CuCl_2 + H_2O$

The net reaction:

$C_2H_4 + ½ O_2 \rightarrow CH_3CHO$

In the catalytic cycle (***Scheme 1.2***) the key step is the nucleophilic attack of H_2O or OH^- on coordinated ethene. There has been much debate about this mechanism, in particular whether this attack by water is external or intramolecular. It was originally argued that a proton from $[Pd(OH_2)(C_2H_4)Cl_2]^-$ was lost and that the resultant complex might undergo an alkene insertion into the Pd-OH bond, or the OH might attack the coordinated ethene as a nucleophile. The resulting hydroxyethyl palladium complex might β-eliminate to give CH_2CHOH which tautomerises to yield CH_3CHO. Recent elegant stereochemical studies conducted by Bäckvall[15] and Stille[16] support an external nucleophilic attack on coordinated ethene by water, rather than the often postulated intramolecular migration of OH^-. ***Scheme 1.2*** gives the currently accepted mechanism.

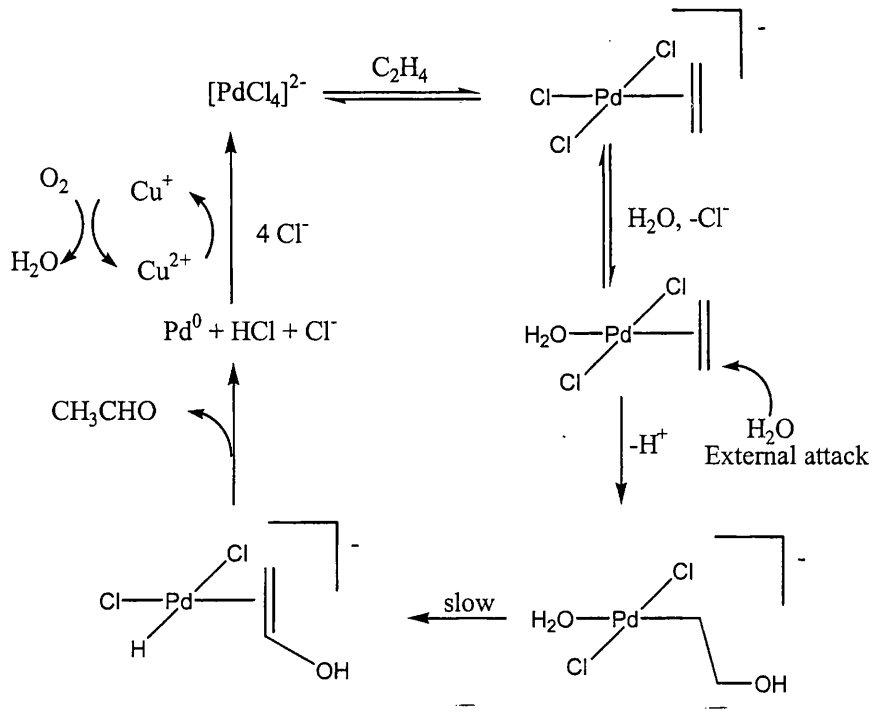

Scheme 1.2: *Hoechst-Wacker catalytic oxidation of ethene to ethanal.*[10]

1.4 Transition metal aqua complexes

It is becoming apparent that water is not just an innocuous solvent as it can take part in hydrogen bonding, hydrogen exchange and protonation, and that a second approach to make complexes that are compatible with water is by coordinating water as a ligand. Water is relatively rare as a ligand in 18-electron organometallic complexes because the hard oxygen atom binds only weakly to late transition metal atoms,[17] in accordance with the 'Jørgensen rule'; a metal ion will bond to either hard or soft ligands, but not both at the same time.[18,19] Thus, second or third row late transition metal complexes with a strong affinity for soft ligands such as CO and phosphines are expected to form only weak bonds to hard water ligands. It is this hard-soft contradiction that gives organometallic aqua complexes high reactivity and peculiar features, which has led to potential application in organic synthesis, catalysis and medicinal chemistry. Water favours ionic reactions due to

its high dielectric constant and its ability to solvate cations as well as anions. Water is positioned midway in the spectrochemical series between O-bound anions and N-donors, and favours formation of both high and low spin complexes (***Scheme 1.3***).[3]

$I^- < Br^- < Cl^- < F^- < OH^- < CH_3CO_2^- <$ oxalate < **H_2O** < pyridine ≈ $NH_3 < NO_2^- <$RNC< $CN^- \approx$ CO

Scheme 1.3: *The spectrochemical series.*[3]

The water molecule has decent crystal field splitting properties and is a good σ-donor ligand, with negligible π-backbonding potential. Thus higher valent transition metals will form the more stable complexes with water but, as can be seen from the data in ***Table 1.1***, the nature of the metal itself is important too.

Metal	Rate [sec^{-1}]	Electron configuration
Cr^{2+}	7×10^9	d^4
Cr^{3+}	3×10^{-6}	d^3
Mn^{2+}	3×10^7	d^5
Fe^{2+}	3×10^6	d^6
Fe^{3+}	3×10^3	d^5
Co^{2+}	1×10^6	d^7
Ni^{2+}	3×10^4	d^8
Cu^{2+}	8×10^9	d^9
Rh^{3+}	4×10^{-8}	d^6

Table 1.1: *Rates of water exchange of hexaqua metal complexes.*[20]

Water can bind to transition metal complexes in a number of ways,[21] either as a planar or pyramidal aquo ligand, or a "non-classical" fashion analogous to η^2-H_2 (***Figure 1.6***).

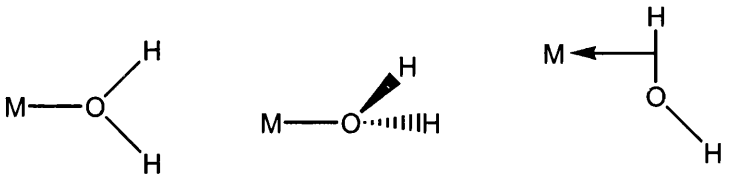

Planar Pyramidal Non-classical

Figure 1.6: *Water binding to metal centre.*[3]

Hydrogen bonding appears to be an important factor in stabilising many coordinated aqua ligands. In the solid state, hydrogen bonding of the aqua ligand to counterions or oxygen donor solvent molecules is often observed.[22,23] The majority of the aqua complexes reported are cationic species, which contain weakly coordinating anions such as BF_4^-, PF_6^- or OTf^-. This type of interaction is considered a hydrogen bond if the distance between the donor and acceptor atoms is less than 3.0 Å (***Figure 1.7***).

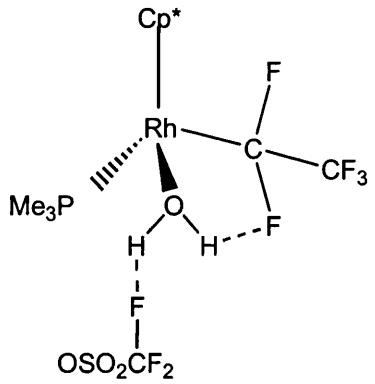

Figure 1.7: *Example of hydrogen-bonding from a coordinated aqua ligand to a free triflate anion.*[22]

Very few organometallic aqua complexes have been isolated. Taube and co-workers,[24] recognised this as a prejudice of organometallic chemists, fighting the moisture sensitivity of many of their compounds.

The principal features that determine the stability of aqua ions are:

(I) redox potentials;

(II) acidity of coordinated water;

(III) water exchange kinetics.

Potentially all of these properties may be affected by the presence of a π- ligand. The first property concerns the thermodynamic stability of a given oxidation state to disproportionate to the metal and oxide. The acidity determines the ability to deprotonate to the hydroxo species which can have a different structure and hence reactivity. The last property is the most studied and, concerns the lability of the coordinated water lignads in solution.[20]

$[Ir(H_2O)_6]^{3+}$ has been found to have the slowest documented water exchange (residence time of *ca* 300 years). Inserting a simple organometallic group, C_5Me_5 (Cp*), to form the half sandwich complex $[\eta^5\text{-Cp*Ir}(H_2O)_3]^{2+}$, the rate of water exchange is increased by 10^{14}.[25] Also exemplified by the couples $[Ru(H_2O)_6]^{2+}/[Ru(\eta^6\text{-}C_6H_6)(H_2O)_3]^{2+}$ and $[Ru(CH_3CN)_6]^{2+}/[Ru(\eta^6\text{-}C_6H_6)(CH_3CN)_3]^{2+}$, the rates of the solvent exchange in the half-sandwich solvento complexes are accelerated drastically by factors of about 640 (H_2O) and 4.6×10^5 (CH_3CN). Many kinetic studies have now been conducted in to this area.[26,27]

Merbach and co-workers[28,29] have studied the labilising effects of π-arene ligands on the rates of water exchange. Taking $[Ru^{II}(H_2O)_6](tos)_2$ (Tos = *p*-toluenesulfonate) and

substituting three of the bound water molecules to form $[Ru(\eta^6\text{-}C_6H_6)(H_2O)_3]^{2+}$ led to some interesting findings and comparisons for the rates of water exchange and mechanistic details (***Table 1.2***).

Compound	k^{298}/s^{-1}	$\Delta H^{298}/JK^{-1}mol^{-1}$	$\Delta V^{298}/cm^3mol^{-1}$
$[Ru(H_2O)_6]^{2+}$	1.8×10^{-2}	$+16 \pm 15$	-0.4 ± 0.7
$[Ru(H_2O)_6]^{3+}$	3.5×10^{-6}	-48 ± 14	-8 ± 2
$[Ru(\eta^6\text{-}C_6H_6)(H_2O)_3]^{2+}$	11.5	$+30 \pm 11$	$+1.5 \pm 0.4$

***Table 1.2**: Comparison of kinetic results.*[29]

The rate of water exchange in $[Ru(\eta^6\text{-}C_6H_6)(H_2O)_3]^{2+}$ is 3 orders of magnitude faster than that for $[Ru(H_2O)_6]^{2+}$. The faster rate of water exchange was ascribed to transition state properties as expected, the higher valent hexaqua complex is more stable and hence has a slower rate of water exchange.

From studying the activation parameters, conclusions can be drawn as to the mechanism of the water exchange. A variation in $\Delta S^{\#}$ is indicative of different pathways for water substitution, and the same conclusions can be drawn from $\Delta V^{\#}$

The three main mechanisms of water exchange, which could be in operation are outlined below.[30] The dissociative, *D* mechanism (**1**) which involves a transition metal ion and six water molecules, in which the rate determining step is bond breakage. The associative, *A* mechanism (**2**) involves seven water molecules around the metal centre and the rate is dependent on the entering group. **3** shows an interchange *I* mechanism where one water molecule is undergoing bond cleavage and the other bond formation.

1. $[M(OH_2)_6]^{n+} \longrightarrow \{[M(OH_2)_5 \text{------} OH_2]^{n+}\}^{\#}$

2. $[M(OH_2)_6.OH_2]^{n+} \longrightarrow \{[M(OH_2)_6 \text{------} OH_2]^{n+}\}^{\#}$

3. $[M(OH_2)_6.OH_2]^{n+} \longrightarrow \{[M(OH_2)_5 \text{-----} (OH_2)_2]^{n+}\}^{\#}$

As $\Delta V^{\#}$ is effectively zero for $[Ru(H_2O)_6]^{2+}$, an interchange mechanism (I) with equal contributions of bond making and bond breaking can be ascribed. $[Ru(H_2O)_6]^{3+}$ has a negative $\Delta V^{\#}$ which is indicative with an associative mechanism (I_a). The small positive value for $[Ru(\eta^6\text{-}C_6H_6)(H_2O)_3]^{2+}$ is consistent with an interchange mechanism where bond breaking is ahead of bond making, and can be explained by the strong *trans* labilising effect of the aromatic ligand on coordinated water. Later studies by Merbach et al[28] also found that the rate of water exchange is decreased by a factor of 2 when two of the aqua ligands in $[Rh(\eta^5\text{-}C_5Me_5)(H_2O)_3]^{2+}$ are replaced by 2, 2'-bipyridine (bpy) to give $[Rh(\eta^5\text{-}C_5Me_5)(bpy)(H_2O)]^{2+}$. This has been ascribed to a change in electronic properties due to the coordinated bpy ligand affecting the lability of the coordinated H_2O ligand.

Therefore, it also important to consider the *cis* and *trans* effects of coordinated ligands on the lability of the coordinated H_2O ligands. $[Ru(H_2O)_6]^{2+}$ represents an ideal starting material for the synthesis of iso-structural compounds, $[Ru(H_2O)_{ax}(H_2O)_{4eq}(L)]^{2+}$. The ligands (L) studied include H_2O, CH_3CN, N_2, $(CH_3)_2SO$, C_2H_4, CO and C_2F_4.[31] From the studies it was found that L can affect the rate and mechanism of the exchange reactions of the coordinated water molecules of $[Ru(H_2O)_5L]^{2+}$. The following increasing *cis* effect series was established from the lability of the equatorial water molecules: $C_2F_4 \cong CO < (CH_3)_2SO < N_2 < C_2H_4 < CH_3CN < H_2O$. Also an increasing *trans* effect series was established from the lability of the axial water molecule, $N_2 << CH_3CN < H_2O < CO < (CH_3)_2SO < C_2H_4 < C_2F_4$. From the two series it can seen that L effects the lability of the coordinated H_2O ligands differently depending upon whether the water molecule is

coordinated in an axial or equatorial position. It is well known that, phosphine ligands exert a labilising effect on ligands *trans* to themselves. Early reactivity studies between the complex *cis, mer*-$Ru^{II}Cl_2(CO)(PMe_2Ph)_3$ and I^- showed that the chloride ligand *trans* to PMe_2Ph is replaced much more readily than that *trans* to CO. It was concluded that the phosphine ligand exerted a greater KTE (that which describes the effect on the lability of a *trans* ligand), and was ascribed to its stronger σ-donor strength when compared to the very weakly basic CO.[32]

Koelle[20] has reported preparative routes for many carbocycle containing organometallic aqua complexes. His studies have concluded that this class of aqua compounds become highly unstable if the metal centre is too hard, resulting in loss of the carbocycle. Cobalt is at the limit of stability, only isolable using the more basic Cp* ligand as in $[Cp^*Co(H_2O)_3]^{2+}$. For 3d organometallic aqua ions a sequence of decreasing stability emerges as $Ni^{II}>Cr^{III}>Co^{III}>>Fe^{II}$. Rh^{III} and Ru^{II} have been found to offer the ideal compromise between "softness and acidity" of complexed water and backbonding into π* orbitals of carbon π ligands.

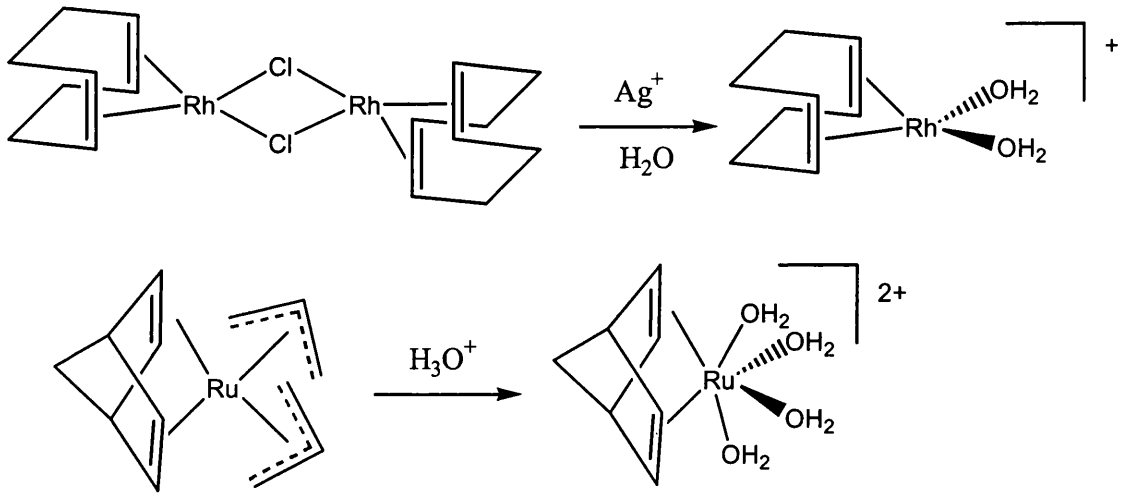

Figure 1.8: *Examples of carbocycle organometallic aqua complexes.*[20]

1.5 Catalysis using aqua complexes

One of the largest uses of catalysts in industry is in polymerisation reactions. The whole property of a polymer can be affected by the functional group substituents along its backbone. Thus the synthesis of such polymers, through the polymerisation of functionalised monomers would be ideal. This enables a direct incorporation of functionality, thus avoiding difficult transformations later on. One over-riding problem in the past has been the deactivation of many early transition metal ROMP (Ring Opening Metathasis Polymerisation) catalysts by the polar functionalities (-OH, RCOR and RCO_2R). As a result, many of the industrially useful polymers only contain alkenic functionalities (***Figure 1.9***).[33] Due to its facile synthesis $[Ru^{II}(H_2O)_6](Tos)_2$ (Tos = *p*-toluenesulfonate) is an ideal starting material for a series of new aqua complexes with ligands as varied as phosphines, arenes, alkenes and small gaseous molecules such as H_2, N_2 and CO.

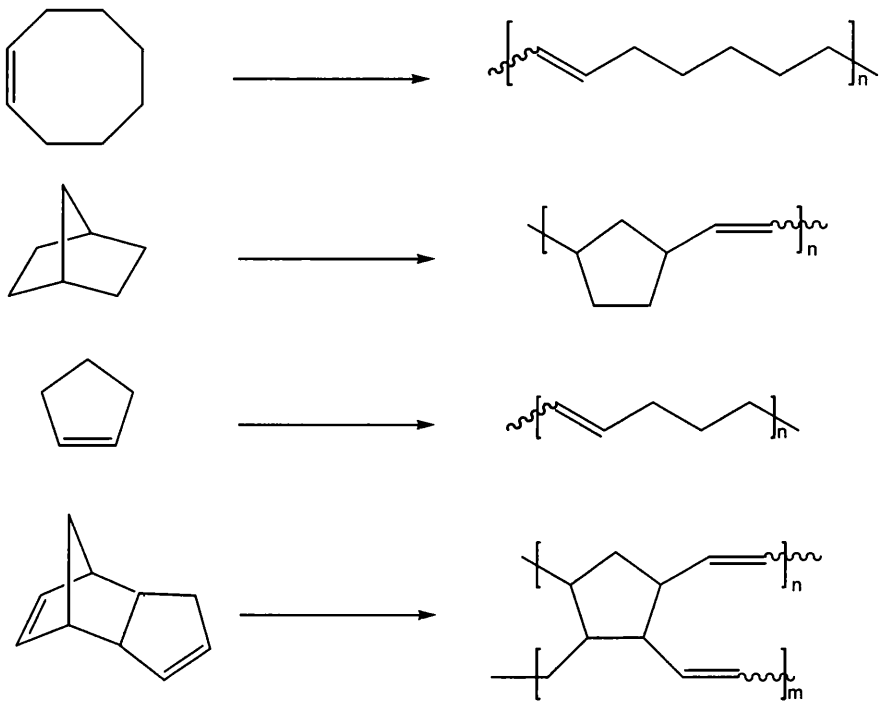

***Figure 1.9**: Industrially useful alkenic- polymers prepared via ROMP.*[34]

Grubbs and coworkers have studied the ROMP reaction of 7-oxanorbornene derivatives in organic solvents using a variety of transition metal salts. These polymerisations using group 8 metals are sometimes preceded by a lengthy initiation period. It is during this period that a small amount of reactive metal carbene is formed which then rapidly polymerises the cyclic alkene present. During efforts to decrease this initiation period (typically 22-24 h in organic solvents) it was found that rigorous exclusion of water from the reaction mixture actually had an unexpected effect. Rather than deactivating these metal catalysts, water acted as a co-catalyst by dramatically decreasing the initiation period required for the reaction. The polymerisation of 7-oxanorbornene derivatives proceeds rapidly in water alone to produce the desired ROMP polymer in nearly quantitative yields. Initiation times decreased from 22-24 h to 30-35 min in aqueous solution.[34,35] Further, on examining the used aqueous ruthenium solution after an initial polymerisation, the solution was recyclable and also the catalysts more active. Initiation times dropped from the initial value of 37.5 min to (after 2-3 polymerisations) 10-12 sec. These solutions were recyclable up to 14 times. $[Ru(H_2O)_6]^{2+}$ was found to be the most active catalyst precursor employed giving high molecular weights, low polydispersity materials in almost quantitative yield and was found to be active for 7-oxanorbornene derivatives incorporating OH, COOH and alkoxy substituents.[36]

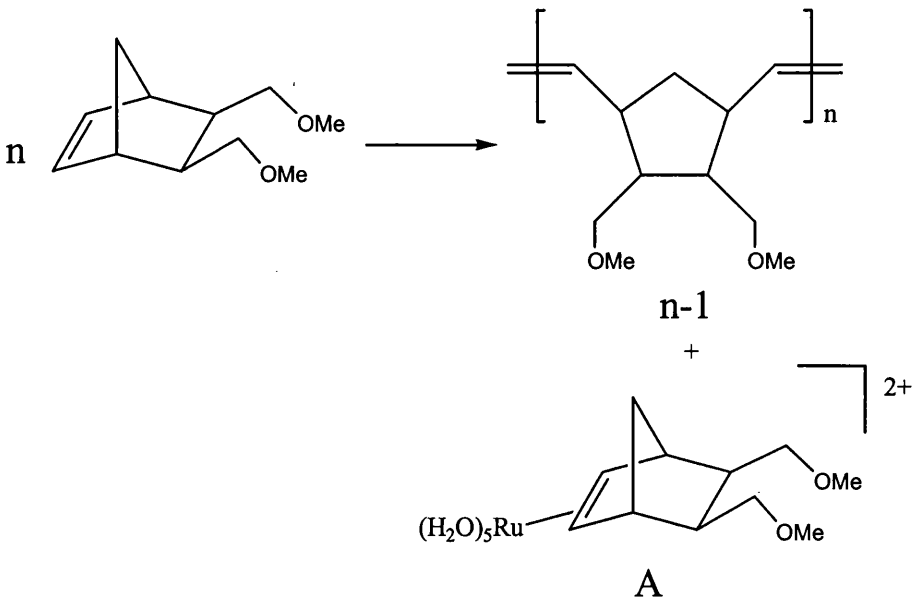

***Figure 1.10**: Postulated ruthenium-alkene catalyst complex and ROMP example.*[37]

When n equivalents of 7-oxanorbornene are allowed to react with $[Ru(H_2O)_6]^{2+}$ in D_2O, n-1 equivalents are polymerised and conversion of the catalyst to a mono alkene adduct (**A**) was observed by NMR. Aqueous solutions of **A** are highly active in subsequent polymerisations, however it is not clear how the precatalyst **A** converts into the active a metal carbene species (***Figure 1.10***).[37]

$[Ru^{II}(H_2O)_6](Tos)_2$ was also found to be the catalyst precursor for the dimerisation of ethene under mild conditions (ambient temperature and 60 bar pressure of ethene) in fully aqueous solution over a period of 72 h, resulting in the formation of butenes (***Figure 1.11***).[38] Both *mono*-and *bis*-ethene complexes of Ru^{II} have been isolated (dependent upon reaction time) and should prove to be potential starting reagents and catalysts for further reactions. It was found that the catalyst, the *bis*-ethene complex $[Ru(H_2O)_4(C_2H_4)_2]^{2+}$, adopts a *cis* arrangement of the ethenes because a *trans* geometry is disfavoured between two strong π-acceptor ligands.[39]

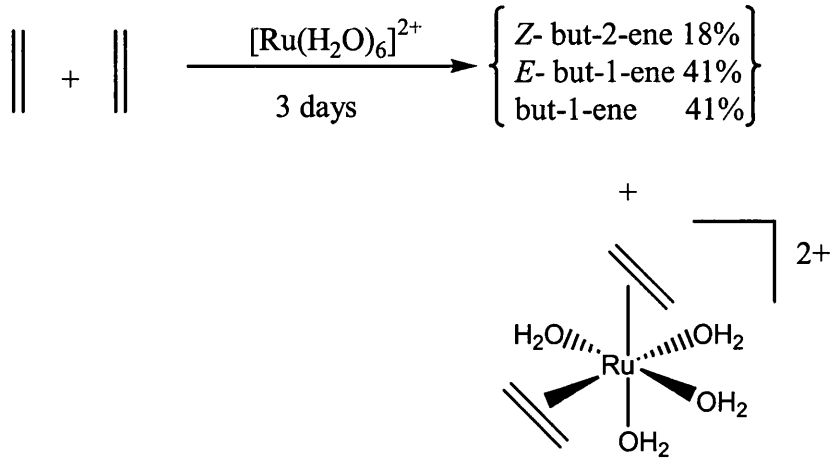

***Figure 1.11**: The aqueous catalytic dimerisation of ethene.*[38]

Fachinetti et al[1] have studied the relationship between the WGSR and alkene carbonylations with CO/H_2O in aqueous solution using *fac*-$[Ru(H_2O)_3(CO)_3]^{2+}$. From a mechanistic point of view, attack of a strong nucleophile such as OH^- on a neutral metal carbonyl generates a hydrido carbonyl intermediate both for H_2 production in WGSR and for organic product formation in the presence of olefin. A catalytic cycle for the conversion of ethene into propanoic acid is depicted in ***Scheme 1.4.***

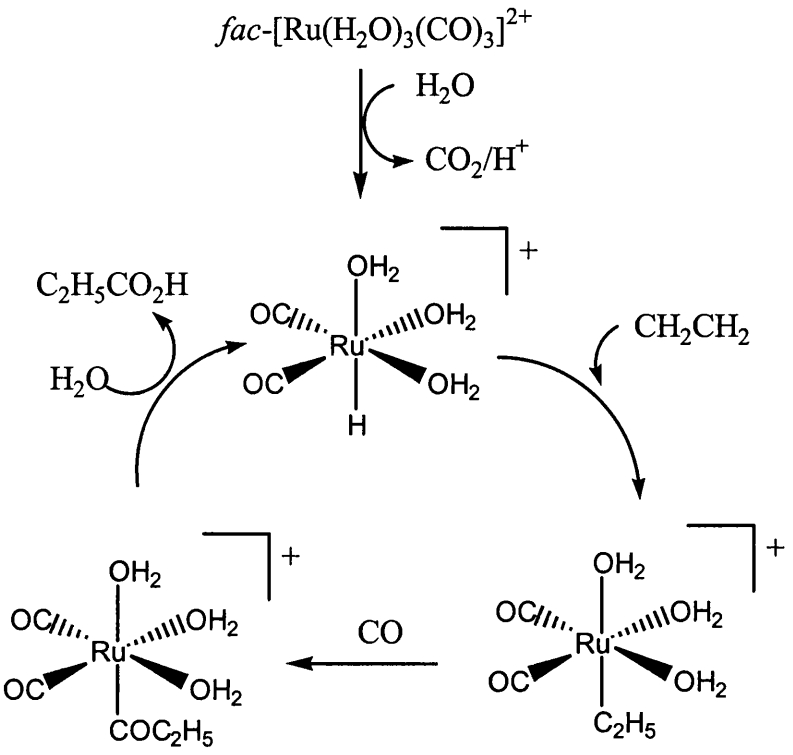

Scheme 1.4: *Alkene carbonylations with CO/H_2O in aqueous solution using fac-$[Ru(H_2O)_3(CO)_3]^{2+}$.*

1.6 Catalysis using organometallic aqua complexes

If a simple coordination complex such as hexaqua ruthenium(II) can catalyse the dimerisation of ethene, polymerise functional monomers and isomerise alkenes, then there is a large scope of potential for substituted aqua complexes. One such example is pH-selective catalysis, since the structures and properties of organometallic aqua complexes change drastically depending upon pH, due to deprotonation of the aqua ligands. Little is known about the acidity (pK_a) of M-OH_2 groups or the rates of deprotonation. Transition metal hydroxo complexes are recognised as versatile precursors and can be readily prepared by deprotonation of aqua complexes (***Scheme 1.5***).[40]

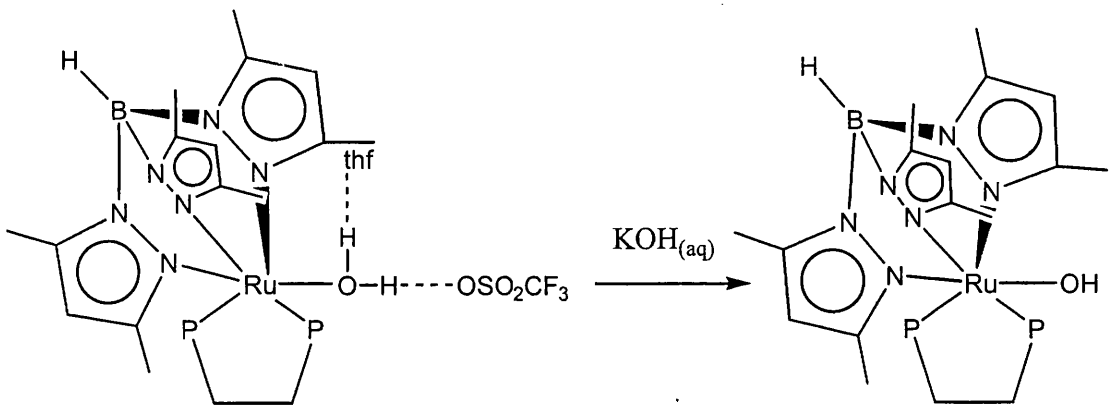

Scheme 1.5: *An example of Ru-OH_2 deprotonation to afford an Ru-OH complex.*[40]

Ogo et al[41,42] have investigated the aqueous hydrogenation of water soluble substrates as a function of pH in the range of –1 to 4 using $[Cp^*Ir(H_2O)_3]^{2+}$ as the catalyst precursor. The pH selectivity is discussed on the basis of; pH dependent structural change of $[Cp^*Ir(H_2O)_3]^{2+}$; stability of an Ir-hydride active catalyst in the acidic media; Lewis basicity of the carbonyl O-atoms of the carbonyl compounds and the C=C moieties of the alkenes. The Ir-H catalyst species has not been characterised and its formation is depicted in ***Figure 1.12*** and, the water soluble carbonyl compounds and the products formed are depicted in ***Figure 1.13***.

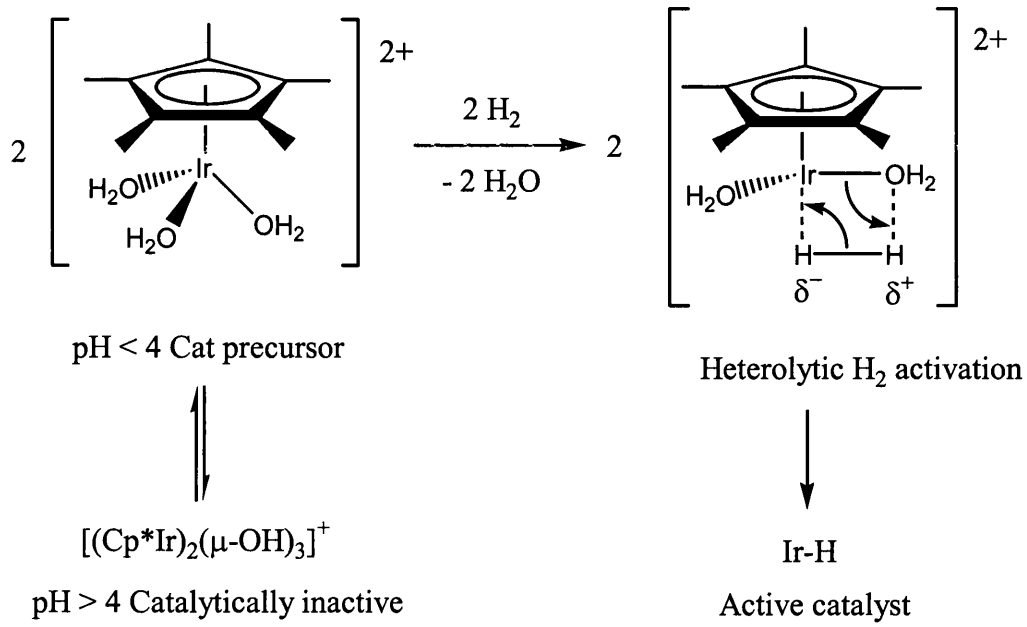

Figure 1.12: *Depiction of pH dependent species.*[41,42]

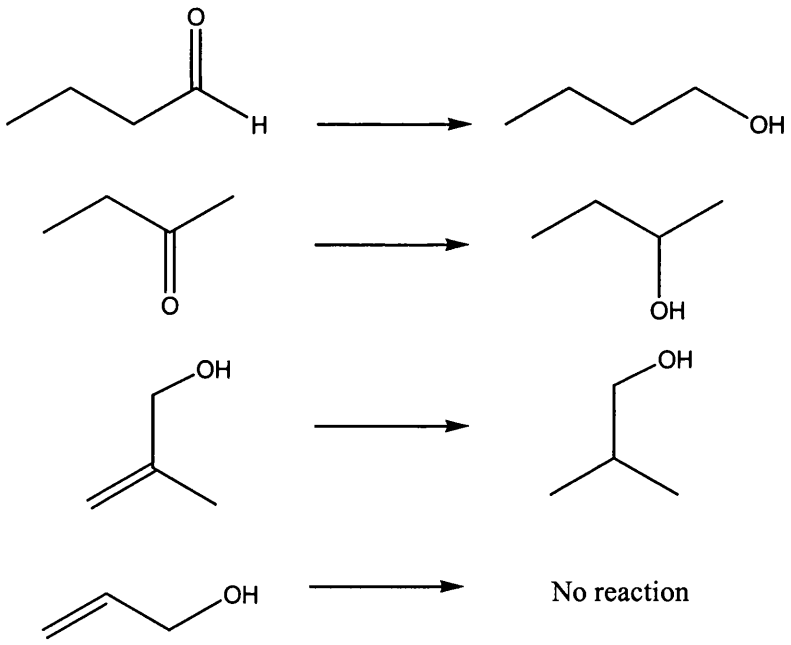

Figure 1.13: *Water soluble carbonyl and alkene substrates and products formed from reaction with the Ir-H catalyst.*[41,42]

Further studies by Ogo et al[43] on $[Cp^*Ir(H_2O)_3]^{2+}$ have focused on altering the Lewis acidity by substituting two of the coordinated water ligands with a bpy ligand to form $[Cp^*Ir^{III}(bpy)(H_2O)]^{2+}$ or by replacing the Cp* ligand by Cp^py (η^5-(tetramethylcyclopentadienyl)methylpyridine) forming $[(Cp^{\wedge}py)Ir^{III}(H_2O)_2]^{2+}$. These complexes were found to act as catalyst precursors for the transfer hydrogenation, reductive amination and dehalogenation of water soluble substrates, some examples of which are depicted in ***Figure 1.14*** (HCOONa and $HCOONH_4$ were the hydrogen donors used).

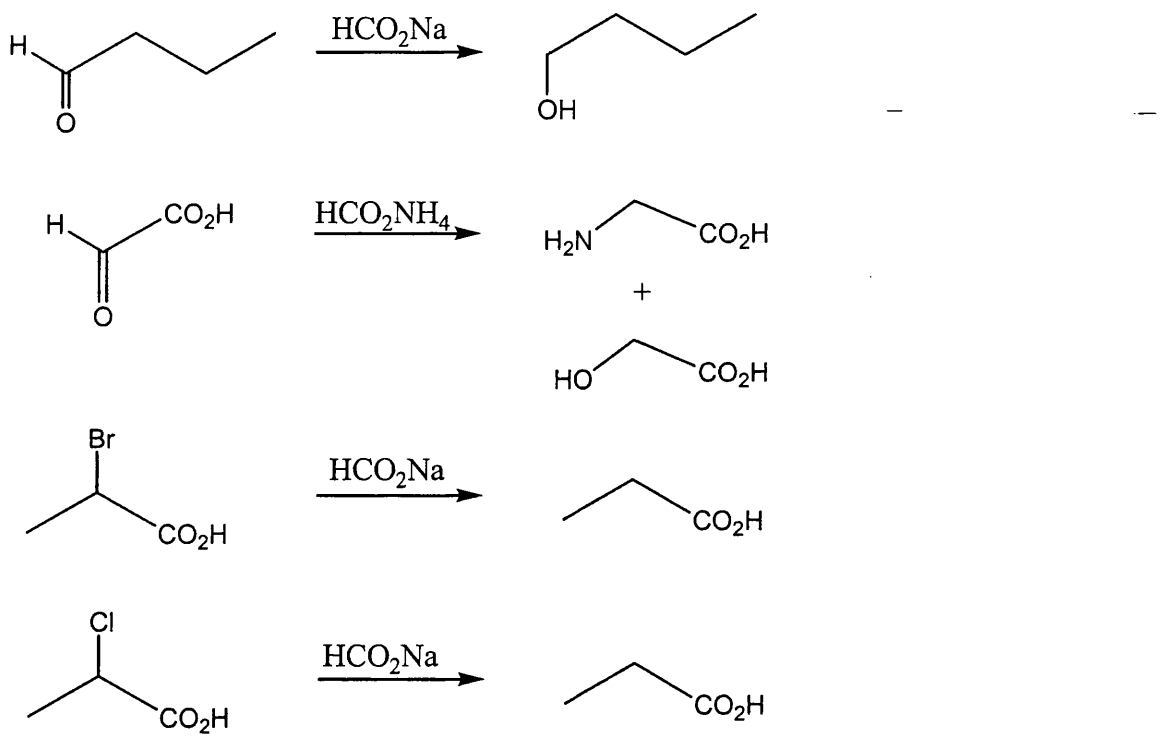

Figure 1.14: *Examples of transfer hydrogenation, reductive amination and dehalogenation of water soluble substrates using* $[(Cp^{\wedge}py)Ir^{III}(H_2O)_2]^{2+}$ *or* $[Cp^*Ir^{III}(bpy)(H_2O)]^{2+}$ *as the catalyst precursor. The hydrogen donors for each reaction are shown in the figure.*[43]

More recent work by Ogo et al[44] has resulted in the discovery of a new class of water soluble organometallic aqua complexes for the pH dependent transfer hydrogenation of ketones with HCO_2Na as the hydrogen donor. The highly water soluble (136.2 mg/mL) $[(\eta^6\text{-}C_6Me_6)Ru(bpy)(H_2O)][SO_4]$ complex was found to be the catalyst precursor for this reaction. Koelle et al have reported that the pk_a value of the aqua ligand is 7.3 (***Equation 1.2***).[28]

$$[(\eta^6\text{–}C_6Me_6)Ru(bpy)(H_2O)]^{2+} \overset{pK_{a\ 7.3}}{\rightleftharpoons} [(\eta^6\text{–}C_6Me_6)Ru(bpy)(OH)]^{+} + H^{+}$$

Equation 1.2: *Formation of the hydroxo species.*

It was found that in the absence of reduceable ketones $[(\eta^6C_6Me_6)Ru(bpy)(H_2O)]^{2+}$ reacts with HCO_2Na to produce the formato complex $[(\eta^6\text{-}C_6Me_6)Ru(bpy)(HCO_2)]^{+}$ as the intermediate of β-H elimination and the hydrido complex $[(\eta^6\text{-}C_6Me_6)Ru(bpy)(H)]^{+}$ as the catalyst for the transfer hydrogenation via an η^6 to η^4 arene coordination shift (a ring slippage mechanism), with the evolution of CO_2. This hydrido species then goes on to react with the ketones to give the corresponding alcohols (***Scheme 1.6***). Ketones include cyclic, straight chain, keto acid and acetophenone (***Figure 1.15***). These catalytic reactions were performed at pH > 3.6 (pK_a value of HCO_2H) in order to form the active species for the transfer hydrogenation.

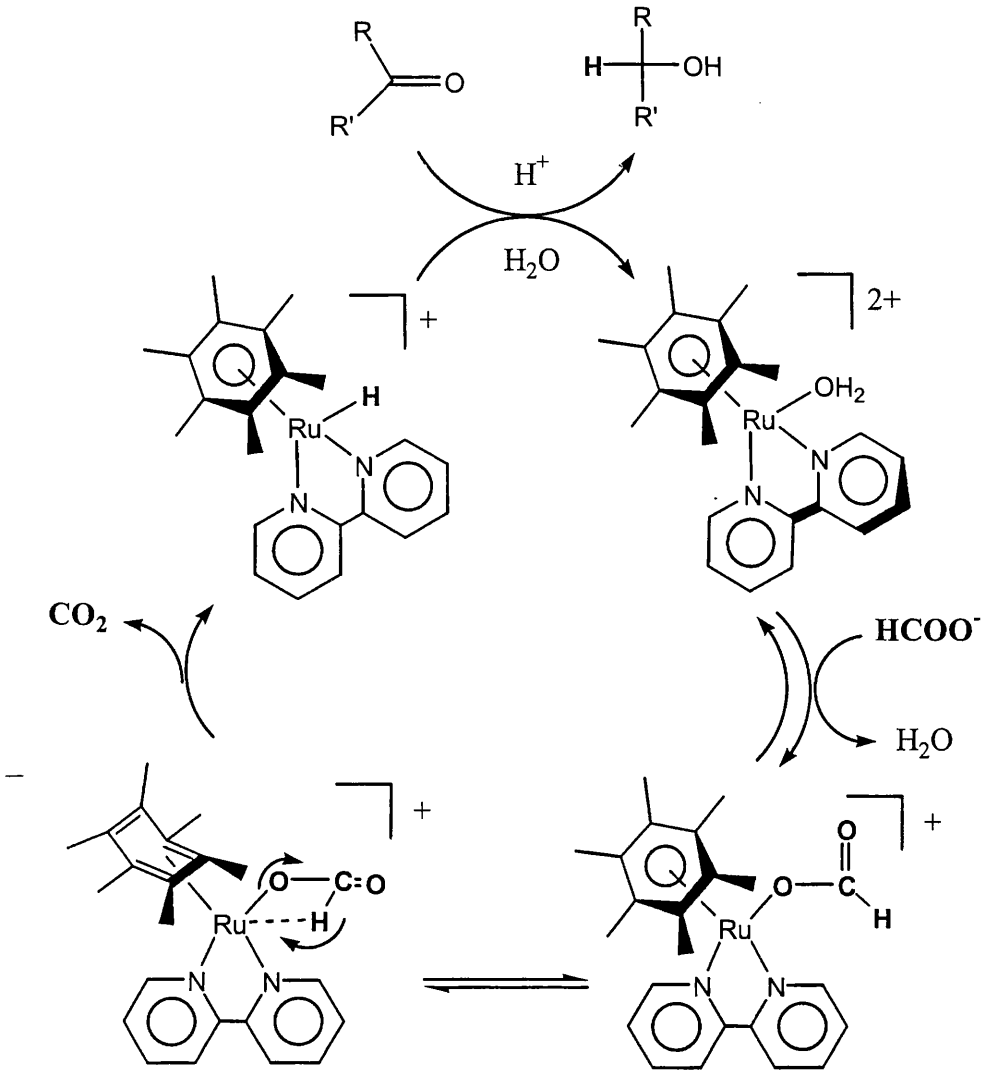

Scheme 1.6: *Catalytic cycle for the pH dependent transfer hydrogenation of water soluble and water insoluble ketones with HCO_2Na acting as a hydrogen donor and $[(\eta^6\text{-}C_6Me_6)Ru(bpy)(H_2O)][SO_4]$ acting as the catalyst precursor.*[44]

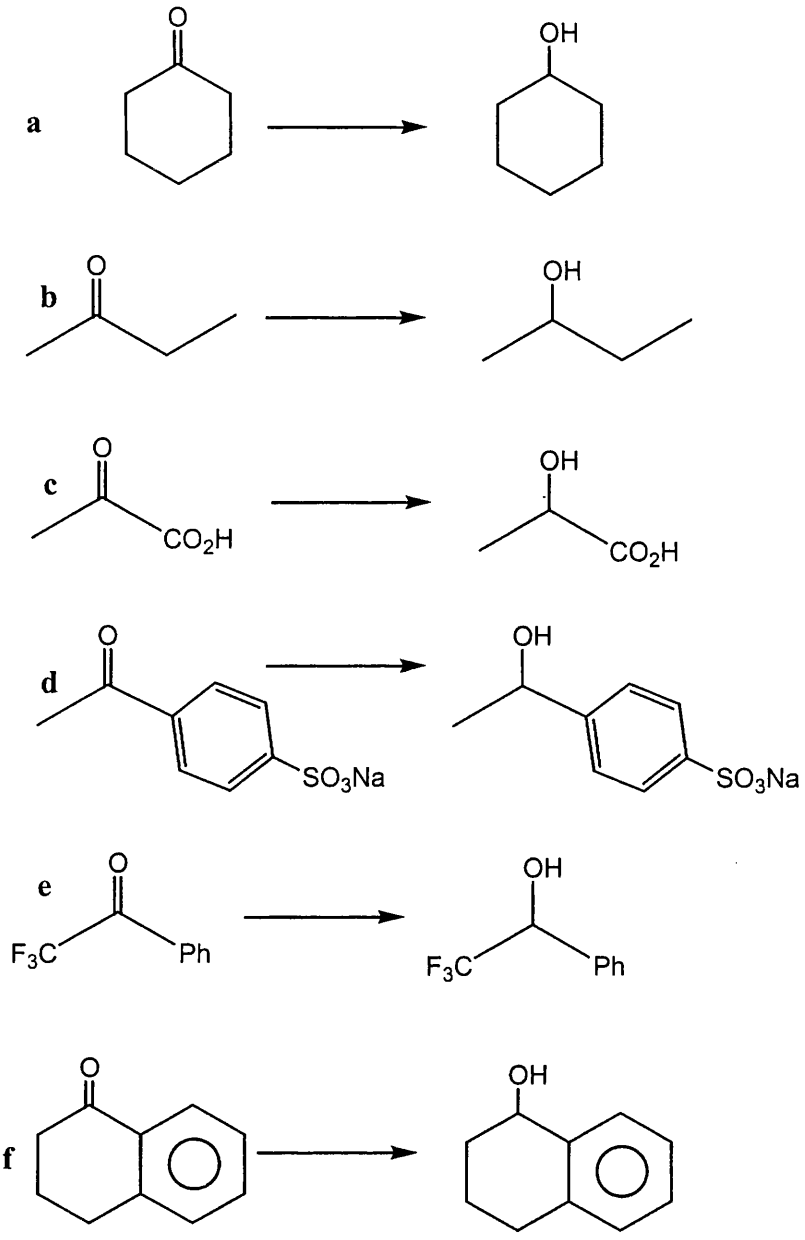

Figure 1.15: *Examples of some of the ketones which undergo transfer hydrogenation in basic media at pH 4.0 from* ***Scheme 1.6****. Ketones* ***a-d*** *are water soluble* ***e*** *and* ***f*** *are not water soluble.*

1.7 Medicinal chemistry of organometallic aqua complexes

The application of organometallic complexes in nuclear medicine is one of the prominent fields where radio-nuclides of transition metals have played an important role in the diagnosis of cancer, myocardial diseases, inflammation and others. Organometallic technetium and rhenium complexes in low oxidation states have received considerable attention in the development of novel target specific radiopharmaceuticals in recent years due to their features of reduced size and kinetic inertness. ^{99m}Tc is an inexpensive andimportant radionuclide in medicinal chemistry, which is readily available in most hospitals and has a long half lifetime of 212000 years.[45] Its low energy β-decay allows convenient handling. Similarly rhenium is considered to have excellent decay properties for applications in cancer therapy as high dose deposition at the tumour site is expected with a lower whole-body radiation burden than is currently observed with ^{131}I radionuclide.[46] The application of these compounds in medicinal chemistry would have to be based on a preparation, which would provide a quantitative yield.

The convenient and fully aqueous preparation of the precursor *fac*-$[M(OH_2)_3(CO)_3]^+$, [M = ^{99m}Tc, $^{186/188}Re$] by dissolution of $(NEt_3)[M(CO)_3(Br)_3]$ in water was devised by Alberto and co-workers. Starting with the precursor *fac*-$[M(OH_2)_3(CO)_3]^+$, a broad variety of organometallic complexes are now accessible for diagnostic and therapeutic pre-clinical and clinical studies.

This new precursor is water-soluble and also has good stability in aqueous solutions over a broad pH range (pH = 2-12) for several hours. The three water molecules coordinated to the *fac*-$[M(CO)_3]$-core are readily substituted by a broad variety of functional groups such as amines, thioethers, thiols and phosphine. This holds well for the combination of an organometallic moiety and a receptor targeting molecule. The metal complex should be "innocent" in terms of interference with the bioaffinity. The fac-

$[M(CO)_3]$-core (M = ^{99m}Tc, $^{186/188}Re$) is almost ideal in this respect. It allows a straightforward functionalization and radioactive labelling of even the smallest biomolecules under retention of their binding affinity (***Figure 1.16***).

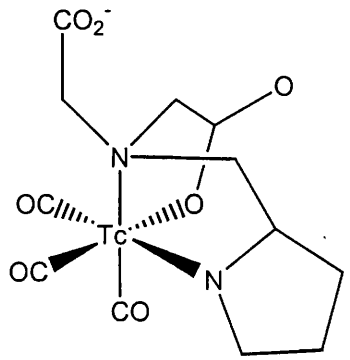

***Figure 1.16**: Complextion to PADA (aminopolycarboxylic acid).*[45]

This was demonstrated with various examples of receptor avid molecules, e.g., *fac*-$[M(CO)_3]$-labelled derivatives of biotin or an analogue of a central nervous system ligand (WAY-100635) which targets the stereogeneric receptor (5-HT1A). In both cases the functionalised Tc^{I}-carbonyl labelled biomolecules exhibit almost the same affinity and selectivity as the native ligand.

It should be noted that it is of fundamental importance to understand the structures of organometallic aqua complexes as a function of pH in order to understand both catalytic function in order to make modifications and *in vivo* stability.

For example determining the structure of $[Cp^*Rh(H_2O)_3][OTf]_2$ as a function of pH has been crucial in following the interaction of the rhodium centre with DNA/RNA nucleobases.[47]

1.8 Rationale for Research

As can be seen from Chapter 1, organometallic aqua chemistry is a rich area of research with many potential applications in catalysis and medicinal chemistry. A research programme was begun 3 years ago to prepare new organometallic aqua complexes of ruthenium(II). Ruthenium(II) was selected as a suitable oxidation state as Ru^{II} exhibits the ideal compromise between "hard" and "soft" ligands. A core Ru(P-P)(CO) (P-P = bidentate phosphine) structure was used as the starting point, to allow for asymmetry in the molecule and a *fac*-$Ru(H_2O)_3$ arrangement which also affords the possibility of studying *cis* and *trans* effects on the lability of the coordinated waters towards a range of incoming ligands, L.

The aqua complex synthesised and described in most detail throughout this thesis has the general formula $[Ru(dppe)(CO)(H_2O)_3]\ [X]_2$ (**4**) where X = OTf^-, BF_4^- or SbF_6^-, the synthesis of which is described in Chapter 2. Prior to the undertaking of kinetic studies, an understanding of the solution chemistry of **4** towards various ligands was essential. The substitution reactions of **4** are described in Chapter 3. Chapter 4 discusses the attempts to synthesise analogues of **4** with substituted dppe ligands in an attempt to alter the lability of the coordinated H_2O ligands. Chapter 5 concerns the synthesis of an aqua complex containing an N-N donor (Me_2bpy) rather than P-P (dppe) ligand.

1.9 References

1. Funaioli, T.; Cavazza, C.; Marchetti, F.; Fachinetti, G. *Inorg. Chem.* **1999**, *38*, 3361.
2. Dinell, L. R.; Batista, A. A.; Queirioz, S. L.; Bonfadini, M. R.; Oliva, G.; Nasciminto, O. R.; Cyr, P. W.; Macfarlane, H. S.; James, B. R. *Inorg. Chem.* **1999**, *38*, 5341.
3. Cornils, B.; Herrmann, W. A. *Aqueous Phase Organometallic Catalysis: Concepts and Applications*, Wiley-VCH, Weinheim. **1998**, 35.
4. Kuntz. E. G. *Chemtech*, **1987**, 570.
5. Kalck, P.; Monteil, F. *Adv. Organometallic. Chem.***1992**, *34*, 219.
6. Avery. A.; Schut, D. M.: Weakley, T. J. R.; Tyler, D. R. *Inorg. Chem.* **1993**, *32*, 233.
7. Baxley, G. T.; Lyon, D. K.; Weakley, T. J. R.; Miller, W. K.; Tyler, D. R. *J. Mol.Catalysis A. Chem.* **1997**, *116*, 191.
8. Baxley, G. T.; Miller, W. K.; Lyon, D. K.; Miller, B. E.; Nieckarz, G. F.; J. Tyler, D. R. *Inorg. Chem.* **1996**,
9. Brießen-Hölscher, B.; Heinen, J. *J. Organometal. Chem.* **1998**, *570*, 141.
10. Bochmann, M. *Organometallics 1. Complexes with Transition metal-carbon σ-bonds. Oxford University Press,* **1994**.
11. Hieber, W.; Leutet, F. Z. *Anorg. Allg. Chem.* **1934**, *204*, 145.
12. Fachinetti, G.; Funaiolli, T.; Lecci, L.; Marchetti, F. *Inorg. Chem.* **1996**, *35*, 7217.
13. Ishida, H.; Tanaka, K.; Morimento, M.; Tanaka, T. *Organometallics.* **1986**, *5*, 724.
14. Ziesel, R. *J. Am. Chem. Soc.* **1993**, *115*, 118.
15. Bäckvall, J. E.; Ållermark,B.; Ljunggren, S. O. *J. Am. Chem. Soc.* **1979**, *101*, 2411.
16. Stille, J. K.; Divakaruni, R. *J. Organomet. Chem.* **1979**, *169*, 239.
17. Sun, Y.; Taylor, N. J.; Corly, A. J. *Inorg. Chem.* **1993**, *32*, 4457.
18. Köelle, U.; Flunkert, G.; Görissen, R.; Schmidt, M. U.; Englert, U. *Angew. Chem., Int. Ed. Engl.* **1992**, *31*, 440.

19. Jørgensen, C. K. *Inorg. Chem.* **1964**, *3*, 1201.

20. Köelle, U. *Coord. Chem. Rev.* **1994**, *135/136*, 623.

21. Kubas, G. J.; Burns, C. J.; Khalsa, G. R. K.; Kiss, L. S. G.; Hoff, C. D. *Organometallics* **1992**, *11*, 3390.

22. Mahon, M. F.; Whittlesey, M. K.; Wood, P. T. *Organometallics* **1999**, *18*, 4068.

23. Hughes, R. P.; Lindner, D. C.; Smith, J. M.; Zhang, D.; Incarvito, C. D.; Lam, K. C.; Liable-Sands, L. M.; Sommer, R. D.; Rheingold, A. L. *J. Chem. Soc. Dalton. Trans.* **2001**, *15*, 2270.

24. Hung, Y.; Kung, W. J.; Taube, H. *Inorg. Chem.* **1981**, *20*, 457.

25. Cusanelli, A.; Frey, U.; Richens, D. T.; Merbach, A. E. *J. Am. Chem. Soc.* **1996**, *118*, 5265.

26. Cayemittes, S.; Poth, T.; Fernandez, M. J.; Peter, G. L.; Becker, M.; Elias, H.; Merbach, A. E. *Inorg. Chem.* **1999**, *38*, 4309.

27. Stebler-Röthlisberger, M.; Hummel, W.; Pittet, P. A.; Bürgi, H. B.; Ludi, A.; Merbach, A. E. *Inorg. Chem.* **1988**, *27*, 1358.

28. Schneider, J. S.; Dadci, L.; Elias, H.; Frey, U.; Hierning, A.; Koelle, U.; Merbach, A. E.; Paulus, H. *Inorg. Chem.* **1995**, *34*, 306.

29. Rapaport, I.; Helm, L.; Merbach, A. E.; Bernard, P.; Ludi, A. *Inorg. Chem.* **1988**, *27*, 873.

30. De Vito, D.; Sidorenkova, H.; Rotzinger, F. P.; Weber, J.; Merbach, A. E. *Inorg. Chem.* **2000**, *39*, 5547.

31. Aebischer, N.; Sidorenkowa, E.; Ravera, M.; Laurenczy, G.; Osella, D.; Weber, J.; Merbach, A. E. *Inorg. Chem.* **1997**, *36*, 6009.

32. Coe, B. J.: Glenwright, S. J.; *Coord. Chem. Rev.* **2000**, *203*, 5.

33. Hillmyer, M. A.; Lepetitt, C.; McGrath, D. V.; Novak, B. M.; Grubbs, R. H. *Macromolecules.* **1992**, *25*, 3345.

34. Novak, B. M.; Grubbs, R. H. *J. Am. Chem. Soc.* **1988**, *110*, 96.

35. Novak, B. M.; Grubbs, R. H. *J. Am. Chem. Soc.* **1988**, *110*, 7542.

36. McGrath, D. V.; Grubbs, R. H. *J. Am.Chem. Soc.* **1991**, *113*, 3611.

37. France, M. B.; Paciello, R. A.; Grubbs, R. H. *Macromolecules* **1993**, *26*, 4742.

38. Laurenczy, G.; Merbach, A. E. *J. Chem.Soc., Chem. Commun.* **1993**, 187.

39. Grunder, P. V.; Laurenczy, G.; Merbach, A. E. *Helev. Chim. Acta.* **2001**, *84*, 2854.

40. Akita, M.; Takakashi, Y.; Hikichi, S.; Moro-oka, Y. *Inorg. Chem.* **2001**, *40*, 169.

41. Ogo, S.; Matuhara, N.; Watanabe. *Organometallics* **1999**, *18*, 5470.

42. Ogo, S.; Makihara, N.; Kaneko, Y.; Watanabe, Y. *Organometallics* **2001**, *20*, 4903.

43. Makihara, N.; Ogo, S.; Watanabe, Y. *Organometallics.* **2001**, *20*, 497.

44. Ogo, S.; Abura, T.; Watanabe, Y. *Organometallics* **2002**, *21*, 2964.

45. Alberto, R.; Schibli, R.; Egli, A.; Schubiger, A. P. *J. Am. Chem. Soc.* **1998**, *120*, 7987.

46. Alberto, R.; Egli, A.; Abram, U.; Hegetschweiler, K.; Gramlich, V.; Schubiger, P. A. *J. Chem. Soc. Dalton. Trans.* **1994**, 2815.

47. Fish, R. H. *Coord. Chem. Rev.* **1999**, *185-186*, 569.

Chapter 2

Preparation of tris-aqua compounds and their precursors

2.1 Introduction

A research programme was begun 3 years ago to prepare new organometallic aqua complexes of ruthenium[1] that could have potential applications in catalysis[2] and medicinal chemistry.[3] $[Ru(dppe)(CO)(H_2O)_3]$ $[OTf]_2$ (**4a**) contains important spectroscopic reporter ligands for use in ^{31}P, ^{19}F, ^{13}C and ^{1}H NMR spectroscopy and ν_{co} stretches that are observable by IR spectroscopy. The X-ray structure determination of **4a** shows the molecule contains a *fac*-$Ru(H_2O)_3$ moiety, which affords the possibility of studying *cis* and *trans* effects on the lability of the coordinated waters towards a range of incoming ligands, L.[4] Ruthenium(II) was selected as a suitable oxidation state as Ru^{II} exhibits the ideal compromise between the "hard" and "soft" contradiction of the 'Jørgensen rule' for binding to soft conventional ligands such as CO and also to hard ligands like water.[5] A core Ru(P-P)(CO) (P-P = bidentate phosphine) structure was used as the starting point, to provide asymmetry in the molecule. The bidentate phosphine backbone allows for easy modifications to be made with respect to stereochemistry. The cationic nature of the complex means that studies can be conducted with respect to change of the anion. In order to retain the ^{19}F NMR spectroscopic handle, anions such as BF_4^- and SbF_6^- were used in addition to triflate (OTf).

2.2 Synthesis and characterisation of $Ru(dppe)(CO)_2(OTf)_2$ (2)

The ideal precursor was found to be all-*cis*-$Ru(dppe)(CO)_2(Cl)_2$ (**1**) from which $Ru(dppe)(CO)_2(OTf)_2$ (**2**) was synthesised. Many ruthenium(II) triflate complexes are prepared from chlorides of Ru(II) using AgOTf as a dehalogenating agent.[6] The starting precursor, all-*cis*-$Ru(dppe)(CO)_2(Cl)_2$ (**1**), was made from $RuCl_3$ via a four step process which is summarised in ***Scheme 2.1***. The characterisation of $[Ru(CO)_2Cl_2(dppe)_{1.14}]$ was described by Barnard,[7] while optimisation of conversion of this polymeric species to the all-*cis* dichloride complex was performed by Taylor.[8]

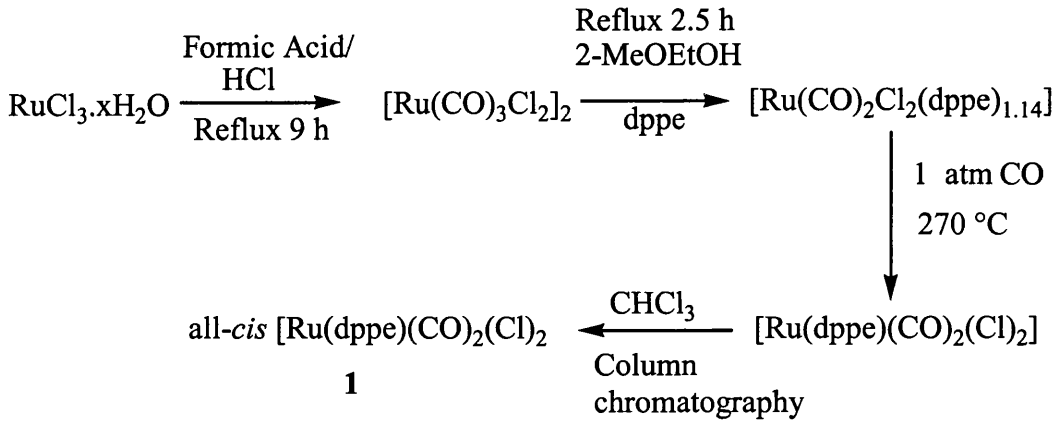

Scheme 2.1: *Summarised reaction for the preparation of* ***1****.*

$[Ru(CO)_2Cl_2(dppe)_{1.14}]$ when heated to approximately 270 °C under an atmosphere of CO melts forming a yellow glass on cooling. When the glass is dissolved in $CHCl_3$ and CO passed through the solution, the required product all-*cis* $Ru(dppe)(CO)_2Cl_2$ is produced in 50% yield. However this conversion yields $Ru(dppe)(CO)_2Cl_2$ as a mixture of isomers. On subjecting the mixture to chromatography on a silica column and elution with $CHCl_3$ yielded three separate isomeric fractions. The first fraction contained the major

product which was identified from NMR and IR spectroscopy as all-*cis* $Ru(dppe)(CO)_2Cl_2$. The $^{31}P\{^1H\}$ NMR spectrum ($CDCl_3$) showed two doublet resonances at δ 38.1 and 63.0 (J_{PP} = 9.7 Hz), while the solution IR spectrum in $CHCl_3$ contained two bands at 2079 and 2004 cm^{-1}. These data confirm that this isomer contained inequivalent phosphorus nuclei and that the two carbonyl ligands are *cis* to one other. Further evidence for the stereochemistry was obtained from the $^{13}C\{^1H\}$ NMR spectrum in $CDCl_3$ solution which included two distinct doublet of doublet resonances in the carbonyl region at δ 189.7 (J_{PC} = 9.6 and 117.5 Hz) and δ 192.9 (J_{PC} = 10.7 and 13.7 Hz). The large carbon-phosphorus coupling constant of 117.5 Hz for the resonance at δ 189.7 implies that this carbonyl ligand is *trans* to a phosphorus nucleus while the relatively small coupling constants on the second resonance indicates that this carbonyl is *cis* to both phosphorus nuclei. All three fractions are depicted in ***Figure 2.1***.

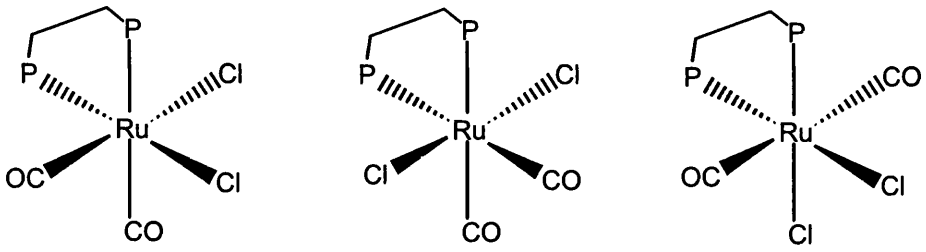

1st fraction (**1**) 2nd fraction 3rd fraction

Figure 2.1: *Isomers of $Ru(dppe)(CO)_2(Cl)_2$ as collected from the column.*

The second and third fractions were collected in a low yield and proved to be unsuitable for the preparation of $[Ru(dppe)(CO)_2(OTf)_2]$ (**2**). Treatment of a CH_2Cl_2 solution of **1** with addition 2.2 equivalents of AgOTf at room temperature (with exclusion of light to prevent formation of AgCl) (***Figure 2.2***), gave a pale yellow solution from which complex **2** was isolated by vigorous stirring with diethyl ether. This new compound

contains the desired core set-up of spectroscopic reporter ligands and asymmetry within the molecule around the bidentate phosphine ligand. Also present are the weakly coordinating anionic triflate ligands which are recognised as facile leaving groups even under mild conditions.[9]

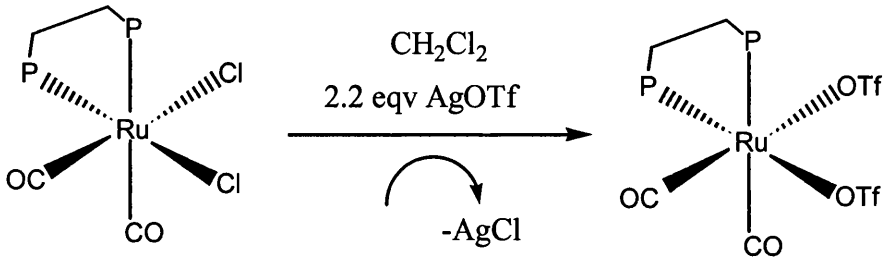

1 2

Figure 2.2: *Formation of Ru(dppe)(CO)$_2$(OTf)$_2$ (2).*[10]

The IR spectrum of **2** in CH_2Cl_2 solution displays two carbonyl bands at 2106 and 2030 cm^{-1} of equal intensity, consistent with a *cis* geometry. These peaks are shifted 26-27 cm^{-1} to higher frequency relative to the dichloride precursor (**1**) (2079 and 2004 cm^{-1}) reflecting the weaker π-donor ability of triflate.[11] Evidence for coordinated triflate ligands is also clear from the IR spectrum. Thus, absorption bands at 1013 and 1329 cm^{-1} arise from ν_{SO}, while bands at 1199 and 1232 cm^{-1} arise from $\nu(CF_3)$. Lawrance[12] has reported that ν_{SO} stretching frequencies occur at 1270 and 1043 cm^{-1} for free anionic triflate and the $\nu(CF_3)$ stretches occur at 1237 and 1167 cm^{-1}. When triflate is coordinated to a metal the band at 1270 cm^{-1} is typically shifted to higher wavenumber in the region around 1380 cm^{-1}. An example of this is the monodentate terminally bound OTf group found in $Ru(PPh_3)_2(CO)_2(OTf)_2$, where the ν_{SO} stretching band is seen at 1328 cm^{-1}.[6] The $^{31}P\{^1H\}$ NMR spectrum of **2** in $CDCl_3$ shows two doublet resonances for the dppe ligand at δ 44.5 and 66.3 (J_{pp} = 16.2 Hz). The $^{13}C\{^1H\}$ NMR spectrum exhibits two carbonyl resonances at

δ 186.0 (dd, J_{PC} = 108.0 Hz, J_{PC} = 9.9 Hz) and 193.6 (t, J_{PC} = 14.9 Hz). These coupling constants indicate a geometry in which the carbonyl ligands are *cis* to one phosphorus atom and *trans* to the other. The room temperature ^{19}F NMR spectrum shows two quartet resonances at δ –76.91 (J = 3.45 Hz) and δ –77.66 (J = 3.45 Hz) for the two inequivalent triflate ligands. Thus ^{19}F-^{19}F experiments were designed to elucidate the nature of this coupling and are described in further detail in ***Section 2.4***. Ludi and Robinson[13-14] have reported for $Ru(PPh_3)_2(CO)(H_2O)(OSO_2R)_2$ that M-O_3SR (R= CH_3 or CF_3) *trans* to CO are less labile than those *trans* to PPh_3 (***Figure 2.3***).

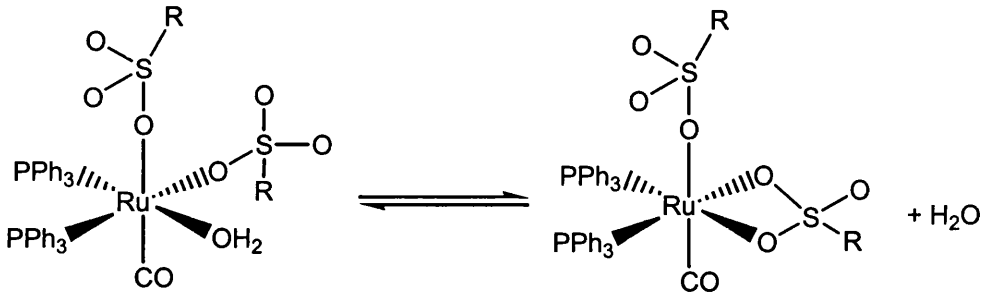

Figure 2.3: *Temperature dependent fluxionality of -OSO_2R as seen in $Ru(PPh_3)_2(CO)(H_2O)(OSO_2R)_2$.*[13-14]

Crystals of **2** suitable for X-ray crystallography were grown from CH_2Cl_2/hexane solution. ***Figure 2.4*** shows the expected octahedral coordination geometry about the ruthenium centre with the dppe ligand *trans* to one carbonyl and one triflate. The bite angle for the phosphine is 84.30(6)°, which is comparable to that in related ruthenium complexes such as Ru(dppe)$(CO)_2$[C(O)N(*p*-chlorophenyl)O],[15,16] which has a phosphine

bite angle of 83.64(8)°. The Ru-O bond distances of 2.197(4) Å for Ru-O(3) and 2.182(4) Å for Ru-O(6) are shorter than those in the bis(triflate) phosphine complex $Ru(Cyttp)(CO)(OTf)_2$ (Cyttp = $PhP(CH_2CH_2CH_2PCy_2)_2$; distances of 2.221(3) and 2.233(3) Å),[17] but significantly longer than those in the more electrophilic half-sandwich complex $(\eta^5\text{-}C_5Me_5)Ru(NO)(OTf)_2$ (Ru-O distances of 2.125(5) and 2.133(5) Å).[18] The triflate groups in **2** clearly point away from one another in the crystal structure with the closest intramolecular F-F distance of 8.54 Å. There is a significant difference in the two Ru-CO bond distances (Ru-C(1) = 1.859(7) Å, Ru-C(2) = 1.992(7) Å), reflecting the different *trans* effects of the phosphine and triflate ligands. Selected bond lengths [Å] and angles [°] for **2** are given in ***Table 2.1***.

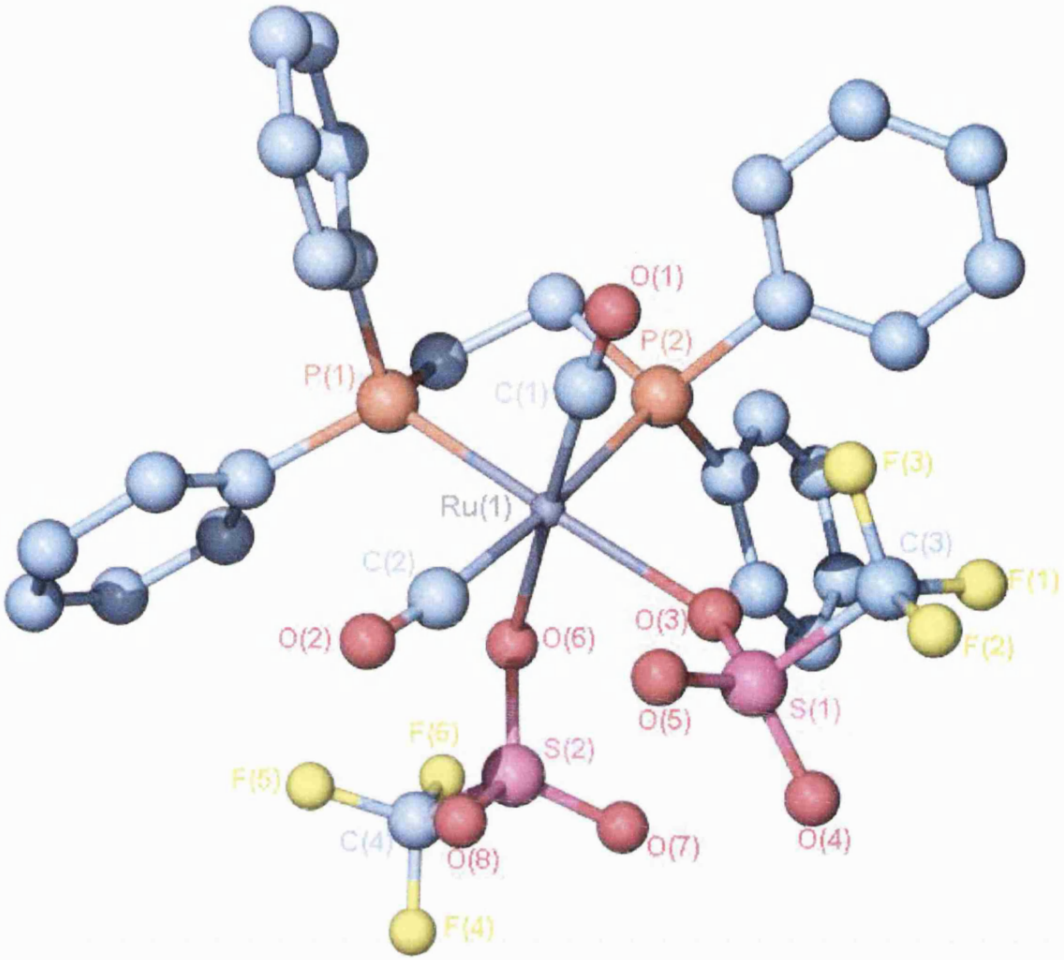

***Figure 2.4**: Plot of Ru(dppe)(CO)$_2$(OTf)$_2$ (**2**)*

Ru(1)-C(1)	1.859(7)	C(3)-F(3)	1.326(10)
Ru(1)-C(2)	1.992(7)	C(3)-F(2)	1.329(10)
Ru(1)-O(6)	2.182(4)	S(2)-O(8)	1.407(5)
Ru(1)-O(3)	2.197(4)	S(2)-O(7)	1.417(6)
Ru(1)-P(1)	2.324(2)	S(2)-O(6)	1.488(4)
Ru(1)-P(2)	2.418(2)	S(2)-C(4)	1.818(11)
S(1)-O(4)	1.396(6)	C(4)-F(6)	1.225(13)
S(1)-O(5)	1.441(7)	C(4)-F(4)	1.287(10)
S(1)-O(3)	1.480(4)	C(4)-F(5)	1.32(2)
S(1)-C(3)	1.803(11)	C(1)-O(1)	1.152(7)
C(3)-F(1)	1.288(12)	C(2)-O(2)	1.126(8)

C(1)-Ru(1)-C(2)	90.0(3)	P(1)-Ru(1)-P(2)	84.30(6)
C(1)-Ru(1)-O(3)	92.8(2)	O(4)-S(1)-O(5)	118.5(5)
C(2)-Ru(1)-O(3)	95.8(2)	O(4)-S(1)-O(3)	114.0(4)
O(6)-Ru(1)-O(3)	85.8(2)	O(5)-S(1)-O(3)	113.2(3)
C(1)-Ru(1)-P(1)	93.0(2)	O(4)-S(1)-C(3)	102.0(5)
C(2)-Ru(1)-P(1)	91.9(2)	O(5)-S(1)-C(3)	103.8(5)
O(6)-Ru(1)-P(1)	88.34(12)	O(3)-S(1)-C(3)	102.6(4)
O(3)-Ru(1)-P(1)	170.41(12)	O(8)-S(2)-O(7)	115.2(5)
C(1)-Ru(1)-P(2)	88.6(2)	O(8)-S(2)-O(6)	114.9(3)
C(2)-Ru(1)-P(2)	175.9(2)	O(7)-S(2)-O(6)	113.8(3)
O(6)-Ru(1)-P(2)	90.77(12)	O(8)-S(2)-C(4)	104.8(6)
O(3)-Ru(1)-P(2)	88.16(13)	O(7)-S(2)-C(4)	103.9(6)

Table 2.1: *Selected Bond Lengths [Å] and Angles [°] for Ru(dppe)(CO)$_2$(OTf)$_2$ (2).*

2.3 Preparation of Ru(dppe)(CO)(H_2O)($OTf)_2$ (3)

The OTf ligand is considered as a poor coordinating anion, and its derivatives are largely used in organic syntheses and inorganic chemistry, such as in the reactions of Re(triphos)$(CO)_2$(OTf) (triphos = $(PCH_2)_3CH$).[19] Here the OTf ligand is labile and can be easily replaced by different halides and pseudohalides ($X = CN^-, N_3^-, SCN^-, SeCN^-, OCN^-$) to give new mononuclear octahedral Re^I octahedral complexes of the general formula Re(triphos)$(CO)_2$(X).

During the synthesis of **2** an additional species was detected, as shown by the appearance of a further carbonyl band in the IR spectrum at 2001 cm^{-1}. This peak was seen to become more intense if the glassware was not rigorously flame-dried prior to use, suggesting that this species arises from reaction with water. Precedence for this comes from the reaction of the moisture sensitive species $Ru(PPh_3)_2(CO)_2(OTf)_2$[6] which undergoes triflate displacement forming $[Ru(PPh_3)_2(CO)_2(H_2O)_2][OTf]_2$. We assign our compound as the mono carbonyl aqua complex Ru(dppe)(CO)(H_2O)($OTf)_2$ (**3**), resulting from a carbonyl displacement rather than substitution of an OTf ligand. In some cases OTf ligands are better ligands than water, as in the case of $[Rh(PPh_3)_2(CO)(OH_2)][OTf]$ which contains two coordinated water ligands.[20]

Complex **3** was prepared by exposure of a solid sample of **2** to atmospheric moisture over a period of three weeks (***Figure 2.5***).

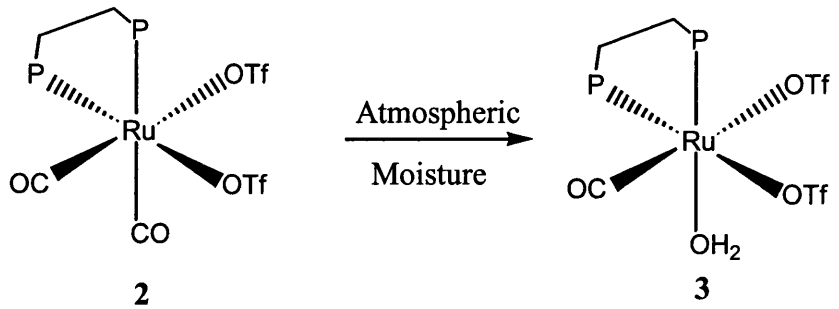

2 **3**

Figure 2.5: *Formation of Ru(dppe)(CO)(H_2O)($OTf)_2$ (3) from 2.*

Two doublets are seen in the $^{31}P\{^{1}H\}$ NMR spectrum of **3** at δ 65.5 and δ 67.5 (J_{PP} = 19.3 Hz), indicating that the two ends of the dppe ligand are in different environments. The $^{13}C\{^{1}H\}$ NMR spectrum contained a single carbonyl resonance at δ 197.1 with coupling to two *cis* phosphorus nuclei (J_{CP} = 17.7 Hz). The ^{19}F NMR spectrum of **3** is similar to that of **2** and shows two quartet resonances for the coordinated triflate ligands, although the ^{19}F-^{19}F coupling is marginally larger (3.84 Hz) than that seen in **2**. Both the ^{19}F and ^{31}P $\{^{1}H\}$ NMR spectra are unchanged between 25 and – 60 °C.

The solid state structure of **3** was determined by X-ray crystallography, as shown in ***Figure 2.6***, selected bond lengths [Å] and angles [°] for

(**3**) are reported in ***Table 2.2***. The triflate groups adopt an orientation very similar to that found in the structure of **2**. The water ligand is located *trans* to P(1) with a Ru-O(8) distance of 2.198(5) Å. This distance is close to that found in the related ruthenium(II) complex $Ru(PPh_3)_2(CO)(H_2O)(OSO_2\text{-}p\text{-}C_6H_4CH_3)_2$ (Ru-O = 2.206(6) Å),[14] but substantially longer than the sum of the Pauling covalent radii for ruthenium and oxygen (1.99 Å), demonstrating the weak nature of the Ru-O bond.[21]

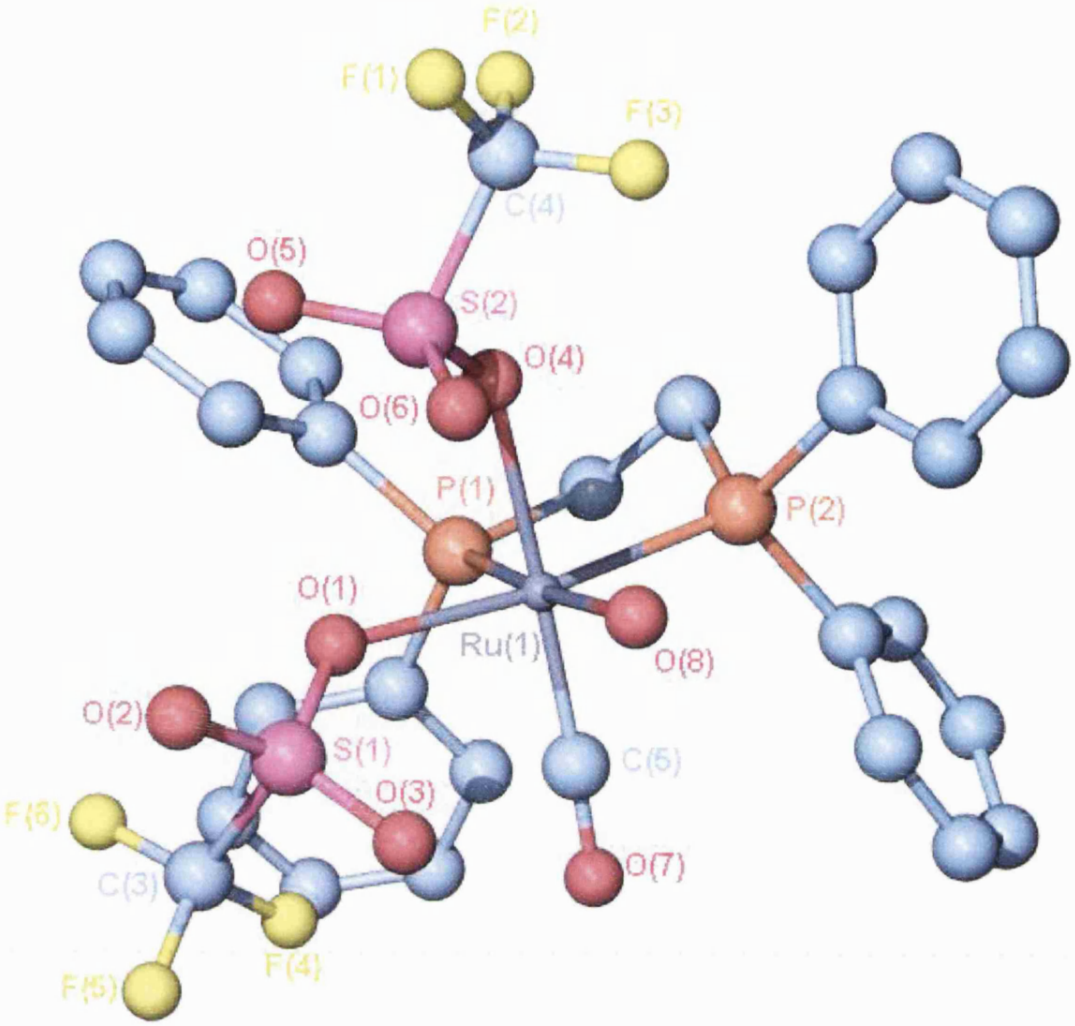

Figure 2.6: *Plot of Ru(dppe)(CO)(H_2O)($OTf)_2$* ***(3)****.*

Ru(1)-C(5)	1.817(8)	F(6)-C(3)	1.225(11)
Ru(1)-O(4)	2.187(4)	S(1)-O(2)	1.395(5)
Ru(1)-O(8)	2.198(5)	S(1)-O(3)	1.428(5)
Ru(1)-O(1)	2.199(4)	S(1)-O(1)	1.472(4)
Ru(1)-P(2)	2.300(2)	S(1)-C(3)	1.827(11)
Ru(1)-P(1)	2.331(2)	S(2)-O(5)	1.407(6)
F(1)-C(4)	1.354(11)	S(2)-O(6)	1.430(5)
F(2)-C(4)	1.250(11)	S(2)-O(4)	1.473(4)
F(3)-C(4)	1.311(12)	S(2)-C(4)	1.814(12)
F(4)-C(3)	1.308(10)	O(7)-C(5)	1.163(8)
F(5)-C(3)	1.347(10)		

C(5)-Ru(1)-O(4)	177.0(2)	O(2)-S(1)-O(3)	117.1(4)
C(5)-Ru(1)-O(8)	94.4(2)	O(2)-S(1)-O(1)	114.5(3)
O(4)-Ru(1)-O(8)	83.8(2)	O(3)-S(1)-O(1)	113.4(3)
C(5)-Ru(1)-O(1)	93.5(3)	O(2)-S(1)-C(3)	103.6(5)
O(4)-Ru(1)-O(1)	84.0(2)	O(3)-S(1)-C(3)	104.2(5)
O(8)-Ru(1)-O(1)	88.8(2)	O(1)-S(1)-C(3)	101.5(4)
C(5)-Ru(1)-P(2)	93.5(2)	O(5)-S(2)-O(6)	116.7(4)
O(4)-Ru(1)-P(2)	89.03(12)	O(5)-S(2)-O(4)	113.4(3)
O(8)-Ru(1)-P(2)	91.86(14)	O(6)-S(2)-O(4)	114.0(3)
O(1)-Ru(1)-P(2)	172.90(12)	O(5)-S(2)-C(4)	105.9(5)
C(5)-Ru(1)-P(1)	89.0(2)	O(6)-S(2)-C(4)	103.5(5)
O(4)-Ru(1)-P(1)	92.92(12)	O(4)-S(2)-C(4)	101.1(4)
O(8)-Ru(1)-P(1)	175.33(13)	S(1)-O(1)-Ru(1)	131.2(3)
O(1)-Ru(1)-P(1)	94.16(13)	S(2)-O(4)-Ru(1)	128.8(3)
P(2)-Ru(1)-P(1)	84.73(7)	O(7)-C(5)Ru(1)	177.5(6)

Table 2.2: *Selected Bond Lengths [Å] and Angles [°] for* $Ru(dppe)(CO)(H_2O)(OTf)_2$ ***(3).***

There are close contacts between the coordinated water ligand and the two triflate groups in the asymmetric unit as presented (O(8)-H···O(3) = 2.835(7) Å), supporting intramolecular hydrogen bonding (***Figure 2.7***). The water ligand also exhibits a close

contact with a triflate in an adjacent molecule (O(8)-H···O(3A) = 3.006(8) Å) generated by the symmetry operation *–x*, *-y*, *-z*, suggesting the presence of intermolecular hydrogen bonding.

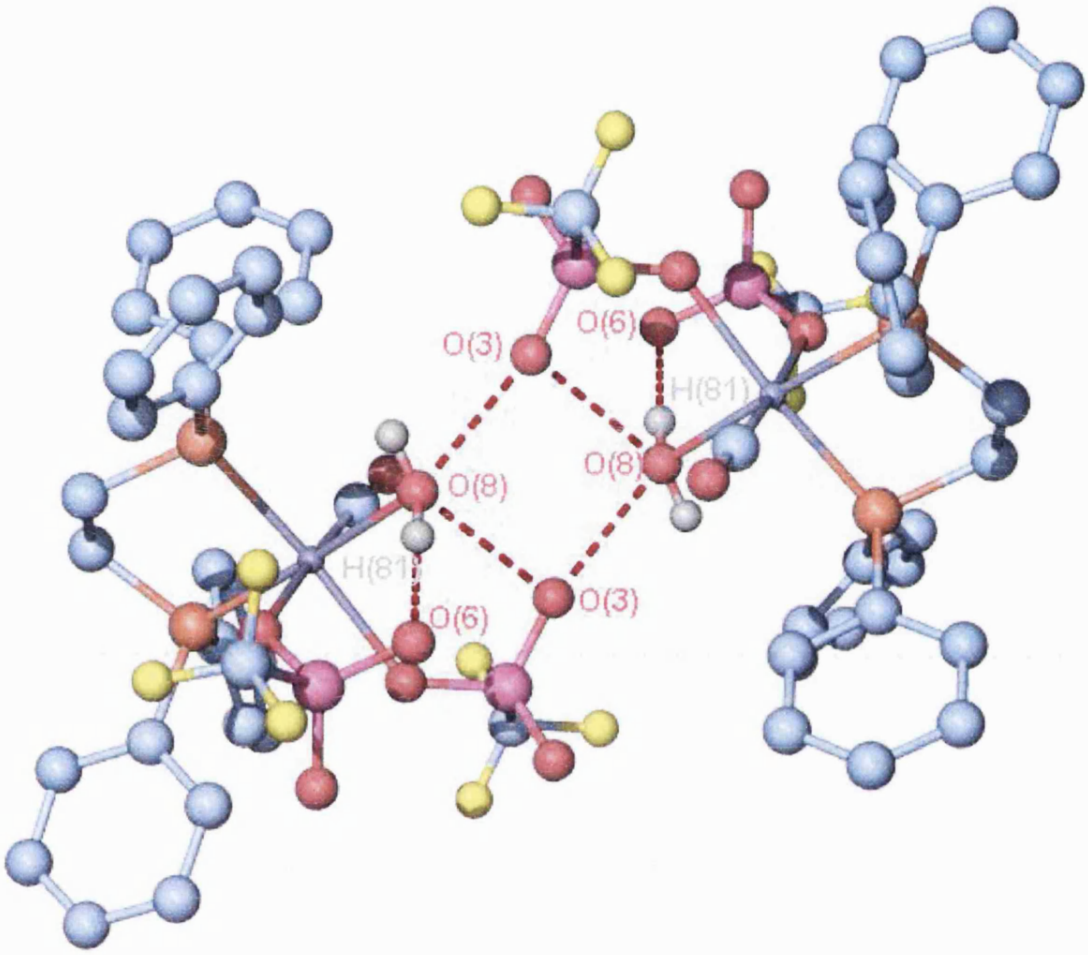

***Figure 2.7**: Inter and intra molecular hydrogen bonding interactions within Ru(dppe)(CO)(H_2O)($OTf)_2$ (**3**).*

The weakly coordinated water ligand in Ru(dppe)(CO)(H_2O)($OTf)_2$ proved to be substitutionally labile. Exposure of a CH_2Cl_2 solution of **3** to CO for 10 minutes resulted in conversion back to **2** in a quantitative yield. Studies using ^{13}CO also reveal that the label is

incorporated exclusively *trans* to dppe by direct substitution of the water molecule (***Figure 2.8***).

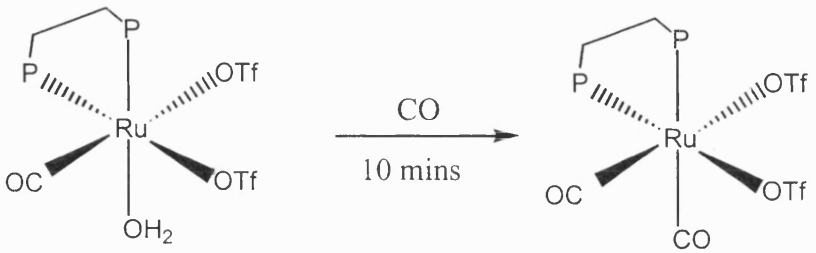

3 **2**

Figure 2.8: *Formation of Ru(dppe)(CO)$_2$(OTf)$_2$ (2) from 3.*

The triplet carbonyl resonance at δ 193.6 for the carbonyl *cis to* both phosphine groups is not ^{13}C enhanced and is thus not observed, proving that the substitution is selective (***Figure 2.9***).

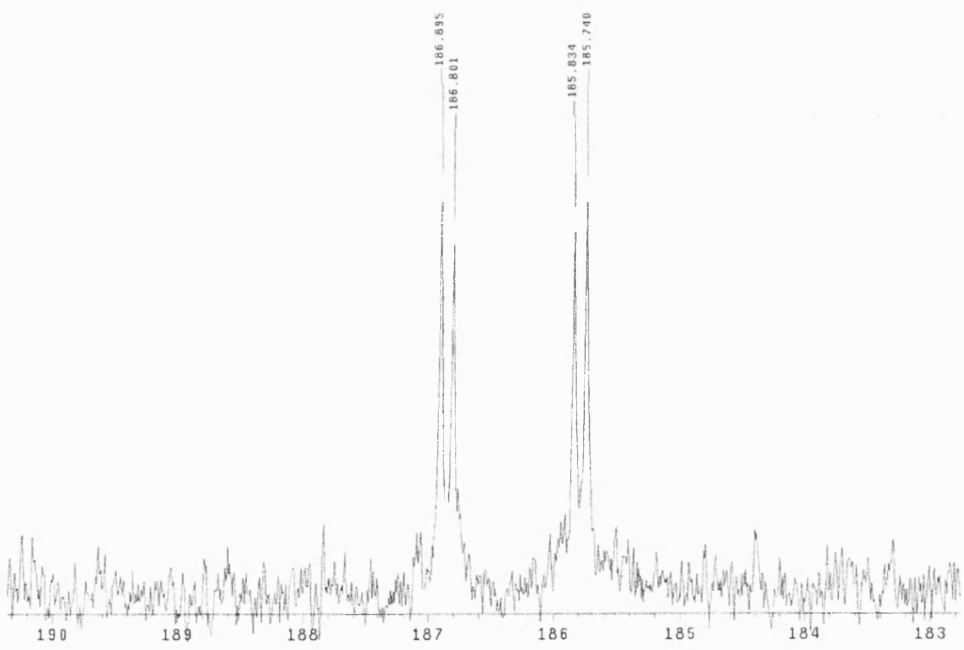

Figure 2.9: *^{13}C{^{1}H} NMR spectrum (75 MHz) showing the selective incorporation of a ^{13}CO label, forming Ru(dppe)(CO)(*CO) (OTf)$_2$ (2*) from 3.*

2.4 ^{19}F-^{19}F NOESY studies of 2 and 3

The coupling between the triflate groups seen in the ^{19}F NMR spectra of both **2** and **3** appear at first sight to be too large for through-bond coupling (the fluorine atoms are separated by eight bonds) and suggests through space coupling. This is well-established in organofluorine compounds by Mallory et al,[22] (***Figure 2.10***) who theorise their findings to result from overlap interactions between 2p lone-pair orbitals on the two crowded fluorines. They also reason that the effectiveness of the overlap depends not only on the intramolecular distance between the two fluorine atoms, but also the angular orientation of the overlapping lone pairs. Such phenomena are much scarcer in transition metal complexes. A sizeable F-F coupling has been seen between the two triflate groups for $Ru(bpy)(CO)_2(OTf)_2$ (J_{FF} = 3.1 Hz). The F-F separation is 8 bonds as in our system but, has been explained as a *trans* coupling (as the triflate groups are *trans* to bpy) rather than a through space effect.[23]

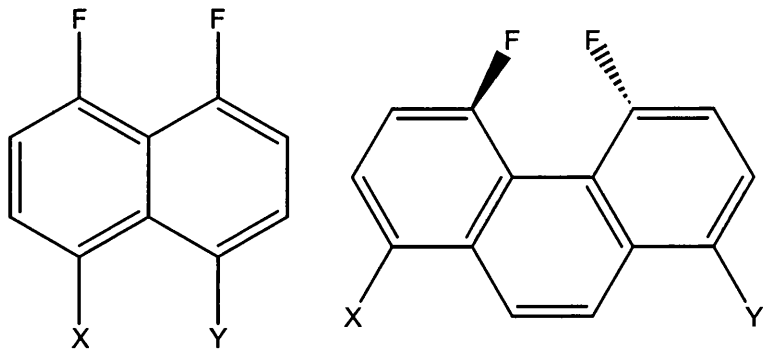

J_{FF} = 60-85 Hz
1,8-difluoronaphthalene

J_{FF} = 165-175 Hz
4,5-difluorophenanthrene

Figure 2.10: *Example of the sensitivity of through space F-F coupling to F-F distance.*

Using a published correlation of coupling constant[24] (J_{FF}) with distance (d_{FF}) based on a series of difluorocyclophanes with rigidly constrained geometries, the ^{19}F-^{19}F coupling constant of 3.45 Hz observed for **3** would imply a separation of 3.51 Å between the fluorine atoms of the two triflate ligands. The X-ray structure (***Figure 2.6***) gives the closest intramolecular interaction at 8.54 Å; while the solution and solid state structures must not necessarily be the same, we investigated the nature of the fluorine interaction in solution by ^{19}F-^{19}F NOESY.

A ^{19}F-^{19}F NOESY spectrum of a $CDCl_3$ solution containing a mixture of **2** and **3** (and also a small amount of free triflate) was recorded at 300 K (***Figure 2.11)*** with a mixing time (τ_m) of 400 ms. The spectrum shows that surprisingly the two triflate groups in **2** exchange with each other and also undergo intermolecular exchange with free triflate. Intra- and intermolecular exchange (with free triflate) is also observed for **3**. When the temperature is lowered to 255 K (***Figure 2.12***), these exchange processes are halted and weak NOE cross-peaks (ca. 1%) are observed between the two CF_3 groups in **2** and between the CF_3 groups in **3**. The observation of only a weak NOE effect (ca. 1%) appears to indicate that while there is some through-space F-F coupling in **2** and **3**, there must also be a contribution from through-bond coupling. It is not possible to quantify this effect any further.

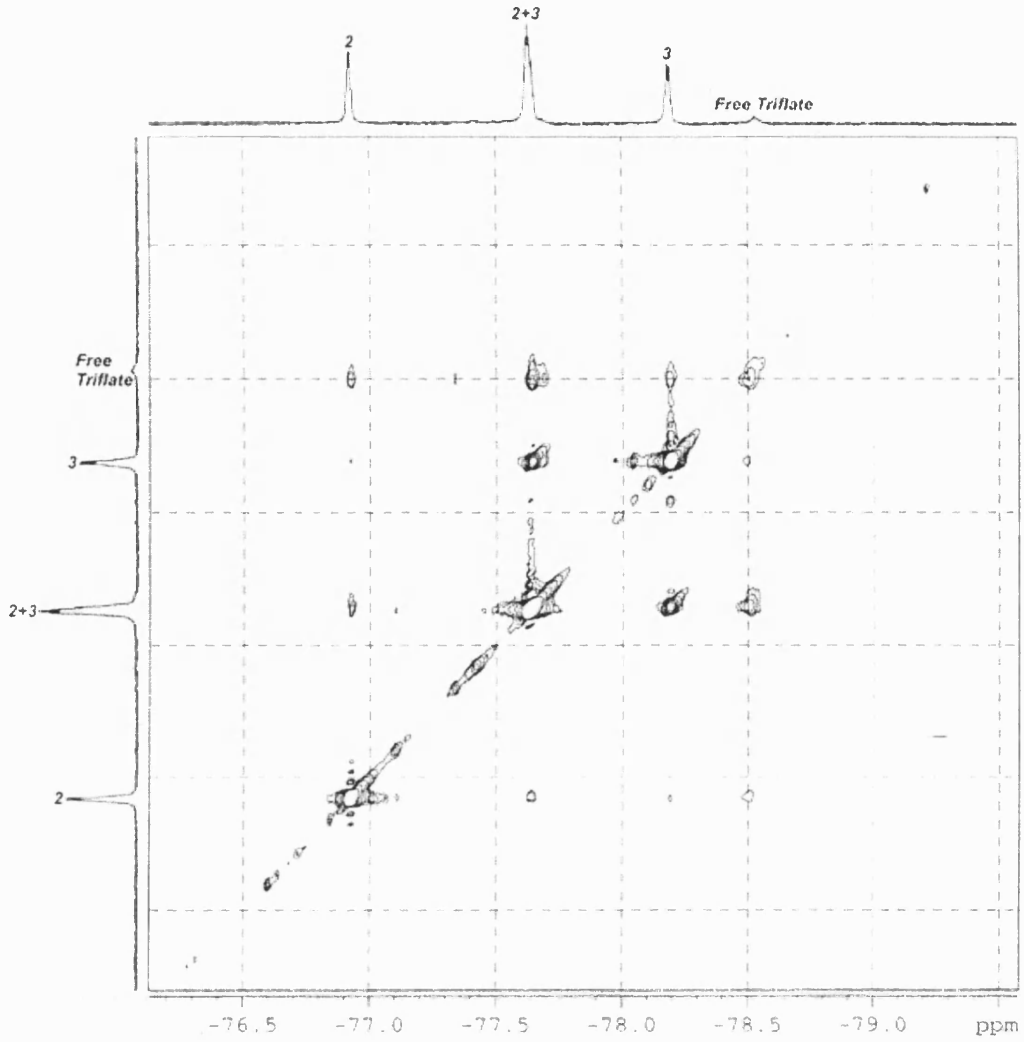

Figure 2.11: *^{19}F-^{19}F NOESY spectrum containing a mixture of* ***2*** *and* ***3*** *(and also a small amount of free triflate) recorded at 300 K, mixing time (τ_m) of 400 ms.*

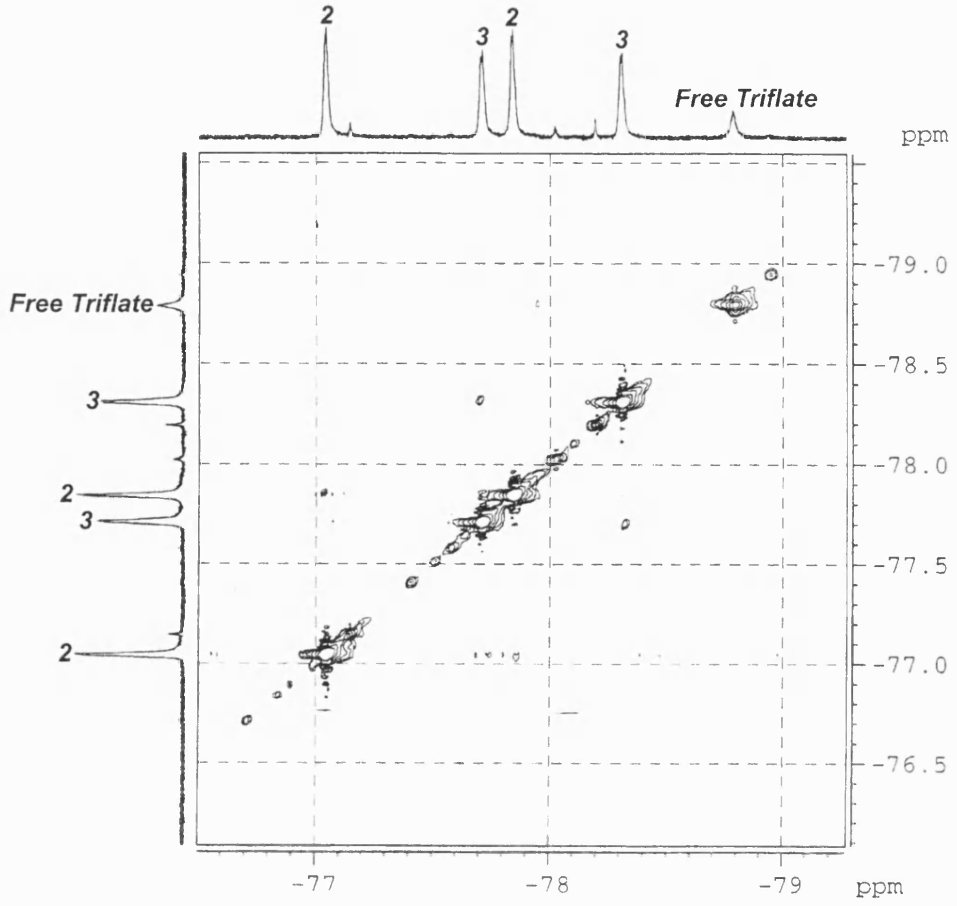

Figure 2.12: *^{19}F-^{19}F NOESY spectrum at 255 K.*

2.5 Preparation and characterisation of $[Ru(dppe)(CO)(H_2O)_3][OTf]_2$ (4a)

Given the facile displacement of a CO ligand from **2** by water in the solid state, an investigation into the reactivity of this complex with water in solution was conducted in the hope of also substituting the OTf ligands as in the case of $Ru(PPh_3)_2(CO)_2(OTf)_2$.[6] Addition of ten equivalents of water to a CH_2Cl_2 solution of **2** resulted in an immediate reaction which, by $^{31}P\{^1H\}$ NMR spectroscopy, showed the presence of at least six dppe containing complexes, none of which corresponded to **2**. The reaction does not go to completion yielding a single species, as pale yellow cubed crystals of $[Ru(dppe)(CO)(H_2O)_3][OTf]_2$ (**4a**) precipitate after 48 h at room temperature or after 24 h at 5 °C. The pale yellow crystals of **4a** proved suitable for X-ray crystallography and the resulting structure is shown in ***Figure 2.13***. Selected bond lengths [Å] and angles [°] for **4a** are given in ***Table 2.3***. It was found that **4a** could also be synthesised from the isomeric mixture of dichlorides $Ru(dppe)(CO)_2Cl_2$ by an *in situ* preparation upon adding AgOTf and H_2O all together.

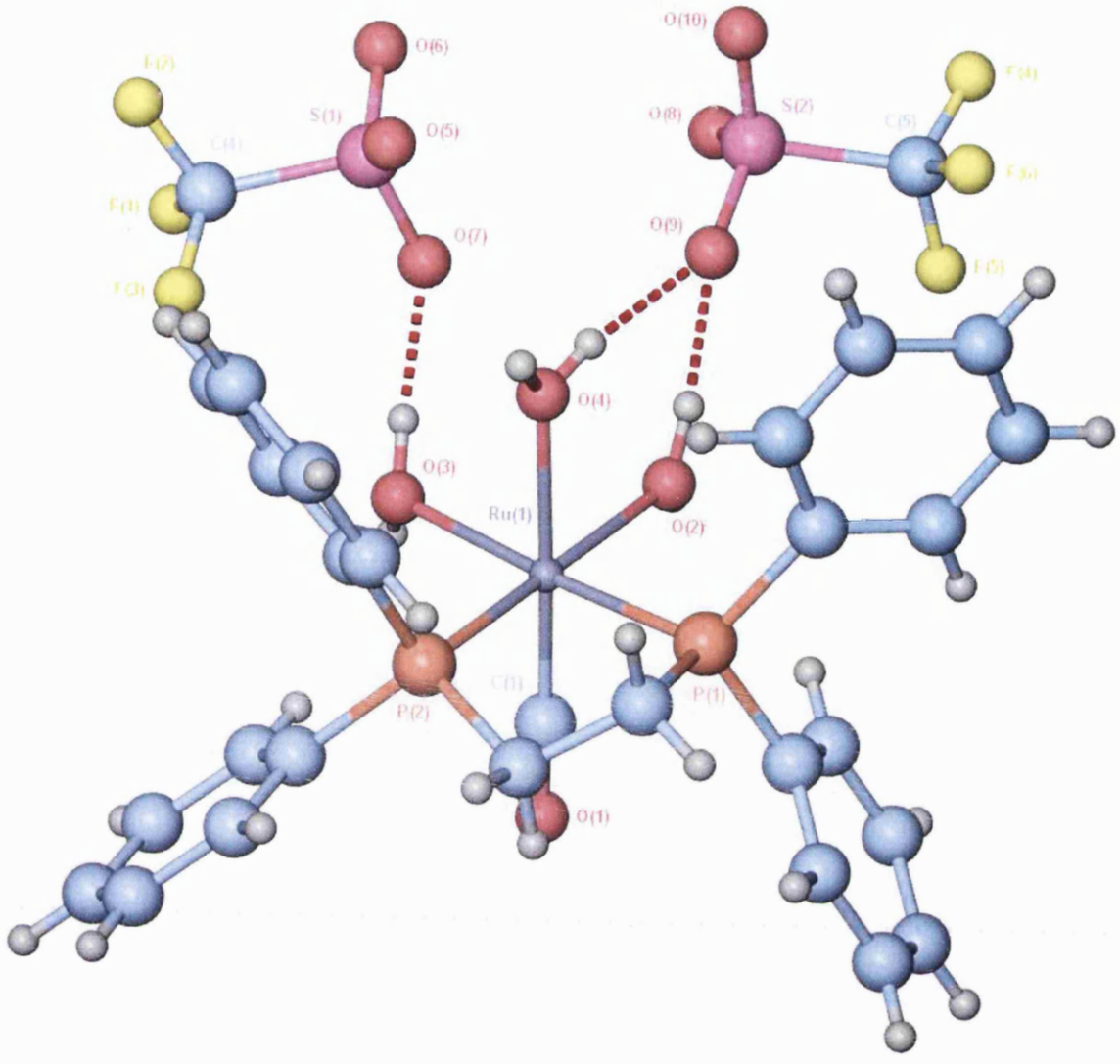

Figure 2.13: *Plot of* $[Ru(dppe)(CO)(H_2O)_3][OTf]_2$ ***(4a)***.

Ru(1)-C(1)	1.833(3)	S(2)-O(8)	1.435(2)
Ru(1)-O(4)	2.157(2)	S(2)-O(9)	1.446(2)
Ru(1)-O(3)	2.170(2)	S(2)-C(5)	1.813(4)
Ru(1)-O(2)	2.180(2)	O(1)-C(1)	1.145(3)
Ru(1)-P(2)	2.2654(7)	C(4)-F(3)	1.317(4)
Ru(1)-P(1)	2.2876(7)	C(4)-F(2)	1.320(4)
S(1)-O(5)	1.420(3)	C(4)-F(1)	1.325(4)
S(1)-O(6)	1.432(3)	C(5)-F(5)	1.309(4)
S(1)-O(7)	1.450(2)	C(5)-F(6)	1.322(4)
S(1)-C(4)	1.822(3)	C(5)-F(4)	1.333(4)
S(2)-O(10)	1.431(2)		

C(1)-Ru(1)-O(4)	176.53(10)	P(2)-Ru(1)-P(1)	85.44(3)
C(1)-Ru(1)-O(3)	95.47(10)	O(5)-S(1)-O(6)	116.5(2)
O(4)-Ru(1)-O(3)	81.40(8)	O(5)-S(1)-O(7)	115.1(2)
C(1)-Ru(1)-O(2)	96.19(10)	O(6)-S(1)-O(7)	112.87(14)
O(4)-Ru(1)-O(2)	82.17(8)	O(5)-S(1)-C(4)	103.5(2)
O(3)-Ru(1)-O(2)	86.80(8)	O(6)-S(1)-C(4)	104.0(2)
C(1)-Ru(1)-P(2)	86.05(8)	O(7)-S(1)-C(4)	102.64(14)
O(4)-Ru(1)-P(2)	95.70(6)	O(10)-S(2)-O(8)	114.4(2)
O(3)-Ru(1)-P(2)	95.09(6)	O(10)-S(2)-O(9)	114.75(14)
O(2)-Ru(1)-P(2)	176.92(6)	O(8)-S(2)-O(9)	114.96(14)
C(1)-Ru(1)-P(1)	88.31(8)	O(10)-S(2)-C(5)	104.8(2)
O(4)-Ru(1)-P(1)	94.81(6)	O(8)-S(2)-C(5)	103.0(2)
O(3)-Ru(1)-P(1)	176.21(6)	O(9)-S(2)-C(5)	102.8(2)
O(2)-Ru(1)-P(1)	92.51(6)	O(1)-C(1)-Ru(1)	77.4(2)

Table 2.3: *Selected Bond Lengths [Å] and Angles [°] for [Ru(dppe)(CO)(H_2O)$_3$][OTf]$_2$ (4a).*

As can be seen from the crystal structure diagram, the three coordinated water molecules are arranged in a *fac* configuration. The asymmetric unit contains the octahedral ruthenium dicationic complex, two free triflate anions and 1.8 molecules of free water.

Two of the aqua ligands are located *trans* to the dppe ligand and one is *trans* to CO (***Table 2.3***). The Ru-O bond lengths for the two equivalent waters are of comparable length (Ru-O(2) = 2.180(2) Å, Ru-O(3) = 2.170(2) Å), while the Ru-O distance *trans* to CO is slightly shorter (Ru-O(4) = 2.157(2) Å). The Ru-O (H_2O) bond length in **3** is 2.198(5) Å and lies *trans* to phosphorus. This is longer than in **4a**, and could indicate greater lability as seen in the reversible reaction with CO. The average Ru-P bond length distance in **4a** is 2.2765 Å, and is comparable to that found in **3**. The phosphine bite angle is 84.44(3)°, comparable to that established in the structures of both **2** and **3**.

Analysis of the supramolecular array reveals that the gross structure is dominated by hydrogen bonding chains parallel to the *c* axis of the unit cell and that these are propagated by two sets of alternating interactions (***Figure 2.14***). Each dicationic centre is hydrogen-bonded to the lattice neighbour (generated as a consequence of the inversion centre) closest to its ligated waters. In particular, the two protons attached to O(2) and O(3), along with one of the protons attached to O(4), interact with the oxygen atoms of the triflate counterions from the same asymmetric unit along with those generated by the inversion centre. These units are then "cemented" further by interaction of the remaining proton on O(4) and a lattice water molecule (O(12)). This cementing is consolidated by interaction of O(12) with O(5) of a triflate ion.

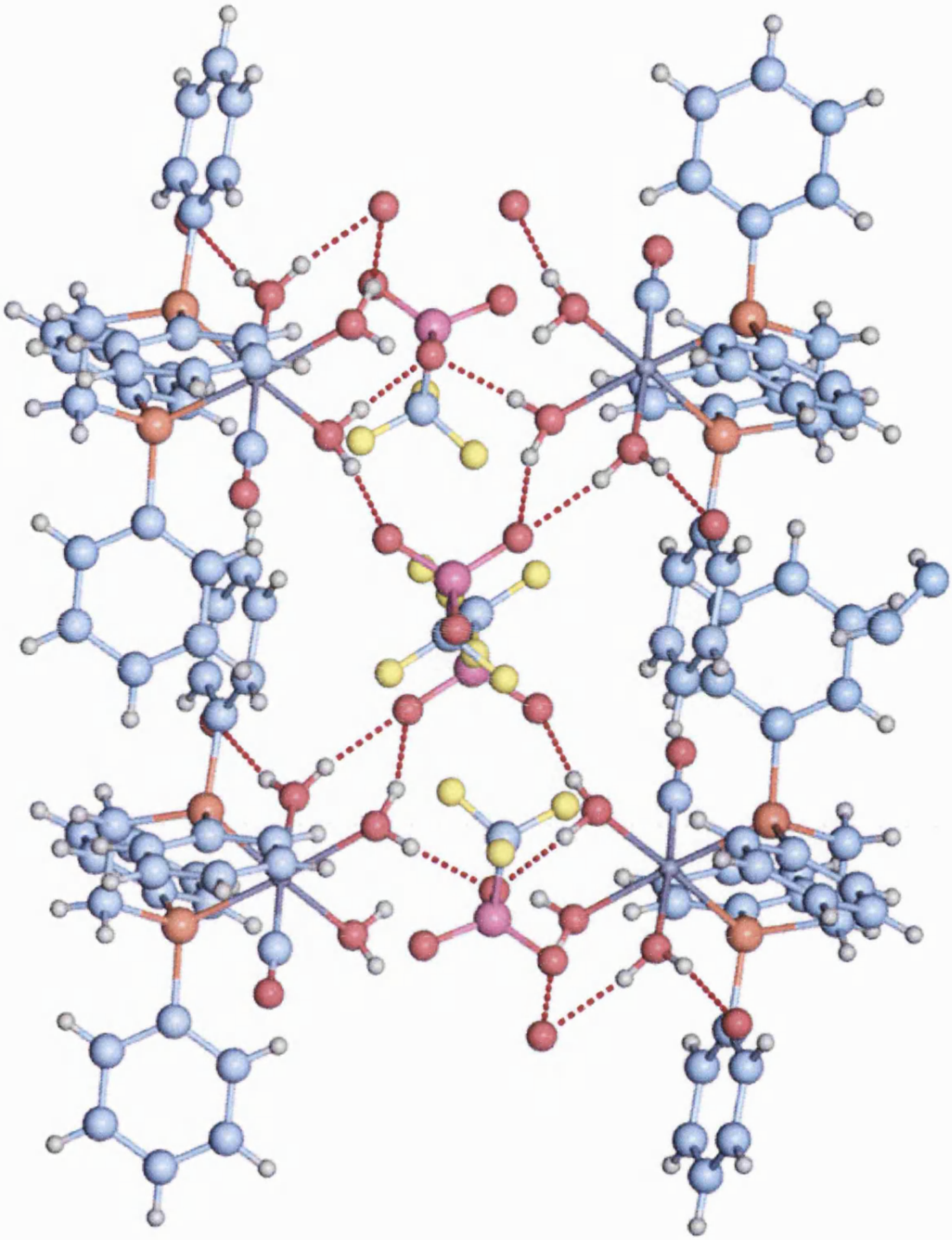

***Figure 2.14**: Plot illustrating the hydrogen bonding interactions within the crystal of **4a**.*

Hydrogen bonding appears to be an important factor in stabilising many coordinated aqua ligands. In the solid state, hydrogen bonding of the aqua ligand to counterions or oxygen donor solvent molecules is often observed.[25] The majority of the aqua complexes reported are cationic species, which contain weakly coordinating anions such as BF_4^-, SbF_6^- or OTf.[26,27] This type of interaction is considered to represent a hydrogen bond if the distance between the donor and acceptor atoms is less than 3.0 Å.[28]

2.6 Solution characterisation of 4a

Solubility studies revealed that **4a** is not very soluble at all in water but is soluble in either CH_2Cl_2 or $CHCl_3$. However in these cases the tris-aqua structure was not retained as evidenced by $^{31}P\{^1H\}$ NMR which showed the appearance of two doublets at δ 65.1 and 67.0 (J_{PC} = 19.2 Hz) and an unidentified singlet resonance at δ 67.7. Dissolution of **4a** in a mixture of acetone and water provided a suitable solvent mixture to study **4a**. A singlet peak was seen in the $^{31}P\{^1H\}$ NMR spectrum at δ 66.5 while the ^{19}F NMR spectrum displayed a single sharp peak at δ –79.20 for the free triflate counterions. The $^{13}C\{^1H\}$ NMR spectrum displayed a triplet carbonyl resonance at δ 198.3 (J_{PC} = 17.9 Hz), the coupling constant being consistent with a *cis* geometry to the coordinated dppe ligand. The coordinated water ligands were not seen in the ^1H NMR spectrum. The IR spectrum of **4a** in KBr displayed a single carbonyl band at 1990 cm^{-1}, and a band associated with uncoordinated triflate at 1232 cm^{-1}.

2.7 Kinetic studies on the synthesis of 4a

The formation of **4a** was investigated by monitoring the $^{31}P\{^1H\}$ NMR spectrum of a solution of **2** in CD_2Cl_2 upon addition of 10 equivalents of water. The reaction was

performed in J. Young's resealable NMR tube, studied at set time intervals and plotted as a kinetic stack plot (***Figure 2.16***). An initial spectrum before the addition of water was recorded and is shown below in ***Figure 2.15***.

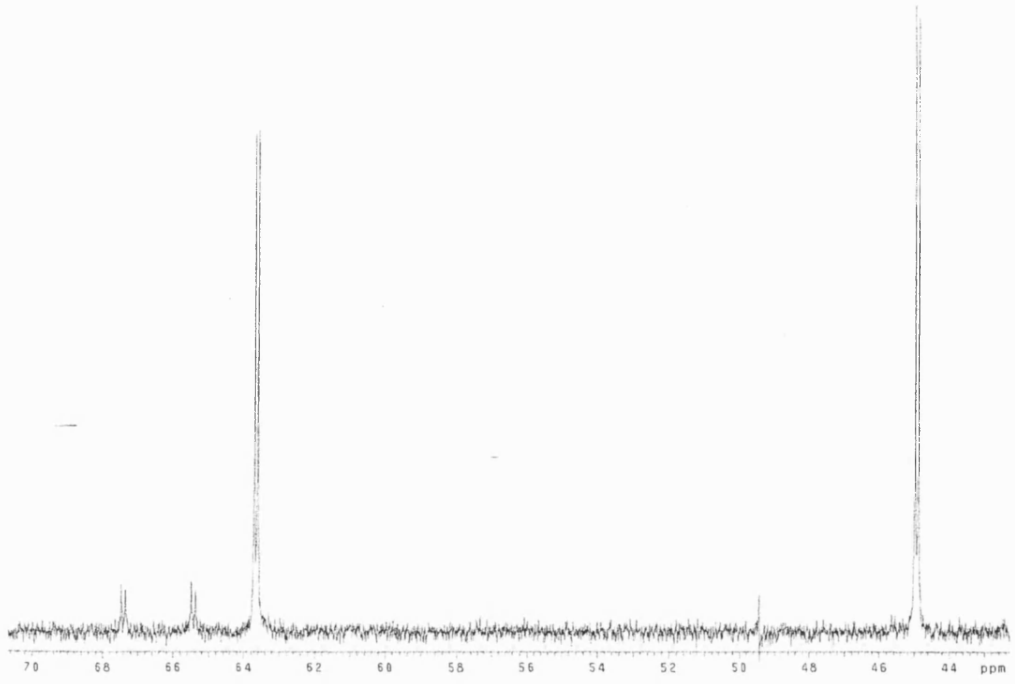

Figure 2.15: *$^{31}P\{^{1}H\}$ NMR spectrum (162 MHz) of* ***2*** *in CD_2Cl_2, before addition of water; the doublet peaks at δ 65.5 and 67.5 are associated with the mono aqua complex $Ru(dppe)(CO)(H_2O)(OTf)_2$ (**3**).*

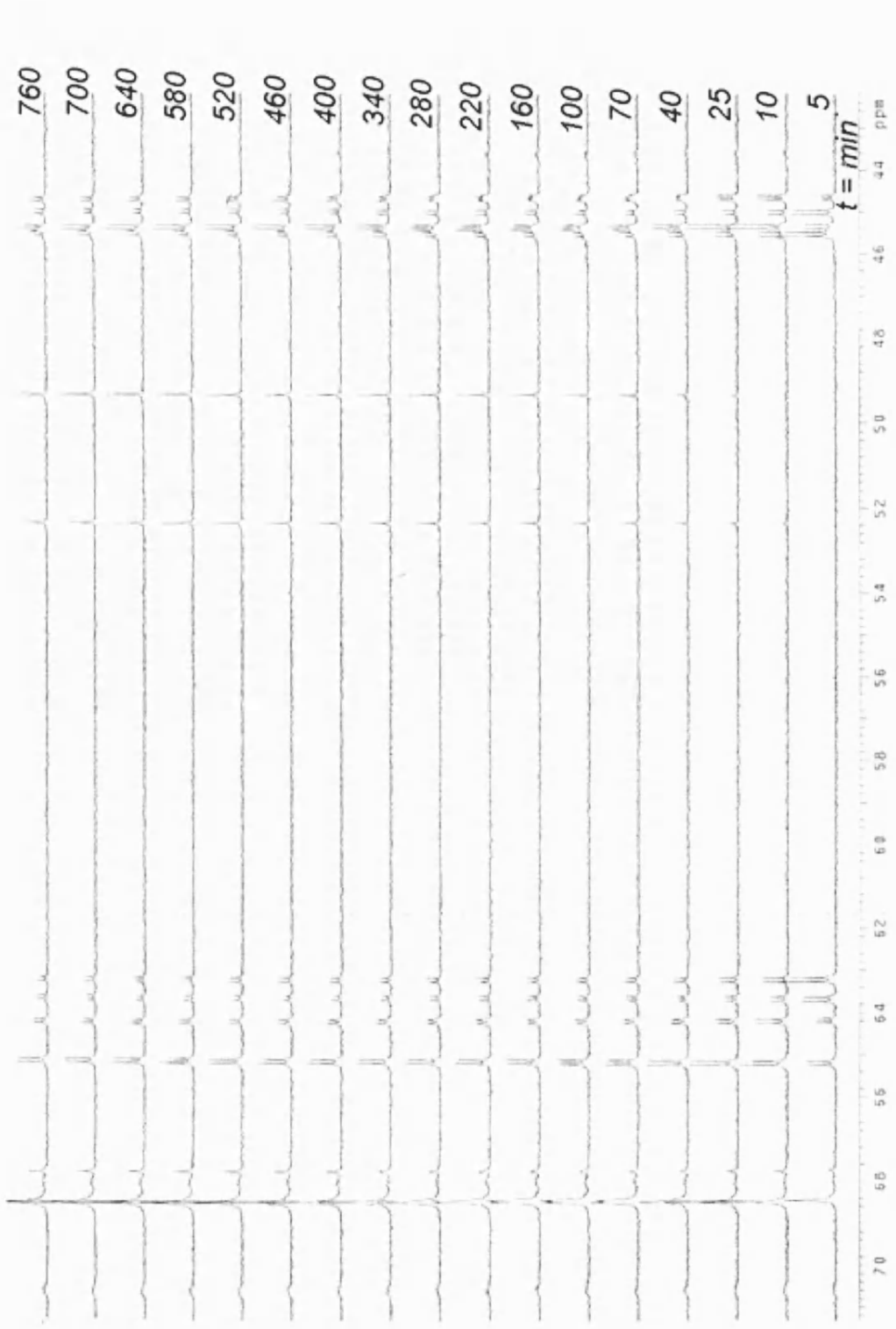

Figure 2.16: *$^{31}P\{^{1}H\}$ NMR spectrum (162 MHz) were recorded at 5, 10, 25, 40, 70, 100 minutes and subsequently at 60 minute intervals after addition of 10 equivalents of water to a CD_2Cl_2 solution of* ***2****.*

When the reaction was started, the mono aqua species **3** reacted rapidly so that it was consumed by t = 5 min. Complex **2** is seen to decrease but less quickly. New peaks are seen early on at δ 68.3 (s), δ 65.2 and 45.5 (d+d) even at t = 5 min. The singlet peak associated with **4a** at δ 52.9 appears early on at t = 10 min. This kinetic experiment was repeated numerous times with varying concentrations of water. However full conversion to **4a** was never seen even with a maximum acquisition time of $17^3/_4$ h, since crystals of **4a** always precipitate from solution before this time.

We do not know the identity of any of the species that give rise to these resonances but, we propose that the singlet peak seen at δ 68.5 may be associated with the bis-aqua complex $[Ru(dppe)(CO)_2(H_2O)_2][OTf]_2$. Attempts were made to try and synthesise this complex starting from a CH_2Cl_2 solution of **2** with addition of 2 equivalents of water. However the same reactivity was observed as in ***Figure 2.16***, and crystals of **4** were isolated after 24 h.

Further details pertaining to the formation of **4a** from **2** with respect to water-gas shift chemistry are explained in ***sections 3.13*** and ***3.14***.

2.8 Preparation of $[Ru(dppe)(CO)(H_2O)_3][BF_4]_2$ (4b) and $[Ru(dppe)(CO)(H_2O)_3][SbF_6]_2$ (4c)

During the past nine months a considerable amount of effort has gone into synthesising new water-soluble ruthenium(II) aqua species. Previous work conducted on $[Ru(dppe)(CO)(H_2O)_3](OTf)_2$ (**4a**) revealed that this compound was soluble in acetone/water but not in water alone. One of the routes proposed in order to achieve better water-solubility was to modify the nature of the counter-anion associated with the $[Ru(dppe)(CO)(H_2O)_3]^{2+}$ dication. Among the group of weakly coordinating anions considered were BF_4^- and SbF_6^-, both of which would potentially present hydrogen

bonding opportunities in the crystal lattice and in solution. Beck and Sünkel[9] have conducted extensive studies on such weakly coordinating anions along with PF_6^- and AsF_6^- .

Attempts were made to synthesise and isolate the $Ru(dppe)(CO)_2X_2$ ($X = BF_4^-$ and SbF_6^-) species, but these proved unsuccessful, presumably because of the lability of the ligands towards water. Fortunately, during the attempted syntheses of these compounds, it was found that good conversion to the tris-aqua species took place upon treatment of **1** with ~2 equivalents of AgX ($X = BF_4^-$ or SbF_6^-) in the presence of 10 equivalents of water.

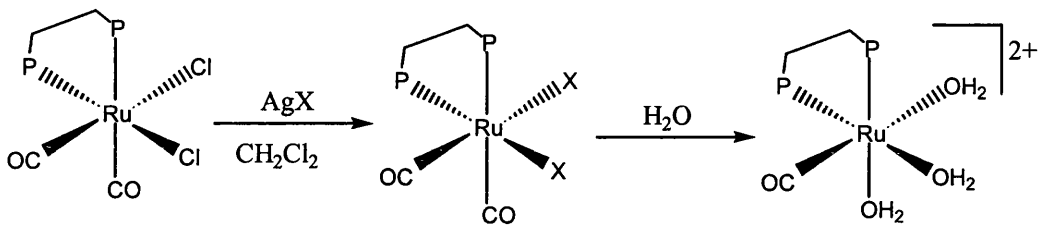

Scheme 2.2: *Proposed synthesis of* $[Ru(dppe)(CO)(H_2O)_3][X]_2$ *(*$X = BF_4^-$ *or* SbF_6^-*)*

2.9 Synthesis and characterisation of $[Ru(dppe)(CO)(H_2O)_3][BF_4]_2$ (4b)

To a solution of **1** in CH_2Cl_2, were added 10 equivalents of H_2O and 2.2 equivalents of $AgBF_4$. The solution was left stirring for 1 h in the absence of light and monitored by IR spectroscopy. Changes were observed in the carbonyl region, as the two bands corresponding to $Ru(dppe)(CO)_2Cl_2$ at 2079 and 2004 cm^{-1} were replaced by a single band at 1992 cm^{-1}. The solution was filtered and the filtrate was reduced to half of the original volume *in vacuo* and left at 5 °C in an attempt to crystallise the product. After 48 h at 5 °C, pale yellow crystals of what was later characterised as $[Ru(dppe)(CO)(H_2O)_3][BF_4]_2$ (**4b**) had precipitated from solution. This compound was

characterised by IR and NMR spectroscopy, elemental analysis and X-ray crystallography. This compound showed fairly good solubility in water (10 mg/mL). The $^{31}P\{^{1}H\}$ NMR spectrum of $[Ru(dppe)(CO)(H_2O)_3][BF_4]_2$ in D_2O exhibited a singlet at δ 67.3, which is comparable to that seen for the OTf analogue in acetone/water (δ 66.5). The $^{19}F\{^{1}H\}$ NMR spectrum displayed two signals at δ -150.466 and –150.417 (ratio 1:4) due to the presence of ^{10}B and ^{11}B (I = 3 and $^{3}/_{2}$ respectively). In the $^{13}C\{^{1}H\}$ NMR spectrum, a triplet signal at δ 198.0 (J_{PC} = 18.0 Hz) is seen for the carbonyl ligand.

Single crystals of **4b** suitable for X-ray crystallography were isolated and the resultant structure determined as shown in ***Figure 2.17***. The structure of $[Ru(dppe)(CO)(H_2O)_3][BF_4]_2$ is very similar to that of $[Ru(dppe)(CO)(H_2O)_3][OTf]_2$ around the metal centre, however it presents a completely different hydrogen-bonded network throughout the crystal lattice. The hydrogen-bonding network for $[Ru(dppe)(CO)(H_2O)_3][BF_4]_2$ can be seen in ***Figure 2.18***. Selected bond lengths [Å] and angles [°] for **4b** are given in ***Table 2.4.*** There is significant hydrogen bonding throughout the lattice of **4b** involving free H_2O and BF_4^- anions. The hydrogens of the coordinated water O(2), is hydrogen bonded to the free water molecule O(5) which is in turn hydrogen bonded to F(7) of B(2) (free BF_4^-) and the other lattice water molecule O(6). The lattice water molecules were found to act as a lattice cement.

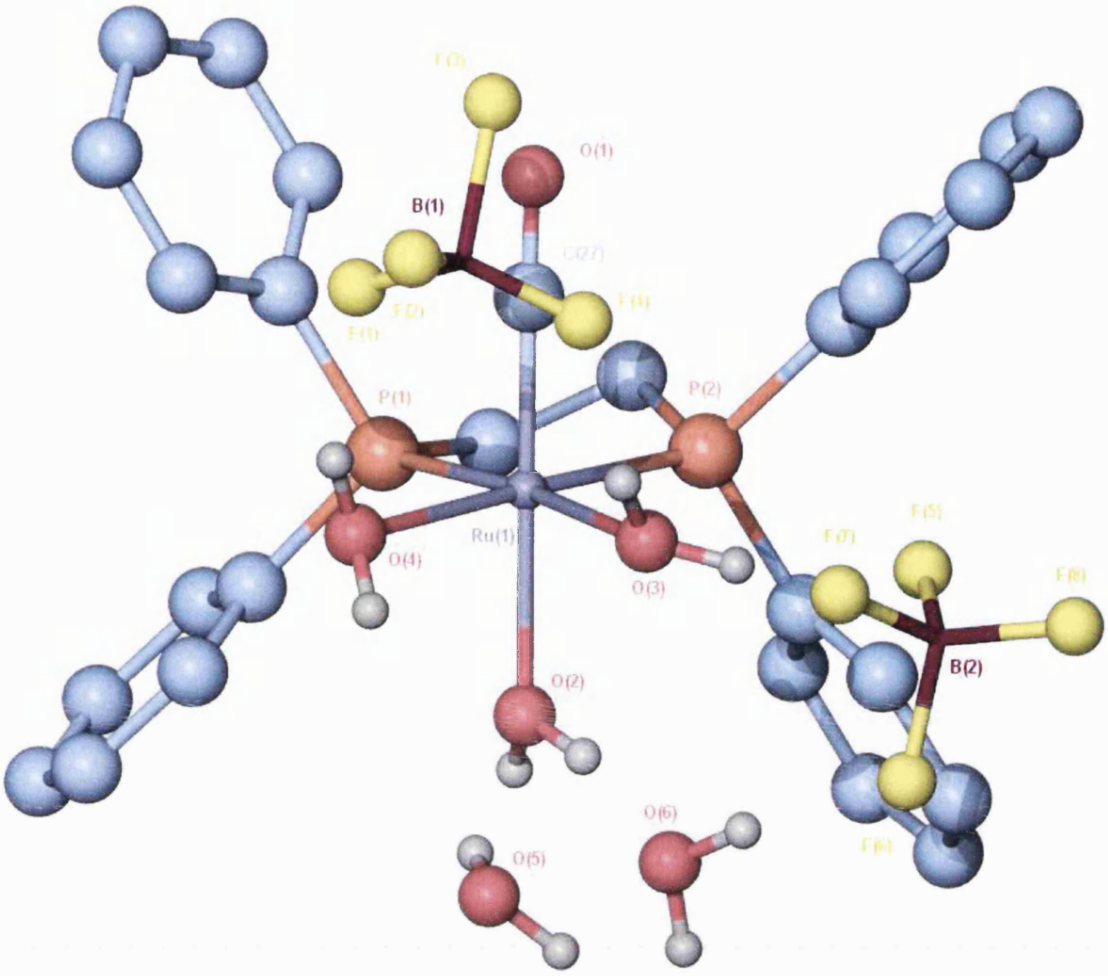

Figure 2.17: *Plot of* $[Ru(dppe)(CO)(H_2O)_3][BF_4]_2.2\ H_2O$, ***4b***.

C(27)-O(1)	1.144(4)	Ru(1)-C(27)	1.836(3)
Ru(1)-O(3)	2.186(2)	Ru(1)-O(4)	2.196(2)
Ru(1)-O(2)	2.142(2)	Ru(1)-P(1)	2.2876(8)
Ru(1)-P(2)	2.2780(8)		

P(1)-Ru(1)-P(2)	84.95(3)	O(3)-Ru(1)-O(4)	78.69(9)
C(27)-Ru(1)-O(2)	176.80(11)	O(2)-Ru(1)-O(3)	81.18(9)
O(2)-Ru(1)-O(4)	81.76(9)	C(27)-Ru(1)-O(3)	95.92(11)
C(27)-Ru(1)-O(4)	96.40(12)		

Table 2.4: *Selected bond lengths [Å] and angles [°] for* ***4b****.*

As can be seen from the crystal structure, the water molecules are coordinated in a *fac* arrangement with two BF_4^- counter ions and two waters of crystallisation present. The Ru-O bond lengths for the two equivalent waters are of a comparable length at 2.186(2) and 2.196(2) Å for O(3) and O(4) respectively, which are noticeably longer than in **4a**, which has bond lengths of 2.170(2) and 2.180(2). These bond length differences presumably reflect the different anion-cation interactions, the differing extent of lattice water hydrogen bonding or general packing effects. The average Ru-P bond length is 2.2828(8) Å and the phosphine bite angle is 84. 95° which are comparable to **4a**.

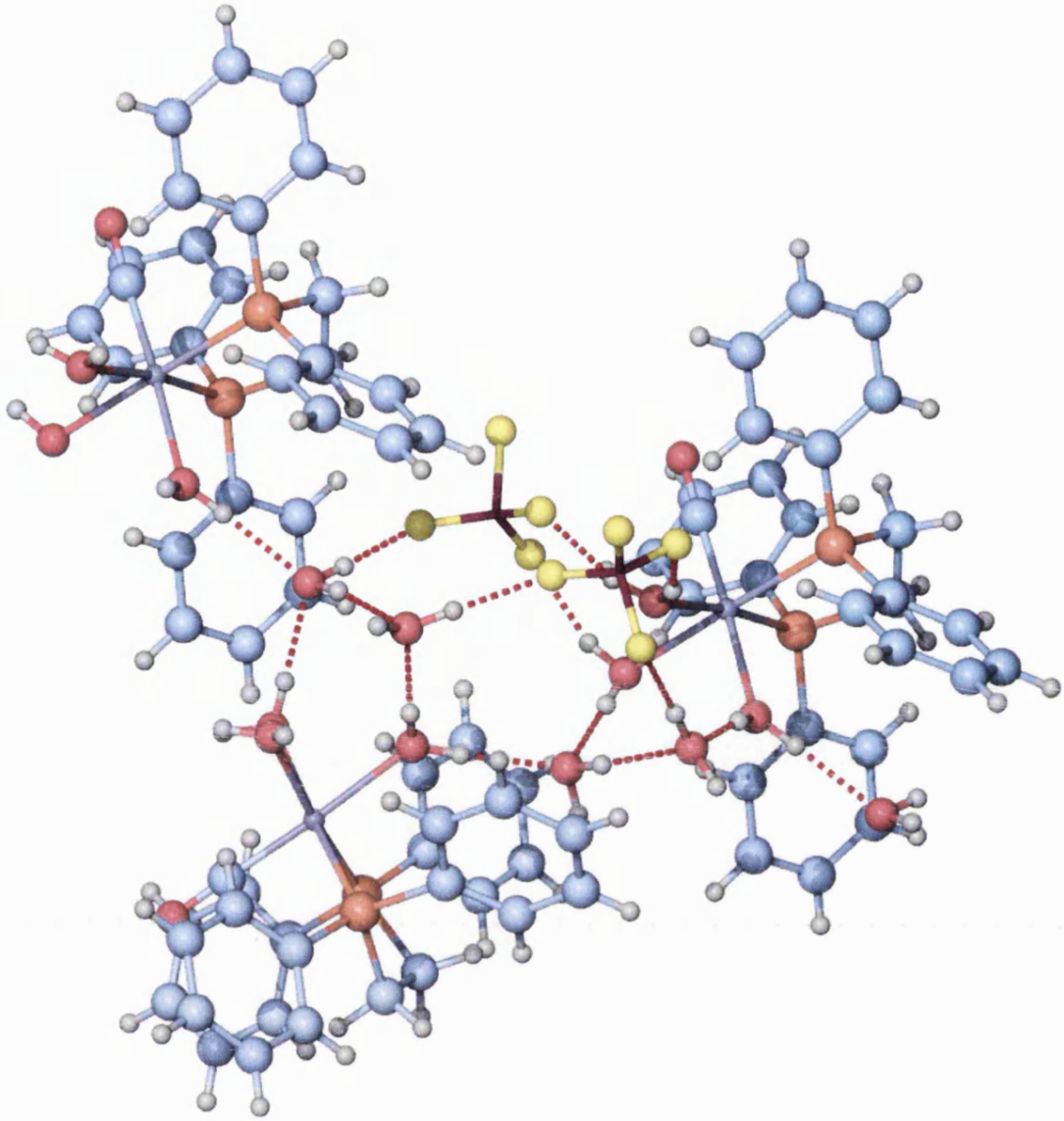

Figure 2.18: *Plot illustrating the hydrogen bonding interactions within the crystal of* ***4b****.*

2.10 Synthesis and characterisation of $[Ru(dppe)(CO)(H_2O)_3][SbF_6]_2$ 4c

The synthesis of $[Ru(dppe)(CO)(H_2O)_3][SbF_6]_2$ was carried out using the same technique as for $[Ru(dppe)(CO)(H_2O)_3][BF_4]_2$. **4c** was characterised by IR and multinuclear NMR spectroscopy, elemental analysis and X-ray crystallography. This compound, showed even better water solubility than the BF_4^- analogue at 14 mg/mL. The difference in solubility between these compounds will be described later in this chapter (***Section 2.11***). The $^{31}P\{^1H\}$ NMR and $^{13}C\{^1H\}$ NMR data of the cationic unit are identical to those of **4a** and **4b**. The IR spectrum recorded in water between CaF_2 plates showed a ν_{CO} stretching frequency at 1994 cm^{-1}. The $^{19}F\{^1H\}$ NMR spectrum showed a characteristic complex signal at δ – 126.45 due to free SbF_6^-.

Suitable crystals for X-ray crystallography of the SbF_6^- complex were obtained and the resulting structure is shown in ***Figure 2.19*** with selected bond lengths [Å] and angles [°] reported in ***Table 2.5.*** As can be seen from the crystal structure, the water molecules are coordinated in a *fac* arrangement as in **4a** and **4b**. The Ru-O bond lengths for the two equivalent waters are of a comparable length at 2.173(3) and 2.182(3) Å for O(2) and O(4) respectively, closer than those seen in **4a** rather than **4b**. The Ru-O bond length for the water *trans* to CO is 2.163(3) Å, close to that found in **4**. There are hydrogen bonding interactions present all throughout the crystal lattice as can be seen in ***Figure 2.20***. The anion based on Sb1 has disorder in the 4:1 positional disorder of fluorines in the belt. The gross structure is dominated by the presence of hydrogen bonding to form sheet–like arrays within the lattice. CH_2Cl_2 molecules fill the small cavities in the lattice, and there may be C–H…F and/or C–H…O interactions present involving the hydrogens therein. Water hydrogens were located and refined at a distance of 0.89Å from the relevant parent atom and at a distance of 1.45 Å from each other within individual water molecules. H4a and H4b were also restrained to be 2.6 Å from the central ruthenium.

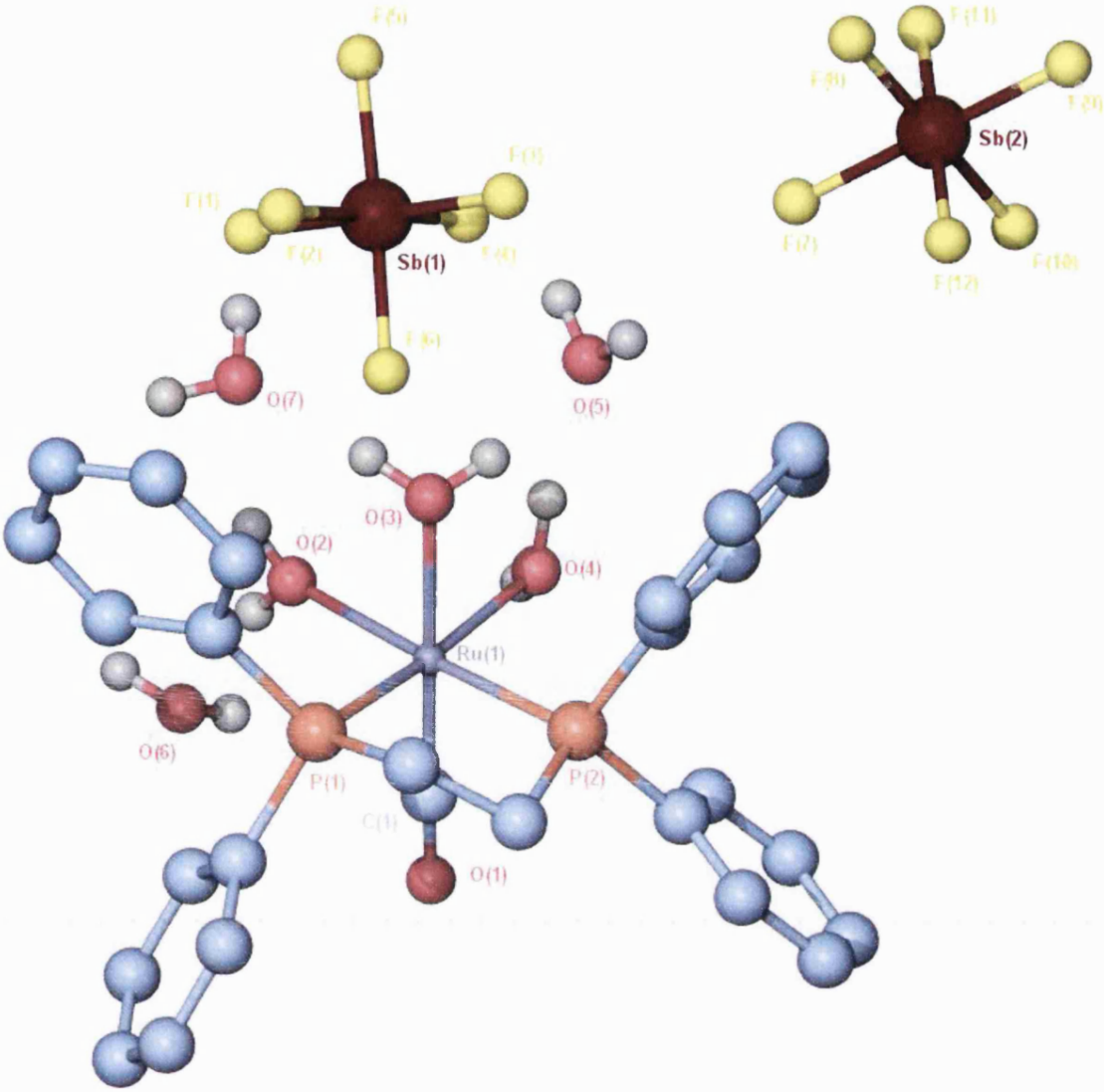

Figure 2.19: *Plot of* $[Ru(dppe)(CO)(H_2O)_3][SbF_6]_2.3\ H_2O.CH_2Cl_2$.

Ru(1)-C(1)	1.843(4)	Ru(1)-O(1)	2.173(3)
Ru(1)-O(3)	2.163(3)	Ru(1)-O(4)	2.182(3)
C(1)-O(1)	1.146(5)	Ru(1)-P(1)	2.3046(9)
Ru(1)-P(2)	2.2860(9)		

P(1)-Ru(1)-P(2)	84.94(3)	O(4)-Ru(1)-O(2)	83.91(11)
C(1)-Ru(1)-O(3)	179.55(14)	O(3)-Ru(1)-O(2)	83.48(11)
O(3)-Ru(1)-O(4)	85.40(11)	C(1)-Ru(1)-O(4)	95.04(14)
C(1)-Ru(1)-O(2)	96.62(14)		

Table 2.5: *Selected bond lengths [Å] and angles [°] for* ***4c****.*

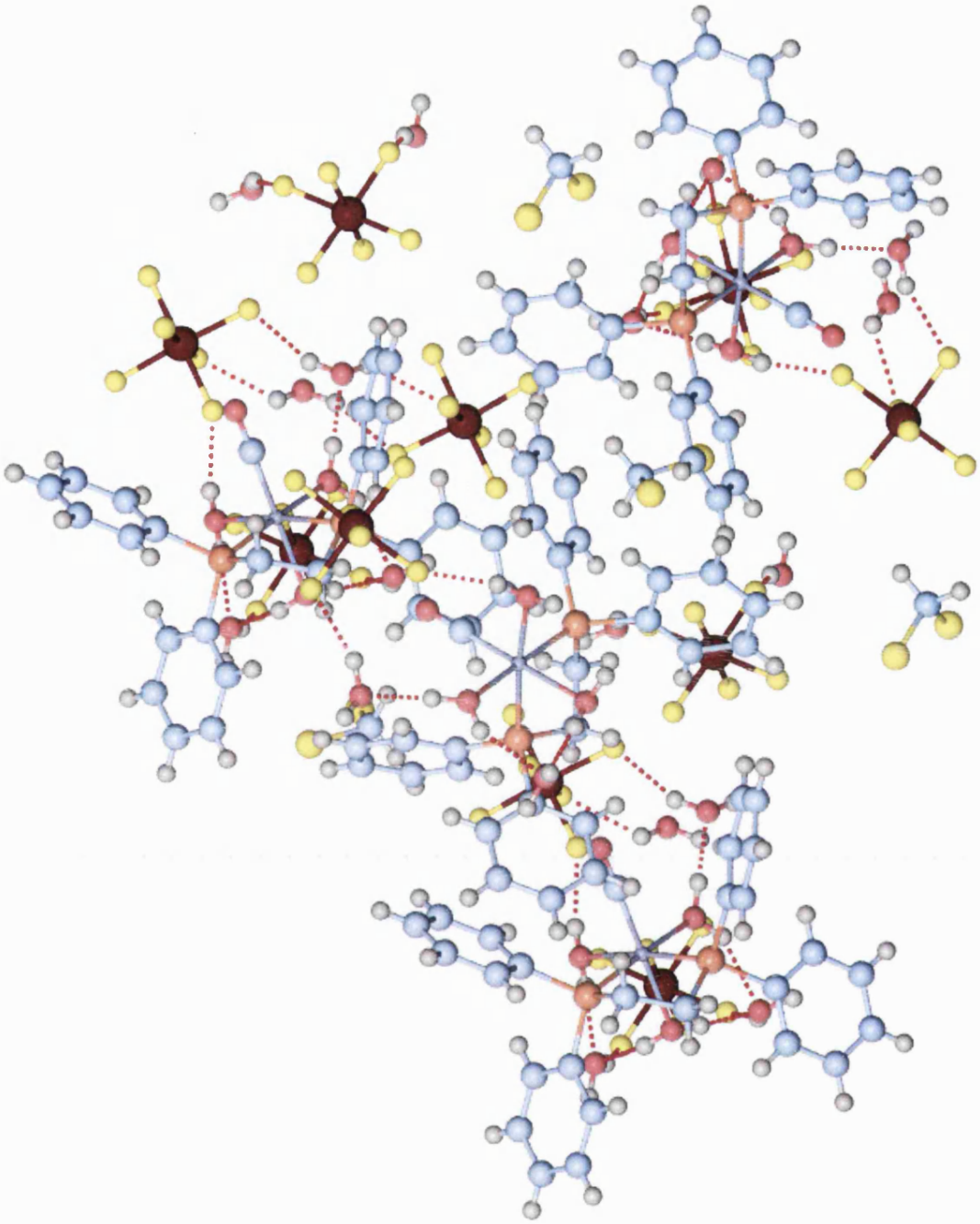

Figure 2.20: *Crystal packing diagram for* ***4c.***

2.11 Cation-anion interactions in solution

Preliminary Pulsed Gradient Spin-Echo (PGSE) experiments have been performed in collaboration with Professor Paul Pregosin (ETH, Zurich) to establish the extent of the interaction between $[Ru(dppe)(CO)(H_2O)_3]^{2+}$ and OTf^-, BF_4^- and SbF_6^- in solution. Spin echo is a relatively old NMR technique but has found little application in organometallic chemistry. Valentini et al[28] have conducted ^1H and ^{19}F PGSE experiments on a selection of cationic ruthenium(II) arene complexes (***Figure 2.21)*** in order to determine relative molecular size in solution. This is achieved by measuring diffusion coefficients ***D*** of the both the cation and the anion. Similar values of ***D*** for both cation and anion imply that hydrogen bonding exists between the two species.

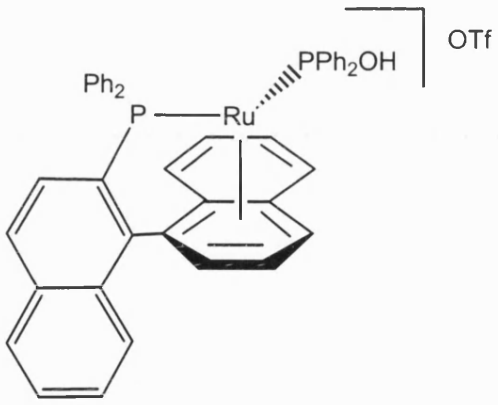

Figure 2.21: *Ruthenium(II) arene complex.*

In the ruthenium arene system shown in the figure, hydrogen bonding occurs via the $P(OH)Ph_2$ ligand to the anion.[29]

The results from the experiments conducted with $[Ru(dppe)(CO)(H_2O)_3]^{2+}$ and OTf^-, BF_4^- and SbF_6^- are given in ***Table 2.6***.

Anion	Solvent	^{1}H $\boldsymbol{D}$ (10^{-10} m^2s^{-1})	^{19}F $\boldsymbol{D}$ (10^{-10} m^2s^{-1})
OTf^-	D_2O	3.47	9.25
BF_4^-	D_2O	3.44	15.29
SbF_6^-	D_2O	3.30	
OTf^-	Acetone/H_2O	9.24	15.58
BF_4^-	Acetone/H_2O	9.36	19.88
SbF_6^-	Acetone/H_2O	9.95	

Table 2.6: *The diffusion coefficients* ***D*** *from* ^{1}H *and* ^{19}F *NMR for two solvent systems of* $[Ru(dppe)(CO)(H_2O)_3]^{2+}$.

The results indicate that OTf^- and BF_4^- behave similarly, whereas the faster diffusion of the SbF_6^- complex suggests it is more isolated thus possibly explaining the differences in water solubility. Also taking into account the ***D*** values for the anions (by ^{19}F NMR) in acetone/water were smaller than we expected. This suggests that hydrogen bonding interactions are occurring between anion and cation. The data suggest two particular things:

(a) comparison of D_2O and acetone/H_2O as solvents revealed different behaviour of the cations. Due to differences in solvent viscosity, the value of ***D*** in acetone/water should be 3.3 greater than that in water. For OTf^-, one calculated a diffusion coefficent of 3.47 x 3.3 = 11.45 which compares to the experimentally determined value of 9.24. This implies that different behaviour is occurring for OTf^- (and BF_4^-) in water and acetone/water solutions.

(b) In acetone/water, the diffusion coefficent for $[Ru(dppe)(CO)(H_2O)_3][SbF_6]_2$

(i.e. ***D*** for the cationic fragment) is higher for SbF_6^- than for OTf^- and BF_4^- (9.95 vs. 9.24 and 9.36). This implies that the cation is moving faster and is thus more isolated (less interaction with the anion).

2.12 Conclusion

As we have seen, four new organometallic aqua complexes of ruthenium(II) have been prepared and characterised. All have been prepared by the facile substitution of carbonyl and triflate groups from $Ru(dppe)(CO)_2(OTf)_2$ (**2**). The formation of **4a-c**, $[Ru(dppe)(CO)(H_2O)_3][X]_2$ ($X= OTf^-, BF_4^-$ or SbF_6^-) involved the substitution of CO by H_2O, which was unexpected, but was also seen for $[Ru(dppe)(CO)_2(OTF)_2]$, in the solid state which afforded $[Ru(dppe)(CO)(H_2O)(OTf)_2]$.

Hydrogen bonding is vital to the solid state structures of the tris-aquas, and all show complex patterns of hydrogen bonding between the cations and anions and also lattice water. The solution reactivity of the tris-aquas will be described in detail in the next chapter.

2.13 References

1. Kölle, U. *Coord. Chem. Rev.* **1994**, *135-6*, 623.
2. Makihara, N; Ogo, S; Watanabe, Y. *Organometallics* **2001**, *20*, 497.
3. Alberto, R.; Schibili, R.; Egli, A.; Schubiger, A. P. *J. Am. Chem. Soc.* **1998**, *120*, 7987.
4. Coe, B. J.; Glenwright, S. J. *Coord. Chem. Rev.* **2000**, *203*, 5.
5. Jørgensen, C. K. *Inorg. Chem.* **1964**, *3*, 1201.
6. Dell'Amico, D. B.; Calderazzo, F.; Grazzini, A.; Labella, L.; Marchetti, F. *Inorg. Chim. Acta.* **2002**, *334*, 411.
7. Barnard, C. F. J. D. Phil Thesis, University of York, York, UK, **1978**.
8. Taylor, A. J. D. Phil Thesis, University of York, York, UK, **1993**.
9. Beck, W.; Sünkel, K. *Chem. Rev.* **1988**, *88*, 1405.
10. Mahon, M. F.; Whittlesey, M. K.; Wood, P. T. *Organometallics.* **1999**, *18*, 4068.
11. Stang, P. J.; Huang. Y.; Arif, A. M. *Organometallics* **1992**, *11*, 231.
12. Lawrance, G. A. *Chem. Rev.* **1986**, *86*, 17.
13. Bailey, O. H.; Ludi, A. *Inorg. Chem.* **1985**, *24*, 2582.
14. Harding, P. A.; Robinson, S. P.; Henrick, K. *J. Chem. Soc, Dalton. Trans.* **1988**, 415.
15. Gargulak, J. D.; Berry, A. J.; Noirot, M. D.; Gladfelter, W. L. *J. Am. Chem. Soc.* **1992**, *23*, 8933.
16. Gargulak, J. D.; Gladfelter, W. L. *Inorg. Chem.* **1994**, *33*, 253.
17. Blosser, P. W.; Gallucci, J. D.; Wojcicki, A. *Inorg. Chem.* **1992**, *31*, 2376.
18. Svetlanova-Larsen, A.; Zoch, C. R.; Hubbard, J. L. *Organometallics* **1996**, *15*, 3076.
19. Bergamini, P.; DeBiani, F. F.; Marvelli, L.; Mascellani, N.; Peruzzini, M.; Rossi, R.; Zanello, P. *New. J. Chem.* **1999**, 207.
20. Svetlanova-Larsen, A.; Hubbard, J. L. *Inorg. Chem.* **1996**, *35*, 3073.

21. Pauling, L. *The Nature of the Chemical Bond*, 3rd edn.; Cornell University Press: Ithaca, NY, **1960**.

22. Mallory, F. B.; Mallory, C. W.; Butler, K. E.; Lewis, M. B.; Xia, A. Q.; Luzik, E. D.; Fredenburgh, L. E.; Ramanjulu, M. M.; Van, Q. N.; Francl, M. M.; Freed, D. A.; Wray, C. C.; Hann, C.; Nerz-Stormes, M.; Carroll, P. J.; Chirlian, L. E. *J. Am. Chem. Soc.* **2000**, *122*, 4108.

23. Gemel, C.; Folting. K.; Caulton, K. G. *Inorg. Chem.* **2000**, *39*, 1593.

24. Ernest, L.; Ibron, K. *Angew. Chem., Int. Ed. Engl.* **1995**, *34*, 1881.

25. Kickham, J. E.; Loeb, S. J. *Inorg .Chem.* **1995**, *34*, 5656.

26. Bauer, H.; Nagel, U.; Beck, W. *J. Organomet. Chem.* **1985**, *290*, 219.

27. Tahiri, A.; Guerchais, V.; Toupet, L.; Lapinte, C. *J. Organomet. Chem.* **1990**, *381*, C47.

28. Stout, G. H.; Jensen, L. H. *X-ray Structure Determination: A Practical Guide.*; Mcmillan Publishing, NY, **1968**, 303.

29. Valentini, M.; Pregosin, P. S.; Rüegger, H. *J. Chem. Soc, Dalton Trans.* **2000**, 4507.

30. Valentini, M.; Pregosin, P. S.; Rüegger, H. *Helv. Chim. Acta.* **2001**, *84*, 2833.

Chapter 3

Solution reactivity studies of

$[Ru(dppe)(CO)(H_2O)_3][X]_2$

($X = OTf^-, BF_4^-$ and SbF_6^-)

3.1 Introduction

The X-ray crystal structure determinations of $[Ru(dppe)(CO)(H_2O)_3][X]_2$ (X = OTf^- (**4a**), BF_4^- (**4b**) and SbF_6^- (**4c**)) display a stereochemistry containing a *fac*-$Ru(H_2O)_3$ moiety with two different types of ligand (two *trans* to P, one *trans* to CO). This affords the possibility of studying *trans* effects of P and CO on the lability of these coordinated waters. Prior to embarking on kinetic work and studies aimed at establishing potential catalytic applications, we set out to elucidate the types of products that may be formed in reactions with a range of incoming ligands. We have found that both mono and bi-nuclear Ru^{II} complexes can be formed upon substitution of either two or all three water ligands.

3.2 Solubility of 4 a-c

As mentioned in the previous chapter, attempts to find an appropriate solvent in which to study the reactions of $[Ru(dppe)(CO)(H_2O)_3][OTf]_2$ (**4a**) initially caused some problems. The complexes **4a**, **4b** and **4c** were not stable in chlorinated solvents and similarly did not remain intact in acetone, where a number of products believed to be mixed acetone-water adducts were formed. This was shown clearly by $^{31}P\{^1H\}$ NMR spectroscopy as a number of doublet resonances demonstrated that the integrity of the *fac*-$Ru(H_2O)_3$ unit had been lost. However, upon addition of ten equivalents of water to this mixture of species in acetone solution, **4a** was the only species observed. Hence, unless stated, all of the following reactions were performed in acetone/water mixtures. For complexes **4b** and **4c**, reactions were performed in water alone, unless otherwise stated.

3.3 Reaction of $[Ru(dppe)(CO)(H_2O)_3][OTf]_2$ (4a) with monodentate ligands (L $=CH_3CN$, $(CH_3)_2SO$, Me_3CNC, C_5H_5N)

Dissolution of **4a** in the coordinating solvents CH_3CN or $(CH_3)_2SO$ leads to facile substitution of all three coordinated water ligands (***Equation 3.1***) and formation of $[Ru(dppe)(CO)(CH_3CN)_3][OTf]_2$ (**5a**) and $[Ru(dppe)(CO)(CH_3)_2SO)_3][OTf]_2$ (**6a**) respectively, which have been characterised by NMR spectroscopy, elemental analysis and X-ray crystallography. The $^{31}P\{^1H\}$ NMR spectra of **5a** and **6b** show only singlet resonances in accord with a *fac* arrangement of the coordinating solvent molecules as in **4a** (however this alone is not conclusive as *bis*-substitution could have occurred *trans* to the phosphine ligand).

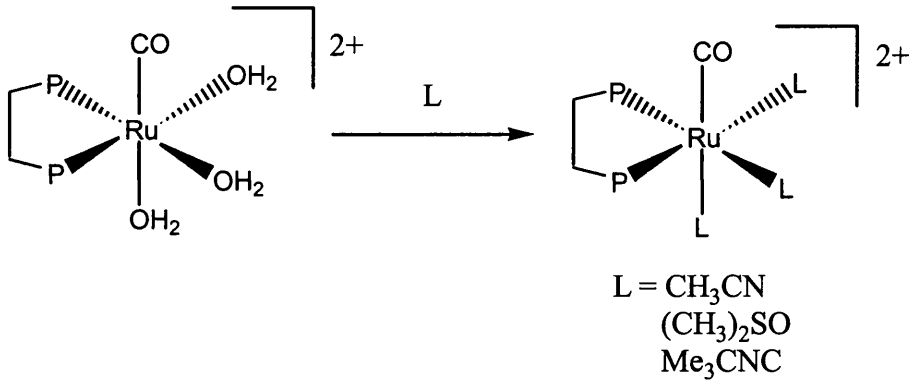

Equation 3.1: *General reaction equation representing tris-substitution.*

3.4 Reaction of $[Ru(dppe)(CO)(H_2O)_3][OTf]_2$ (4a) with CH_3CN

Dissolution of **4a** in neat CD_3CN led to an immediate reaction, as evidenced by the formation of a coloured solution. $^{31}P\{^1H\}$ NMR spectroscopy showed the formation of one species which appeared as a singlet at δ 62.3 and which was identified as $[Ru(dppe)(CO)(CH_3CN)_3][OTf]_2$ (**5a**). A repeat of the reaction in CH_3CN and dissolution of the resulting product in d^6-acetone produced two CH_3CN signals in both the ^1H and $^{13}C\{^1H\}$ NMR spectra. The ^1H NMR spectrum showed two methyl singlet resonances at δ 2.78 and 2.00 which integrated in a 2:1 ratio. This is consistent with the $^{13}C\{^1H\}$ NMR spectrum, which displayed the methyl singlet resonances at δ 3.5 and 2.2. A triplet carbonyl resonance appeared at δ 194.1 (J_{PC} = 16.1 Hz). In the ^{19}F NMR spectrum, there was a sharp singlet resonance at δ – 79.2, corresponding to non-coordinated triflate anions. The IR spectrum of **5a** exhibited two ν_{CN} stretches at 2324 and 2294 cm^{-1},[1] while the carbonyl band appeared 30 cm^{-1} higher than that in **4a** at 2020 cm^{-1} reflecting the poorer donor ability of the acetonitrile ligands relative to that of water.

Removal of the solvent and dissolution of **5a** in $CHCl_3$ solution doped with three equivalents of CH_3CN and layered with diethyl ether produced colourless crystals of analytically pure material, which were suitable for X-ray crystallography. A plot representing the asymmetric unit in the X-ray structure of **5a** (***Figure 3.1***) demonstrates the expected octahedral coordination geometry about the ruthenium centre. Selected bond distances [Å] and angles [°] are given in ***Table 3.1***.

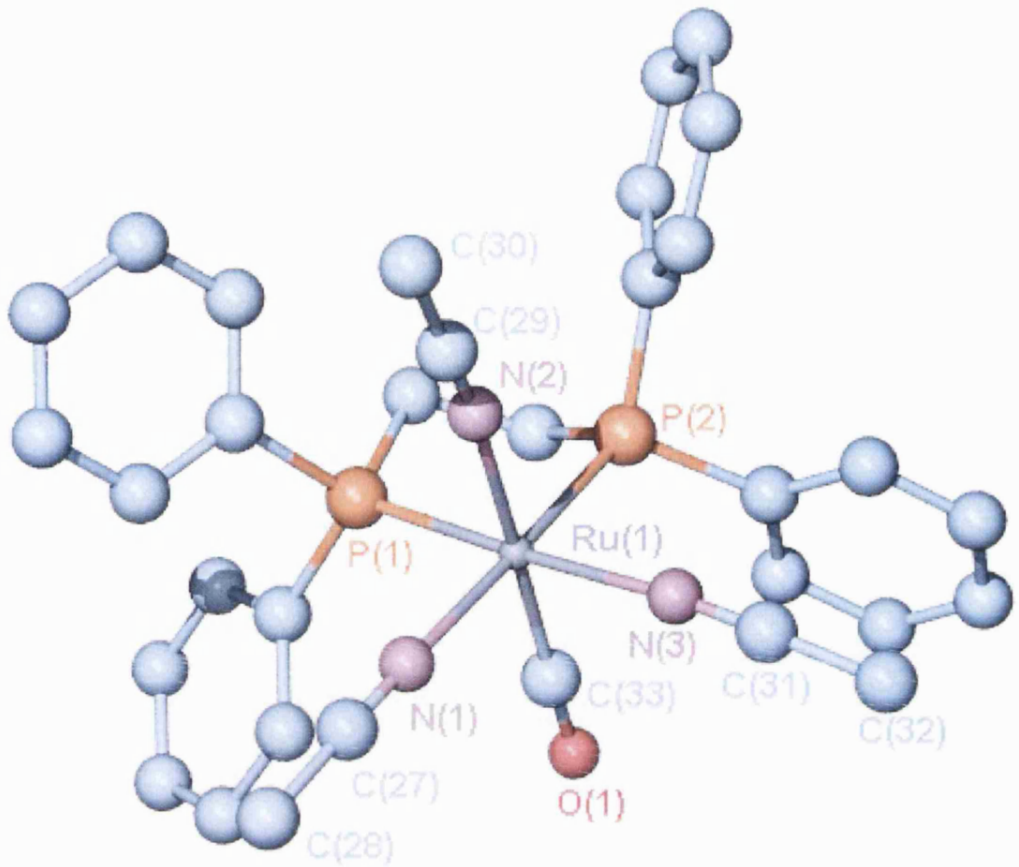

Figure 3.1: *Plot of* $[Ru(dppe)(CO)(CH_3CN)_3][OTf]_2.2CHCl_3$ ***(5a)***.

Ru(1)-C(33)	1.870(3)	Ru(1)-N(2)	2.095(3)
Ru(1)-N(1)	2.107(3)	Ru(1)-N(3)	2.116(3)
Ru(1)-P(1)	2.3098(8)	Ru(1)-P(2)	2.3115(9)

C(33)-Ru(1)-N(3)	90.04(11)	C(33)-Ru(1)-N(2)	176.18(12)
C(33)-Ru(1)-N(1)	93.59(12)	N(2)-Ru(1)-N(1)	83.10(10)
N(1)-Ru(1)-N(3)	89.70(10)	N(2)-Ru(1)-N(3)	88.06(10)
P(1)-Ru(1)-P(2)	84.49(3)		

Table 3.1: *Selected bond lengths [Å] and angles [°] for* $[Ru(dppe)(CO)(CH_3CN)_3][OTf]_2.2CHCl_3$ ***(5a)***.

The coordination geometry of $[Ru(dppe)(CO)(CH_3CN)_3][OTf]_2$ is approximately octahedral, with the average angle at ruthenium being close to 90°. All three Ru-N distances are similar, although the average value (2.106(3) Å) is considerably longer than the average Ru-N distances found in the related ruthenium(II) complexes, $[Ru(CH_3CN)_6]^{2+}$ (2.028(1) Å),[2] $[(\eta^5\text{-}C_5H_5)Ru(CH_3CN)_3]^+$ (2.083(1) Å)[3] or $[TpRu(CH_3CN)_3]^+$ (2.045(7) Å)[4] (Tp = hydridotris(pyrazolyl)borate). This is an indication that d → π* bonding is much less important in **5a** than in these three other reported cases, a fact that is further supported by the high frequency of the ν_{CN} IR absorption bands. The crystal structure of **5a** contains discrete Ru^{II} cations, two triflate anions and solvent molecules. There is evidence for C-H···O interactions using the criteria of Desiraju.[5] Thus, in the lattice array, the cation is linked to both of the OTf^- anions via weak C-H···O interactions involving hydrogens in two of the bound acetonitrile groups (C(28)-H(28A)...O(4) = 3.56 Å, C(32)-H(32B)...O(6) = 3.29 Å). The average Ru-P bond length is 2.130(8) Å and the phosphine bite angle is 84.49(3)°. Complex **5a** has a Ru-CO bond length of 1.870(3) Å, which is longer than that of **4a** at 1.833(3) Å. Compound **5a** can also be made by dissolution of **2** in neat CH_3CN, however the reaction is slower than the analogous reaction using **4a**. Compound **5a** also proved to be unstable in neat chlorinated solvents (CD_2Cl_2 or $CDCl_3$) as evidenced by $^{31}P\{^1H\}$ NMR spectroscopy (***Figure 3.2***). Complex **5a** was present as a singlet resonance at δ 62.2 but also with an unknown species represented by a pair of doublets at δ 69.7 and 59.2 (J_{PP} = 15.7 Hz). However addition of three equivalents of CH_3CN reformed **5a** as the only species seen in solution.

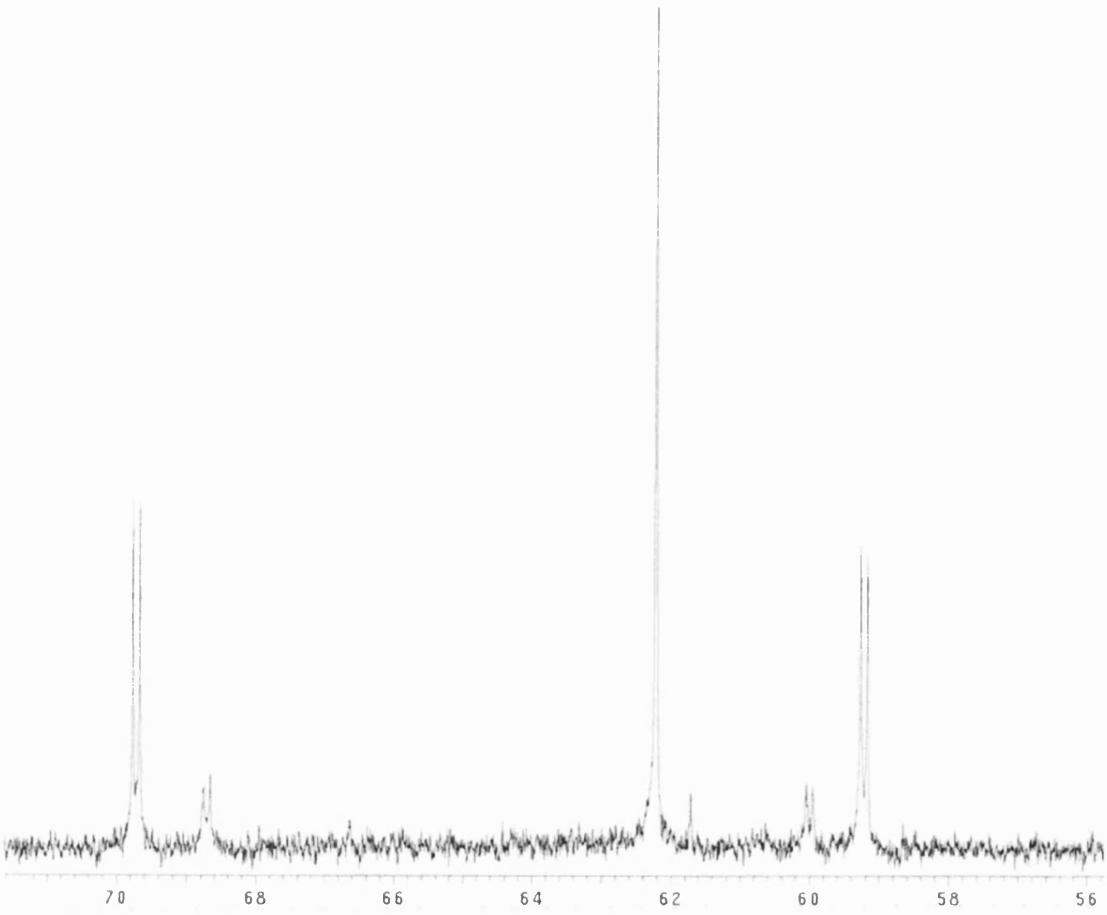

Figure 3.2: *$^{31}P\{^{1}H\}$ NMR (162MHz) spectrum of* ***5a*** *recorded in $CDCl_3$.*

The reaction of $[Ru(dppe)(CO)(H_2O)_3][BF_4]_2$ (**4b**) with CH_3CN formed $[Ru(dppe)(CO)(CH_3CN)_3][BF_4]_2$ (**5b**). The NMR and IR spectroscopic data were identical to that of **4a** as the same cationic fragment is present, $[Ru(dppe)(CO)(CH_3CN)_3]^{2+}$.

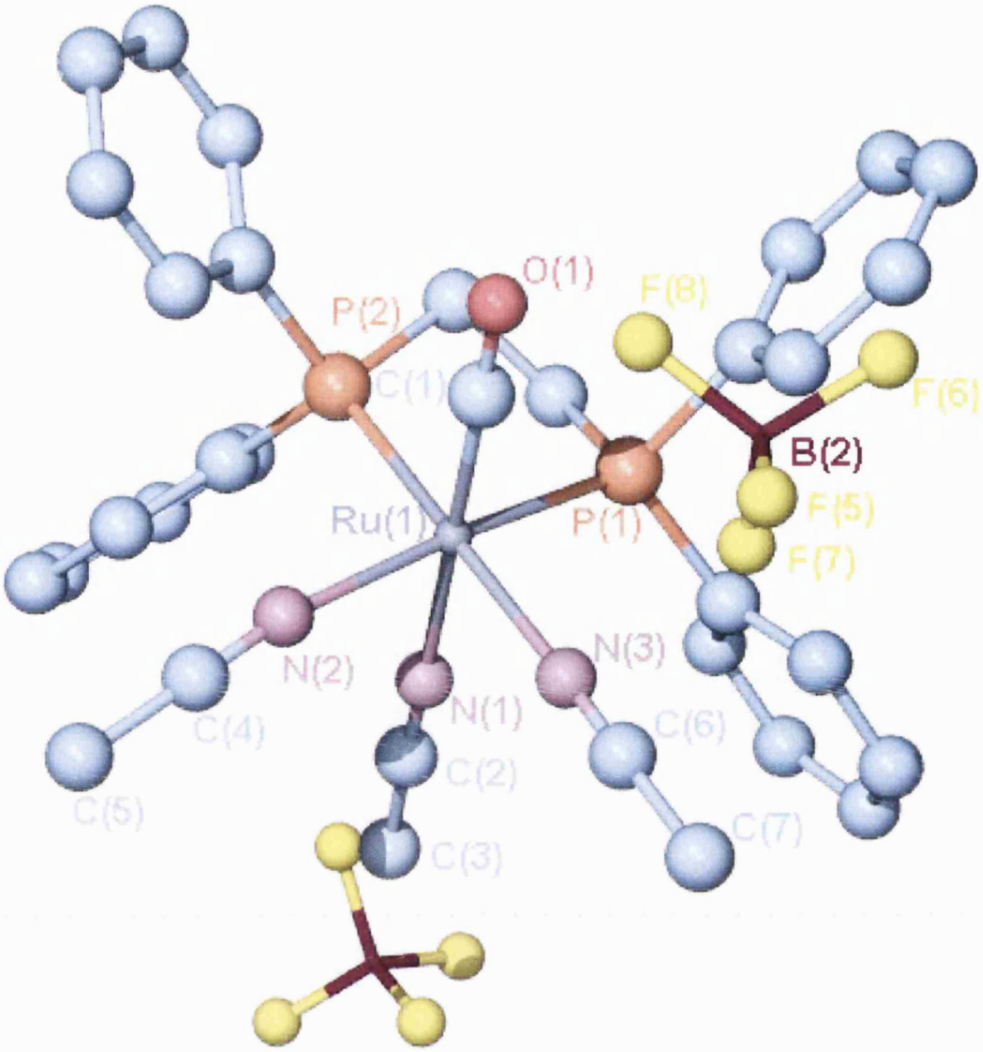

Figure 3.3: *Plot of* [Ru(dppe)(CO)(CH_3CN)$_3$][BF_4] 0.5 *(CH_3)$_2$CO* ***(5b)***.

Ru(1)-C(1)	1.864(2)	C(1)-O(1)	1.130(3)
Ru(1)-N(1)	2.085(5)	Ru(1)-N(2)	2.111(2)
Ru(1)-N(3)	2.115(2)	Ru(1)-P(1)	2.3175(6)
Ru(1)-P(2)	2.3195(6)		

C(1)Ru(1)-N(1)	177.75(13)	P(1)-Ru(1)-P(2)	84.92(2)
C(1)-Ru(1)-N(2)	95.24(10)	C(1)-Ru(1)-N(3)	94.04(9)
N(1)-Ru(1)-N(2)	86.46(10)	N(2)-Ru(1)-N(3)	85.55(8)

Table 3.2: *Selected bond lengths [Å] and angles [°] for [Ru(dppe)(CO)(CH$_3$CN)$_3$][BF$_4$]$_2$. 0.5 (CH$_3$)$_2$CO (**5b**).*

Crystals suitable for X-ray determination were grown from an acetone solution of **5b** doped with 3 equivalents of CH_3CN and layered with diethyl ether. A plot of **5b** is shown in ***Figure 3.3***, and selected bond lengths [Å] and angles [°] are given in ***Table 2***. No real effect of the change of anion from OTf^- to BF_4^- was seen in the structural features of the $[Ru(dppe)(CO)(CH_3CN)_3]^{2+}$ dication. The average Ru-N bond length of 2.103(3) Å is comparable to that in **5** of 2.106(3) Å as would be expected.

3.5 Reaction of 4a with $(CH_3)_2SO$ to yield $[Ru(dppe)(CO)((CH_3)_2SO)_3][OTf]_2$ (6a)

The $^{31}P\{^1H\}$ NMR spectrum recorded minutes after dissolution of **4a** in neat d^6 $(CH_3)_2SO$ showed no residual starting material was present and indicated the formation of a single new species as evidenced by the appearance of a singlet resonance at δ 64.7. This was assigned to the tris-$(CH_3)_2SO$ complex $[Ru(dppe)(CO)((CH_3)_2SO)_3]^{2+}$. The ^1H NMR spectrum displayed the two expected methyl singlet resonances at δ 3.34 and δ 2.99 in a ratio of 2:1. The ^{19}F NMR spectrum yielded a sharp singlet at –79.33 for free triflate. The

$^{13}C\{^{1}H\}$ NMR spectrum showed a triplet carbonyl resonance at δ 199.1 (J_{PC} = 17.4 Hz) but, at higher field, it was not possible to conclusively assign the methyl peaks for the coordinated $(CH_3)_2SO$ ligands. A single carbonyl band was detected at 1973 cm^{-1} in the IR spectrum but it was not possible to assign from the infra-red spectrum whether the $(CH_3)_2SO$ ligands were O and/or S bound to the metal. Alessio et al[6,7] have reported that O bound $(CH_3)_2SO$ appears around 900 cm^{-1} while S bound $(CH_3)_2SO$ comes around 1100 cm^{-1}. The IR spectrum of **6a** showed no discernable bands in either region. Removal of the solvent and recrystalisation of the residue from acetone with three equivalents of $(CH_3)_2SO$ and layered with diethylether produced large yellow cubed crystals of **6a**, which were suitable for X-ray crystallography. ***Figure 3.4*** represents the asymmetric unit cell of **6a**, with the relevant bond angles [°] and distances [Å] given in ***Table 3.3***.

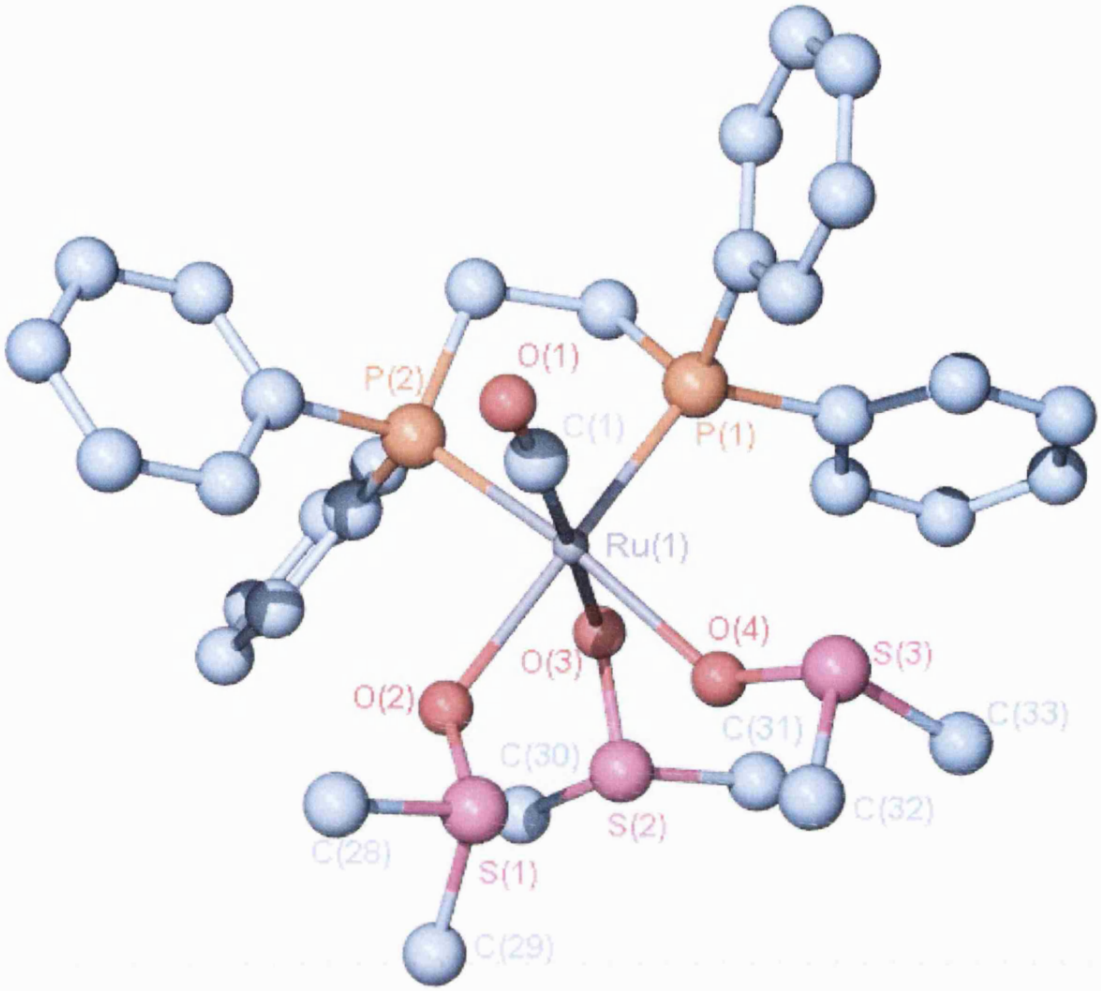

Figure 3.4: *Plot of [Ru(dppe)(CO)((CH$_3$)$_2$SO)$_3$][OTf]$_2$.2 CHCl$_3$ (**6a**).*

Ru(1)-C(1)	1.831(2)	Ru(1)-O(3)	2.1353(16)
Ru(1)-O(4)	2.1524(17)	Ru(1)-O(2)	2.1808(17)
Ru(1)-P(2)	2.2866(5)	Ru(1)-P(1)	2.2941(6)

C(1)-Ru(1)-O(3)	176.18(9)	C(1)-Ru(1)-O(4)	103.35(10)
O(3)-Ru(1)-O(4)	80.47(7)	C(1)-Ru(1)-O(2)	95.20(9)
O(3)-Ru(1)-O(2)	85.21(7)	O(4)-Ru(1)-O(2)	83.48(7)
C(1)-Ru(1)-P(2)	88.07(8)	O(3)-Ru(1)-P(2)	88.12(4)
O(4)-Ru(1)-P(2)	168.00(5)	O(2)-Ru(1)-P(2)	91.93(5)
C(1)-Ru(1)-P(1)	91.06(8)	O(3)-Ru(1)-P(1)	88.33(5)
O(4)-Ru(1)-P(1)	98.25(6)	O(2)-Ru(1)-P(1)	172.94(5)
P(2)-Ru(1)-P(1)	85.03(2)		

Table 3.3: *Selected bond lengths [Å] and angles [°] for* *[Ru(dppe)(CO)((CH$_3$)$_2$SO)$_3$][OTf]$_2$* ***(6a)****.*

As expected in a cationic ruthenium complex, all three $(CH_3)_2SO$ ligands are oxygen bound to the metal with Ru-O bond lengths in the range of 2.13-2.18 Å. Although O-bonded $(CH_3)_2SO$ is sterically less demanding than *S*-bonded $(CH_3)_2SO$,[7] the cation in **6a** is still subject to steric crowding in the metal coordination sphere, as reflected by the large Ru-O-S angles of the equatorial $(CH_3)_2SO$ ligands (121.8 and 131.4°) relative to the axial bound group (118.5°). One of the triflate anions shows an interaction with the hydrogens on one of the $(CH_3)_2SO$ ligands (C(28)-H(28A)...O(7) = 3.54 Å). The Ru-C carbonyl bond length is 1.831(2) Å which is comparable to that seen in **4a** where the ruthenium-carbonyl (Ru-C) bond length is 1.833(3) Å, both of which are significantly shorter than that seen for **5a**, where the comparable distance is 1.870(3) Å. This can be explained in terms of σ-donor ability and metal carbonyl back bonding. CH_3CN is a worse σ-donor than both H_2O and $(CH_3)_2SO$. This is confirmed by comparing the C-O bond lengths and

the infrared carbonyl stretching frequencies. **4a** and **6a** exhibit C-O bond lengths of 1.145(3) and 1.148(3) Å respectively, whereas the C-O bond length in **5a** is a lot shorter at 1.135(4). The shorter bond C-O bond seen in **5a** is consistent with a ν_{CO} band at 2020 cm^{-1} compared to 1990 cm^{-1} for **4a** and 1973 cm^{-1} for **6a** (shortest C-O bond length). The coordinated $(CH_3)_2SO$ ligand *trans* to CO has a significantly shorter Ru-O(3) bond length (2.1353(6)) than the two coordinated $(CH_3)_2SO$ ligands which are *trans* to phosphorus and have under gone a *trans*-labilising effect (Ru-O(4), 2.1524(17) and Ru-O(2), 2.1808(17) Å).

As with **3a** and **4a**, compound **6a** proved to be unstable in the absence of $(CH_3)_2SO$. Dissolution of a solid sample of **6a** in either $CDCl_3$ or acetone required the presence of at least 3 equivalents of $(CH_3)_2SO$ to stabilise it in solution.

3.6 Reaction of $[Ru(dppe)(CO)(H_2O)_3][OTf]_2$ (4a) with Me_3CNC to yield $[Ru(dppe)(CO)(CNCMe_3)_3][OTf]_2$ (7a)

The reaction of **4a** with excess Me_3CNC was also found to lead to the substitution of all three water ligands by the isocyanide affording $[Ru(dppe)(CO)(CNCMe_3)_3][OTf]_2$ (**7a**). The $^{31}P\{^1H\}$ NMR spectrum displayed a singlet resonance at δ 52.4 and, the ^1H NMR spectrum showed the coordinated Me_3CNC ligands at δ 1.79 and 1.05 in a 2:1 ratio respectively. The $^{13}C\{^1H\}$ NMR spectrum displayed Me_3CNC singlet resonances at δ 62.2, 61.6, and δ 30.0, 29.2. The IR spectrum of **7a** displayed a single carbonyl band at considerably higher frequency (2071 cm^{-1}) than found for either **5a** or **6a**, and two, ν_{CN} stretches at 2233 and 2212 cm^{-1}. Analytically pure crystals of **7a** suitable for X-ray determination were grown, from the reaction mixture by layering with diethyl ether (***Figure 3.5***). Selected bond lengths [Å] and angles [°] for $[Ru(dppe)(CO)(CNCMe_3)_3][OTf]_2.(CH_3)_2CO$ (**7a**) are given in ***Table 3.4***.

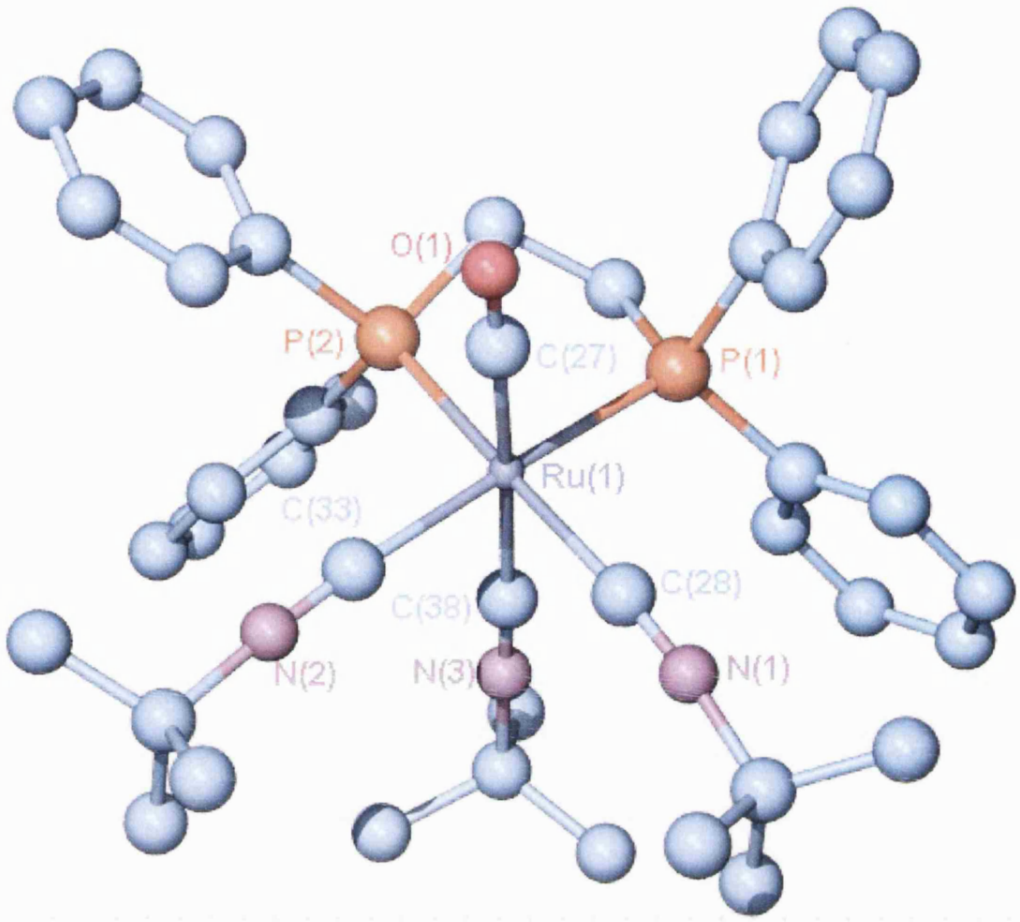

Figure 3.5: *Plot of [Ru(dppe)(CO)(CNCMe$_3$)$_3$][OTf]$_2$.(CH$_3$)$_2$CO (**7a**).*

Ru(1)-C(27)	1.937(3)	Ru(1)-C(28)	2.030(3)
Ru(1)-C(38)	2.041(3)	Ru(1)-C(33)	2.025(3)
Ru(1)-P(1)	2.3660(7)	Ru(1)-P(2)	2.3583(7)
C(28)-N(1)	1.141(4)	C(33)-N(2)	1.140(4)
C(38)-N(3)	1.140(4)	C(27)-O(1)	1.121(4)

C(27)-Ru(1)-C(33)	91.33(14)	C(27)-Ru(1)-C(28)	94.31(12)
C(33)-Ru(1)-C(28)	88.76(12)	C(27)-Ru(1)-C(38)	177.42(12)
C(33)-Ru(1)-C(38)	86.09(13)	C(28)-Ru(1)-C(38)	85.60(12)
C(27)-Ru(1)-P(2)	90.36(9)	C(33)-Ru(1)-P(2)	94.91(9)
C(28)-Ru(1)-P(2)	173.99(8)	C(38)-Ru(1)-P(2)	89.90(8)
C(27)-Ru(1)-P(1)	92.84(10)	C(33)-Ru(1)-P(1)	175.79(10)
C(28)-Ru(1)-P(1)	91.51(8)	C(38)-Ru(1)-P(1)	89.74(8)
P(2)-Ru(1)-P(1)	84.48(3)		

Table 3.4: *Selected bond lengths [Å] and angles [°] for* $[Ru(dppe)(CO)(CNCMe_3)_3][OTf]_2.(CH_3)_2CO$ ***(7a).***

Although the Ru-CO distance is significantly longer than the comparable distances in either **5a** or **6a** (1.937(3) vs. 1.870(3) and 1.831(2) Å), this reflects the competition between CO and the three other π-acceptor isocyanide ligands for electron density on the metal (Me_3CNC is isoelectronic to CO). The solvent of recrystallisation in **7a** acts solely as a lattice 'cement', although one of the triflate anions displays weak hydrogen bonding interactions to hydrogen atoms in one of the equatorial $CNCMe_3$ groups (C(30)-H(30C)...O(6) = 3.48 Å, C(32)-H(32B)...O(2) = 3.40 Å).

Complete substitution of all 3 waters in **4a** was not as facile as in the previous examples. Addition of excess $CNCMe_3$ to an acetone/water solution immediately gave a colourless solution. $^{31}P\{^1H\}$ NMR spectroscopy showed no remaining starting material at δ 66.5 but, instead a signal at δ 55.1. This new resonance was seen to deplete after 24

hours and was completely replaced by the singlet resonance at δ 52.4 for **7a** after 48 hours. We propose that the initial species is $[Ru(dppe)(CO)(H_2O)(Me_3CNC)_2]^{2+}$ in which the two water ligands *trans* to the dppe are readily substituted. Formation of the final product $[Ru(dppe)(CO)(Me_3CNC)_3]^{2+}$ (**7a**) occurs upon the much slower displacement of the H_2O ligand *trans* to CO. The reaction (showing stereochemistry) is summarised below in ***Scheme 3.1***.

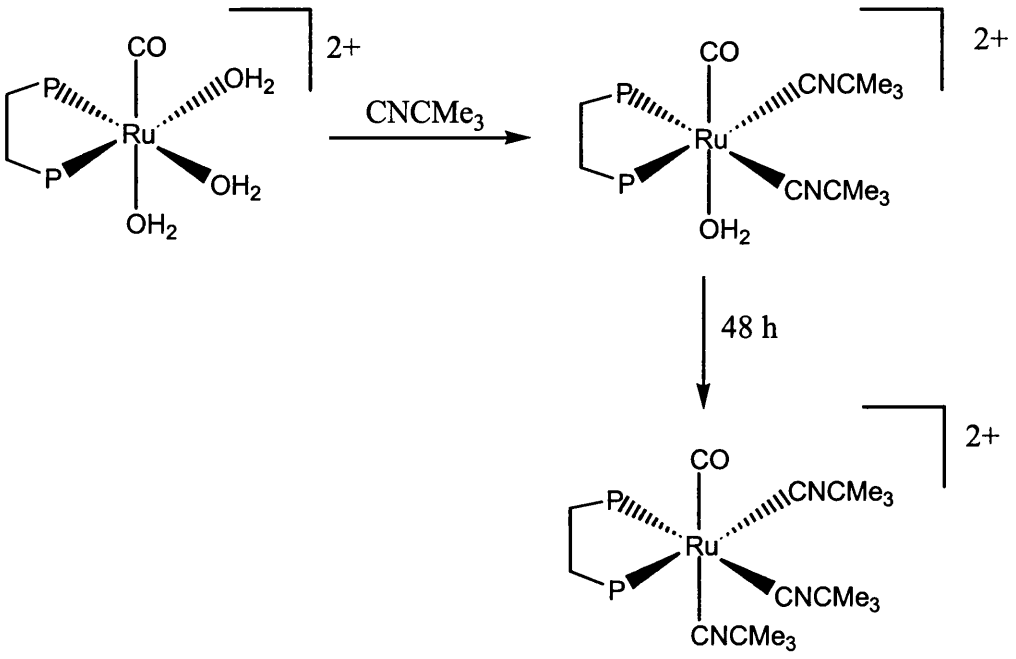

Scheme 3.1:*Formation of* ***7a*** *from reaction of* ***4a*** *with* $CNCMe_3$.

An identical reaction was seen when **4b** was reacted with Me_3CNC forming the analogous species $[Ru(dppe)(CO)(CNCMe_3)_3][BF_4]_2$, **7b**. The spectroscopic data were identical to those found for **7a**. Crystals were precipitated from the reaction mixture over night at room temperature by layering with hexane. However these crystals did not prove suitable for X-ray determination.

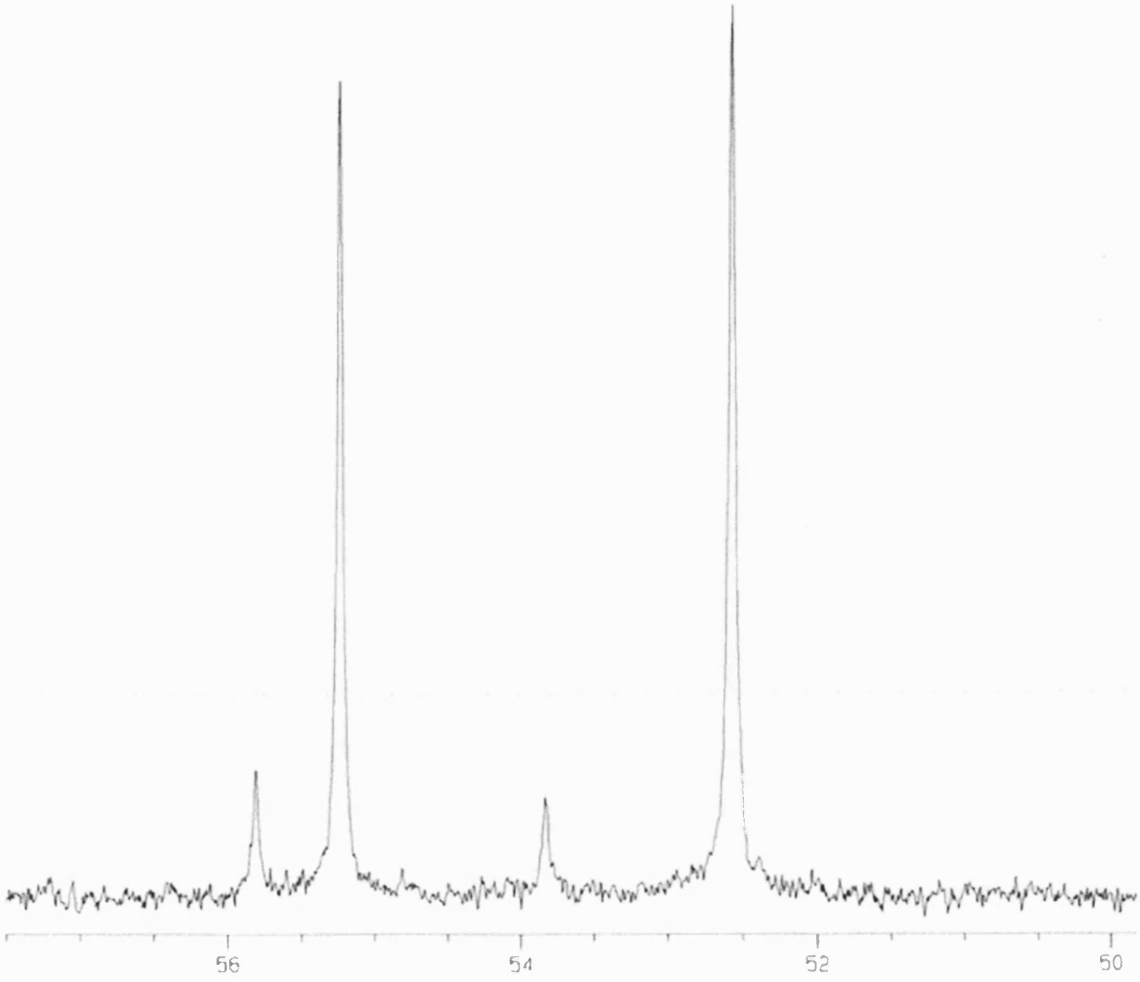

Figure 3.6: *$^{31}P\{^{1}H\}$ NMR (162 MHz) spectrum of the reaction of* ***4a*** *with Me_3CNC after 12 hours.*

3.7 Reaction of $[Ru(dppe)(CO)(H_2O)_3][OTf]_2$ (4a) with C_5H_5N to yield $[Ru(dppe)(CO)(H_2O)(C_5H_5N)_2](OTf)_2$ (8a).

Addition of 3 equivalents of C_5H_5N to an acetone/H_2O mixture of **4a** led to an immediate reaction, with a colour change being observed from pale yellow to colourless, and the appearance of a new singlet species in the $^{31}P\{^1H\}$ NMR spectrum at δ 58.1. In contrast to the isocyanide chemistry described in the preceding section, the $^{31}P\{^1H\}$ NMR spectrum in the pyridine case remained unchanged even after one week. Due to overlap of the dppe and pyridine resonances in the aromatic region of the ^1H NMR spectrum we were unable to ascertain the number of coordinated pyridine ligands. The $^{13}C\{^1H\}$ NMR spectrum showed a triplet carbonyl resonance at δ 201.4 (J_{PC} = 16.2 Hz) and this was complimented by IR (KBr) spectroscopy with a single υ_{CO} band at 1983 cm^{-1}. The extent of the substitution was elucidated by isolation of analytically pure crystals of this new species and indicated the presence of two pyridine ligands. Removal of the solvent and dissolution in $CDCl_3$ /H_2O layered with diethyl ether produced single crystals which proved suitable for X-ray crystallography. ***Figure 3.7*** shows a plot of $[Ru(dppe)(CO)(H_2O)(C_5H_5N)_2](OTf)_2$ (**8a**). Selected bond lengths [Å] and angles [°] are shown in ***Table 3.5***.

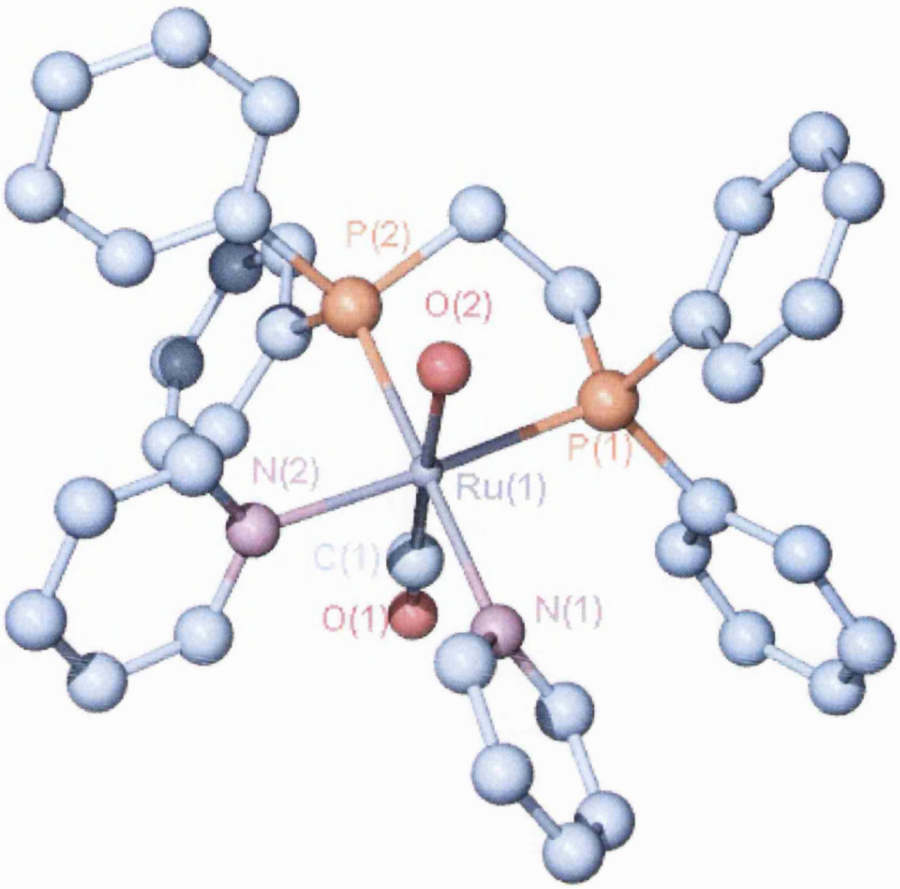

Figure 3.7: *Plot of* $[Ru(dppe)(CO)(H_2O)(C_5H_5N)_2](OSO_2CF_3)_2 \cdot 3H_2O$ ***(8a)***.

Ru(1)-O(2)	2.134(4)	O(1)-C(1)	1.143(6)
Ru(1)-C(1)	1.838(5)	Ru(1)-N(1)	2.178(4)
Ru(1)-N(2)	2.177(4)	Ru(1)-P(2)	2.3384(12)
Ru(1)-P(1)	2.3316(12)		

C(1)-Ru(1)-O(2)	177.88(17)	C(1)-Ru(1)-N(2)	95.59(17)
O(2)-Ru(1)-N(2)	84.97(14)	C(1)-Ru(1)-N(1)	88.51(18)
O(2)-Ru(1)-N(1)	89.52(16)	N(2)-Ru(1)-N(1)	84.57(14)
C(1)-Ru(1)-P(1)	88.71(14)	P(1)-Ru(1)-P(2)	84.24(4)

Table 3.5: *Selected bond lengths [Å] and angles [°] for* $[Ru(dppe)(CO)(H_2O)(C_5H_5N)_2](OSO_2CF_3)_2 \cdot 3H_2O$ ***(8a)***.

The bond lengths and angles of **8a** are unremarkable. The average Ru-P bond length is 2.313(12) Å, and the phosphine bite angle is 84.24°, which is comparable to the value found in compounds previously synthesised in this chapter. The ruthenium-oxygen water bond length (2.134(4)) is far greater than the sum of the Pauling covalent radii (1.99 Å). Within the asymmetric unit are also found three waters of recrystallisation, which are involved with the triflate anions to form a dense network of hydrogen bonding interactions within the gross structure.

Whereas in the previous substitution reactions all three of the water ligands had been substituted by the incoming ligands, the reaction with pyridine resulted in substitution of the two water ligands *trans* to dppe. Longer reaction times, heating or the addition of up to 20 equivalents of C_5H_5N did not result in substitution of the remaining axial water ligand in **8a**.

As in the previous examples, dissolution of **8a** in "dry" $CDCl_3$ forms a new singlet species by $^{31}P\{^1H\}$ NMR at δ 54.9 in addition to the resonance seen for **8a** at δ 58.1. ^{19}F NMR spectroscopy recorded two singlet resonances at δ – 79.04 and – 79.44 which can be

assigned to coordinated and free triflate respectively. Upon addition of water to the mixture, the ^{19}F NMR spectrum displayed only one singlet resonance at δ – 79.44, which is associated with uncoordinated triflate. The $^{31}P\{^{1}H\}$ NMR spectrum recorded after the addition of water displayed a singlet at δ 58.1 showing the reformation of **8a**.

Due to the initial problems of determining the extent of the substitution in the reaction of **4a** with pyridine, reactions were also performed using 2,4,6-collidine and 2,6-lutidine (***Figure 3.8***), in the hope of using the methyl groups as spectroscopic handles.

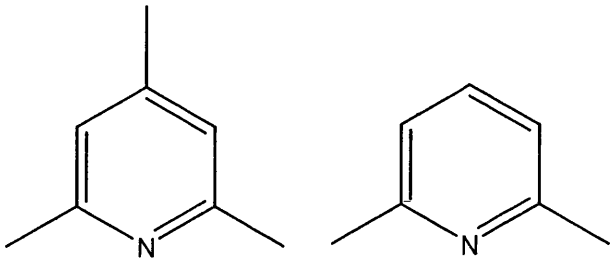

Figure 3.8: *2,4,6-collidine and 2,6-lutidine structures.*

Addition of 2,4,6-collidine or 2,6-lutidine to **4a**, although different to the pyridine pathway, gave similar reactivity patterns as each other. Upon initial addition of either reagent to acetone/water solutions of **4a**, immediate reactions occurred forming colourless solutions. The reactions were followed by $^{31}P\{^{1}H\}$ NMR which showed the appearance of a singlet species at δ 63.6 and two doublets at δ 69.6 and 66.3 (J_{PP} = 13.8 Hz) for both 2,4,6-collidine and 2,6-lutidine (***Figure 3.9***). Clearly the minor differences between 2,4,6-collidine and 2,6-lutidine (additional *p*-methyl group in 2,4,6-collidine) leads to very little effect on the NMR spectra.

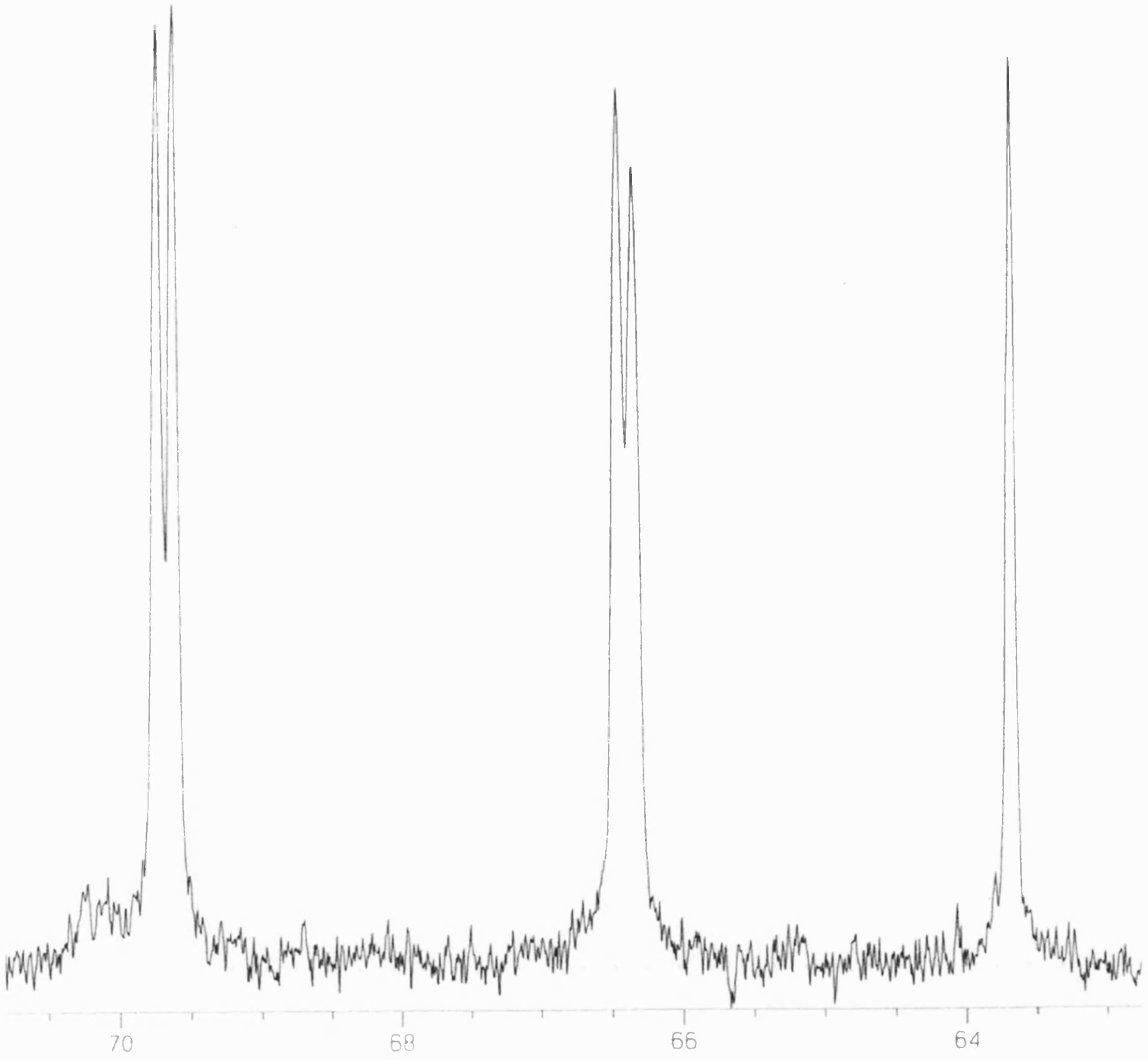

Figure 3.9: *$^{31}P\{^{1}H\}$ NMR spectrum (162 MHz) showing reaction of* ***4a*** *with 2,4,6-collidine.*

The intensity of these two species did not alter over time or after prolonged heating (with or without excess addition of ligand). Again the ^{1}H NMR spectrum did not give a clear enough indication of the number of the methyl groups to determine the symmetry around the metal centre.

3.8 Reaction of $[Ru(dppe)(CO)(H_2O)_3][OTf]_2$ (4a) with bidentate ligands L {L = 2,2'-bipyridyl (bpy) and 4,4'-dimethyl-2,2'-bipyridyl (Me_2bpy)}

Addition of 1 equivalent of 2,2'-bipyridyl (bpy) to an acetone/water solution of **4a** resulted in the rapid formation of $[Ru(dppe)(CO)(H_2O)(bpy)][OTf]_2$, **9a**, as evidenced by the appearance of a singlet in the $^{31}P\{^1H\}$ NMR spectrum at δ 58.6. This indicates that the bipyridyl ligand must be in the same plane as the bidentate phosphine. The symmetrical structure of this product was confirmed through the ^1H NMR spectrum, which showed only four pyridyl resonances as expected for an equatorial Ru(P-P)(N-N) unit. A single carbonyl stretching band was observed by IR spectroscopy at 1996 cm^{-1}.

Species **9a** readily converted over approximately 1 h at room temperature into a second species **9a'**, which displayed two doublets in the $^{31}P\{^1H\}$ NMR spectrum at δ 64.1 and 51.7 (J_{PP} = 13.1 Hz) (***Figure 3.10***).

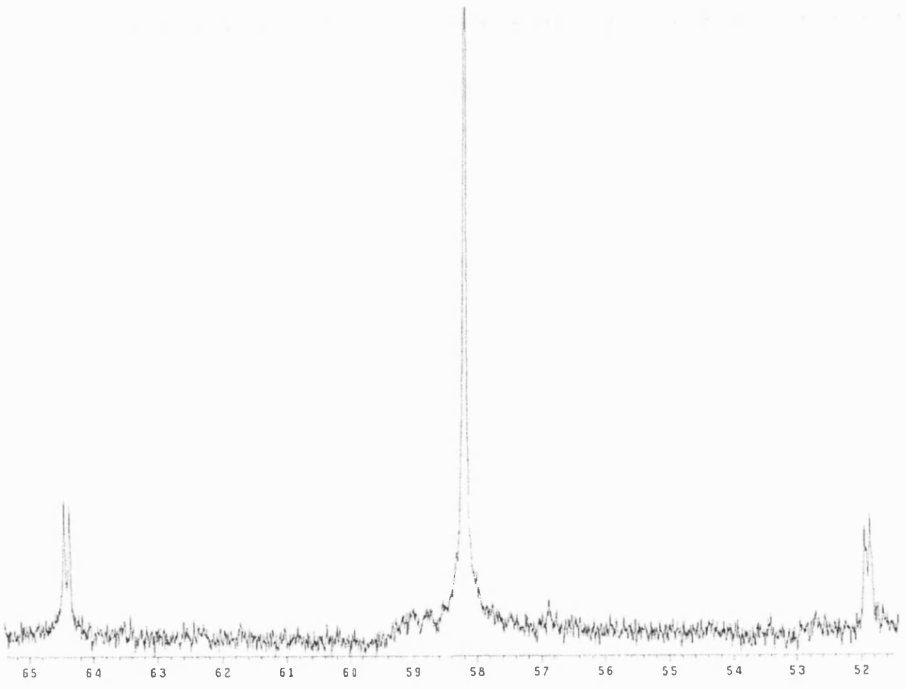

Figure 3.10: *$^{31}P\{^1H\}$ NMR spectrum (162 MHz) showing conversion of **9a** to **9a'**.*

Extensive overlap of the pyridyl and phenyl signals in the aromatic region of the ^{1}H NMR spectrum prevented **9a'** from being fully characterised (***Figure 3.11***). We were able to show by IR spectroscopy however, that **9a'** retained a CO ligand due to the presence of an intense CO stretch at 2000 cm^{-1}.

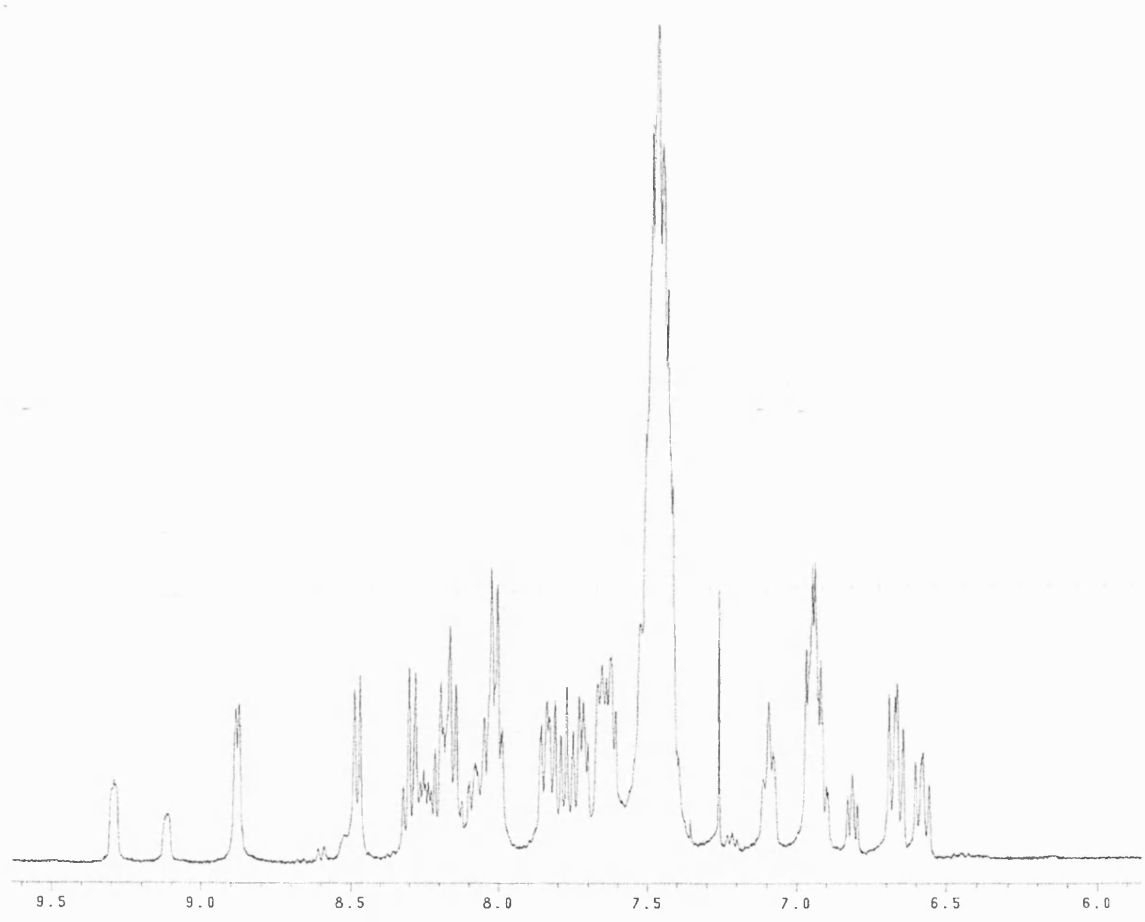

Figure 3.11: *^{1}H NMR spectrum (400 MHz) of* ***9a****, showing extensive overlap in the aromatic region.*

The reaction of **4a** with 4,4'-dimethyl-2,2'-bipyridyl (Me_2bpy) was conducted on the grounds that the methyl substituents would give a clearer spectroscopic handle as to the process responsible for converting **9a** to **9a'** and the identity of the latter. The low

temperature (258 K) ^{1}H and $^{13}C\{^{1}H\}$ NMR spectra of [Ru(dppe)(CO)(H_2O)(Me_2bpy)][$OTf]_2$, **10a**, showed only one methyl signal at δ 2.55 (***Figure 3.12***) and δ 29.2 respectively as expected for a symmetrical arrangement of the two pyridyl rings.

Conversion of **10a** to **10a'** occurred upon warming to room temperature. The ^{1}H NMR spectrum of **10a'** showed two singlet methyl resonances at δ 2.61 and 2.30 (***Figure 3.13***); the $^{13}C\{^{1}H\}$ spectrum displayed two CH_3 signals δ 21.2 and 20.7. The latter also showed a carbonyl signal at δ 199.4 (t, J_{CP} = 16.1 Hz). The size of this coupling constant implies that the CO is *cis* to the dppe ligand. The $^{31}P\{^{1}H\}$ NMR spectrum displayed two doublets at δ 64.7 and 52.1 (J_{PP} = 13.1 Hz). The IR spectrum yielded a ν_{CO} absorption band at 2004 cm^{-1}. The spectroscopic data suggest the transformation of **9** (**a, a'**) to **10** (**a, a'**) involves an isomerisation in which (for **10a'**) the coordinated Me_2bpy ligand lies *trans* to one end of the dppe and CO (***Scheme 3.2***).

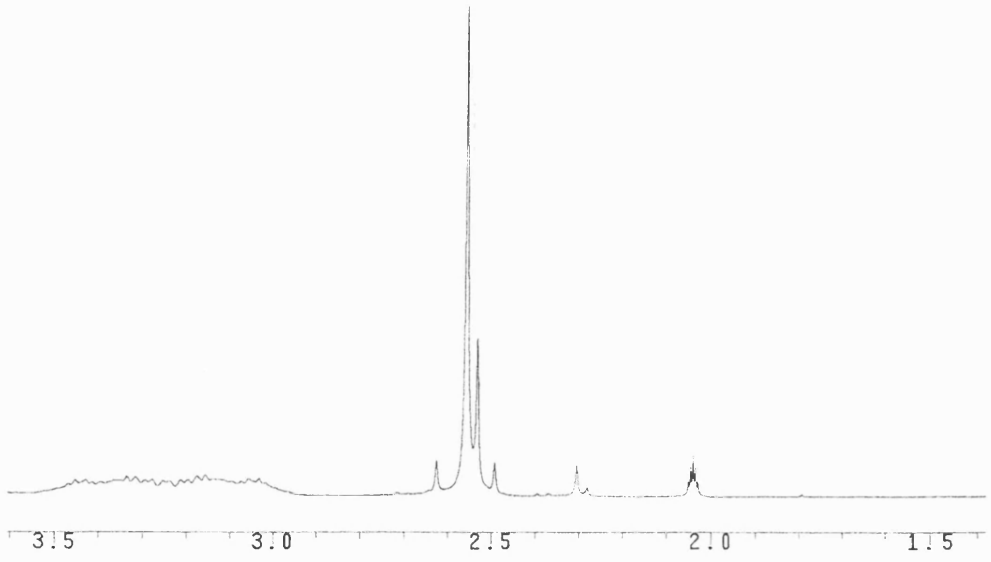

Figure 3.12: *^{1}H NMR spectrum (400 MHz) of* ***10a*** *showing one methyl spectroscopic handle resonance.*

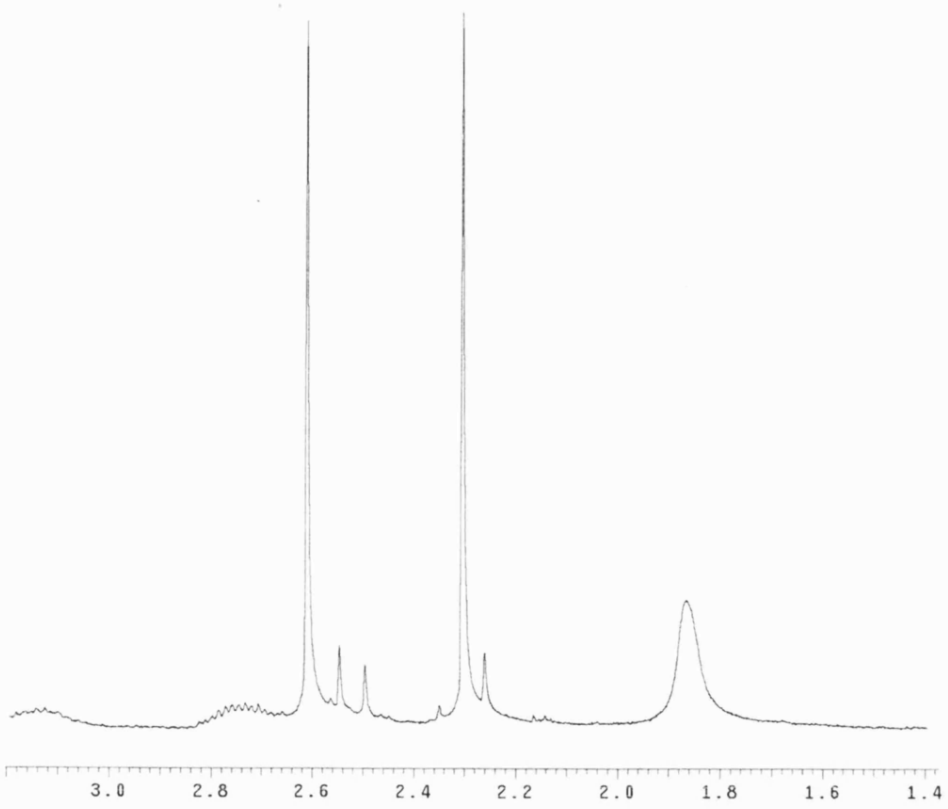

Figure 3.13: *^{1}H NMR spectrum (400MHz) of **10a'** showing two methyl resonances.*

Compounds **9a** and **10a** are fully symmetrical products in which both H_2O ligands *trans* to dppe are displaced by the bidentate N-N donor. These subsequently isomerise to **9a'**, **10a'** in which the N-N donor is now *trans* CO and the water ligand *trans* to dppe.

While **9a** and **10a** proved to be unstable at room temperature and hence were not isolable, the stereochemistry at **9a'** and **10a'** was confirmed by the isolation of the product from reaction **10a'** with CH_2Cl_2/Et_2O in which displacement of H_2O by OTf^- afforded the triflate complex [Ru(dppe)(CO)(OTf)(Me_2bpy)][OTf] (**11a**).

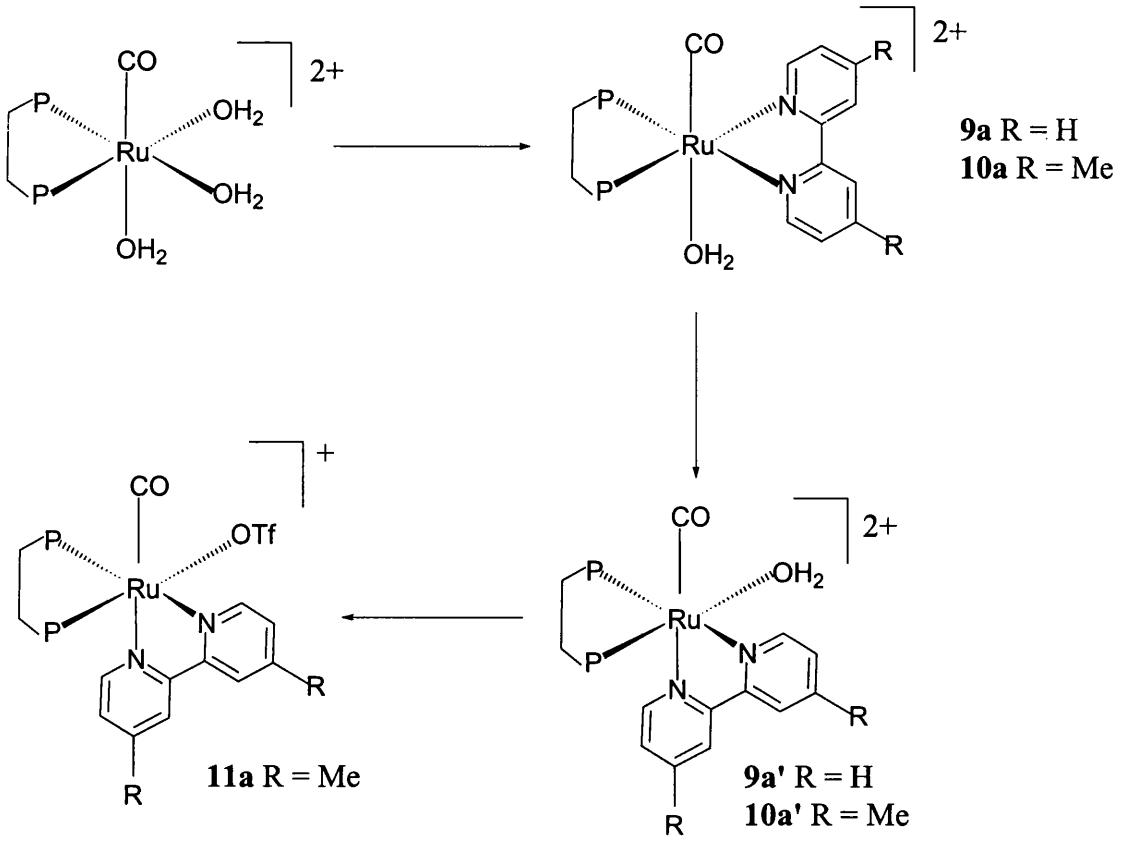

*Scheme 3.2: Reactivity scheme for **4a** with bpy and Me_2bpy.*

3.9 Synthesis and X-ray characterisation of [Ru(dppe)(CO)(OTf)(Me_2bpy)][OTf] (11a)

The coordinated water ligand in **10a'** proved to be labile and hence dissolution in 'dry' $CDCl_3$ or CD_2Cl_2 afforded [Ru(dppe)(CO)(OTf)(Me_2bpy)][OTf] (**11a**). The ^{19}F NMR spectrum showed two signals in a 1:1 ratio at δ – 78.97 and – 79.07 for coordinated and uncoordinated triflate respectively (***Figure 3.14***). The related replacement of H_2O by OTf^- in dry solvents is reminiscent of the chemistry seen with **8a**. The $^{31}P\{^1H\}$ NMR spectrum of **11a** showed two doublet resonances at δ 67.3 and 51.8 (J_{PP} = 14.3 Hz) while the ^1H NMR spectrum displayed the expected two CH_3 resonances at δ 2.61 and 2.30. The

IR spectrum showed a strong ν_{CO} band at 2005 cm^{-1}.

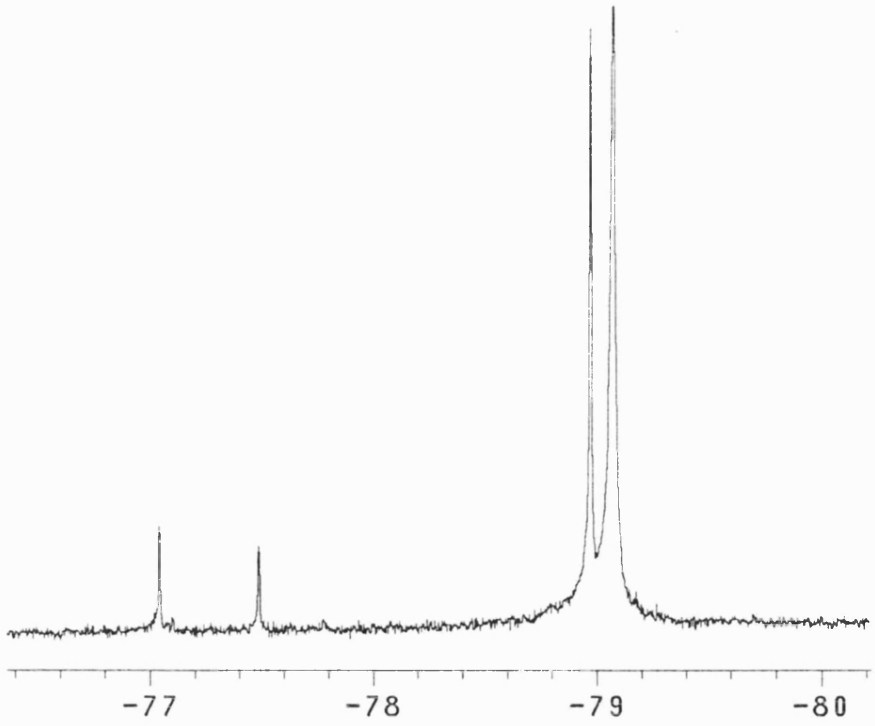

Figure 3.14: *^{19}F NMR spectrum (376 MHz) of [Ru(dppe)(CO)(OTf)(Me$_2$bpy)][OTf] (**11a**) in CD_2Cl_2.*

Complex **11a** rapidly precipitated from solution preventing full characterization by NMR spectroscopy. However, the structure of **11a** was unambiguously established using X-ray crystallography. ***Figure 3.15*** reveals the contents of the asymmetric unit while selected bond lengths [Å] and angles [°] are given in ***Table 3.6***. The geometry about the ruthenium centre in **11a** is largely dictated by the steric demands of the chelating bipyridyl ligand (N(1)-Ru-N(2) = 76.73(7)°).[8] This results in severe distortion away from a regular octahedral geometry as shown by the P(2)-Ru-P(1), C(27)-Ru-N(2) and C(27)-Ru-O-(2) angles (85.17(2), 171.96(8)° and 99.48(8)° respectively).

There are large differences in the Ru-N(1) (2.126(2) Å) and Ru-N(2) (2.267(2) Å)

distances of **11a**. The notable lengthening of the latter bond arises from differing *trans* influences of the phosphine (P1) and carbonyl ligands (C27). This is further apparent from the significant differences in the Ru-P(1) and Ru-P(2) bond distances (2.3392(5) Å, 2.2826(6) Å respectively). There appears to be a weak intramolecular interaction between a phenyl C-H and the coordinated triflate group (C(8)-H(8)...O(3), 3.396 Å) as well as an intermolecular interaction between C(11)-H(11) and O(5) of a symmetry related anion in the lattice, at 3.451(3) Å.

Ru(1)-C(27)	1.869(2)	Ru(1)-O(2)	2.212(2)
Ru(1)-N(1)	2.126(2)	Ru(1)-P(2)	2.2826(6)
Ru(1)-N(2)	2.267(2)	Ru(1)-P(1)	2.3392(5)

C(27)-Ru(1)-N(1)	96.25(8)	N(1)-Ru(1)-P(2)	95.60(5)
C(27)-Ru(1)-N(2)	171.96(8)	N(2)-Ru(1)-P(2)	86.35(5)
N(1)-Ru(1)-N(2)	76.73(7)	O(2)-Ru(1)-P(2)	169.85(5)
C(27)-Ru(1)-O(2)	99.48(8)	C(27)-Ru(1)-P(1)	84.33(7)
N(1)-Ru(1)-O(2)	85.26(6)	N(1)-Ru(1)-P(1)	179.11(5)
N(2)-Ru(1)-O(2)	84.00(6)	N(2)-Ru(1)-P(1)	102.74(5)
C(27)-Ru(1)-P(2)	90.50(7)	O(2)-Ru(1)-P(1)	93.98(4)
P(2)-Ru(1)-P(1)	85.17(2)		

Table 3.6: *Selected bond lengths [Å] and angles [°] for [Ru(dppe)(CO)(OTf)(Me$_2$bpy)][OTf] (**11a**).*

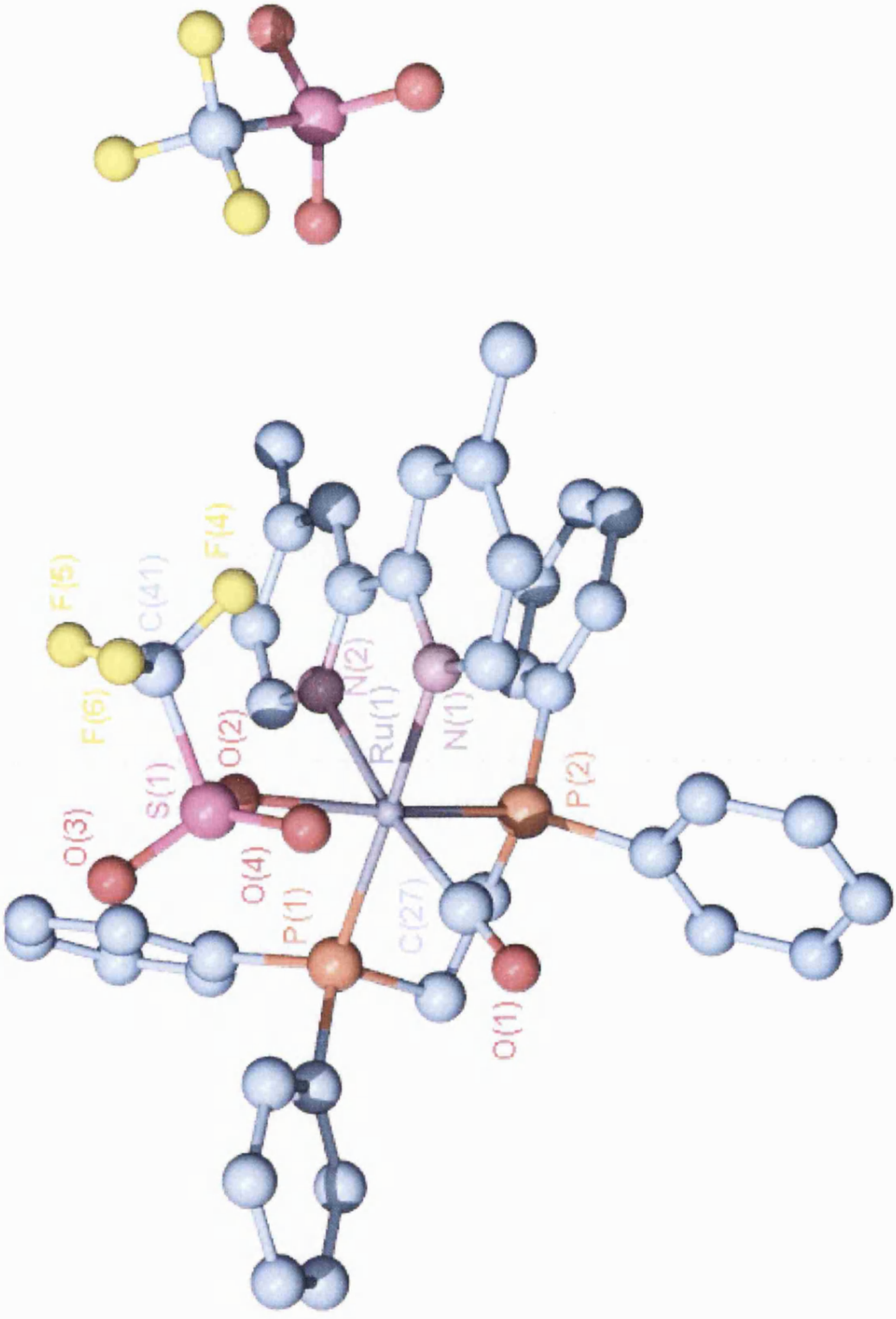

Figure 3.15: *Plot of [Ru(dppe)(CO)(OTf)(Me$_2$bpy)][OTf]* ***(11a)****.*

3.10 Reaction of 4a with 2,2'-bipyrimidine (bipim)

The reaction of **4a** with bipim was conducted in the attempt of forming a dimeric species with the possibility of adding linkage ligands later to form a molecular box as in the case of a $Re(CO)_5Cl$ example which formed a tetrametallic square.[9]

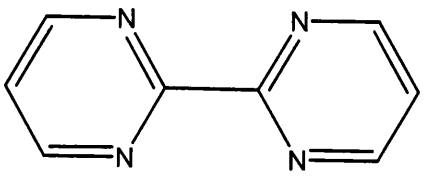

Figure 3.16: *Structure of bipim.*

The reaction of bipim with **4** followed a similar pattern to that of the bpy and Me_2bpy reactions described earlier. Initially a singlet resonance was recorded in the $^{31}P\{^1H\}$ NMR spectrum at δ 60.1 after the addition of 0.5 equivalent of bipim (a stoichiometric amount in an attempt to form a dimer), which slowly converted to two doublet resonances at δ 64.9 and 52.7 (J_{PP} = 12.9 Hz). This conversion was accelerated by the addition of 3 equivalents of bipim. The $^{13}C\{^1H\}$ NMR spectrum of the final product showed a triplet resonance for the carbonyl ligand at δ 197.8 (J_{PC} = 16.1 Hz), while the IR spectrum displayed a single ν_{CO} stretching frequency at 2006 cm^{-1}. Although this product could be precipitated from acetone/water by stirring with diethylether, it was not pure enough by elemental analysis to determine the elemental composition, while single crystals suitable for an X-ray crystallographic determination proved impossible to obtain. A proposed pathway for the reaction of **4a** with bipim is depicted in ***Scheme 3.3*** below. Initial loss of both water ligands *trans* to dppe and coordination of bipim gives $[Ru(dppe)(CO)(H_2O)(bipim)]^{2+}$ (**A**), which would appear as the singlet. Isomerisation (as

in the case of bpy and Me_2bpy) afforded **B** which would display two doublet resonances.

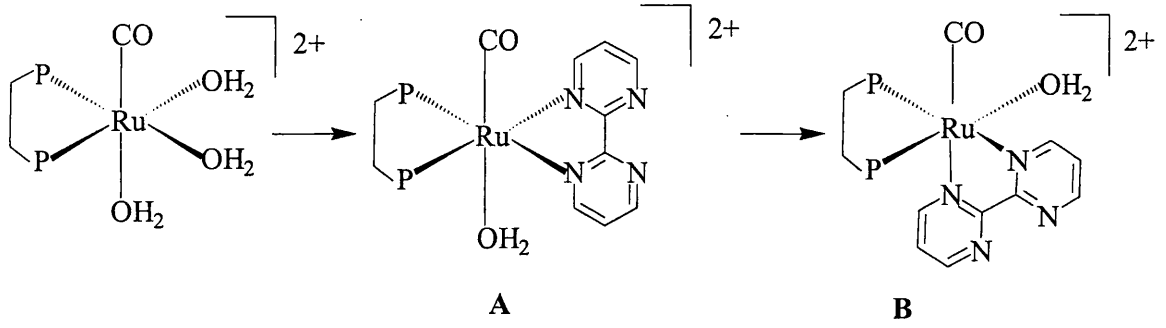

Scheme 3.3: *Proposed pathway for the reaction of* ***4a*** *with bipim.*

3.11 Reaction of $[Ru(dppe)(CO)(H_2O)_3][OTf]_2$ (4a) with 1-propanethiol

Addition of 1-propanethiol (3 equivalents) to an acetone/water solution of **4a** led to an immediate colour change from pale yellow to deep yellow, which over the course of 24 h became deep red. A new singlet species at δ 47.0 was seen immediately in the $^{31}P\{^1H\}$ NMR spectrum, which did not change when the solution became deep red. The IR spectrum (KBr) showed the appearance of a new carbonyl stretching band at 1953 cm^{-1}, a marked shift from **4a** which appears at 1990 cm^{-1}.

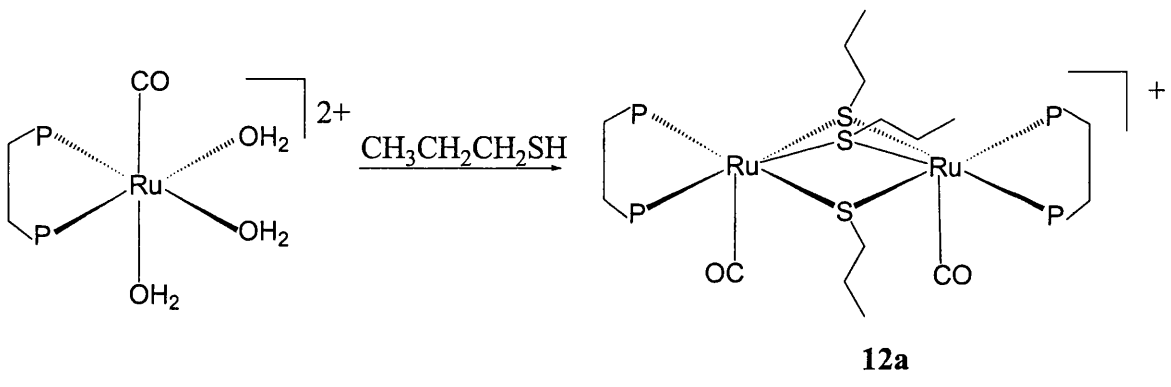

12a

Equation 3.2: *Formation of* $[\{Ru(dppe)(CO)\}_2(\mu\text{-}SCH_2CH_2CH_3)_3][OTf]$ ***(12a)*** *from* ***4a.***

Removal of the solvent and dissolution of the red/orange residue in acetone and layering with diethylether gave yellow/orange crystals which were isolated in 32% yield and shown to be the dimeric complex, $[\{Ru(dppe)(CO)\}_2(\mu\text{-}SCH_2CH_2CH_3)_3][OTf]$ (**12a**), by X-ray crystallography (***Equation 3.2***). Dissolution of these crystals in acetone gave a deep yellow solution, which did not become deep red over a prolonged period of time. The asymmetric unit in **12a** (***Figure 3.16***) shows the presence of a cationic dinuclear ruthenium(II) core bridged by the sulfur atoms of three thiolate groups. Selected bond distances [Å] and angles [°] for **12a** are given in ***Table 3.7***.

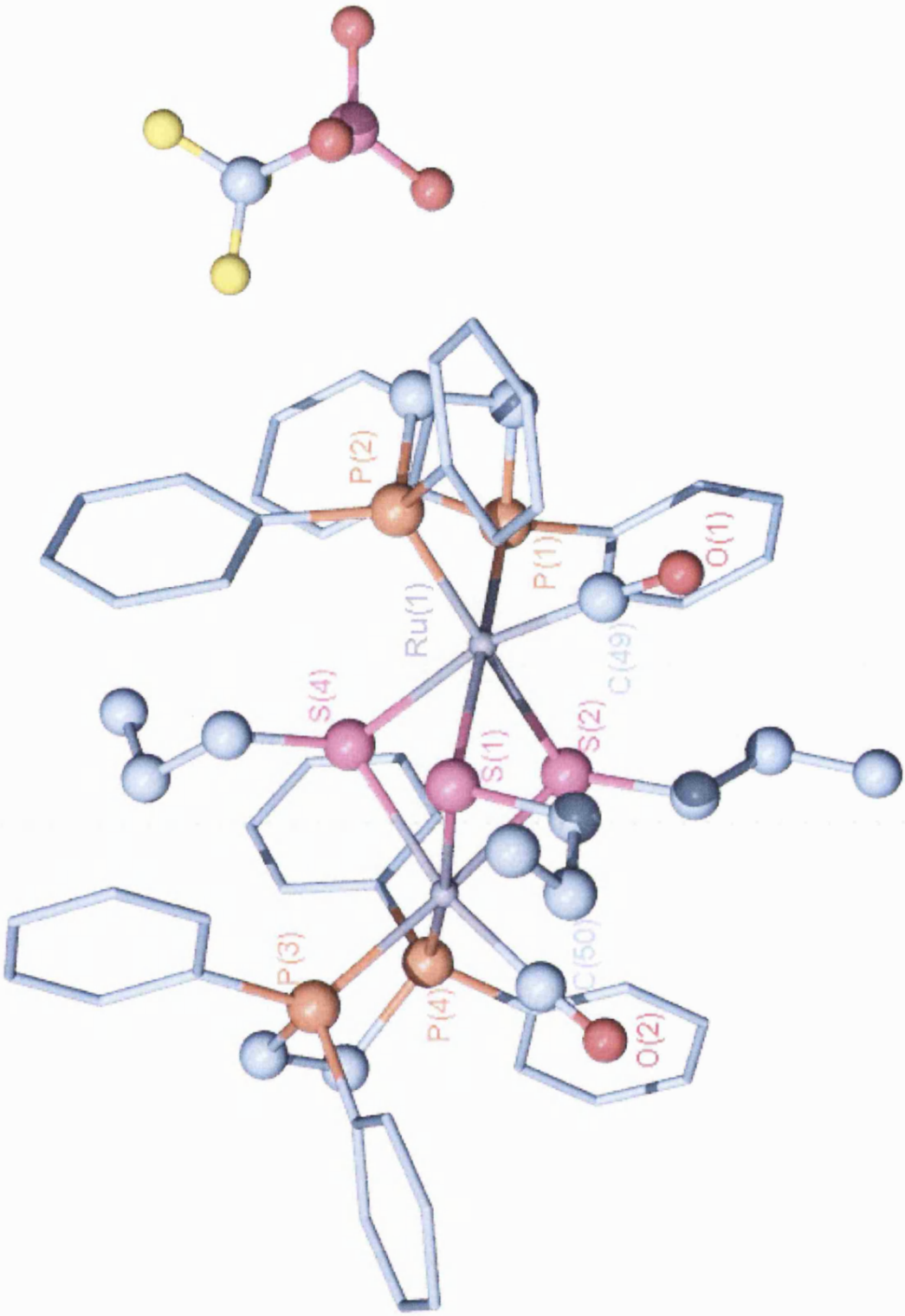

Figure 3.16: *Plot of [{Ru(dppe)(CO)}$_2$(μ-SCH$_2$CH$_2$CH$_3$)$_3$][OTf]* ***(12a)***.

Ru(1)-C(49)	1.851(2)	Ru(1)-P(1)	2.3340(5)
Ru(1)-P(2)	2.3539(5)	Ru(1)-S(2)	2.4387(5)
Ru(1)-S(1)	2.4662(5)	Ru(1)-S(4)	2.4964(5)
Ru(2)-C(50)	1.861(2)	Ru(2)-P(4)	2.3211(5)
Ru(2)-P(3)	2.3547(5)	Ru(2)-S(2)	2.4473(5)
Ru(2)-S(4)	2.4654(5)	Ru(2)-S(1)	2.4653(5)

C(49)-Ru(1)-P(1)	87.77(6)	C(49)-Ru(1)-P(2)	87.54(7)
P(1)-Ru(1)-P(2)	82.657(18)	C(49)-Ru(1)-S(2)	93.56(7)
P(1)-Ru(1)-S(2)	94.968(17)	P(2)-Ru(1)-S(2)	177.346(17)
C(49)-Ru(1)-S(1)	95.30(6)	P(1)-Ru(1)-S(1)	176.421(18)
P(2)-Ru(1)-S(1)	99.279(17)	S(2)-Ru(1)-S(1)	83.030(16)
C(49)-Ru(1)-S(4)	165.59(7)	P(1)-Ru(1)-S(4)	99.830(17)
P(2)-Ru(1)-S(4)	105.468(17)	S(2)-Ru(1)-S(4)	73.711(16)
S(1)-Ru(1)-S(4)	76.777(16)	C(50)-Ru(2)-P(4)	93.84(6)
C(50)-Ru(2)-P(3)	89.89(6)	P(4)-Ru(2)-P(3)	83.926(17)
C(50)-Ru(2)-S(2)	94.69(6)	P(4)-Ru(2)-S(2)	92.056(17)
P(3)-Ru(2)-S(2)	174.107(17)	C(50)-Ru(2)-S(4)	167.23(6)
P(4)-Ru(2)-S(4)	92.708(17)	P(3)-Ru(2)-S(4)	101.709(17)
S(2)-Ru(2)-S(4)	74.111(16)	C(50)-Ru(2)-S(1)	95.43(6)
P(4)-Ru(2)-S(1)	169.757(17)	P(3)-Ru(2)-S(1)	100.411(17)
S(2)-Ru(2)-S(1)	82.871(16)	S(4)-Ru(2)-S(1)	77.367(16)
Ru(2)-S(1)-Ru(1)	86.412(15)	Ru(1)-S(2)-Ru(2)	87.419(16)
Ru(2)-S(4)-Ru(1)	85.753(15)		

Table 3.7: *Selected bond lengths [Å] and angles [°] for [{Ru(dppe)(CO)}$_2$(μ-SCH$_2$CH$_2$CH$_3$)$_3$][OTf]* ***(12a)***.

Particularly striking is the distortion away from an octahedral geometry at the ruthenium centres; the angles between the carbonyl ligands and the unique sulfur lying below the plane of the phosphines are 165.56(7)° and 167.22(6)° for Ru(1) and Ru(2) respectively. The Ru-S distances in **12a** (average 2.463(5) Å) are comparable to those reported in the literature for $[\{(arene)Ru\}_2(\mu\text{-}SPh)_3]^+$ (arene = hexamethylbenzene, *p*-cymene) where the average Ru-S distance is 2.3935(2) (***Figure 3.21***).[10,11] While there is only small deviation in the Ru-S-Ru angles (average 86.5°) from 90°, for $[\{(arene)Ru\}_2(\mu\text{-}SPh)_3]^+$ the average is 88.8°.

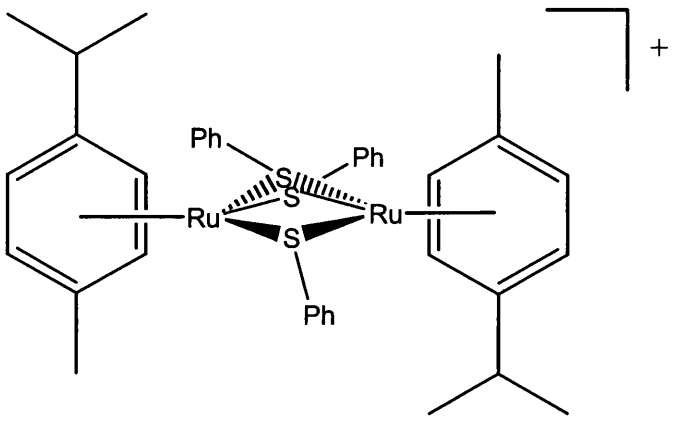

Figure 3.17: *Structure of related complex* $[\{(p\text{-cymene})Ru\}_2(\mu\text{-}SPh)_3][PF_6]$.

When viewed along the metal–metal vector, the structure of **12a** reveals that the bridging sulfurs are staggered with respect to the phosphorus and carbonyl carbon atoms at both ends of the molecule, reflecting the local octahedral coordination sphere at both metal centres (***Figure 3.18***). This highly distorted geometry is exemplified in the angles subtended by the carbonyl carbon and the *trans* sulfur at each of the ruthenium atoms, which have values of 165.59(7)° and 167.23(6)° for Ru(1) and Ru(2) respectively. The metal–metal distance in **12a** is 3.376 Å, which precludes the presence of a Ru-Ru interaction.

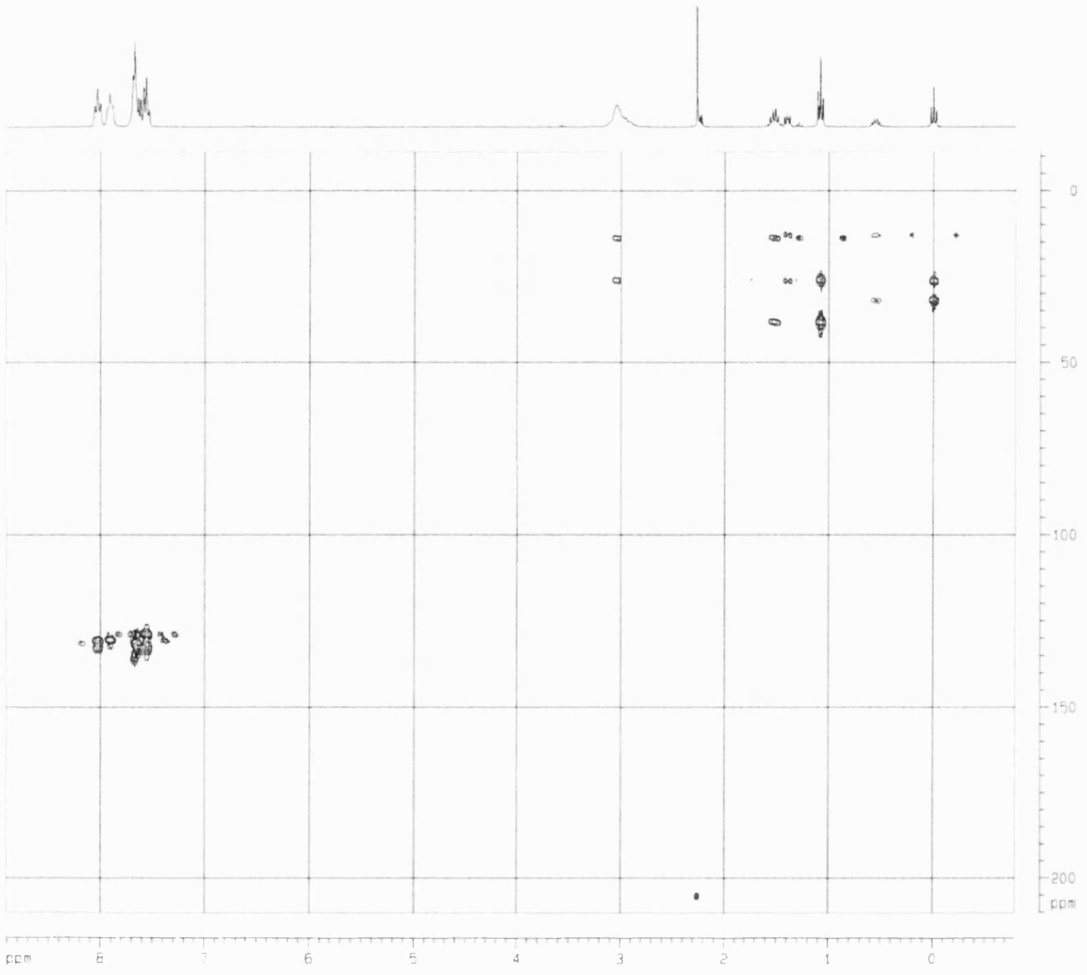

Figure 3.21: *^{13}C -^{1}H Long Range Correlation Spectrum HMQC of* ***12a****.*

The same reactivity with 1-propanethiol was seen with compound **4b**, forming the BF_4^- analogue of **12b**. A singlet resonance was seen at δ 46.8 in the $^{31}P\{^{1}H\}$ NMR spectrum. The ^{19}F NMR spectrum showed a sharp singlet resonance at δ - 151.25. The carbonyl absorption band was seen at 1957 cm^{-1} in the IR spectrum comparable to that of **12a**. Crystals of this species were not obtainable and as a result full characterisation of this species was not pursued.

3.12 Reactions of 4a with other thiols

The reaction of **4a** with other thiols did not proceed in the same manner as for the formation of **12a**. Experiments were conducted using $C_6H_{11}SH$ and *p*-$CH_3C_6H_4SH$. These two proceeded in a similar way, immediately forming a deep yellow solution and later deep red. It was not possible in either of these reactions to form just one species upon addition of either excess RSH reagent or heating.

Addition of 3 equivalents of *p*-$CH_3C_6H_4SH$ to an acetone/water mixture of **4a** led to an immediate reaction. The $^{31}P\{^1H\}$ NMR spectrum showed the appearance of two singlet species at δ 55.7 and 52.1, neither of which corresponded to the starting material, **4a**. After 24 hours, the singlet at δ 55.7 has been replaced by two doublets at δ 54.6 and 51.0 (J_{PP} = 10 Hz). However, the major species was still the singlet at δ 52.1 (***Figure 3.22***). From observing previous experiments, we tentatively assigned the identity of these three reaction products. The singlet at δ 55.7 could be a direct substitution of the two equatorial water ligands *trans* to dppe, which as in the case of the bipyridyl experiments subsequently, isomerises to yield the two doublets at δ 54.6 and 51.0. However, it was not possible to monitor the methyl resonances in the ^1H NMR due to many overlapping signals seen in this region. The singlet at δ 52.1 could be a bridged dimer species as in the case of **12a**, which displayed a singlet resonance at δ 47.0. However it is too unclear to even postulate if it is a two or three thiolate bridged species.

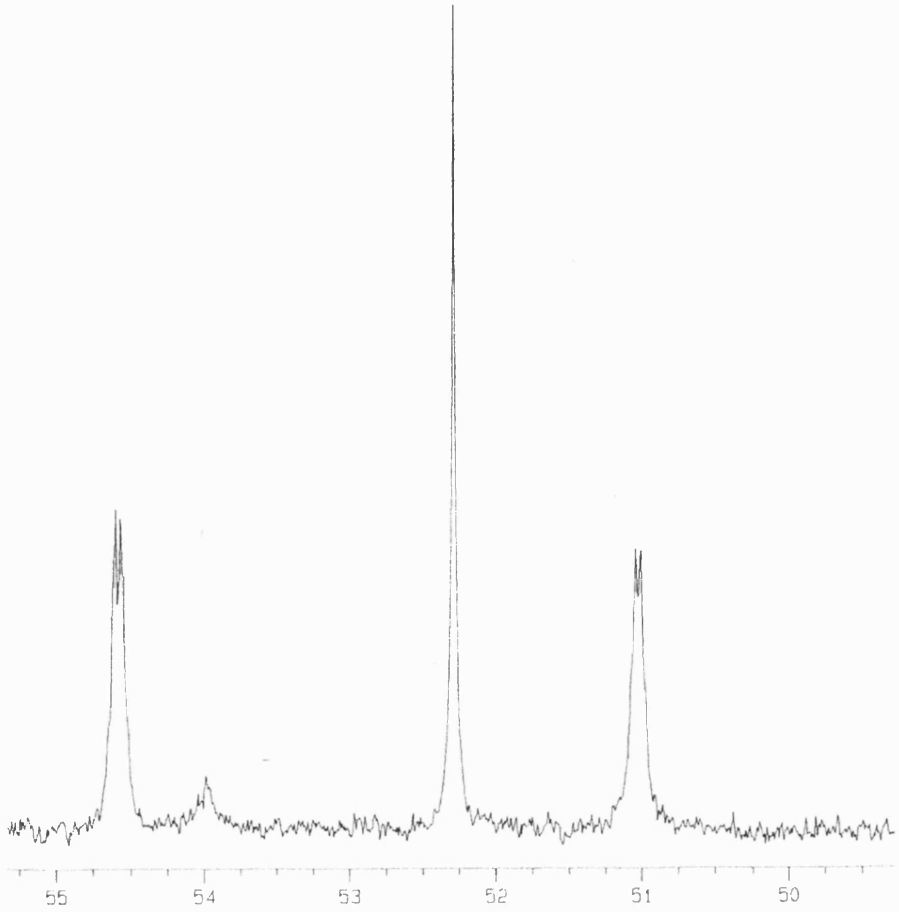

Figure 3.22: *$^{31}P\{^{1}H\}$ NMR spectrum (162 MHz) of* ***4a*** *in acetone/water after addition of p-$CH_3C_6H_4SH$.*

3.13 Reaction of $[Ru(dppe)(CO)(H_2O)_3][OTf]_2$ (4a) with CO

In contrast to the rapid displacement of the water ligands in **4a** by strongly coordinating groups such as CH_3CN or $(CH_3)_2SO$, the reaction of **4a** with CO (1 atmosphere) proceeded very slowly with complete conversion to a single, new ruthenium-containing complex taking place only after three weeks at room temperature. Surprisingly the product proved to be the cationic tricarbonyl hydride complex, $[Ru(dppe)(CO)_3H][OTf]$, (**13a**) which was identified through a combination of NMR, IR spectroscopy and X-ray crystallography. The IR spectrum showed three bands (2110, 2062 and 2051 cm^{-1}), which is consistent with the analogous $[Ru(dppe)(CO)_3H][BF_4]$ species prepared by Gladfelter et al (2105, 2068 and 2053 cm^{-1}).[12] A triplet hydride resonance was observed at δ –7.57 (J_{HP} = 17.80 Hz) in the ^1H NMR (***Figure 3.23***) of **13a** and a singlet resonance seen at δ 64.6 in the $^{31}P\{^1H\}$ NMR spectrum which is again consistent with data reported for $[Ru(dppe)(CO)_3H][BF_4]$, (triplet hydride resonance at δ –7.63 (J_{HP} = 18.10 Hz) and a singlet $^{31}P\{^1H\}$ resonance at δ 64.2). The spectroscopic data are consistent with a *fac* arrangement of the CO ligands and are in good agreement with that reported by Gladfelter et al for the PF_6^- salt of **13a**, which was synthesised upon hydrogen atom abstraction from Bu_3SnH by the radical cation $[Ru(dppe)(CO)_3]^+$.[13] A ^{13}C enriched $^{13}C\{^1H\}$ NMR spectrum depicting the carbonyl region is shown in ***Figure 3.24***, a triplet resonance is seen at δ 190.0 (J_{CP} = 7.9 Hz) and at δ 192.2 (dd, J_{CP} = 76.3, 17.4 Hz).

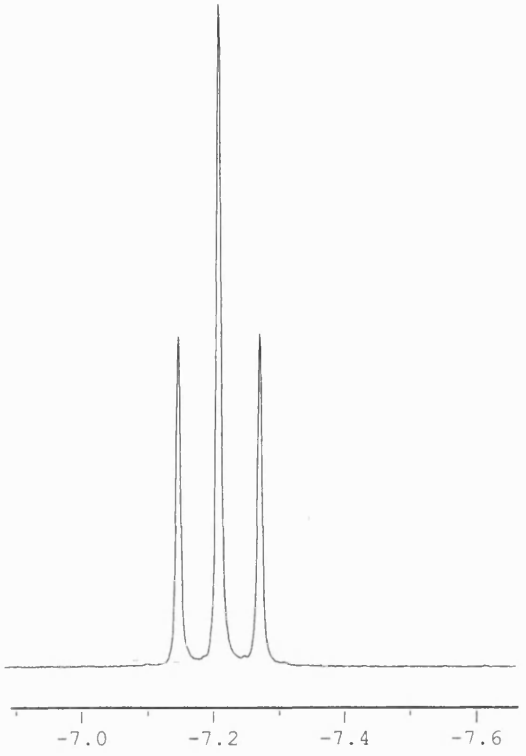

Figure 3.23: *^{1}H NMR spectrum (300 MHz) showing Ru-H.*

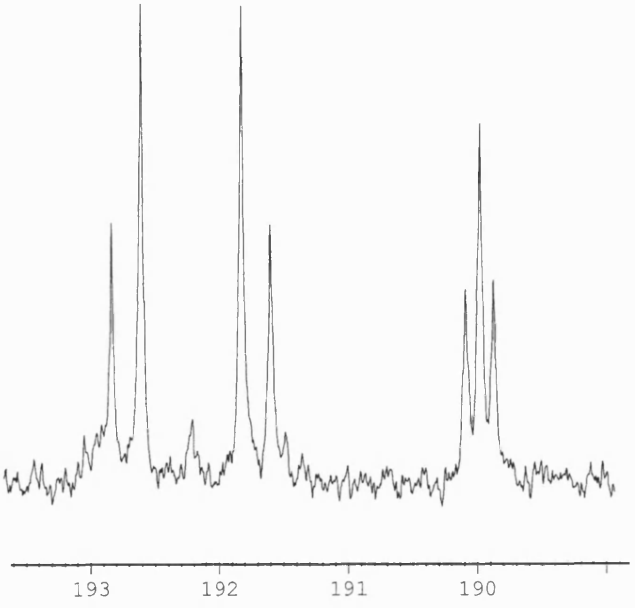

Figure 3.24: *$^{13}C\{^{1}H\}$ (75 MHz) NMR spectrum showing Ru-CO.*

Attempts to isolate **13a** from the reaction mixture were unsuccessful, partly due to its apparent instability in solution in the absence of CO. However, we were able to prepare the complex independently by protonation of $Ru(dppe)(CO)_3$ with triflic acid under a CO atmosphere in CO saturated C_6H_6 solution. Single crystals slowly precipitated from the reaction solution after a two-week period. An X-ray structure determination was performed on this complex, although the poor quality of the crystals and disorder in the triflate anion prevented the structure from being solved with the same high degree of accuracy as for the other compounds reported in this thesis. Nevertheless, the stereochemistry at the ruthenium centre was established beyond doubt as illustrated in ***Figure 3.25***. The *fac* arrangement of the CO ligands imposed by the chelating phosphine ligands contrasts with the *mer* geometry in the structure of $[Ru(PPh_3)_2(CO)_3H][HC(SO_2CF_3)_2]^+$ as reported by Siedle et al.[14] Due to the *mer* arrangement of the CO ligands, only two ν_{CO} bands are seen in the IR spectrum at 2072 and 2052 cm^{-1}.

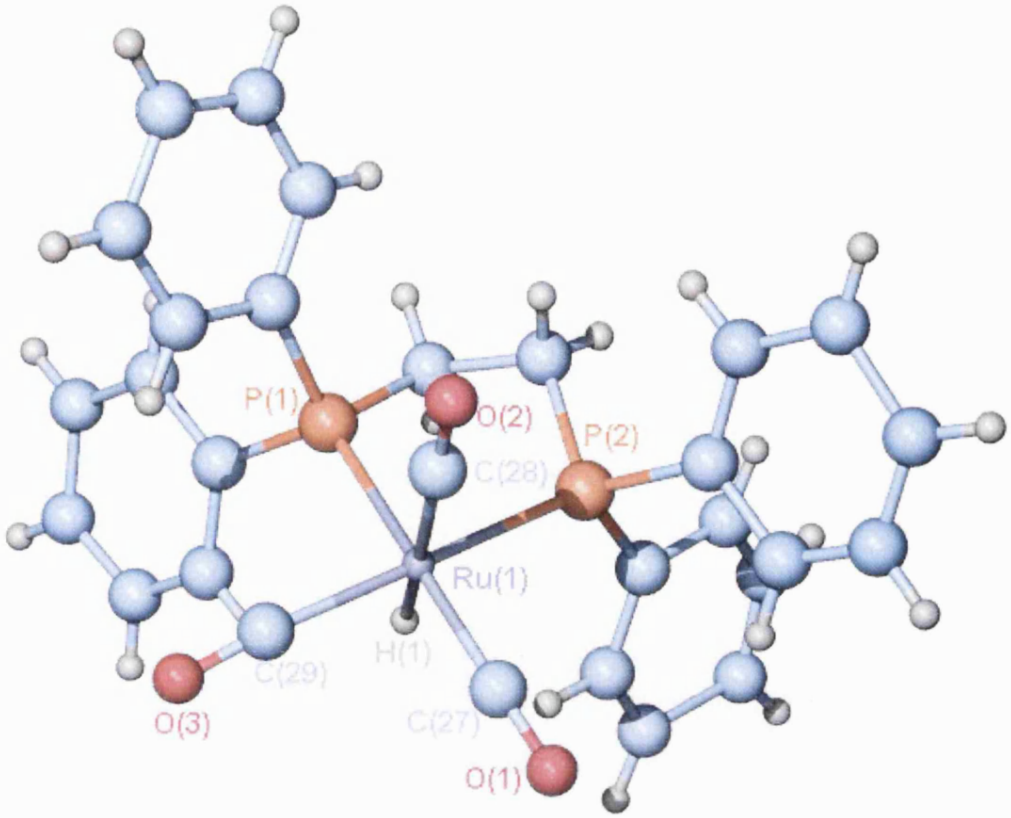

Figure 3.25: *Plot of* ***13a****, depicting the stereochemistry around the metal centre.*

The formation of a hydride product by reaction of the aqua complex **4a** with CO prompted us to investigate the reaction in detail using ^{13}CO labelling. Monitoring by $^{31}P\{^{1}H\}$ NMR spectroscopy showed the appearance after 3 days of an initial product believed to be $[Ru(dppe)(CO)_2(H_2O)_2][OTf]_2$, (***Equation 3.3)*** which appeared as two doublets of doublets at δ 64.5 (J_{PC} = 9.3 Hz, J_{PP} = 14.0 Hz) and 42.8 (J_{PC} = 102.3 Hz, J_{PP} = 14.0 Hz). The size of the P-C coupling constants indicates substitution of water at an equatorial site by ^{13}CO. The $^{13}C\{^{1}H\}$ NMR spectrum showed a single ^{13}C-enhanced carbonyl resonance at δ 187.0 with coupling to two inequivalent ^{31}P nuclei.

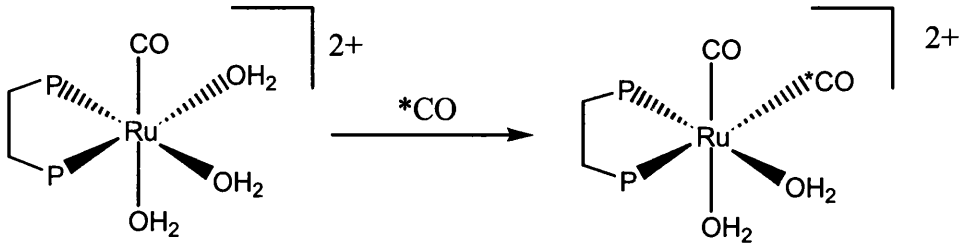

Equation 3.3: *Conversion of **4a** to intermediate species during reaction with CO.*

The ^{31}P signals from $[Ru(dppe)(CO)_2(H_2O)_2][OTf]_2$ diminished over weeks at room temperature and were replaced by a signal for **13a**, showing coupling to ^{13}CO. In addition to two CO resonances for **13a**, the $^{13}C\{^1H\}$ NMR spectrum indicated incorporation of ^{13}CO into residual amounts of **4a**, but most importantly, displayed a signal for $^{13}CO_2$ at δ 126.3. The formation of **13a**, ^{13}CO incorporation into **4a** and evolution of CO_2 can all be rationalised by a mechanism based on nucleophilic attack by water on a coordinated CO ligand leading to a water-gas shift reaction. A postulated pathway is shown in ***Scheme 3.4*** overleaf.[15] The initial reaction step involves the displacement of a H_2O ligand *trans* to phosphorus in **4a** by a *CO ligand (*CO = labelled ^{13}CO) yielding the *bis*-aqua, *bis*-carbonyl species $[Ru(dppe)(CO)_2(H_2O)_2]^{2+}$. The incorporated *CO then undergoes nucleophilic attack by H_2O forming a *COOH group which yields $*CO_2$ forming the hydride species $[Ru(dppe)(CO)(H_2O)_2H]^+$. This reforms **4a** by reaction with H_2O and H^+

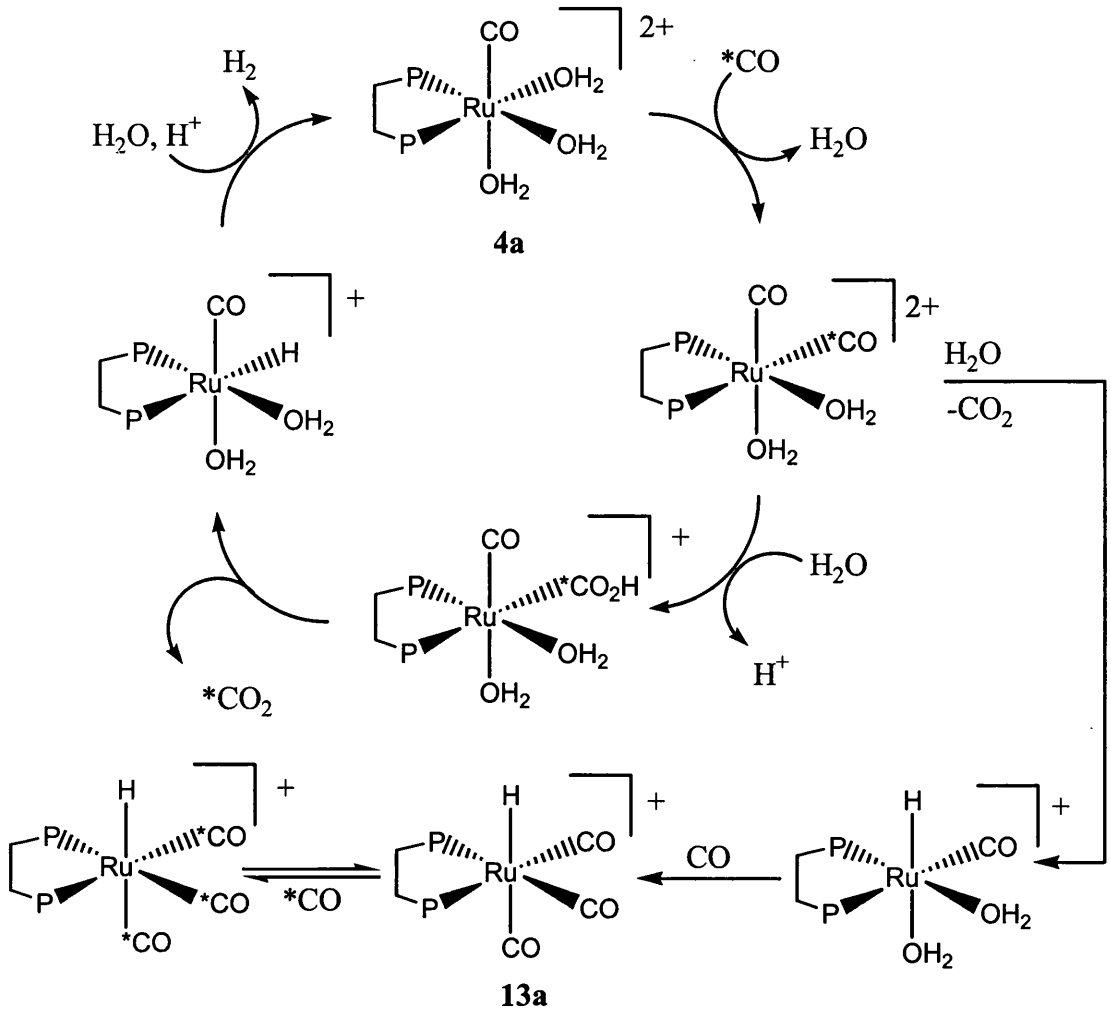

Scheme 3.4: *Postulated water-gas shift pathway/mechanism for the formation of* ***13a*** *from* ***4a****.*

Thus, the formation of **13a** constitutes the trapping of an intermediate on the cycle by addition of excess CO. This is confirmed by the observation that reaction of $[Ru(dppe)(^{12}CO)_3H][OTf]$ with ^{13}CO results in incorporation of the label, but does not yield $^{13}CO_2$.

A number of recent examples of water-gas shift chemistry involving electrophilic non-phosphine stabilised ruthenium (II) carbonyl complexes have been reported.[16-20] In most of these cases, the isolation of hydrido complexes has proved elusive, although Fachinetti and co-workers have been able to trap $[Ru(H_2O)_3(CO)_2H]^+$ with either pyridine

or ethene to give $[Ru(py)_3(CO)_2H]^+$ and $[Ru(H_2O)_3(CO)_2(C_2H_5)]^+$ respectively.[21] Normally when P or As ligands are present, the H atom is generally *trans* to these rather than *trans* to CO, if this π-acid ligand is also present. Without either P or As ligands present, the H is found *trans* to N or O hard σ-donor atoms. This increases the hydridic nature of the H-Ru bond. An H-Ru-N *trans* configuration exists in *cis*-$[Ru(bpy)_2(CO)H]^+$, which has been associated as an intermediate in the homogeneous WGSR.[22]

3.14 The formation of 4a in a water-gas shift type mechanism

The discovery of WGSR as a pathway towards the production of **13a** prompted us to reinvestigate the formation of **4a**, which occurs via substitution of CO and triflate in $[Ru(dppe)(CO)_2(OTf)_2]$ upon addition of water. Thus, addition of water to a chloroform solution of partially ^{13}CO labelled $[Ru(dppe)(CO)_2(OTf)_2]$ resulted in the formation of $^{13}CO_2$, implying that nucleophilic attack of water on a coordinated CO in the bis-triflate complex is responsible for the formation of **4a**. In order to incorporate a label into **2**, a solid sample of **2** was left in air for three weeks to form the mono-aqua species **3** in a quantitative yield. Subsequent addition of 1 atmosphere of ^{13}CO to a degassed "dry" CD_2Cl_2 solution of **3** in a J. Young's resealable NMR tube so that, the extent of the reaction could be monitored by $^{31}P\{^1H\}$ NMR brought about the reformation of **2** in quantitative yield but, now with the incorporation of a ^{13}CO label in place of the substituted water (**2***). Addition of ten equivalents of water to **2*** was conducted as before (***Equation 3.4***), and monitoring of the $^{13}C\{^1H\}$ NMR spectrum (***Figure 3.26***) revealed the formation of $^{13}CO_2$ at δ 126.2, which is consistent with the attack of H_2O on a CO ligand, a characteristic of a *water-gas* shift type mechanism.

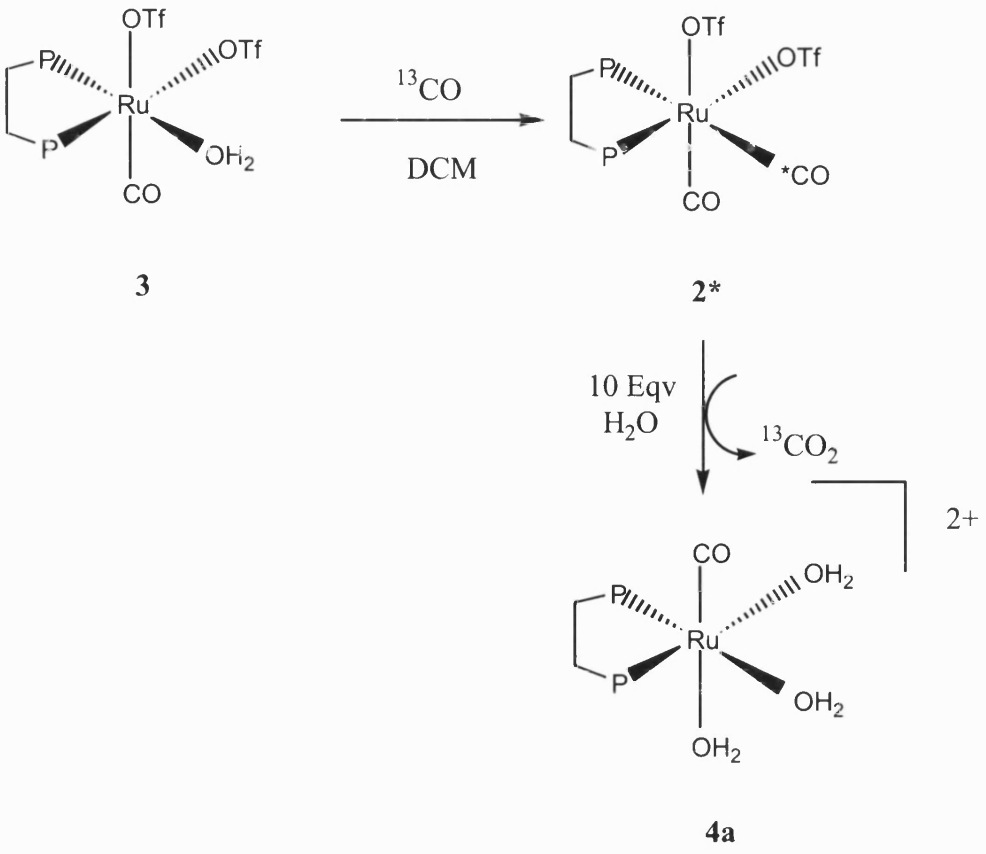

Equation 3.4: *Reaction scheme for generation of $^{13}CO_2$ from **2***.*

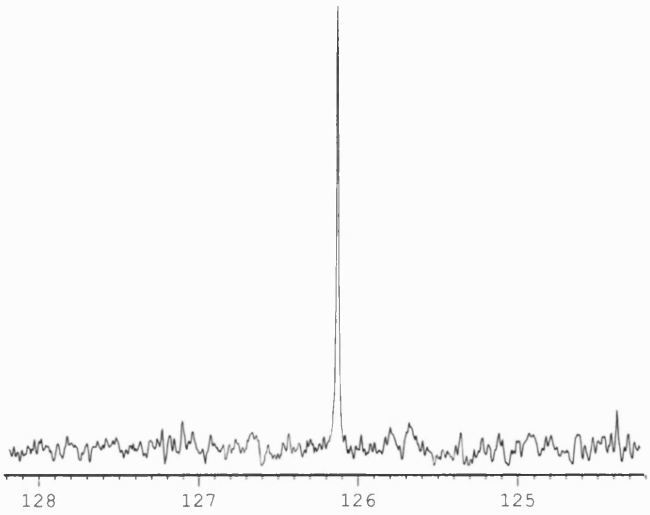

Figure 3.26: *$^{13}C\{^1H\}$ NMR spectrum (75 MHz) showing the formation of $^{13}CO_2$ from reaction of **3*** with 10 equivalents of H_2O.*

3.15 Conclusions

Substitution of one, two or all three water ligands in $[Ru(dppe)(CO)(H_2O)_3][OTf]_2$ (**4a**) by a range of donor ligands has been demonstrated resulting in the formation of both mononuclear and dinuclear ruthenium products. In all cases, we have shown at least qualitatively, that initial substitution of the equatorial water ligands (*trans* to dppe) occurs. This is in agreement with kinetic studies on *trans*-$[Ru(NH_3)_4(H_2O)(PR_3)]^{2+}$ which have established that the kinetic *trans* effect of dppe is much greater than that of CO.[23]

The triflate anion appears to play an important role in the reactivity of **4a**.[24,25] While hydrogen bonding interactions have been reported in helping to stabilise many organometallic aqua complexes, we find that OTf^- also plays the role of hydrogen bond acceptor in weak C-H...O hydrogen bonding interactions in the solid state structures of **5a**, **6a** and **7a**. Dissolution of $[Ru(dppe)(CO)(H_2O)(Me_2bpy)][OTf]_2$, **10a'**, in non-protic solvents results in triflate playing an even more interactive role in substituting water to afford **11a**.

3.16 References

1. Thornburn, I. S.; Rettig, S. J.; James, B. R. *J. Organomet. Chem.* **1985**, *296*, 103.
2. Luginbühl, W.; Ludi, A.; Raselli, A.; Bürgi, H.-B. *Acta Crystallogr., Sect. C* **1989**, *C45*, 1428.
3. Luginbühl, W.; Zbinden, P.; Pittet, P.A.; Armbruster, T.; Bürgi, H.-B.; Merbach, A.E.; Ludi, A. *Inorg. Chem.* **1991**, *30*, 2350.
4. Rüba, E.; Simanko, W.; Mereiter, K.; Schmid, R.; Kirchner, K *Inorg. Chem.* **2000**, *39*, 382.
5. Desiraju, G.R. *Acc. Chem. Res.* **1996**, *29*, 441.

6. Iengo, E.; Mestroni, G.; Geremia, S.; Calligaris, M.; Alessio, E. *J. Chem. Soc., Dalton Trans.* **1999**, 3361.

7. Alessio, E.; Bolle, M.; Milani, B.; Mestroni, G.; Faleschini, P.; Geremia, S.; Calligaris, M. *J. Chem. Soc., Dalton Trans.* **1995**, 4716.

8. Anderson, P.A.; Deacon, G.B.; Haarmann, K.H.; Keene, F.R.; Meyer, T.J.; Reitsma, D.A.; Skelton, B.W.; Strouse, G.F.; Thomas, N.C.; Treadway, J.A.; White, A.H. *Inorg. Chem.* **1995**, *34*, 6145.

9. Benkstein, K. D.; Hupp, J. T.; Stern, C. L. *J. Am. Chem. Soc.* **1998**, *120*, 12982.

10. Maskima, K.; Mikami, A.; Nagamura, A. *Chem. Lett.* **1992**, 1795.

11. Seino, H.; Mizobe, Y.; Hidai, M. *New J. Chem.* **2000**, *24*, 907.

12. Skoog, S.J.; Jorgenson, A.L.; Campbell, J.P.; Douskey, M.L.; Munson, E.; Gladfelter, W.L. *J. Organomet. Chem.* **1998**, *557*, 13.

13. Sherlock, S.J.; Boyd, D.C.; Moasser, B.; Gladfelter, W.L. *Inorg. Chem.* **1991**, *30*, 3626.

14. Siedle, A.R.; Newmark, R.A.; Gleason, W.B. *Inorg. Chem.* **1991**, *30*, 2005.

15. Ford, P.C.; Rokicki, A. *Adv. Organomet. Chem.* **1988**, *28*, 139.

16. Fachinetti, G.; Funaioli, T.; Lecci, L.; Marchetti, F. *Inorg. Chem.* **1996**, *35*, 7217.

17. Lavigne, G. *Eur. J. Inorg. Chem.* **1999**, 917.

18. Faure, M.; Maurette, L.; Donnadieu, B.; Lavigne, G. *Angew. Chem., Int. Ed.* **1999**, *38*, 518.

19. Funaioli, T; Cavazza, C.; Marchetti, F.; Fachinetti, G. *Inorg. Chem.* **1999**, *38*, 3361.

20. Hill, A.F. *Angew. Chem., Int. Ed.* **2000**, *39*, 130.

21. Fachinetti, G.; Funaioli, T.; Marchetti, F. *J. Organomet. Chem.* **1995**, *498*, 20.

22. Morimoto, M.; Tanaka, T.; Ishida, H.; Tanaka, K. *Organometallics* **1986**, *5*, 724.

23. Franco, D. W. *Coord. Chem. Rev.* **1992**, *119*, 199.

24. Lawrance, G. A. *Chem. Rev.* **1986**, *86*, 17.

25. Beck, W.; Sünkel, K. *Chem. Rev.* **1988**, *88*, 1405.

Chapter 4

Attempted synthesis of substituted dppe analogues of $[Ru(dppe)(CO)(H_2O)_3]^{2+}$

4.1 Introduction

As part of the ongoing investigation into $[Ru(dppe)(CO)(H_2O)_3]^{2+}$ (**4**), one idea was to alter the bidentate chelating phosphine ligand, either by extension of the chain length or by incorporating substituents on to the Ph groups. Three substituted dppe variants were investigated; $(p\text{-R-}C_6H_4)_2PCH_2CH_2P(p\text{-R-}C_6H_4)_2$ (dppe-R), where R = -F, -OMe, -Me. All three were readily synthesised by known Grignard preparations[1,2] and attached to $[Ru(CO)_3(Cl)_2]_2$ as in Taylor's preparation of all-*cis*-$[Ru(dppe)(CO)_2(Cl)_2]$ (**1**),[3] and then following the same preparative route as to the synthesis of **4**.[5] The plan to synthesise the dppe-OMe and dppe-F substituents might allow an interesting study of phosphine influence on M-OH_2 bond reactivity through the electron donating (OMe) and electron withdrawing (F) substituents. The effect of R on reactivity has been observed by Chatt and co-workers in $[Re(P\text{-}P)_2(X_2)Y]$,[4] where R can be any number of different substituents. A linear variation was found in the oxidation potential (E^{OX}) of the metal with changing of the R substituent, (***Figure 4.1***). The dppe containing compounds are $[ReCl(N_2)(dppe)_2]$ (**10**), $[ReCl(N_2)\{(p\text{-}ClC_6H_4)_2PCH_2CH_2P(C_6H_4Cl\text{-}p)_2\}_2]$ (**11**), $[ReCl(N_2)\{(p\text{-}CF_3C_6H_4)_2PCH_2CH_2P(C_6H_4CF_3\text{-}p)_2\}_2]$ (**12**), $[ReCl(N_2)\{(p\text{-}MeC_6H_4)_2PCH_2CH_2P(C_6H_4Me\text{-}p)_2\}_2]$ (**13**) and $[ReCl(N_2)\{(p\text{-}MeOC_6H_4)_2PCH_2CH_2P(C_6H_4OMe\text{-}p)_2\}_2]$ (**14**). Interestingly compounds **12** (dppe-CF_3) and **13** (dppe-Me) are anomalous, which has been attributed to a change in the relative π acceptance of the phosphine being predominant and σ donation being relatively weaker.

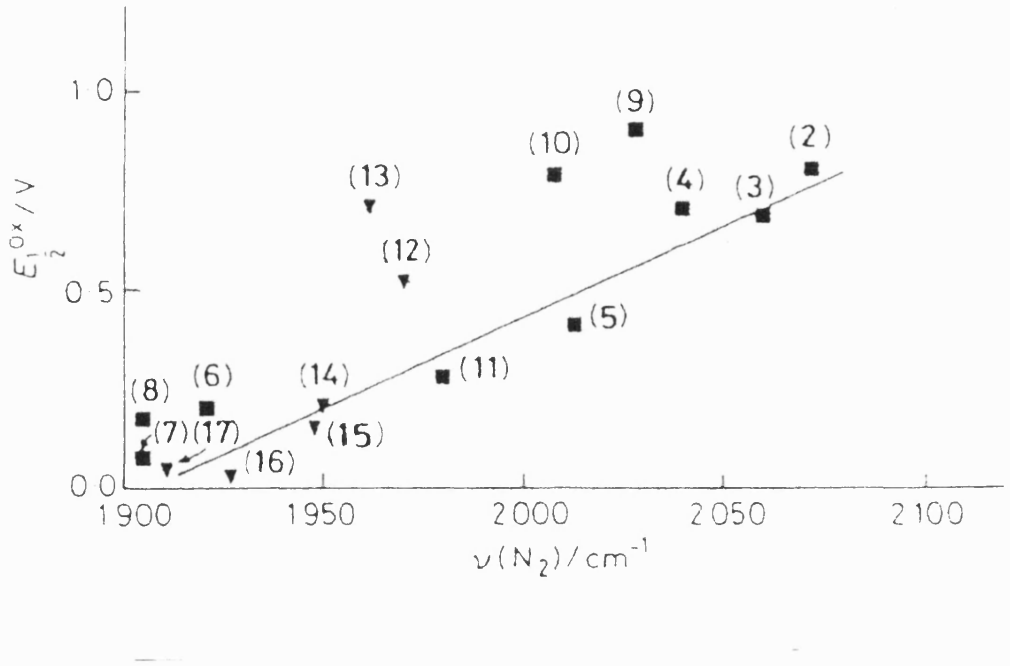

FIGURE 4.1: *Plot of $\nu(N_2)$ versus $E_{0.5}$ for a range of rhenium complexes.*

4.2 Synthesis of $(p\text{-R-}C_6H_4)_2PCH_2CH_2P(p\text{-R-}C_6H_4)_2$

The three substituted variants of dppe, were prepared by reaction of $Cl_2PCH_2CH_2PCl_2$ with the appropriate Grignard reagent (***Equation 4.1***).

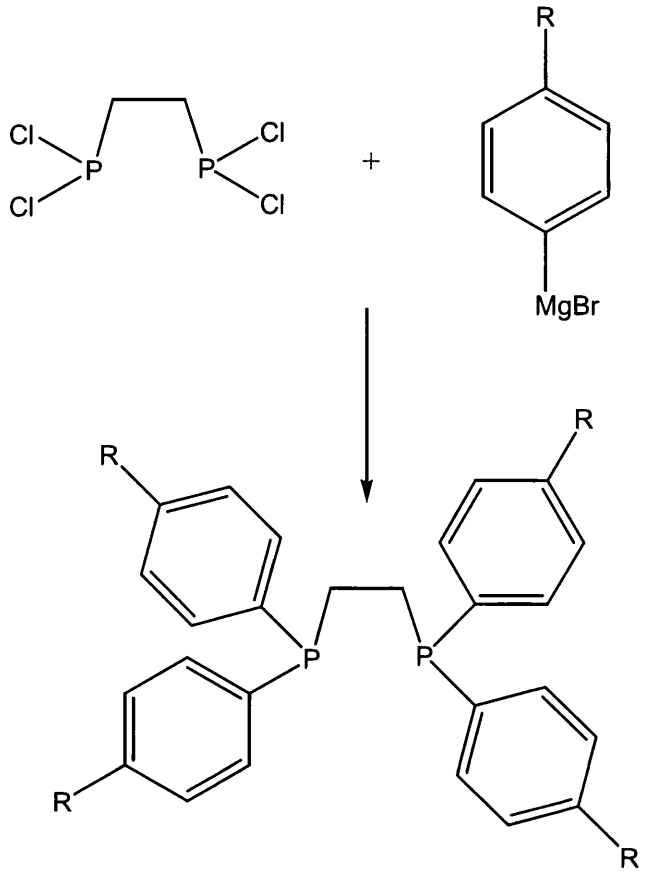

Equation 4.1: *General reaction equation for the syntheses of* $(p\text{-R-}C_6H_4)_2PCH_2CH_2P(p\text{-R-}C_6H_4)_2$ *where R = -F, -OMe and -Me.*

Only for the preparation of dppe-F was the Grignard reagent synthesised. For dppe-Me and dppe-OMe, solutions of the respective Grignard reagents were purchased from Aldrich. All three phosphines were extracted in similar ways, although the yields were always lower than those quoted in the literature. This was found to cause problems later on due to the nature of the synthesis of **1** and its respective analogues (***Scheme 4.1***).

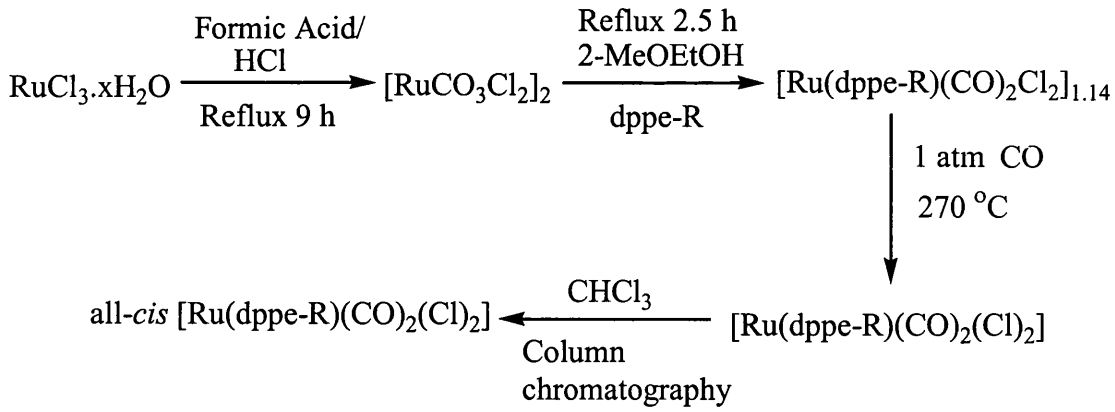

Scheme 4.1: *Reaction steps in the synthesis of [Ru(dppe-R)(CO)$_2$(Cl)$_2$] (**1R**) analogues where R = -F, -OMe, -Me.*

4.3 Synthesis of all-*cis*-[Ru(dppe-F)(CO)$_2$Cl$_2$] (1F)

The synthesis of dppe-F was checked by multi-nuclear NMR and melting point values. A singlet was seen in the $^{31}P\{^1H\}$ NMR spectrum at δ – 14.5 while a triplet was displayed in the ^{19}F NMR spectrum at δ – 112.15 (J_{HF} = 18.05 Hz). The phosphine melted between 128-130 °C, in good agreement with the literature.[1] The yield obtained was around 40% compared to the 77% reported by Mirabelli et al.[1]

Two equivalents of dppe-F were reacted with one equivalent of [Ru(CO)$_3$(Cl)$_2$]$_2$,[6] under reflux in 2-methoxyethanol to afford a creamy insoluble precipitate after 2 h, which was collected by filtration and dried in air. The solid state IR spectrum (nujol) of the precipitate displayed two ν_{CO} bands at 2051 and 1988 cm^{-1} which compare favourably to the dppe analogue [Ru(dppe)(CO)$_2$(Cl)$_2$]$_{1.14}$ (2047 and 1985 cm^{-1}).

Portions of [Ru(dppe-F)(CO)$_2$(Cl)$_2$]$_{1.14}$ were placed under 1 atm of CO in an ampoule and heated to 270 °C.[3] However, unlike the dppe analogue, the dppe-F dimer did not melt but rapidly turned yellow upon warming and, with prolonged heating, began to

char and burn. The yellow compound proved to be soluble in $CHCl_3$ and was extracted by filtration for analysis by $^{31}P\{^1H\}$ NMR spectroscopy (***Figure 4.2***).

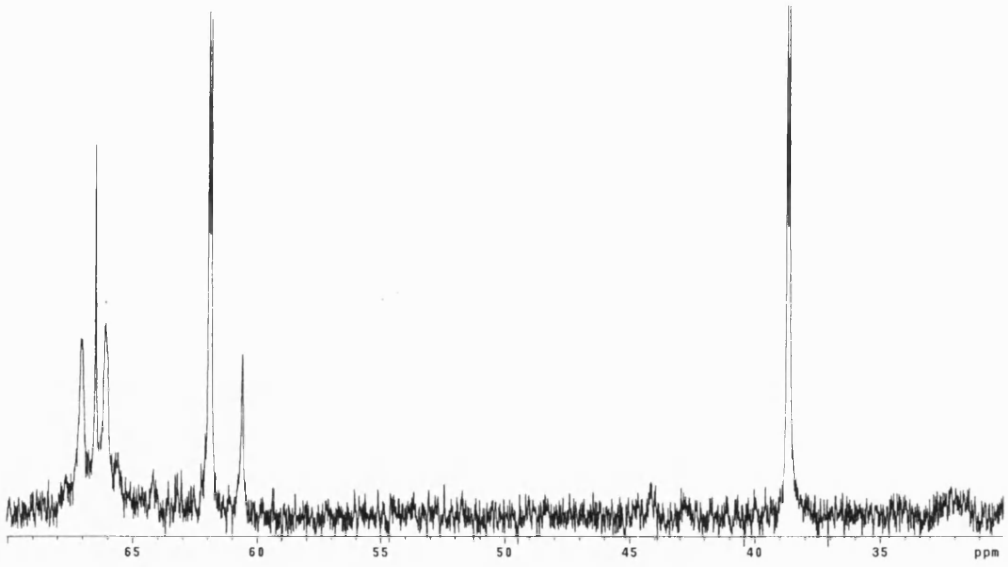

Figure 4.2: *$^{31}P\{^1H\}$ NMR spectrum (162 MHz) of Ru(dppe-F)$(CO)_2(Cl)_2$ before purification on a silica gel column.*

From the $^{31}P\{^1H\}$ NMR spectrum it can be seen that there are three species present, the major one giving a pair of doublets at δ 61.9 and 38.7 (J_{PP} = 15.2 Hz). This corresponds favourably with all-*cis*-[Ru(dppe)$(CO)_2(Cl)_2$] which displayed two doublets at δ 63.0 and 38.1 (J_{PP} = 9.7 Hz) and is therefore assigned as all-*cis*-[Ru(dppe-F)$(CO)_2Cl_2$] (**1F**). The two singlets seen at δ 66.5 and 60.6 can also be assigned from Taylor's work as the two other possible isomers of **1F** (***Figure 4.3***).[3]

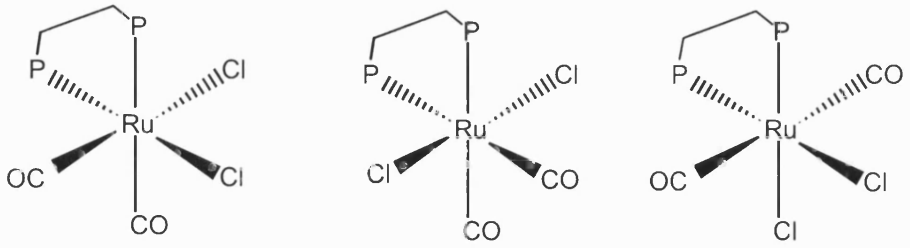

Fraction 1 2nd Fraction 3rd Fraction

Figure 4.3: *Observed isomers of [Ru(dppe-F)(CO)$_2$(Cl)$_2$] (**1F**).*

The separation of the three isomers of **1F** was performed as per the synthesis of **1** on a silica-gel column eluted with a 95:5 eluent mixture of $CHCl_3$ and MeOH respectively. Inspection of the collected fractions revealed that all-*cis*-**1F** had become isomerised on the column (***Figure 4.4***).

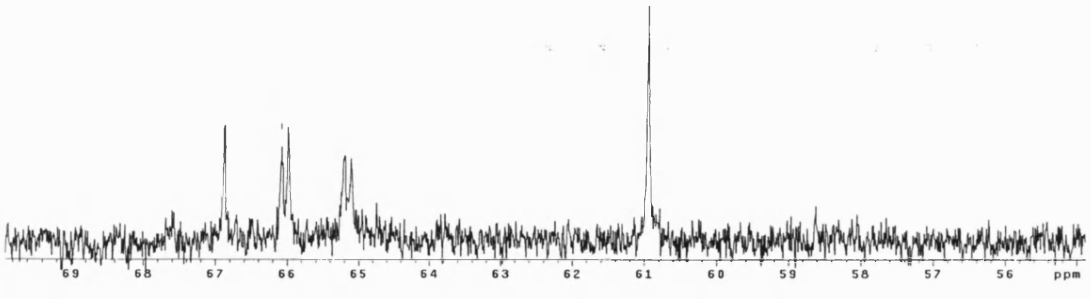

Figure 4.4: *$^{31}P\{^1H\}$ NMR spectrum (162 MHz) of fraction 1, all-cis-**1F** after attempted purification by column chromatography on a silica gel column.*

As can be seen from the $^{31}P\{^{1}H\}$ NMR spectrum (***Figure 4.4***), the all-*cis* species had become isomerised to the *trans* CO species, which was seen as the predominant singlet at δ 60.9. We were unable to isolate this in a pure enough form to characterise further.

4.4 Synthesis of all-*cis*-[Ru(dppe-OMe)(CO)$_2$Cl$_2$] (1OMe)

Following the synthetic route of Burt et al (*p*-OMe-$C_6H_4)_2PCH_2CH_2P$(*p*-OMe-$C_6H_4)_2$ (dppe-OMe) was prepared in 30% yield.[2] The free phosphine was seen as a singlet resonance at δ – 14.9 by $^{31}P\{^{1}H\}$ NMR spectroscopy. Further characterisation was provided by the ^{1}H NMR spectrum with the appearance of a 12H singlet resonance at δ 3.80 corresponding to the *p*–OMe groups.

The reaction of dppe-OMe with $[Ru(CO)_3(Cl)_2]_2$ proceeded as for the dppe analogue forming a creamy precipitate which was assigned as [Ru(*p*-OMe-dppe)$(CO)_2(Cl)_2]_{1.14}$. An IR spectrum in nujol displayed two ν_{CO} bands of similar intensity at 2051 and 1991 cm^{-1} which are comparable to the dppe analogue.

Unlike $[Ru(dppe\text{-}F)(CO)_2(Cl)_2]_{1.14}$, the –OMe analogue did melt on heating under a CO atmosphere, and the orange glass which formed on cooling was extracted with $CHCl_3$. A $^{31}P\{^{1}H\}$ NMR spectrum of the extracted compound revealed that a number of species were present, some of which could not be assigned based on the previous work by Taylor[3] but one did look favourably like the all-*cis*-isomer **1OMe**. Thus separation of the species was attempted through chromatography on silica gel. The first fraction was obtained in a very low yield. The $^{31}P\{^{1}H\}$ NMR spectrum (***Figure 4.5***) showed a pair of doublets at δ 59.9 and δ 37.5 (J_{PP} = 16.8 Hz) and the solution IR displayed two ν_{CO}

stretching bands at 2077 and 2004 cm^{-1}, both of which compared favourably with the dppe analogue. Thus we assign this complex as all-*cis*-[Ru(dppe-OMe)$(CO)_2(Cl)_2$] (**1OMe**).

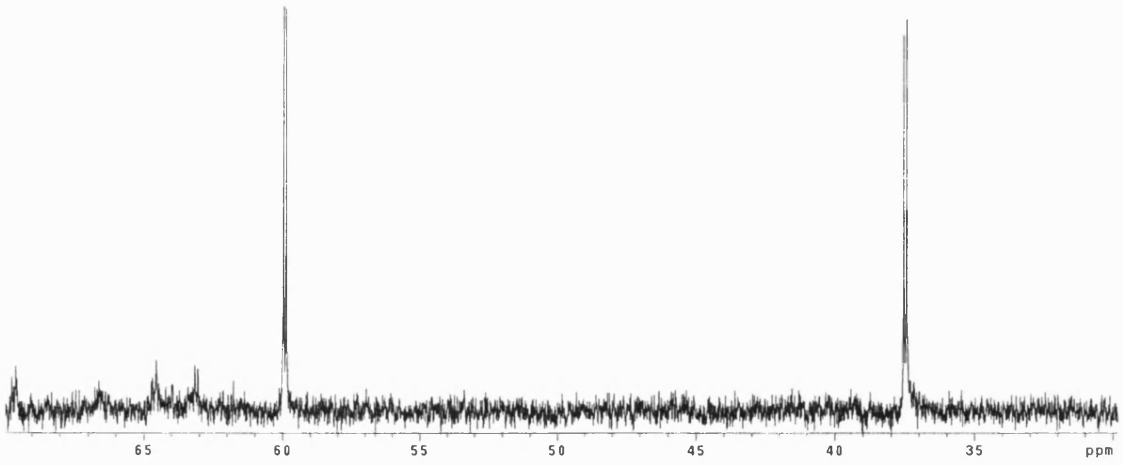

Figure 4.5: *$^{31}P\{^1H\}$ NMR spectrum (162 MHz) of* ***1OMe****.*

The remaining fractions could, neither be identified or separated. Due to the low yields obtained during these syntheses, the ligand was deemed unsuitable for the preparation of [Ru(dppe-R)$(CO)(H_2O)_3]^{2+}$ (**4R**).

4.5 Synthesis of all-*cis*-[Ru(dppe-Me)$(CO)_2(Cl)_2$] (1Me)

The last phosphine to be prepared was (p-Me-$C_6H_4)_2PCH_2CH_2P(p$-Me-$C_6H_4)_2$ (dppe-Me) which proved to be the most successful in terms of synthesis. The phosphine was prepared as in the previous examples by reaction of $Cl_2PCH_2CH_2PCl_2$ with p-Me-

C_6H_4-MgBr and was worked up as in the literature but again in a relatively low yield of 19% compared to the expected 38%.[2]

The free phosphine was collected as pure white crystals and the $^{31}P\{^1H\}$ NMR spectrum showed a singlet resonance at δ – 13.6, while in the ^1H NMR spectrum, a singlet was seen at δ 2.0 for the *p*-Me groups. Two equivalents of this phosphine were reacted with $[Ru(CO)_3(Cl)_2]_2$ under reflux. The IR spectrum of the resultant insoluble precipitate displayed two ν_{CO} stretching bands at 2042 and 1976 cm^{-1} (compared to the dppe analogue 2047 and 1985 cm^{-1}). Thus the insoluble compound was presumed to be [Ru(dppe-Me)$(CO)_2(Cl)_2]_{1.14}$ and was subjected to heating at 270 °C under 1 atm of CO. The solid melted and was extracted with $CHCl_3$. IR and $^{31}P\{^1H\}$ NMR indicated that a mixture of isomers were present. Separation was achieved using a silica gel column using only $CHCl_3$ as the eluent. The first fraction collected was assigned as all-*cis*-Ru(dppe-Me)$(CO)_2(Cl)_2$ (**1Me**) and was characterised using multinuclear NMR and IR. The solution IR spectrum (CH_2Cl_2) displayed two ν_{CO} bands of equal intensity at 2078 and 2006 cm^{-1}, indicating a *cis* carbonyl ligand arrangement (***Figure 4.6***).

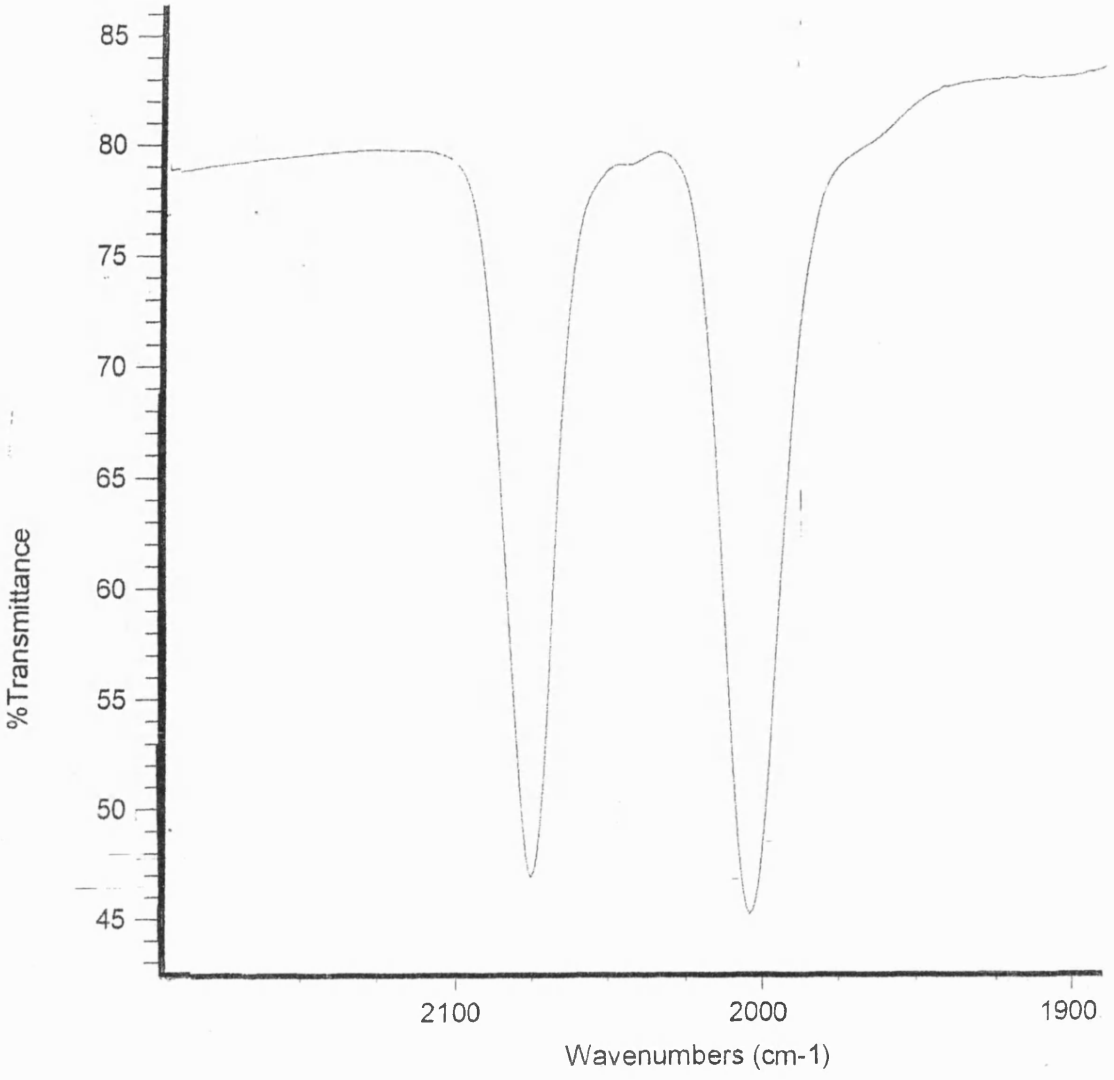

Figure 4.6: *IR spectrum of all-cis-**1Me** in* $CHCl_3$.

In the $^{31}P\{^1H\}$ NMR spectrum, (***Figure 4.7***) a pair of doublets was seen at δ 61.2 and δ 37.9 (J_{PP} = 16.7 Hz) indicating an unsymmetrical arrangement of the bidentate phosphine around the metal centre. $^{13}C\{^1H\}$ NMR spectroscopy (***Figure 4.8***) confirmed the presence of the CO ligands through the appearance of a doublet of doublets at δ 193.1 (J_{PC} = 13.6 Hz, J_{PC} = 10.7 Hz) and a doublet of doublets at δ 189.9 (d, J_{PC} = 9.5 Hz, *cis*-CO; d, J_{PC} = 116.8 Hz, *trans*-CO). The coupling constant reflects the *cis* and *trans* disposition of the CO ligand to dppe-Me. All of the spectroscopic data for **1Me** are comparable to **1**.[3]

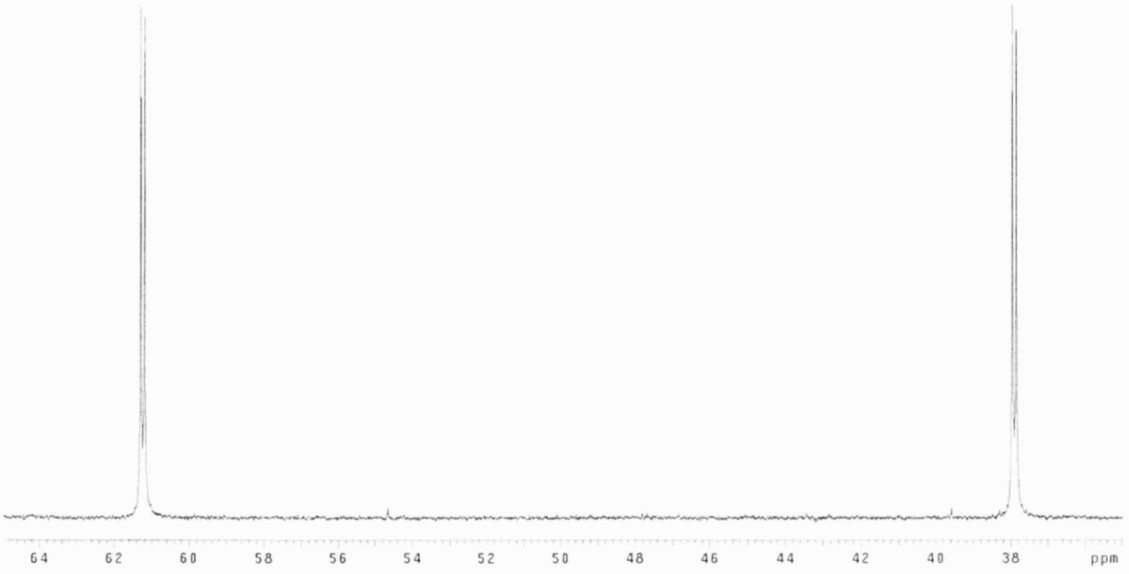

Figure 4.7: *$^{31}P\{^{1}H\}$ NMR spectrum (162 MHz) of* ***1Me***

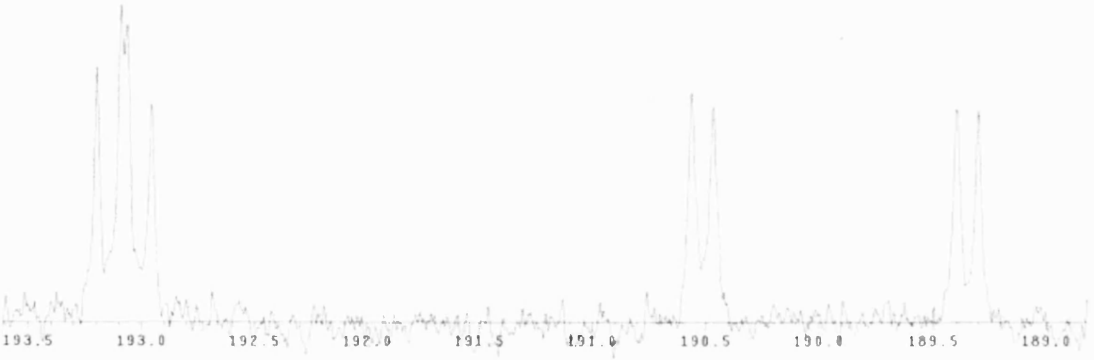

Figure 4.8: *$^{13}C\{^{1}H\}$ NMR spectrum (100 MHz) of* ***1Me*** *showing the carbonyl resonances.*

4.6 Synthesis of [Ru(dppe-Me)(CO)$_2$(OTf)$_2$] (2Me)

Compound **1c** was reacted with AgOTf in dry CH_2Cl_2 in an attempt to synthesise the analogous species to [Ru(dppe)(CO)$_2$(OTf)$_2$] (**2**). The same preparative route (***Equation 4.2***) was followed as for the synthesis of **2** except a less polar solvent (hexane) had to be used to precipitate the product.[5]

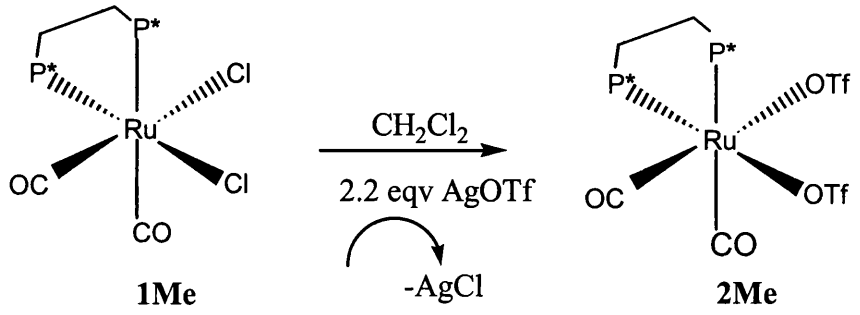

Equation 4.2: *Reaction of all-cis-**1Me** with AgOTf to yield **2Me** (P* = dppe-Me).*

The $^{31}P\{^1H\}$ NMR spectrum of [Ru(dppe-Me)(CO)$_2$(OTf)$_2$] (***Figure 4.9***) displayed a pair of doublets at δ 62.4 and δ 43.6 (J_{PP} = 15.7 Hz) which reflects the unsymmetrical nature of the phosphine ligand around the metal centre. $^{13}C\{^1H\}$ NMR and IR spectroscopy confirmed the retention of a *cis* stereochemical arrangement for the carbonyl ligands. The $^{13}C\{^1H\}$ NMR spectrum (***Figure 4.10***) displayed a doublet of doublets at δ 186.9 (d, J_{PC} = 9.9 Hz; d, J_{PC} = 106.7 Hz) and a triplet resonance at δ 194.2 (J_{PC} = 15.5 Hz). Two ν_{CO} bands at 2102 and 2027 cm^{-1} are observed by IR spectroscopy and are in a comparable position to those in **2** (2106 and 2030 cm^{-1}).

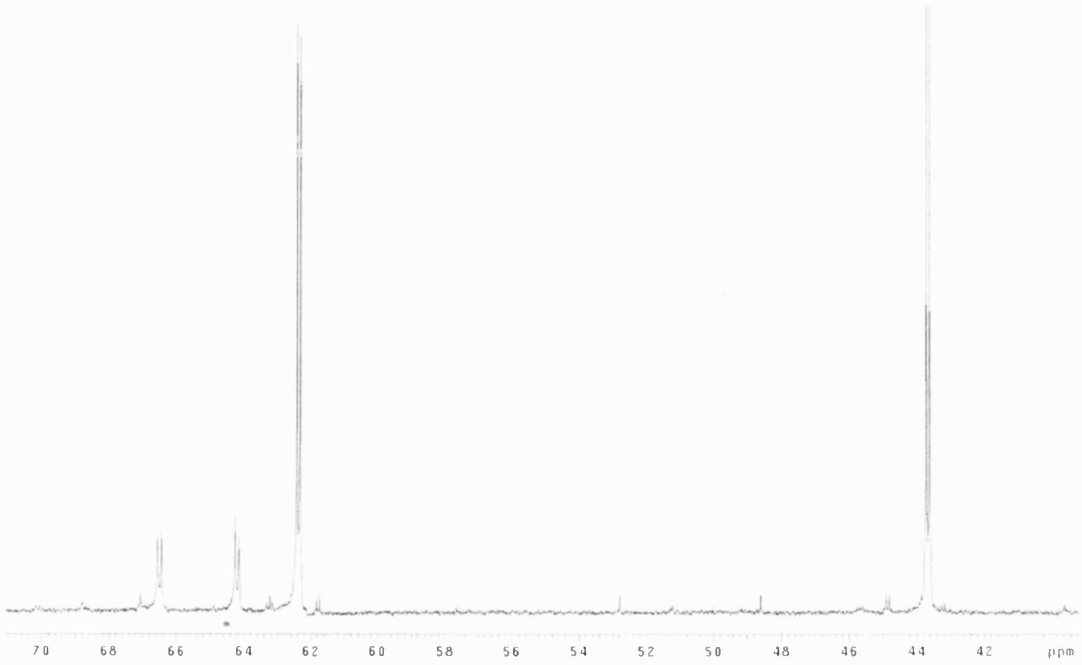

Figure 4.9: *The $^{31}P\{^{1}H\}$ NMR spectrum (162 MHz) of [Ru(dppe-Me)(CO)$_2$(OTf)$_2$] (**2Me**).*

Figure 4.10: *The $^{13}C\{^{1}H\}$ NMR spectrum (100 MHz) of [Ru(dppe-Me)(CO)$_2$(OTf)$_2$] (**2Me**) showing the carbonyl region of the spectrum.*

Of particular interest was the ^{19}F NMR spectrum (***Figure 4.11***) which, as in the case of **2**, displayed two quartet resonances at δ -77.5 and δ -78.2. These resonances had a

significant ^{19}F-^{19}F coupling constant (J_{FF} = 3.2 Hz) which, as in the case of **2**, was too large to be a purely through bond coupling interaction (refer to ***Section 2.4***).[5,7]

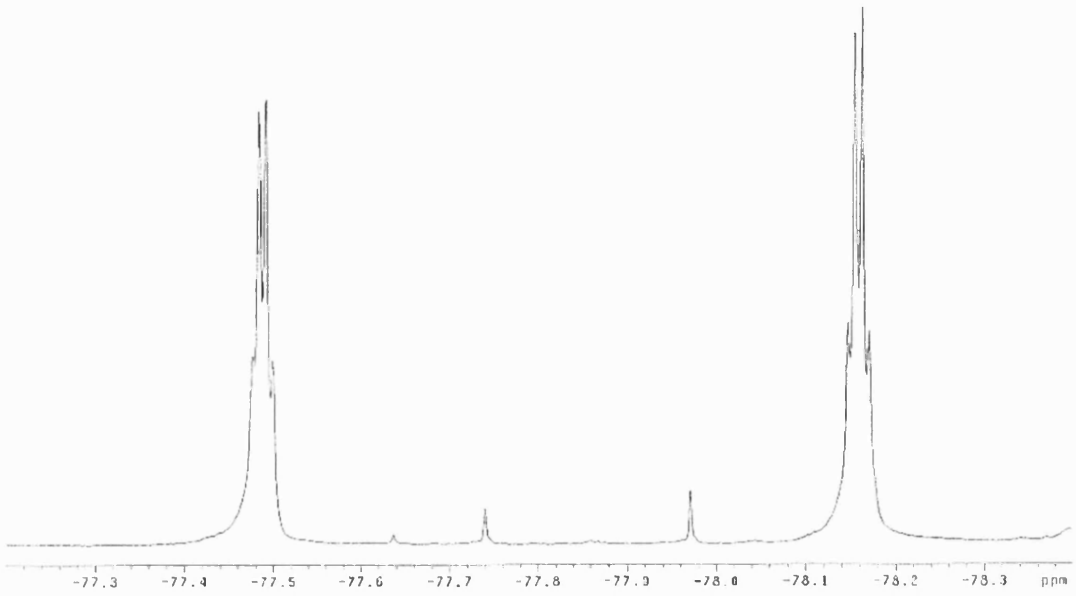

Figure 4.11: *The ^{19}F NMR spectrum (376 MHz) of [Ru(dppe-Me)(CO)$_2$(OTf)$_2$] (**2Me**) showing the large F-F couplings.*

^{19}F-^{19}F NOESY spectra of a CD_2Cl_2 solution of **2Me** were recorded at 300 K and 240 K with a mixing time (τ_m) of 100 ms (***Figure 4.12*** *and* ***4.13*** *respectively*). The spectra show that the two triflate groups at δ -77.5 and –78.2 exchange with each other, and also with free triflate (seen at δ -78.7) at ambient temperature. Lowering the temperature to 240 K eliminates this exchange process and weak NOE cross peaks are observed between the two CF_3 groups. Thus the same conclusion can be reached as from the ^{19}F-^{19}F NOESY experiments of **2** that while there is some through space ^{19}F-^{19}F coupling, there is also a contribution from through bond coupling.

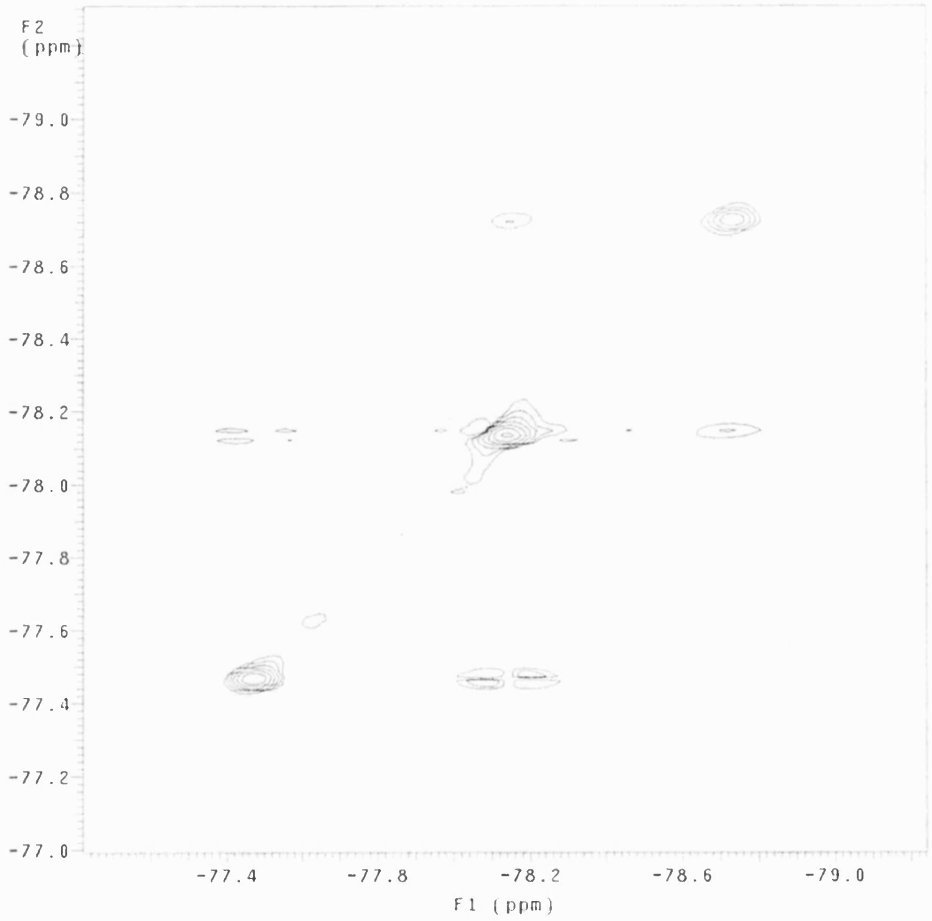

Figure 4.12: *^{19}F NOESY (376 MHz) spectrum (CD_2Cl_2) of [Ru(dppe-Me)$(CO)_2(OTf)_2$] (**2Me**) at 300 K.*

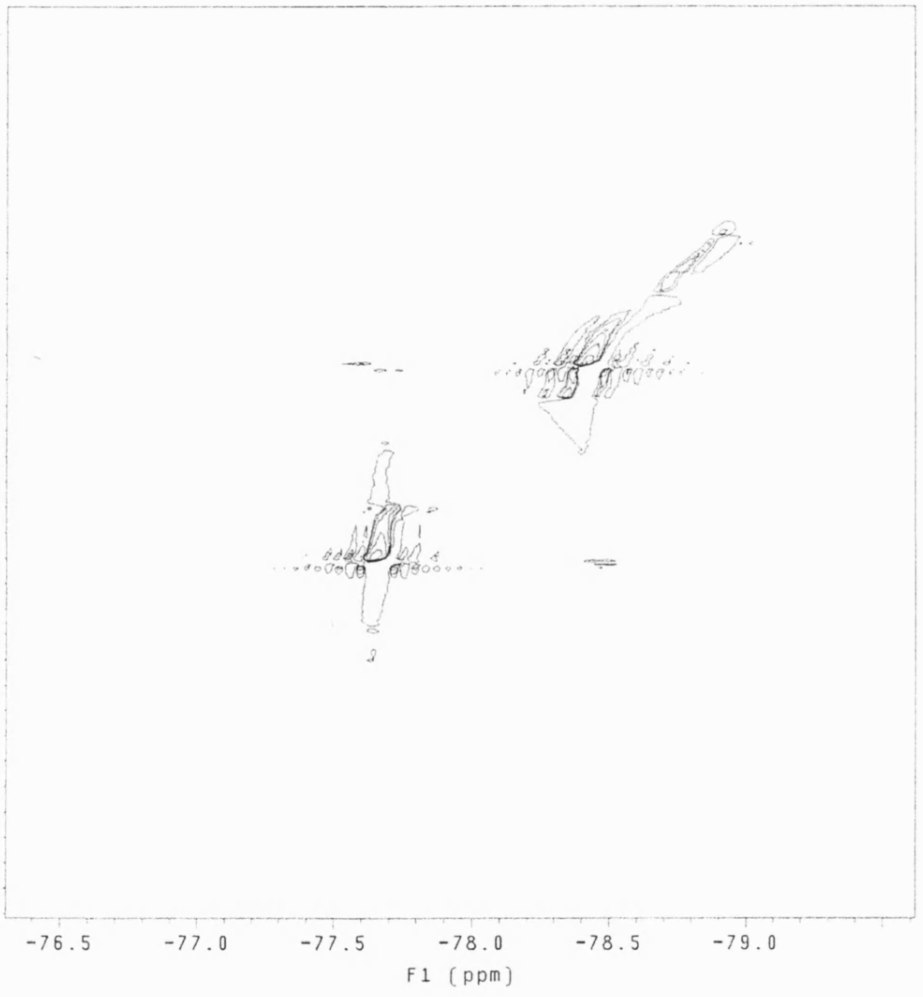

Figure 4.13: *^{19}F NMR NOESY spectrum at 240 K (376 MHz). The extended diagonal peak at δ-78.2 has overlapping contributions from one Ru-OTf and free OTf. Most importantly, there is no cross peak from the free triflate component.*

4.7 Reaction of [Ru(dppe-Me)(CO)$_2$(OTf)$_2$] (2Me) with H_2O

The formation of [Ru(dppe-Me)(CO)$_2$(OTf)$_2$] (**2Me**) was accompanied by the trace quantities of the mono aqua complex [Ru(dppe-Me)(CO)(H_2O)(OTf)$_2$]. This complex appeared as a pair of doublets at δ 66.5 and δ 64.4 (J_{PP} = 19.0 Hz) in the $^{31}P\{^1H\}$ NMR spectrum and as a pair of quartets at δ - 78.73 and δ -78.18 (J_{FF} = 3.0 Hz) in the ^{19}F NMR spectrum. The IR spectrum showed a single ν_{CO} stretching band at 1988 cm^{-1}. Attempts to synthesise **3Me** quantitatively from **2Me** by exposure to atmospheric moisture were not conducted.

Kinetic $^{31}P\{^1H\}$ NMR experiments were run on CD_2Cl_2 solutions of **2Me** upon addition of ~10 equivalents of H_2O. A similar pattern of reactivity was seen to that of as previously for **4a** upon the addition of H_2O (***Figure 4.14***), with the immediate formation of a singlet species at δ 67.3 and rapid consumption of the mono aqua species. However, even upon running experiments with high amounts of H_2O (up to 100 equivalents) coupled with extended reaction times monitored over a number days, never resulted in the reaction going through to completion with the appearance in the spectrum of just [Ru(dppe-Me)(CO)(H_2O)$_3$]$^{2+}$ complex. Heating the reaction mixture up to 50 °C similarly had no effect. More surprising was the fact that the tris aqua analogue (**4Me**), which we assign to the singlet resonance at δ 53.0, did not crystallise from the solution. Numerous solvents were tried but were unsuccessful and this precluded us from further characterisation of the product by either multi nuclear NMR or X-ray crystallography.

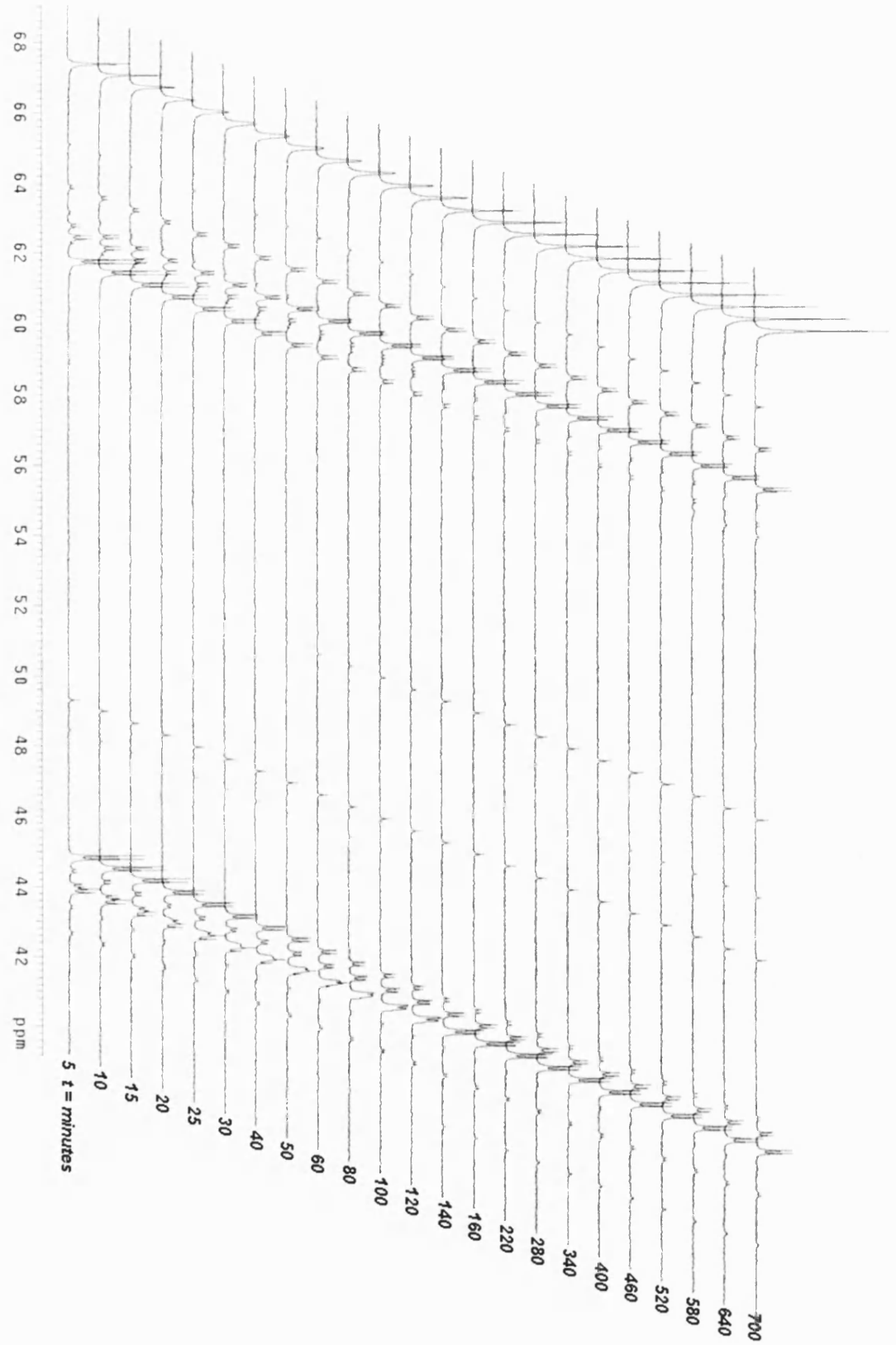

Figure 4.14: *Kinetic $^{31}P\{^{1}H\}$ NMR (162 MHz) spectrum upon addition of H_2O to a CD_2Cl_2 solution of* ***2Me****.*

4.8 Conclusion

Although it was possible to make [Ru(dppe-R)$(CO)_2(Cl)_2$] species poor separation of the isomers combined with low yields proved to make the compounds (where R = F and OMe) unviable for the preparation of their respective tris aqua analogues. The most successful of the phosphines used was dppe-Me, where the tris aqua analogue was identified in solution by $^{31}P\{^1H\}$ NMR, but could not be isolated for further characterisation.

4.9 References

1. Mirabelli, F. L.; Girad, G. R.; Bryan, D. B.; Sutton, B. M.; O'Leary Bartus, J.; Crooke, S. T.; Johnson, R. K. *J. Med. Chem.* **1987**, *30*, 2181.
2. Burt, R. J.; Chatt, J.; Hussain, W.; Leigh, G. J. *J. Organomet. Chem.* **1979**, *182*, 203.
3. Taylor, A. J. D. Phil, University of York, York, UK, **1993**.
4. Chatt, J.; Hussain, W.; Leigh, G. J.; Mohd, Ali. H.; Pickett, C. J.; Rankin, D. A. *J. Chem. Soc, Dalton. Trans.* **1985**, 1131.
5. Mahon, M. F.; Whittlesey, M. K.; Wood. P. T. *Organometallics.* **1999**, *18*, 4068.
6. Barnard, C. F. J. D.Phil, University of York, York, UK, **1978**.
7. Ernst, L.; Ibrom. K. *Angew. Chem, Int. Ed. Engl.* **1995**, *34*, 1881.

Chapter 5

The synthesis of a bidentate N-N aqua complex

5.1 Introduction

Ruthenium poly(bipyridines) have been widely studied because of their activity in water gas shift reactions.[1-4] In these processes the catalytic cycles and the structures of the probable intermediates are relatively well documented.[5,6] The corresponding reactions with ruthenium carbonyl mono(bipyridines) have been studied less frequently. $[Ru(bpy)(CO)_2Cl_2]$, the analogous species to $[Ru(dppe)(CO)_2Cl_2]$, is known to be an excellent catalyst for the photochemical and electrochemical reduction of CO_2 into formate.[7] Ziessel et al have proposed a mechanism for electrocatalytic reduction of CO_2. The mechanism is proposed to proceed through protonation of bound CO_2 to a carboxylic complex followed by rearrangement to a formate complex. Subsequent substitution by Cl^- would release formate.

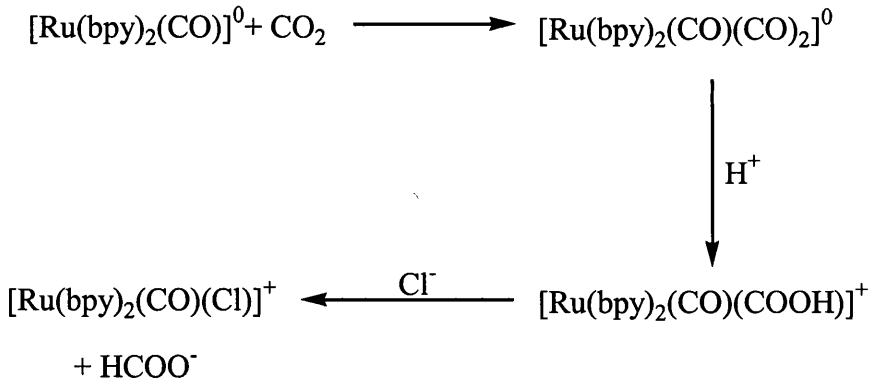

Scheme 5.1: *Proposed mechanism of the photochemical reduction of CO_2 to formate using $[Ru(bpy)_2(CO)]$ and $[Ru(bpy)(CO)_2Cl_2]$ as the catalyst.*[7]

$[Ru(dppe)(CO)_2Cl_2]$ (**1**) was used as the precursor for the formation of **2** and **4**, and thus experiments were conducted using $[Ru(Me_2bpy)(CO)_2Cl_2]$ and the known complex $[Ru(Me_2bpy)(CO)_2(OTf)_2]$ as precursors in an attempt to produce the N-N analogue of **4**, $[Ru(Me_2bpy)(CO)(H_2O)_3]^{2+}$. It should be noted here that we used *trans*-

[$Ru(Me_2bpy)(CO)_2Cl_2$] which however does form all-*cis*-[$Ru(Me_2bpy)(CO)_2(OTf)_2$] which could be used as the precursor into aqua chemistry (***Scheme 5.2***).

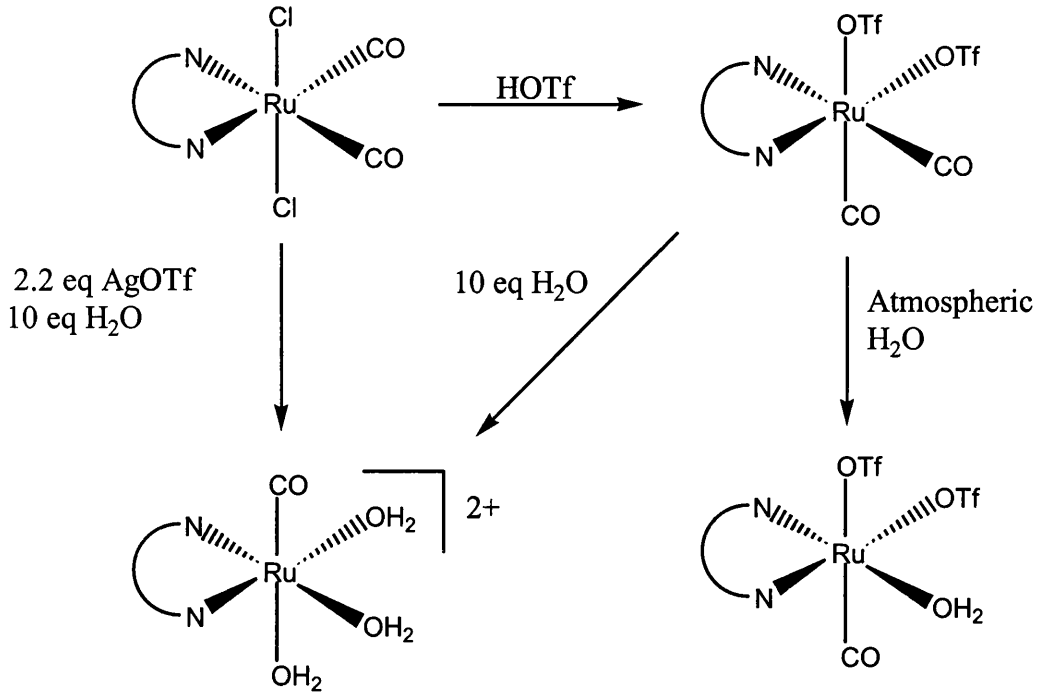

Scheme 5.2: *Proposed route of entry into aqua complexes.*

The replacement of the dppe ligand by a bpy ligand resulted in the loss of the most important spectroscopic reporter ligand and technique, $^{31}P\{^1H\}$ NMR. Thus heavier reliance was placed upon ^1H NMR and IR spectroscopy. As a result of this, Me_2bpy was used rather than bpy in order to obtain a CH_3 spectroscopic handle with which to determine the stereochemistry of the products.

5.2 Synthesis of *trans*-[Ru(Me$_2$bpy)(CO)$_2$Cl$_2$]

In principle [Ru(Me$_2$bpy)(CO)$_2$Cl$_2$] complexes can exist in three stereoisomeric forms, although the *trans*-CO isomer is thermodynamically unfavourable.[8] Several preparative routes have been reported by several different authors,[9,10] but in general the starting precursor is [Ru(CO)$_2$Cl$_2$]$_n$, which is made from RuCl$_3$.xH$_2$O (***Scheme 5.3***).[11]

Cis, cis, trans-[Ru(Me$_2$bpy)(CO)$_2$Cl$_2$] was synthesised using the preparation of Anderson et al,[11] which involved refluxing a methanolic solution of [Ru(CO)$_2$Cl$_2$]$_n$ and Me$_2$bpy for 30 minutes. The product precipitated from the solution and was recrystallised from boiling CHCl$_3$. An IR spectrum of the crystalline material displayed two ν_{CO} stretching bands at 2060 and 1989 cm^{-1}, indicative of a *cis* arrangement of the carbonyl groups.

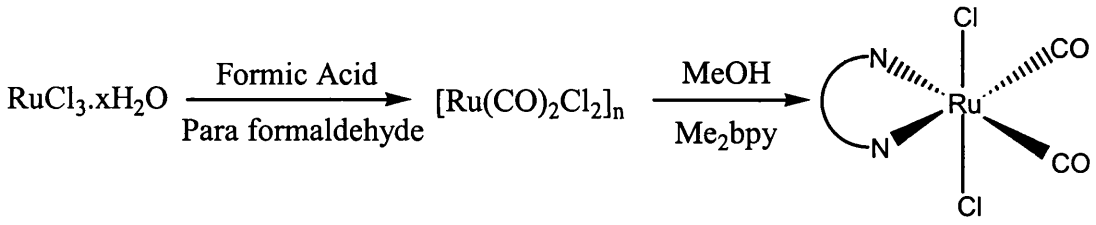

Scheme 5.3: *Synthetic route to trans-[Ru(Me$_2$bpy)(CO)$_2$Cl$_2$].*

It was previously noted by Black et al[12] that *cis, cis, trans*-[Ru(N-N)(CO)$_2$Cl$_2$] complexes can be reacted with HOTf (and other derivatives such as RCO$_2$Ag, where R = Me or CF$_3$) to form [Ru(N-N)(CO)$_2$(OTf)$_2$] species.[12-15] They also noted two important observations; firstly that if the bidentate N-N ligand being used was 1,10-phenanthroline, retention of the stereochemistry occurred in the product; secondly, if bpy

or Me_2bpy were used, the reaction involved a stereochemical change from *cis, cis, trans*-$Ru(N\text{-}N)(CO)_2Cl_2$ to all-*cis*-$[Ru(N\text{-}N)(CO)_2(OTf)_2]$ species (***Scheme 5.4***).

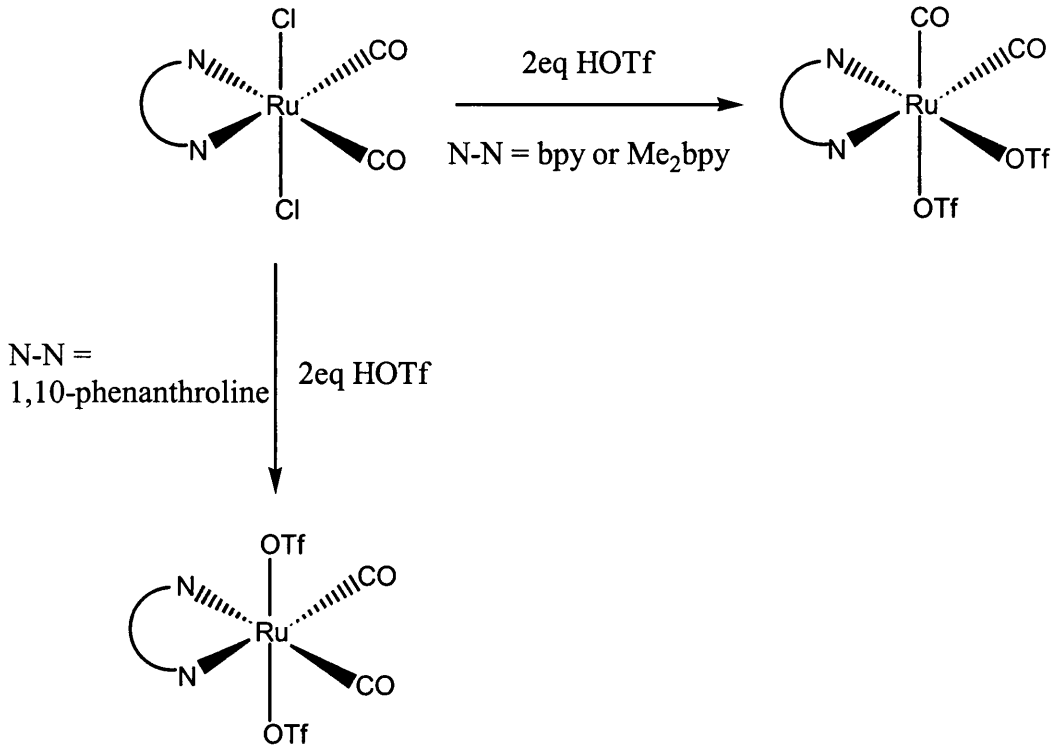

Scheme 5.4: *Stereochemical differences observed for the reaction of cis, cis, trans-[Ru(N-N)(CO)$_2$Cl$_2$] with HOTf dependent upon the bidentate N-N ligand used.*

As $[Ru(dppe)(CO)_2(OTf)_2]$ (**2**) was used as the precursor to make the aqua compounds **3** and **4a**, mainly due to the lability of the coordinated triflate groups, which have also been shown to be labile in $[Ru(N\text{-}N)(CO)_2(OTf)_2]$ compounds (***Figure 5.1***), the same route was tried for the N-N analogue.[12]

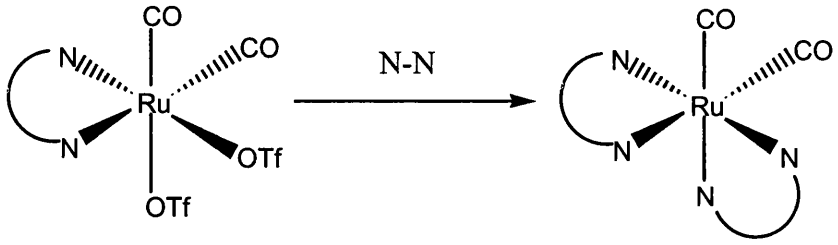

Figure 5.1: *Lability of the coordinated OTf groups where N-N = phen or bpy as demonstrated by Black et al.*[12]

All-*cis*-[Ru(Me_2bpy)(CO)$_2$($OTf)_2$] was prepared by the reaction of *cis*, *cis*, *trans*-Ru(Me_2bpy)(CO)$_2Cl_2$ in 1,2-dichlorobenzene with HOTf added dropwise by a syringe (platinum needle) and the resultant mixture subsequently refluxed for 1.5 hr at 110 °C.[11] The reaction mixture was cooled to 0 °C and the complex precipitated by the addition of Et_2O. An IR spectrum of the compound displayed two ν_{CO} stretching bands at 2099 and 2027 cm^{-1} which are approximately 30 cm^{-1} to higher wave number compared to the di-chloride precursor, reflecting the weaker donor ability of triflate compared to chloride. This is consistent with the preparation of [Ru(dppe)(CO)$_2$($OTf)_2$] which displayed ν_{CO} stretching bands at 2106 and 2030 cm^{-1}, compared to 2079 and 2004 cm^{-1} as seen for the dichloride precursor **1**. The ^{1}H NMR spectrum of all-*cis*-[Ru(Me_2bpy)(CO)$_2$($OTf)_2$] displayed two singlet resonances at δ 1.27 and δ 0.89, which correspond to the two inequivalent CH_3 groups of the Me_2bpy ligand.

Attempts to react [Ru(Me_2bpy)(CO)$_2$($OTf)_2$] in CH_2Cl_2 with 10 equivalents of H_2O using the same methodology as in the synthesis of **4** and also leaving a solid sample of [Ru(Me_2bpy)(CO)$_2$($OTf)_2$] exposed to atmospheric moisture in order to form complex **3** both failed, as no reactions were seen by either route. This is perhaps not unsurprising given that the isolation of Ru(Me_2bpy)(CO)$_2$($OTf)_2$ is reported to require washing the

complex with H_2O to remove residual amounts of 4,4'-dimethyl bipyridinium trifluoromethanesulphonate.

5.3 Synthesis of $[Ru(Me_2bpy)(CO)_2(H_2O)(Cl)]^+$ (14)

The failure to make aqua complexes from all-*cis*-$[Ru(Me_2bpy)(CO)_2(OTf)_2]$ prompted us to investigate the in *situ* method preparation from *cis*, *cis*, *trans*-$Ru(Me_2bpy)(CO)_2Cl_2]$. This produced very different results from those seen with the $[Ru(dppe)(CO)_2Cl_2]$ (**1**). A CH_2Cl_2 solution of $[Ru(Me_2bpy)(CO)_2Cl_2]$ was reacted with 2.2 equivalents of AgOTf and 10 equivalents of H_2O, and the extent of the reaction was monitored by IR spectroscopy. Whereas in the dppe case, the two ν_{CO} bands of the dichloride precursor were completely replaced by a single ν_{CO} band after 1 h, a much slower reaction was observed with $[Ru(Me_2bpy)(CO)_2Cl_2]$. Two new ν_{CO} stretching bands at 2078 and 2018 cm^{-1} were seen to grow in over 2 h of reaction to approximately a 50% conversion (***Figure 5.2***).

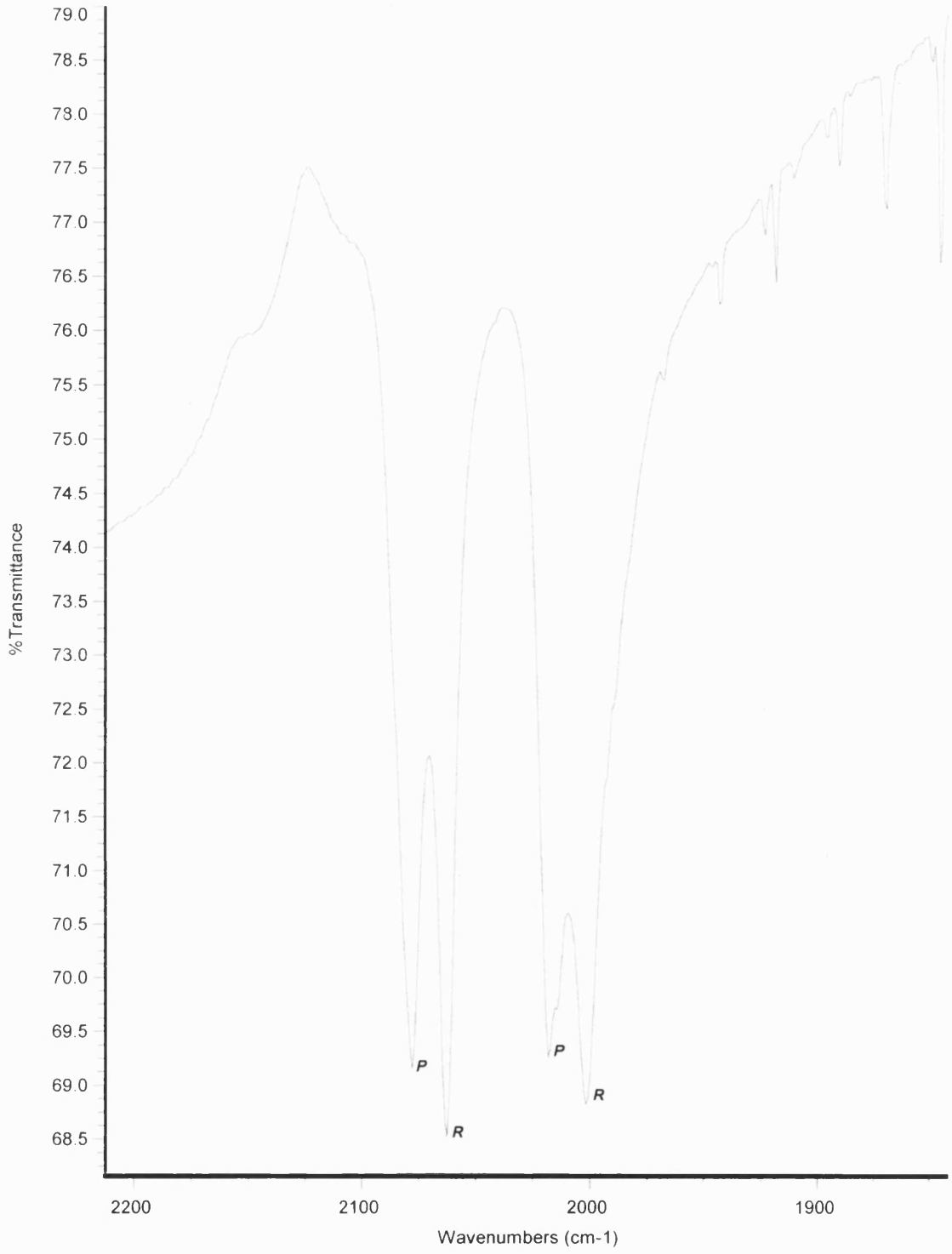

Figure 5.2: *Solution IR spectrum in CH_2Cl_2 showing the extent of the reaction between $[Ru(Me_2bpy)(CO)_2Cl_2]$ (**R**) with AgOTf and H_2O after 2 h forming the product (**P**).*

A further 2 days were required for the reaction to go to completion (as shown by IR) and the resultant product was collected by filter cannula to remove AgCl, which had precipitated during the reaction. The ^{1}H NMR spectrum of the product showed only one – CH_3 singlet resonance at δ 2.74, suggesting that both halves of the Me_2bpy ligand were in a symmetrical environment. Thus with the knowledge that two ν_{CO} bands are observed by IR, then the core structure of the product must be as depicted in ***Figure 5.3***.

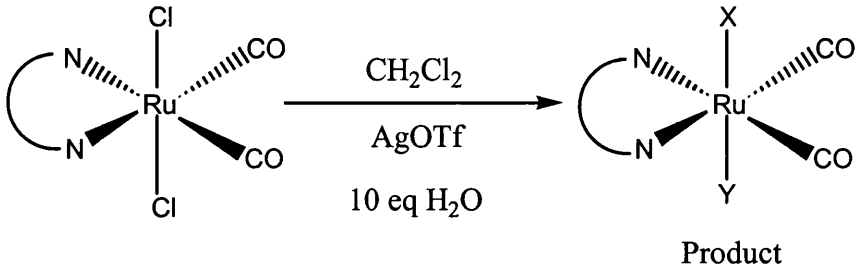

Product

Figure 5.3: *Observation of the product stereochemistry based on IR and ^{1}H NMR spectroscopy.*

The ^{19}F NMR spectrum confirmed that the unknown groups x and y (***Figure 5.3***) in the product, were not coordinated triflate as only a singlet resonance at δ -79.61 corresponding to anionic, uncoordinated triflate was observed. No further evidence for the structure could be obtained from multi-nuclear NMR experiments. Crystals of the product, suitable for X-ray determination, were grown from CH_2Cl_2/H_2O layered with Et_2O. The structure was found to be the mono aqua complex $[Ru(Me_2bpy)(CO)_2(H_2O)(Cl)]^+$ (**14**) (***Figure 5.4***). Selected bond lengths [Å] and angles [°] are given in ***Table 5.1***.

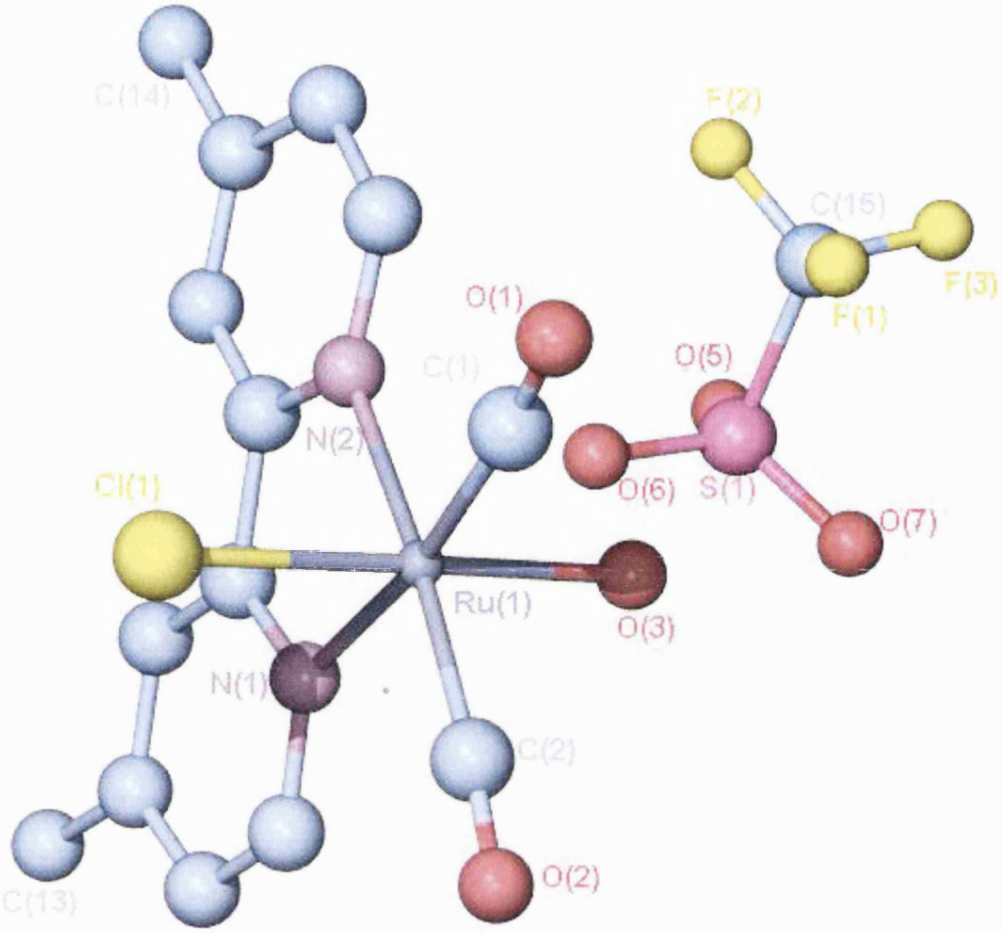

Figure 5.4: *Plot of* $[Ru(Me_2bpy)(CO)_2(H_2O)(Cl)]^+$ ***(14)***.

Ru(1)-C(1)	1.8994(17)	Ru(1)-N(1)	2.1115(13)
Ru(1)-C(2)	1.8856(17)	Ru(1)-N(2)	2.1136(13)
Ru(1)-Cl(1)	2.3569(4)	Ru(1)-O(3)	2.1104(12)
O(1)-C(1)	1.127(2)	O(2)-C(2)	1.135(2)
N(1)-Ru(1)-N(2)	77.36(5)	O(3)-Ru(1)-Cl(1)	175.19(4)
C(2)-Ru(1)-C(1)	89.36(7)	N(1)-Ru(1)-O(3)	87.68(5)
C(2)-Ru(1)-N(2)	174.13(6)	C(1)-Ru(1)-N(1)	172.20(6)
C(2)-Ru(1)-N(1)	96.96(6)		

Table 5.1: *Selected bond lengths [Å] and angles [°] for* ***14****.*

Compound **14** has essentially octahedral geometry around the metal centre without any major distortions. The Ru-N bond distances are essentially equal to each other as expected due to the symmetry within the molecule. These distances are comparable to those found in the starting material where the average Ru-N distance is 2.108 Å.[3] The coordinated H_2O has a Ru-O bond length of 2.110(4) Å which is significantly shorter than those reported for [Ru(dppe)(CO)(H_2O)($OTf)_2$] (**3**) and [Ru(dppe)(CO)(H_2O)($C_5H_5N)_2$]$^{2+}$ (**8a**) where the Ru-O bond distances are 2.198(5) and 2.134(4) Å respectively.

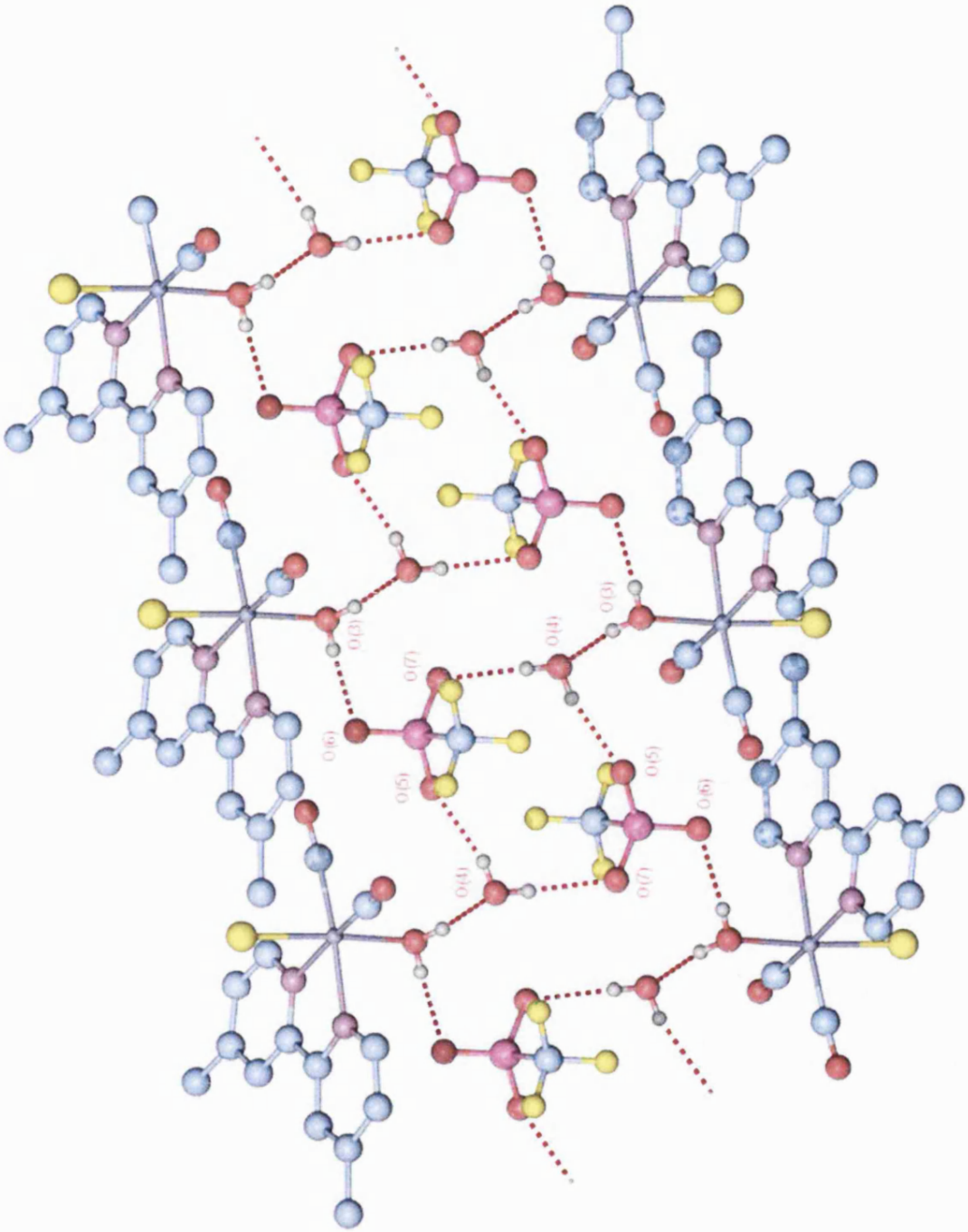

Figure 5.5: *Hydrogen bonding network of* ***14****.*

The gross lattice structure is dominated by hydrogen bonding interactions. The hydrogens of the coordinated water molecule O(3) are hydrogen bonded to the lattice water O(4) and also to O(6) of the free triflate anion, O(4) is hydrogen bonded to O(5) and O(7) of triflate to form a ribbon like structure.

The experiment to form **14** was repeated again using 2.2 equivalents of AgOTf to see if partial metathesis still occurred but also up to 30 equivalents of H_2O was used in an attempt to speed up to the reaction. In both cases, the same product and the same reaction times were observed. Due to the increased amount of H_2O used, two layers formed, a lower yellow coloured CH_2Cl_2 layer containing the precursor and a pale yellow H_2O upper layer which contained the product **14**. It was found that **14** is exceptionally soluble in H_2O and crystals suitable for X-ray determination were grown from a concentrated H_2O solution of **14** in addition to the method described in this section.

5.4 Preliminary solution reactivity studies of 14

Some preliminary reactivity studies were conducted on **14** to probe the lability of the axial H_2O ligand. Firstly, it was observed that as in the case of many of the complexes seen in ***chapter 3*** dissolution of a solid sample of **14** in dry CD_2Cl_2 caused the H_2O ligand to be displaced by an OTf ligand. This was observed by ^{19}F NMR with the appearance of a singlet resonance at δ -77.64, consistent with coordinated triflate.[16] Addition of 10 equivalents of H_2O to this sample caused the coordinated OTf ligand to shift to δ -79.45 in the ^{19}F NMR spectrum (***Figure 5.6***). No reaction was seen when either an acetone/H_2O or H_2O solution of **14** was reacted with one 1 atm of CO. This is consistent with the behaviour of $[Ru(dppe)(CO)(H_2O)(C_5H_5N)_2]^{2+}$ (**8a**) which also did not react with CO.

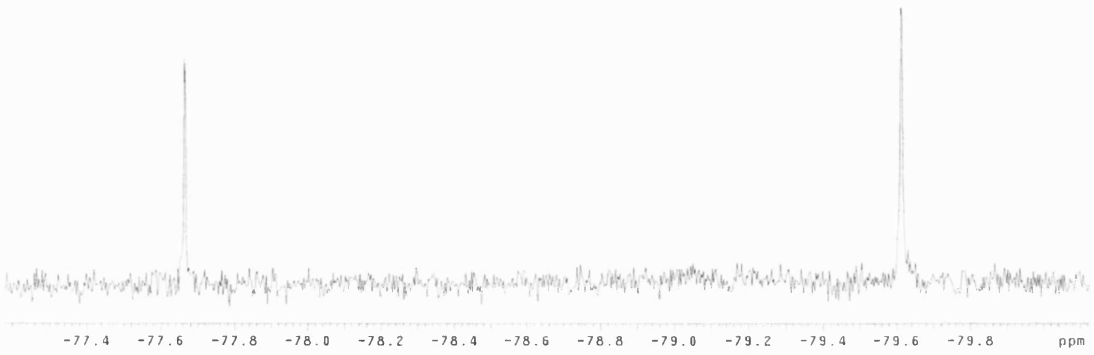

Figure 5.6: *^{19}F NMR spectrum (376 MHz) of* ***14*** *in CD_2Cl_2 solution without the presence of H_2O which shows two species to be present in solution.*

5.5 Conclusion

Although it was possible to synthesise an aqua complex from $[Ru(Me_2bpy)(CO)_2Cl_2]$, it was only possible to form a mono aqua species **14**, rather than a tris aqua species. **14** proved to be exceptionally water soluble and as a result future investigations into the reaction chemistry of the compound should be possible in fully aqueous media.

5.6 References

1. Richmond, M. G. *J. Organomet. Chem.* **1993**, *457*, 121.

2. Kelly, J. M.; Vos, J. G. *Angew. Chem., Int. Ed. Engl.* **1982**, *21*, 628.

3. Haasnoot, J. G.; Hinrichs, W.; Weir, O.; Vos, J. *Inorg. Chem.* **1986**, *25*, 4140.

4. Ishida, H.; Tanaka, K.; Morimoto, M.; Tanaka, T. *Organometallics* **1986**, *5*, 724.

5. Tanaka, H.; Nagao, H.; Tanaka, K. *Inorg. Chem.* **1992**, *31*, 1971.

6. Vleck, A. Jr. *Inorg. Chem.* **1993**, *4*, 1.

7. Lehn, J. M.; Ziesel, R. *J. Organomet. Chem.* **1990**, *382*, 157.

8. Barnard, C. F. J.; Daniels, J. A.; Jefferey, J.; Mawby, R. J. *J. Chem. Soc., Dalton Trans.* **1976**, 953.

9. Haukka, M.; Kiviaho, J.; Ahlgrén, M.; Pakkanen, T. A. *Organometallics.* **1995**, *14*, 825.

10. Chardon-Noblat, S.; Deronzier, A.; Ziessel, R.; Zsoldos, D. *Inorg. Chem.* **1997**, *36*, 5384.

11. Anderson, P. A.; Deacon, G. B.: Haarmann, K. H.; Keene, R. F.; Meyer, T. J.; Reitsma, D. A.; Skelton, B. W.; Strouse, G. F.; Thomas, N. C.; Treadway, J. A.; White, A. H. *Inorg. Chem.* **1995**, *34*, 6145.

12. Black, St. C. D.; Deacon, G. B.; Thomas, N. C. *Polyhedron*, **1983**, *5*, 409.

13. Colton, R.; Farthing, R. H. *Aust. J. Chem.* **1967**, *20*, 1283.

14. Colton, R.; Farthing, R. H. *Aust. J. Chem.* **1971**, *24*, 903.

15. Collman, J. P.; Roper, W. R. *J. Am. Chem. Soc.* **1965**, *87*, 4008.

16. Lawrance, G. A. *Chem. Rev.* **1986**, *86*, 17.

Chapter 6

Experimental

6.1 General comments

All reactions were carried out using standard Schlenk and high vacuum techniques. CH_2Cl_2 was distilled from either CaH_2 or P_2O_5. Water was doubly distilled and degassed prior to use. Diethyl ether, THF and hexane were distilled from purple solutions of sodium dispersion / benzophenone and ethanol was distilled from magnesium and iodine. Deuterated solvents (Goss) were dried over CaH_2 ($CDCl_3$ and CD_2C1_2); $(CD_3)_2CO$ $(CD_3)_2SO$ and CD_3CN were freeze-pump-thaw degassed while D_2O was degassed by bubbling with argon. AgOTf, $AgBF_4$ and $AgSbF_6$ (Lancaster) were handled in a nitrogen filled glovebox. 2,2'-bipyridyl (bpy) and 4,4'-dimethyl-2,2'-bipyridyl (Me_2bpy) (Aldrich), propanethiol (Aldrich), CO (BOC, 99.9%), ^{13}CO (Promochem, 99%), $Ru_3(CO)_{12}$ (Aldrich) and $RuCl_3.xH_2O$ (Johnson-Matthey) were used as received. 4-bromofluorobenzene (Aldrich) was used as supplied, except degassed under argon. Bis-1,2-dichlorophosphinoethane (Avocado) was degassed by freeze-pump-thaw techniques. *p*-methoxyphenylmagnesiumbromide and *p*-tolylmagnesiumbromide (Aldrich) were used as supplied from a Sure Seal bottle.

^1H NMR spectra were recorded on Bruker AVANCE 300 or Varian Mercury 400 MHz NMR spectrometers and referenced to residual protio solvent resonances (chloroform δ 7.27, acetone δ 2.05). All spectra were recorded in mixtures of d^6-acetone and H_2O unless otherwise stated. $^{31}P\{^1H\}$ and ^{19}F NMR chemical shifts were referenced externally to 85% H_3PO_4 and $CFCl_3$ respectively (both at δ 0.00). $^{13}C\{^1H\}$ NMR spectra were referenced to d^6-acetone at δ 30.6. ^1H COSY, ^1H-^{13}C HMQC and HMBC experiments were performed on the AVANCE spectrometer using standard Bruker pulse sequences. Peak positions are given in ppm and coupling constants in hertz. IR spectra were recorded on a Nicolet Protégé 460 FTIR spectrometer. Elemental analyses were performed at the University of Bath.

6.2 Compounds relating to Chapter 2

Preparation of all-*cis*-Ru(dppe)$(CO)_2Cl_2$ (1). $RuCl_3.3H_2O$ (4.0 g, 15.0 mmol) in a mixture of conc. HCl (80 mL) and formic acid (80 mL) was refluxed for 9 h until golden yellow. The solvent was removed under reduced pressure to yield the orange/yellow residue, $[Ru(CO)_3(Cl)_2]_2$. The residue was dissolved in 2-methoxyethanol (100 mL) and dppe (5.6 g, 14.0 mmol) was added and stirred until dissolved. The mixture was refluxed for 2.5 h until a creamy precipitate, $[Ru(dppe)(CO)_2(Cl)_2]_{1.14}$ {(IR (nujol mull, cm^{-1}) 2047 (ν_{CO}), 1985 (ν_{CO})} crashed out of solution. This was collected by filtration and dried. Portions of $[Ru(dppe)(CO)_2(Cl)_2]_{1.14}$ were heated to 270 °C in an ampoule placed under 1 atmosphere of CO. The precipitate melted, forming a yellow glass on cooling, which was extracted with $CHCl_3$ and filtered through Celite. IR and NMR studies revealed that isomers of $[Ru(dppe)(CO)_2Cl_2]$ were present. Separation was achieved with column chromatography using silica gel 60 and a 95:5 mixture of $CHCl_3$:MeOH as the eluent. The first fraction obtained was found to be **1**. Analytically pure white crystals were grown from a solution of CH_2Cl_2/hexane. $^{31}P\{^1H\}$ NMR: δ 63.0 (d, J_{PP} = 9.7 Hz), 38.1 (d, J_{PP} = 9.7 Hz). $^{13}C\{^1H\}$ NMR: δ 192.9 (dd, J_{PC} = 13.7 Hz, J_{PC} = 10.7 Hz, CO), 189.7 (dd, J_{PC} = 9.6 Hz, J_{PC} = 117.5 Hz, CO). IR (nujol mull, cm^{-1}): 2079 (ν_{CO}), 2004 (ν_{CO}). Anal. Found (calcd) for $RuC_{28}H_{24}P_2O_2Cl_2$: C, 51.89 (53.68); H, 3.79 (3.86).[1,2]

Ru(dppe)$(CO)_2(OTf)_2$ (2). Silver triflate (0.27 g, 1.06 mmol) was added to a Schlenk tube containing a stirred solution of **1** (0.30 g, 0.48 mmol) in CH_2Cl_2 (10 mL). The solution was stirred at room temperature with the exclusion of light for 1 h and then filtered under argon. The filtrate was then concentrated to 5 mL, and diethyl ether (15 mL) was added to induce precipitation of a white solid. The solution was reduced by 50% to

maximise precipitation and left to stir for 30 minutes with exclusion of light. The remaining solvent was removed by filter-cannula to leave a white solid, which was washed with ether and dried under vacuum (0.18 g, 50% yield). ^{1}H NMR ($CDCl_3$): δ 7.35-7.85 (20H, br, PC_6H_5), 3.06 (2H, m, PCH_2), 2.75 (2H, m, PCH_2). $^{31}P\{^{1}H\}$ NMR: δ 66.3 (d, J_{pp} = 16.2 Hz), 44.5 (d, J_{PP} = 16.2 Hz), ^{19}F NMR: δ -77.66 (q, J_{FF} = 3.45 Hz, CF_3), - 76.91 (q, J_{FF} = 3.45 Hz, CF_3). $^{13}C\{^{1}H\}$ NMR: δ 193.6 (t, J_{PC} = 14.9 Hz, CO), 186.0 (dd, J_{PC} = 108.0 Hz, J_{PC} = 9.9 Hz, CO). IR (CH_2Cl_2, cm^{-1}): 2106 (ν_{CO}), 2030 (ν_{CO}). Anal. Found (calcd) for $RuC_{30}H_{24}P_2O_8S_2F_6 \cdot 1.2H_2O$: C, 41.76 (42.21); H, 2.90 (2.83).[3]

Ru(dppe)(CO)(H_2O)($OTf)_2$ (3). In a typical experiment, a solid sample of **2** (0.04 g, 0.047 mmol) was left in the air at room temperature for 3 weeks. The sample, which slowly changed colour from white to brown, was periodically checked by IR spectroscopy until only a single band for ν_{CO} at 2001 cm^{-1} was seen. Recrystallisation from CH_2Cl_2/hexane afforded colourless crystals of **3** suitable for X-ray diffraction (0.026 g, 0.031 mmol, 66% yield). ^{1}H NMR ($CDCl_3$, 293 K): 7.95-7.38 (20H, m, ph), 2.95 (2H, m, PCH_2), 2.50 (2H, m, PCH_2). $^{31}P\{^{1}H\}$ NMR: δ 67.5 (d, J_{PP} = 19.3 Hz), 65.5 (d, J_{PP} = 19.3 Hz). ^{19}F NMR: δ -78.19 (q, J_{FF} = 3.84 Hz, CF_3), -77.63 (q, J_{FF} = 3.84 Hz, CF_3). $^{13}C\{^{1}H\}$ NMR: δ 197.0 (t, J_{PC} = 17.7 Hz, CO). IR ($CHCl_3$, cm^{-1}): 2001 (ν_{CO}). Anal. Found (calcd) for $RuC_{29}H_{26}P_2O_8S_2F_6$: C, 40.41 (40.80); H, 3.09 (3.11).[3]

[Ru(dppe)(CO)($H_2O)_3$][$OTf]_2$ (4a). To a solution of **2** (0.07 mg, 0.082 mmol) in CH_2Cl_2 (5 mL) was added 10 equivalents of water (15 μL, 0.83 mmol). Pale yellow crystals of **4a** slowly crystallised from the solution after 2 days at 5 °C (0.06 g, yield 85%). ^{1}H NMR (d^6-acetone/H_2O, 293 K): δ 7.98-7.90 (6H, m, PC_6H_5), 7.55-7.50 (10H, m, PC_6H_5), 7.37 (2H, m, PC_6H_5), 6.94 (2H, m, PC_6H_5), 3.49-3.43 (2H, m, PCH_2), 3.14-3.08 (2H, m, PCH_2).

$^{31}P\{^1H\}$ NMR: δ 66.5 (s). ^{19}F NMR: δ -79.20 (s). $^{13}C\{^1H\}$ NMR: δ 198.3 (t, J_{CP} = 17.9, CO).

IR (KBr, cm^{-1}): 1990 vs (ν_{CO}). Anal. Found (calcd) for $RuC_{29}H_{34}P_2O_{12}S_2F_6 \cdot 1.8\ H_2O$: C, 38.56 (38.19): H, 3.57 (3.71). Larger quantities of **4a** were more easily prepared by addition of AgOTf (0.27 g, 1.06 mmol) to a solution of **1** (0.30 g, 0.48 mmol) in 15 mL of CH_2Cl_2 followed immediately by water (86 μL, 4.77 mmol). After the mixture was stirred for 90 min with the total exclusion of light, the precipitate of AgCl was removed by filtration and the pale yellow filtrate concentrated by half. Crystals of **4a** slowly precipitated out of solution (0.13 g, yield 43%).[3]

[Ru(dppe)(CO)(H_2O)$_3$][BF_4]$_2$ (4b). To a solution of **1** (0.10 g, 0.159 mmol) in CH_2Cl_2 (25 mL), 2.2 equivalents of $AgBF_4$ (0.068 g, 0.349 mmol) was added, followed immediately by 30 equivalents of H_2O (86 μL, 4.77 mmol). After the mixture was stirred for 90 minutes with the total exclusion of light, the precipitate of AgCl was removed by filtration and the pale yellow filtrate concentrated by 50%. Crystals of **4b** slowly precipitated out of solution. $^{31}P\{^1H\}$ NMR (D_2O, 293 K): δ 67.3 (s). $^{19}F\{^1H\}$ NMR: δ -150.417 (s), -150.466 (s). $^{13}C\{^1H\}$ NMR: δ 198.0 (t, J_{PC} = 18.0 Hz, CO). IR (H_2O, CaF_2, cm^{-1}): 1992 (ν_{CO}).

[Ru(dppe)(CO)(H_2O)$_3$][SbF_6]$_2$ (4c). To a CH_2Cl_2 (25 mL) solution of **1** (0.10 g, 0.159 mmol) was added 2.2 equivalents of $AgSbF_6$ (0.12 g, 0.349 mmol, followed immediately by 30 equivalents of H_2O (86 μL, 4.77 mmol). After the mixture was stirred for 90 minutes with the total exclusion of light, the precipitate of AgCl was removed by filtration and the pale yellow filtrate concentrated by 50%. Crystals of **4c** slowly precipitated out of solution. $^{31}P\{^1H\}$ NMR (D_2O, 293 K): δ 67.3 (s). $^{19}F\{^1H\}$ NMR: δ -126.45 (br). $^{13}C\{^1H\}$

NMR: δ 198.0 (t, J_{PC} = 18.0 Hz, CO). IR (H_2O, CaF_2, cm^{-1}): 1994 (ν_{CO}). Anal. Found (calcd) for $RuC_{27}H_{30}P_2O_4Sb_2F_{12}$: C, 30.1 (30.8); H, 2.92 (2.87).

6.3 Compounds relating to Chapter 3

[Ru(dppe)(CO)(CH_3CN)$_3$][OTf]$_2$ (5a). A sample of **4a** (0.01 g, 0.011 mmol) was placed in a J. Young's resealable NMR tube and dissolved in CD_3CN (0.6 mL). The $^{31}P\{^1H\}$ NMR spectrum showed immediate conversion to **5a**. Removal of the solvent and recrystallisation of the residue from $CHCl_3/CH_3CN$ layered with Et_2O gave white crystals of **5a** in analytically pure form. ^1H NMR (d^6-acetone, 293 K): δ 8.04-7.60 (20H, m, PC_6H_5), 3.62-3.55 (2H, m, PCH_2), 3.34-3.27 (2H, m, PCH_2), 2.78 (6H, s, CH_3CN), 2.00 (3H, s, CH_3CN). $^{31}P\{^1H\}$ NMR (CD_3CN, 293K): δ 62.3 (s). ^{19}F NMR: δ -79.20 (s). $^{13}C\{^1H\}$ NMR: δ 194.1 (t, J_{CP} = 16.1 Hz, CO), 3.5 (s, CH_3CN), 2.2 (s, CH_3CN). IR (nujol mull, cm^{-1}): 2324 m (ν_{CN}), 2294 m (ν_{CN}), 2020 vs (ν_{CO}). Anal. Found (calcd) for $RuC_{35}H_{33}P_2O_7S_2F_6N_3$: C, 44.2 (44.30): H, 3.77 (3.50): N, 4.59 (4.43).

[Ru(dppe)(CO)(CH_3CN)$_3$][BF_4]$_2$ (5b). A sample of **4b** (0.01 g, 0.013 mmol) was placed into a J. Youngs resealable NMR tube and dissolved in CD_3CN. An immediate reaction was observed as in the case of product **5a**. Colourless crystals of **5b** were grown from a $CHCl_3/CH_3CN$ solution, layered with Et_2O, these were found to be analytically pure. $^{31}P\{^1H\}$ NMR (d^3-acetonitrile, 293K): δ 62.4 (s). IR (nujol mull, cm^{-1}): 2027 vs (ν_{CO}).

[Ru(dppe)(CO)((CH_3)$_2$SO)$_3$][OTf]$_2$ (6a). A sample of **4a** (0.010 g, 0.011 mmol) was placed in a J. Young's resealable NMR tube and dissolved in degassed $(CH_3)_2SO$ (0.6 mL). The $^{31}P\{^1H\}$ NMR spectrum showed immediate conversion to **6a**. Removal of the solvent and

recrystallisation of the residue from acetone/$(CH_3)_2SO$ layered with Et_2O gave pale yellow crystals of **6a** in analytically pure form (0.008 g, 75% yield). ^1H NMR ($(CD_3)_2SO$, 293K): δ 3.34 (12H, s, $(CH_3)_2SO$), 2.99 (6H, s, $(CH_3)_2SO$). $^{31}P\{^1H\}$ NMR: δ 64.7 (s). ^{19}F NMR: δ -79.33 (s). $^{13}C\{^1H\}$ NMR: δ 199.1 (t, J_{CP} = 17.4 Hz, CO). IR (KBr, cm^{-1}): 1973 vs (ν_{CO}). Anal. Found (calcd) for $RuC_{35}H_{42}P_2O_{10}S_5F_6$: C, 39.3 (39.66): H, 3.91 (3.99).

[Ru(dppe)(CO)(CNCMe$_3$)$_3$][OTf]$_2$ (7a). Addition of 81 μL of Me_3CNC (0.72 mmol) to a d^6-acetone/H_2O solution of **4a** (0.12 g, 0.14 mmol) gave an immediate colour change from pale yellow to colourless with the appearance of a new resonance in the $^{31}P\{^1H\}$ NMR spectrum at δ 54.8. This species fully converted to a second product at δ 52.4 over 48 hours. Layering with Et_2O gave white analytically pure crystals of **7a** (0.83 mg, 66% yield). ^1H NMR (d^6-acetone, 293 K): δ 1.79 (9H, s, Me_3CNC), 1.05 (18H, s, Me_3CNC). $^{31}P\{^1H\}$ NMR: δ 52.4 (s). ^{19}F NMR: δ -79.35 (s). $^{13}C\{^1H\}$ NMR: δ 190.8 (t, J_{CP} = 12.0 Hz, CO), 62.2 (s, Me_3CNC), 61.6 (s, Me_3CNC). IR (KBr, cm^{-1}): 2233 s (ν_{CN}), 2212 s (ν_{CN}), 2071 vs (ν_{CO}). Anal. Found (calcd) for $RuC_{44}H_{51}P_2O_7S_2F_6$: C, 48.9 (49.15): H, 4.74 (4.78): N, 3.83 (3.91).

[Ru(dppe)(CO)(CNCMe$_3$)$_3$][BF$_4$]$_2$ (7b). Addition of 38 μL of Me_3CNC (0.33 mmol) to a d^6-acetone/H_2O solution of **4b** (0.06 g, 0.080 mmol) gave an immediate colour change from pale yellow to colourless with the appearance of a new resonance in the $^{31}P\{^1H\}$ NMR spectrum at δ 54.9. This species fully converted to a second product at δ 52.4 over 48 h. Layering with hexanes gave white analytically pure crystals of **7b** (0.04 g, 57% yield). ^1H NMR (d^6-acetone, 293 K): δ 1.80 (9H, s, Me_3CNC), 1.06 (18H, s, Me_3CNC).

$^{31}P\{^1H\}$ NMR: δ 52.4 (s). ^{19}F NMR: δ -151.25 (s), -151.20 (s). $^{13}C\{^1H\}$ NMR: δ 190.8 (t, J_{CP} = 12.1 Hz, CO), 62.2 (s, Me_3CNC), 61.6 (s, Me_3CNC). IR (KBr, cm^{-1}): 2077 vs (ν_{CO}).

[Ru(dppe)(CO)(H_2O)(C_5H_5N)$_2$][OTf]$_2$ (8a). A sample of **4a** (0.05 g, 0.059 mmol) was placed into a J. Youngs resealable NMR tube, dissolved in d^6-acetone/H_2O and 3 equivalents of degassed pyridine (14 μL, 0.17 mmol) added. An immediate reaction was recorded by $^{31}P\{^1H\}$ NMR with the, appearance of a new singlet resonance species at δ 57.9. The product **8a** can be crystallised from $CHCl_3$/H_2O layered with Et_2O. $^{31}P\{^1H\}$ (d^6-acetone, 293K): δ 57.9: ^{19}F NMR: δ -79.43 (s). $^{13}C\{^1H\}$ NMR: δ 201.2 (t, J_{CP} = 16.2 Hz, CO). IR (KBr, cm^{-1}): 1983 vs (ν_{CO}). Anal. Found (calcd) for $RuC_{39}H_{36}N_2S_2P_2F_6O_8$: C, 44.45 (45.0): H, 3.82 (3.63): N, 2.66 (2.52).

Reaction of 4 with 2,2'-bipyridyl to form [Ru(dppe)(CO)(H_2O)(bpy)][OTf]$_2$. A sample of **4a** (0.025 g, 0.029 mmol) was dissolved in d^6-acetone/H_2O and 1 equivalent of 2,2'-bipyridyl (0.005 g, 0.032 mmol) was added. A new species, **9a**, was formed almost immediately as shown by $^{31}P\{^1H\}$ NMR spectroscopy. ^1H NMR (273K): δ 8.89 (2H, d, J_{HH} = 8.05 Hz), 8.53 (2H, d, J_{HH} = 8.05 Hz), 8.42 (2H, d, J_{HH} = 8.05 Hz), 8.07 (2H, dd, J_{HH} = 8.05 Hz), 8.01-7.37 (20H, m, PC_6H_5), 3.15-3.01 (4H, m, PCH_2). $^{31}P\{^1H\}$ NMR: δ 58.3 (s). IR (KBr, cm^{-1}): 1996 vs (ν_{CO}). Conversion to the isomeric product **9a'** was observed upon warming to room temperature for one hour. $^{31}P\{^1H\}$ NMR (293 K): δ 64.7 (d, J_{PP} = 13.1 Hz), 52.2 (d, J_{PP} = 13.1 Hz). IR (KBr, cm^{-1}): 2000 vs (ν_{CO}). Anal. Found (calcd) for $RuC_{39}H_{34}P_2O_8S_2F_6$: C, 47.1 (46.80): H, 3.72 (3.42): N, 2.90 (2.80).

Reaction of 4 with 4,4'-dimethyl-2, 2'-bipyridyl to form [Ru(dppe)(CO)(H_2O)(Me_2bpy)][OTf]$_2$. The reaction of **4a** with Me_2bpy was carried out in a similar manner as above, to give **10a** almost immediately. ^{1}H NMR (258K): δ 2.55 (s, Me). ^{31}P{^{1}H} NMR: δ 58.6 (s). ^{19}F NMR: δ -79.35 (s). ^{13}C{^{1}H}NMR: δ 199.5 (t, J_{CP} = 15.6 Hz, CO), 29.2 (s, CH_3). Upon warming to room temperature for one hour, conversion to the isomeric product **10a'** was observed. ^{1}H NMR (293 K): δ 2.61 (s, CH_3), 2.30 (s, CH_3). ^{31}P{^{1}H} NMR: δ 64.7 (d, J_{PP} = 13.1 Hz), 52.1 (d, J_{PP} = 13.1 Hz). ^{13}C{^{1}H} NMR: δ 199.4 (t, J_{CP} = 16.1 Hz, CO), 21.2 (s, Me), 20.7 (s, Me). IR (KBr, cm^{-1}): 2004 vs (ν_{CO}).

[Ru(dppe)(CO)(OTf)(Me_2bpy)][OTf] (11a). A sample of **4a** (0.062 g, 0.070 mmol) was dissolved in acetone/H_2O and 1 equivalent of Me_2bpy (0.013 g, 0.070 mmol) was added. After one day at room temperature, the solution was pumped to dryness and the residue redissolved in $CDCl_3$. Yellow crystals of **11a** were slowly precipitated from the solution (0.048 g, 68% yield). ^{1}H NMR ($CDCl_3$, 293 K): δ 2.61 (s, CH_3), 2.30 (s, CH_3). ^{31}P{^{1}H} NMR (CD_2Cl_2): δ 67.3 (d, J_{PP} = 14.3 Hz), 51.8 (d, J_{PP} = 14.3 Hz). ^{19}F NMR (CD_2Cl_2): δ -78.97 (s), -79.07 (s). IR (KBr, cm^{-1}): 2005 vs (ν_{CO}). Anal. Found (calcd) for $RuC_{41}H_{36}P_2N_2O_7S_2F_6$: C, 48.3 (48.76): H, 3.56 (3.59): N, 2.57 (2.77).

[{Ru(dppe)(CO)}$_2$(μ-$SCH_2CH_2CH_3$)$_3$][OTf] (12a). 1-propanethiol (38 μL, 0.42 mmol) was added to an acetone/H_2O solution of **4a** (0.125 g, 0.14 mmol) at room temperature. The solution, which became yellow immediately, was pumped to dryness and the residue redissolved in acetone and layered with diethyl ether. Yellow crystals formed overnight (0.04 g, 32% yield). ^{1}H NMR (d^6-acetone, 293 K): δ 7.81 (8H, t, J_{HH} = 8.39 Hz), 7.70 (8H, t, J_{HH} = 8.39 Hz), 7.49 – 7.32 (24H, m), 2.65-2.85 (8H, br, PCH_2 + SCH_2), 1.29 (4H, m, CH_2CH_3), 1.17 (2H, m, SCH_2), 0.86 (6H, t, J_{HH} = 7.20 Hz, CH_3), 0.31 (2H, m, CH_2CH_3), –

0.23 (3H, t, J_{HH} = 7.20 Hz, CH_3). $^{31}P\{^1H\}$ NMR: δ 47.0 (s). $^{13}C\{^1H\}$ NMR: δ 201.4 (t, J_{CP} = 9.6 Hz, CO). IR (KBr, cm^{-1}): 1953 vs (ν_{CO}). Anal. Found (calcd) for $Ru_2C_{64}H_{69}P_4O_5S_4F_3$: C, 53.5 (53.77): H, 5.09 (4.86).

Preparation of Ru(dppe)(CO)$_3$. $Ru_3(CO)_{12}$ (0.38 g, 0.85 mmol) was heated and stirred at 65 °C with excess dppe (1.01g, 2.55 mmol) in C_6H_6 (50 mL) in a high pressure bomb with 8 bar of CO for 1 week. After release of the pressure, the orange/red solution was transferred to a Schlenk tube and the solvent removed under vacuum. Extraction of the residue with hexane gave an orange/yellow solution. Ru(dppe)$(CO)_3$ was obtained as a pale yellow solid (200 mg, 23% yield) upon crystallisation from hexane at –20 °C. $^{31}P\{^1H\}$ NMR (C_6D_6, 293 K): δ 40.0 (s). IR (hexane, cm^{-1}): 2005 (ν_{CO}), 1934 (ν_{CO}), 1915 (ν_{CO}).[4]

[Ru(dppe)(CO)$_3$H][OTf] (13a). One equivalent of HOTf (3.5μL, 0.039 mmol) was added to a CO-saturated C_6D_6 solution of Ru(dppe)$(CO)_3$ (0.023 g, 0.039 mmol) cooled to –78 °C. Upon warming to room temperature, a colour change from orange to yellow was observed consistent with the appearance of a new singlet for **13a** at δ 64.6 in the $^{31}P\{^1H\}$ NMR spectrum. Over a week at room temperature, small yellow crystals appeared, one of which was used for the structure determination. ^1H NMR (C_6D_6, 293 K): δ –7.57 (1H, t, J_{HP} = 17.80 Hz). $^{31}P\{^1H\}$ NMR: δ 64.6 (s). $^{13}C\{^1H\}$ NMR: δ 201.4 (t, J_{CP} = 9.6 Hz, CO). IR (nujol mull, cm^{-1}): 2110 vs (ν_{CO}), 2062 vs (ν_{CO}), 2051 vs (ν_{CO}).

Reaction of 4a with 2,2'-bipyrimidine. Addition of 2, 2'-bipyrimidine (0.006 g, 0.037 mmol) to an acetone/water solution of **4a**, resulted in an immediate reaction with a colour change from pale yellow to bright orange. This was confirmed by $^{31}P\{^1H\}$ NMR by the appearance of a new singlet species at δ 60.3. A new species was seen to grow in within

one hour and complete conversion is seen in 24 hours. $^{31}P\{^1H\}$ NMR (d^6-acetone/D_2O, 293K): δ 64.8 (d, J_{PP} = 13.0 Hz), 52.7 (d, J_{PP} = 13.0 Hz). $^{13}C\ \{^1H\}$ NMR: δ 197.8 (t, J_{CP} = 16.1 Hz, CO). $^{19}F\{^1H\}$ NMR: δ -79.34. IR (KBr, cm^{-1}): 2006 vs (ν_{CO}).

6.4 Compounds relating to Chapter 4

Preparation of (p-F-C_6H_4)$_2$PCH$_2$CH$_2$P(C_6H_4-p-F)$_2$. 4-Bromofluorobenzene (12.0 g, 68.5 mmol in 100 mL of THF) was added dropwise to Mg turnings (1.68 g, 69.1 mmol) in THF (10 mL) in a 3 necked round bottomed flask under argon while the temperature was maintained at 30-40 °C. After being stirred for 2 h under inert atmosphere the reaction mixture was cooled to –80 °C and 1,2-bis(dichlorophosphino) ethane (2.65 g, 11.4 mmol) in THF (40 mL) was added over 40 minutes. The mixture was allowed to warm to ambient temperature over night. Excess Grignard reagent was quenched with saturated aqueous NH_4Cl (50 mL degassed H_2O), the organic layer was separated and, the volatiles were removed at reduced pressure. The residue was extracted with EtOAc and dried ($MgSO_4$) the solvent was removed at reduced pressure to give a white solid which was recrystallised from hot EtOH (2.2 g, 40% yield). ^1H NMR (C_6D_6, 293 K): δ 7.15 (16H, m, PC_6H_5), 1.93 (4H, t, J_{PH} = 4.39 Hz). $^{31}P\{^1H\}$ NMR: δ -14.5 (s). ^{19}F NMR: δ -112.1 (t, J_{HF} = 18.05 Hz). Mp 128-130 °C.[5]

Preparation of (p-MeO-C_6H_4)$_2$PCH$_2$CH$_2$P(C_6H_4-p-OMe)$_2$. 1,2-bis(dichlorophosphino) ethane (1.536 g, 6.60 mmol) in THF (40 mL) was added dropwise over a period of 40 minutes to p-methoxyphenylmagnesium bromide (7.0 g, 3.30 mmol) in THF (66 mL) while maintaining the temperature at –80 °C (the mixture was subjected to vigorous stirring under an inert atmosphere). Excess Grignard reagent was quenched with saturated aqueous NH_4Cl

(50 mL degassed H_2O), the organic layer was separated and dried ($MgSO_4$) and the volatiles were removed at reduced pressure. The residue was extracted with THF and then layered with EtOH which afforded white crystals after 72 h at –10 °C (1.02 g, 30% yield).). ^1H NMR ($CDCl_3$, 293 K): δ 7.05 (16H, m, PC_6H_5), 3.76 (12H, s) 1.98 (4H, s). $^{31}P\{^1H\}$ NMR: δ -14.9 (s). Mp 97-98 °C.[6]

Preparation of (*p*-Me-C_6H_4)$_2$$PCH_2CH_2P(C_6H_4$-*p*-Me)$_2$. *p*-tolylmagnesiumbromide (3.23 g, 16.6 mmol) in Et_2O (50 mL) was cooled to –80 °C and 1,2-bis(dichlorophosphino) ethane (1.93 g, 8.30 mmol) was added drop wise over a 40 minute period. The resultant mixture was allowed to warm to ambient temperature overnight. Excess Grignard reagent was quenched with saturated aqueous NH_4Cl (50 mL degassed H_2O) added dropwise. The residue was extracted from the organic layer and dried ($MgSO_4$). The volatiles were removed at reduced pressure. The residue was extracted with THF and then layered with EtOH and left for 3 days at –10 °C (0.73 g, 19% yield). ^1H NMR (C_6D_6, 293 K): δ 7.05 (16H, br, PC_6H_5), 2.13 (4H, t, J_{PH} = 4 Hz), 2.00 (12H, s, CH_3). $^{31}P\{^1H\}$ NMR: δ - 13.6. Mp 142-144 °C.[6]

Preparation of [Ru(CO)$_2$(Cl)$_2$(dppe-F)]$_{1.14}$. $[Ru(CO)_3(Cl)_2]_2$ (1.1 g, 2.0 mmol) was dissolved in 100 ml of 2-methoxyethanol and 2 equivalents of (*p*-F-$C_6H_4)_2PCH_2CH_2P(C_6H_4$-*p*-F)$_2$ (2 g, 4.0 mmol) was added and stirred for 30 minutes until all of the phosphine had dissolved. The mixture was refluxed for 2.5 h until a creamy white precipitate dropped out of solution, which was filtered and dried

IR (nujol mull, cm^{-1}), 1988 (ν_{CO}), 2051 vs (ν_{CO}).

all-*cis*-Ru(dppe-F)$(CO)_2(Cl)_2$ (1F). Solid samples of $[Ru(CO)_2(Cl)_2(dppe\text{-}F)]_{1.14}$ were melted at 270 °C under a stream of CO and on cooling a yellow product formed. The resultant product was extracted with chloroform and filtered through Celite.
IR and NMR data suggested a mixture of isomers were present one of which corresponding to **1F**. However separation of the isomers could not be achieved. Subjection to $CHCl_3$/silica gel 60 column resulted in destruction and isomerisation of the fractions.
^{31}P $\{^1H\}$ NMR ($CDCl_3$, 293 K): δ 61.9 (d, J_{pp} = 15.2 Hz), 38.7 (d, J_{pp} = 15.2 Hz).
IR ($CHCl_3$, cm^{-1}): 2082 vs (ν_{CO}), 1992.br (ν_{CO}).

Preparation of $[Ru(dppe\text{-}OMe)(CO)_2(Cl)_2]_{1.14}$. $[Ru(CO)_3(Cl)_2]_2$ (0.5 g, 0.97 mmol) was dissolved in 100 ml of 2-methoxyethanol and dppe-OMe (1.02 g, 2.0 mmol) was added and stirred until dissolved. The mixture was refluxed for 2.5 h until a white solid precipitated which was then filtered and dried. IR (nujol mull, cm^{-1}): 1991 vs (ν_{CO}) 2051 vs (ν_{CO}).

Preparation of all-*cis*-Ru(dppe-OMe)$(CO)_2(Cl)_2$ (1OMe). Samples of $[Ru(dppe\text{-}OMe)(CO)_2(Cl)_2]_{1.14}$ were placed in an ampoule under 1 atmosphere of CO and melted at 270 °C. The orange glass, which formed on cooling, was extracted with $CHCl_3$ and filtered through Celite. IR and ^{31}P $\{^1H\}$ NMR showed a mixture of isomers to be present one of which corresponded to **1OMe** which was separated in a low yield using a silica gel 60 column/$CHCl_3$. $^{31}P\{^1H\}$ NMR ($CDCl_3$, 293K): δ 61.2 (d, J_{pp} = 16.8 Hz), 37.9 (d, J_{pp} = 16.8 Hz). IR ($CHCl_3$, cm^{-1}): 2077 vs (ν_{CO}), 2004 vs (ν_{CO}).

Preparation of $[Ru(dppe\text{-}Me)(CO)_2(Cl)_2]_{1.14}$. $[Ru(CO)_3(Cl)_2]_2$ (0.88 g, 1.72 mmol) was dissolved in 100 ml of 2-methoxyethanol and dppe-Me (1.60 g, 3.57 mmol) was added and, stirred until dissolved. The mixture was refluxed for 2.5 h until a white solid

precipitated which was then filtered and dried (0.96 g). IR (nujol mull, cm^{-1}): 2042 vs (ν_{CO}) 1976 vs (ν_{CO}).

Preparation of all-*cis*-Ru(dppe-Me)$(CO)_2(Cl)_2$ (1Me). Samples of [Ru(dppe-Me)$(CO)_2(Cl)_2]_{1.14}$ were placed in an ampoule under 1 atmosphere of CO and heated to 270 °C. The white compound melted and formed an orange glass on cooling. This was extracted with $CHCl_3$ and filtered through Celite.

IR and ^{31}P $\{^1H\}$ NMR showed a mixture of isomers to be present one of which corresponded to **1Me** which was separated using a silica gel 60 column/$CHCl_3$.

$^{31}P\{^1H\}$ NM: δ 59.9 (d, J_{pp} = 16.8 Hz), 37.5 (d, J_{pp} = 16.8 Hz). $^{13}C\{^1H\}$ NMR: δ 193.1 (dd, J_{PC} = 9.5 Hz, J_{PC} = 13.6 Hz, CO), 189.1 (dd, J_{PC} = 116.8 Hz, J_{PC} = 9.5 Hz, CO). IR ($CHCl_3$, cm^{-1}): 2006 vs (ν_{CO}), 2078 vs (ν_{CO}).

Ru(dppe-Me)$(CO)_2(OTf)_2$, (2Me). A rigorously flame dried Schlenk tube was charged with **1Me** (0.1 g, 0.14 mmol), dissolved in CH_2Cl_2 and 2.2 equivalents of AgOTf (0.083 g, 0.32 mmol) were added. The mixture was stirred for 1 h with exclusion of light and then filtered under Ar to remove AgCl. The filtrate was concentrated to 5 mL and hexane (20 mL) was added and stirred for 45 minutes to induce the precipitation of a white solid. The solution was concentrated by 50% to maximise precipitation and the white solid was collected by filtration and washed with hexane (3 x 5 mL) and dried under vacuum (0.08 g, 75% yield). $^{31}P\{^1H\}$ NMR (CD_2Cl_2, 293 K): δ 62.4 (d, J_{PP} = 15.7 Hz), 43.6 (d, J_{PP} = 15.7 Hz). $^{13}C\{^1H\}$ NMR: δ 194.2 (t, J_{PC} = 15.5 Hz, CO), 186.9 (dd, J_{PC} = 106.9 Hz, J_{PC} = 9.9 Hz, CO). ^{19}F NMR: δ -78.2 (q, J_{FF} = 3.2 Hz, CF_3), -77.5 (q, J_{FF} = 3.2 Hz, CF_3). IR (CH_2Cl_2, cm^{-1}): 2102 vs (ν_{CO}), 2027 vs (ν_{CO}).

6.5 Compounds relating to chapter 5

Preparation of $[Ru(CO)_2Cl_2]_n$. $RuCl.xH_2O$ (2.0 g, 9.74 mmol) and paraformaldehyde (1 g) were added to an Ar-sparged solution of 90% formic acid (50 mL). The mixture was refluxed 6 h until pale yellow. The solution was cooled to room temperature and stored under an inert atmosphere at 4 °C overnight to allow complete conversion to the polymer. The solution was evaporated to dryness using an oil bath set at 80–85 °C while under a continuos stream of N_2. The resultant residue was washed with hexane and dried in *vacuo* (2.0 g, 90% yield).
IR (nujol mull, cm^{-1}): 2074 vs (ν_{CO}), 2017 vs (ν_{CO}).[7]

***Cis-cis-trans*-Ru(Me$_2$bpy)(CO)$_2$Cl$_2$.** Me_2bpy (1.0 g, 6.6 mmol) was dissolved in MeOH (15 mL) and the suspension was degassed for 30 minutes. $[Ru(CO)_2Cl_2]_n$ (1.0 g, 4.4 mmol) was added to the degassed suspension and the resultant mixture was refluxed for 30 minutes, during which time the product precipitates from the solution. On cooling the pale yellow precipitate was collected and recrystallised from boiling $CHCl_3$ (0.90g, 50% yield).
IR (nujol mull, cm^{-1}): 2060 vs (ν_{CO}), 1989 vs (ν_{CO}).[7]

all-*cis*-Ru(Me$_2$bpy)(CO)$_2$(OTf)$_2$. A 1,2-dichlorobenzene solution (200 mL) of *cis*, *cis*, *trans*-$Ru(Me_2bpy)(CO)_2Cl_2$ (0.75 g, 1.82 mmol) was deaerated with Ar for 30 minutes, resulting in a cloudy yellow solution. HOTf (0.5 mL) was added drop wise by syringe (platinum needle) and, the solution was heated to 110 °C for 1.5 h. The mixture was cooled to 0 °C and the product was precipitated by the addition of Et_2O (200 mL). The mixture was allowed to stir for 1 h and the complex, $Ru(Me_2bpy)(CO)_2(OTf)_2$ was collected by vacuum filtration under argon and, washed with Et_2O (2 x 5 mL) followed by cold distilled H_2O (2 x 5 mL) (0.99 g, 85% yield). ^1H NMR ($CDCl_3$, 293 K): δ 1.269 (s, CH_3), 0.890 (s, CH_3). ^{19}F NMR: δ -78.69

(s), -78.78 (s). IR (nujol mull, cm^{-1}): 2099 vs (ν_{CO}), 2027 vs (ν_{CO}).[7]

[Ru(Me$_2$bpy)(CO)$_2$(H$_2$O)Cl][OTf] (14). An Ar-sparged Schlenk tube was charged with *cis*, *cis*, *trans*-Ru(Me$_2$bpy)(CO)$_2$Cl$_2$ (0.3 g, 0.72 mmol) dissolved in CH_2Cl_2 (10 mL). 2.2 equivalents of AgOTf (0.4 g, 1.58 mmol) and 20 equivalents of H_2O (260 μL) were added and the mixture was stirred for 3 days with the exclusion of light. The reaction was monitored by IR (CH_2Cl_2) until only the ν_{CO} bands associated with the product were present in solution. The solution was filtered to remove AgCl which, was formed during the reaction and the filtrate was concentrated by 50% and layered with Et_2O from which analytically pure crystals suitable for X-ray determination of **14** were grown. ^{1}H NMR (acetone-d_6): δ 2.74 (s, CH_3). ^{19}F NMR (D_2O): δ -79.445 (s). IR (H_2O, CaF_2, cm^{-1}): 2078 vs (ν_{CO}), 2018 vs (ν_{CO}). Anal. Found (calcd) for $RuC_{15}H_{14}N_2O_6SF_3Cl$: C, 33.7 (33.12): H, 2.25 (2.59): N, 5.38 (5.15).

6.6 References

1. Barnard, C. F. J. D.Phil Thesis, University of York, York, UK, **1978**.
2. Taylor, A. J. D. Phil Thesis, University of York, York, UK, **1993**.
3. Mahon, M. F.; Whittlesey, M. K.; Wood, P. T. *Organometallics* **1999**, *18*, 4068.
4. Bunten, K. A.; Farra, D. H.; Poe, A. J.; Lough, A. J. *Organometallics* **2000**, *19*, 3674.
5. Mirabelli, F. L.; Girad, G. R.; Bryan, D. B.; Sutton, B. M.; O'Leary Bartus, J.; Crooke, S. T.; Johnson, R. K. *J. Med. Chem.* **1987**, *30*, 2181.
6. Burt, R. J.; Chatt, J.; Hussain, W.; Leigh, G. J. *J. Organomet. Chem.* **1979**, *182*, 203.

7. Anderson, P. A.; Deacon, G. B.: Haarmann, K. H.; Keene, R. F.; Meyer, T. J.; Reitsma, D. A.; Skelton, B. W.; Strouse, G. F.; Thomas, N. C.; Treadway, J. A.; White, A. H. *Inorg. Chem.* **1995**, *34*, 6145.

Appendices

Appendix 1: *Crystallographic data for compound* ***2****.*

Crystal data and structure refinement for **2**.

Identification code	Mw1b
Empirical formula	$C_{30}\,H_{24}\,F_6\,O_8\,P_2\,Ru\,S_2 \bullet 1.2\,H_2O$
Formula weight	875.24
Temperature	293(2) K
Wavelength	0.71073 Å
Crystal system	Monoclinic
Space group	$P2_1/c$
Unit cell dimensions	a = 11.637(6)Å $\alpha = 90^\circ$
	b = 18.452(2)Å $\beta = 100.72(3)^\circ$
	c = 17.227(3)Å $\gamma = 90^\circ$
Volume	3635(8) $Å^3$
Z	4
Density (calculated)	1.600 Mg/m^3
Absorption coefficient	0.715 mm^{-1}
F(000)	1760
Crystal size	0.09 x 0.10 x 0.10 mm
Theta range for data collection	1.63 to 24.58°.
Index ranges	-13<=h<=13; -21<=k<=21; -20<=l<=20
Reflections collected	11878
Independent reflections	6091 [R(int) = 0.0481]
Refinement method	Full-matrix least-squares on F^2
Data / restraints / parameters	6086 / 0 / 447
Goodness-of-fit on F^2	0.970
Final R indices [$I>2\sigma(I)$]	R1 = 0.0590 wR2 = 0.1606
R indices (all data)	R1 = 0.0953 wR2 = 0.1885
Largest diff. peak and hole	1.087 and -0.570 $eÅ^{-3}$
Weighting scheme	Calc $w=1/[\sigma^2(Fo^2)+(0.1102P)^2+0.0000P]$ where $P=(Fo^2+2Fc^2)/3$

Appendix 2: *Crystallographic data for compound* ***3****.*

Crystal data and structure refinement for **3**.

Identification code	Compound 2
Empirical formula	$C_{29}\ H_{28}\ F_6\ O_8\ P_2\ Ru\ S_2$
Formula weight	845.64
Temperature	293(2) K
Wavelength	0.71073 Å
Crystal system	Monoclinic
Space group	$P2_1/n$
Unit cell dimensions	a = 11.603(1)Å $\alpha = 90^o$
	b = 18.396(3)Å $\beta = 100.03(1)^o$
	c = 16.840(2)Å $\gamma = 90^o$
Volume	3593.5(10) $Å^3$
Z	4
Density (calculated)	1.587 Mg/m^3
Absorption coefficient	0.728 mm^{-1}
F(000)	1704
Crystal size	0.08 x 0.10 x 0.10 mm
Theta range for data collection	2.10 to 25.46°.
Index ranges	-13<=h<=13; -22<=k<=22; -20<=l<=16
Reflections collected	11981
Independent reflections	6362 [R(int) = 0.0424]
Refinement method	Full-matrix least-squares on F^2
Data / restraints / parameters	6357 / 0 / 436
Goodness-of-fit on F^2	0.942
Final R indices [I>2σ (I)]	R1 = 0.0580 wR2 = 0.1531
R indices (all data)	R1 = 0.1101 wR2 = 0.1900
Largest diff. peak and hole	0.765 and -0.654 $eÅ^{-3}$
Weighting scheme	calc $w=1/[\sigma^2(Fo^2)+(0.1027P)^2+0.0000P]$ where $P=(Fo^2+2Fc^2)/3$

*Appendix 3: Crystallographic data for compound **4a**.*

Crystal data and structure refinement for **4a**.

Identification code	99mw1/uea
Empirical formula	$C_{29}H_{30}F_6O_{10}P_2RuS_2 \bullet 1.8\ H_2O$
Formula weight	912.09
Temperature	198(2) K
Wavelength	0.71069 Å
Crystal system	Monoclinic
Space group	$P2_1/c$
Unit cell dimensions	a = 11.719(1)Å $\alpha = 90^o$
	b = 23.365(3)Å $\beta = 102.54(1)^o$
	c = 13.851(2)Å $\gamma = 90^o$
Volume	3702.1(8) $Å^3$
Z	4
Density (calculated)	1.636 Mg/m^3
Absorption coefficient	0.710 mm^{-1}
F(000)	1848
Crystal size	0.15 x 0.15 x 0.15 mm
Theta range for data collection	2.24 to 25.00°.
Index ranges	0<=h<=13; 0<=k<=27; -16<=l<=16
Reflections collected	7045
Independent reflections	6495 [R(int) = 0.0106]
Refinement method	Full-matrix least-squares on F^2
Data / restraints / parameters	6488 / 6 / 494
Goodness-of-fit on F^2	0.981
Final R indices [$I>2\sigma(I)$]	R1 = 0.0302 wR2 = 0.0731
R indices (all data)	R1 = 0.0369 wR2 = 0.0835
Largest diff. peak and hole	0.701 and -0.538 $eÅ^{-3}$
Weighting scheme	calc $w=1/[\sigma^2(Fo^2)+(0.0358P)^2+6.4816P]$ where $P=(Fo^2+2Fc^2)/3$
Extinction coefficient	0.00039(11)

Extinction expression $Fc^{*}=kFc[1+0.001xFc^{2}\sigma^{3}/\sin(2\sigma)]^{-1/4}$

Bond lengths [Å] and angles [°] for **4a**.

Ru(1)-C(1)	1.833(3)	C(5)-F(6)	1.322(4)
Ru(1)-O(4)	2.157(2)	C(5)-F(4)	1.333(4)
Ru(1)-O(3)	2.170(2)	C(6)-C(11)	1.390(4)
Ru(1)-O(2)	2.180(2)	C(6)-C(7)	1.395(4)
Ru(1)-P(2)	2.2654(7)	C(7)-C(8)	1.383(4)
Ru(1)-P(1)	2.2876(7)	C(8)-C(9)	1.374(5)
P(1)-C(12)	1.811(3)	C(9)-C(10)	1.370(5)
P(1)-C(6)	1.819(3)	C(10)-C(11)	1.386(5)
P(1)-C(2)	1.833(3)	C(12)-C(17)	1.388(4)
P(2)-C(18)	1.813(3)	C(12)-C(13)	1.398(4)
P(2)-C(24)	1.817(3)	C(13)-C(14)	1.384(4)
P(2)-C(3)	1.830(3)	C(14)-C(15)	1.384(5)
S(1)-O(5)	1.420(3)	C(15)-C(16)	1.375(5)
S(1)-O(6)	1.432(3)	C(16)-C(17)	1.383(4)
S(1)-O(7)	1.450(2)	C(18)-C(19)	1.389(4)
S(1)-C(4)	1.822(3)	C(18)-C(23)	1.394(4)
S(2)-O(10)	1.431(2)	C(19)-C(20)	1.378(4)
S(2)-O(8)	1.435(2)	C(20)-C(21)	1.383(5)
S(2)-O(9)	1.446(2)	C(21)-C(22)	1.371(5)
S(2)-C(5)	1.813(4)	C(22)-C(23)	1.386(4)
O(1)-C(1)	1.145(3)	C(24)-C(29)	1.391(4)
C(2)-C(3)	1.528(4)	C(24)-C(25)	1.396(4)
C(4)-F(3)	1.317(4)	C(25)-C(26)	1.383(4)
C(4)-F(2)	1.320(4)	C(26)-C(27)	1.381(5)
C(4)-F(1)	1.325(4)	C(27)-C(28)	1.376(5)
C(5)-F(5)	1.309(4)	C(28)-C(29)	1.391(4)

C(1)-Ru(1)-O(4)	176.53(10)	S(2)-O(9)-O(4)	154.1(2)
O(4)-Ru(1)-O(3)	81.40(8)	S(2)-O(10)-O(12)	123.1(2)
C(1)-Ru(1)-O(2)	96.19(10)	O(12)#2-O(11)-O(4)	128.2(2)
O(4)-Ru(1)-O(2)	82.17(8)	O(12)#2-O(11)-O(11)#2	85.0(2)
O(3)-Ru(1)-O(2)	86.80(8)	O(4)-O(11)-O(11)#2	121.0(2)
C(1)-Ru(1)-P(2)	86.05(8)	O(5)-O(12)-O(10)	91.01(11)
O(4)-Ru(1)-P(2)	95.70(6)	O(1)-C(1)-Ru(1)	177.4(2)
O(3)-Ru(1)-P(2)	95.09(6)	C(3)-C(2)-P(1)	109.1(2)
O(2)-Ru(1)-P(2)	176.92(6)	C(2)-C(3)-P(2)	109.2(2)
C(1)-Ru(1)-P(1)	88.31(8)	F(3)-C(4)-F(2)	108.0(3)
O(4)-Ru(1)-P(1)	94.81(6)	F(3)-C(4)-F(1)	108.0(3)
O(3)-Ru(1)-P(1)	176.21(6)	F(2)-C(4)-F(1)	107.5(3)
O(2)-Ru(1)-P(1)	92.51(6)	F(3)-C(4)-S(1)	111.6(2)
P(2)-Ru(1)-P(1)	85.44(3)	F(2)-C(4)-S(1)	111.3(2)
C(12)-P(1)-C(6)	106.16(13)	F(1)-C(4)-S(1)	110.3(2)
C(12)-P(1)-C(2)	107.79(13)	F(5)-C(5)-F(6)	109.3(3)
C(6)-P(1)-C(2)	105.55(13)	F(5)-C(5)-F(4)	107.5(3)
C(12)-P(1)-Ru(1)	113.17(9)	F(6)-C(5)-F(4)	107.7(3)
C(6)-P(1)-Ru(1)	115.54(9)	F(5)-C(5)-S(2)	110.6(2)
C(2)-P(1)-Ru(1)	108.14(9)	F(6)-C(5)-S(2)	110.7(3)
C(18)-P(2)-C(24)	102.72(12)	F(4)-C(5)-S(2)	111.0(2)
C(18)-P(2)-C(3)	108.13(13)	C(11)-C(6)-C(7)	118.9(3)
C(24)-P(2)-C(3)	105.31(12)	C(11)-C(6)-P(1)	121.7(2)
C(18)-P(2)-Ru(1)	113.18(9)	C(7)-C(6)-P(1)	119.4(2)
C(24)-P(2)-Ru(1)	119.22(9)	C(8)-C(7)-C(6)	120.4(3)
C(3)-P(2)-Ru(1)	107.61(9)	C(9)-C(8)-C(7)	120.1(3)
O(5)-S(1)-O(6)	116.5(2)	C(10)-C(9)-C(8)	120.1(3)
O(5)-S(1)-O(7)	115.1(2)	C(9)-C(10)-C(11)	120.7(3)
O(6)-S(1)-O(7)	112.87(14)	C(10)-C(11)-C(6)	119.9(3)
O(5)-S(1)-C(4)	103.5(2)	C(17)-C(12)-C(13)	118.7(3)
O(6)-S(1)-C(4)	104.0(2)	C(17)-C(12)-P(1)	123.2(2)
O(7)-S(1)-C(4)	102.64(14)	C(13)-C(12)-P(1)	118.1(2)
O(10)-S(2)-O(8)	114.4(2)	C(14)-C(13)-C(12)	120.6(3)
O(10)-S(2)-O(9)	114.75(14)	C(13)-C(14)-C(15)	120.1(3)
O(8)-S(2)-O(9)	114.96(14)	C(16)-C(15)-C(14)	119.3(3)

O(10)-S(2)-C(5)	104.8(2)	C(15)-C(16)-C(17)	121.2(3)
O(8)-S(2)-C(5)	103.0(2)	C(16)-C(17)-C(12)	120.1(3)
O(9)-S(2)-C(5)	102.8(2)	C(19)-C(18)-C(23)	119.4(3)
Ru(1)-O(2)-O(9)	109.19(10)	C(19)-C(18)-P(2)	117.5(2)
Ru(1)-O(3)-O(8)#1	106.03(10)	C(23)-C(18)-P(2)	123.1(2)
Ru(1)-O(3)-O(7)	115.21(9)	C(20)-C(19)-C(18)	120.2(3)
O(8)#1-O(3)-O(7)	110.12(10)	C(19)-C(20)-C(21)	120.4(3)
Ru(1)-O(4)-O(11)	139.06(12)	C(22)-C(21)-C(20)	119.6(3)
Ru(1)-O(4)-O(9)	106.18(9)	C(21)-C(22)-C(23)	120.9(3)
O(11)-O(4)-O(9)	107.98(11)	C(22)-C(23)-C(18)	119.5(3)
S(1)-O(5)-O(12)	131.9(2)	C(29)-C(24)-C(25)	119.5(3)
S(1)-O(7)-O(3)	127.92(12)	C(29)-C(24)-P(2)	122.1(2)
S(2)-O(9)-O(2)	133.50(14)	C(25)-C(24)-P(2)	118.3(2)
C(28)-C(27)-C(26)	120.3(3)	C(26)-C(25)-C(24)	119.9(3)
C(27)-C(28)-C(29)	120.1(3)	C(27)-C(26)-C(25)	120.2(3)
C(24)-C(29)-C(28)	119.9(3)		

Appendix 4: *Crystallographic data for compound* ***4b****.*

Crystal data and structure refinement for **4b**.

Identification code	k00mkw11
Empirical formula	$C_{27}H_{34}B_2F_8O_6P_2Ru$
Formula weight	791.17
Temperature	150(2) K
Wavelength	0.71070 Å
Crystal system	Orthorhombic
Space group	Pbca
Unit cell dimensions	a = 10.81400(10)Å $\alpha = 90^\circ$
	b = 22.9740(2)Å $\beta = 90^\circ$
	c = 26.8330(2)Å $\gamma = 90^\circ$
Volume	6666.41(10) $Å^3$
Z	8
Density (calculated)	1.577 Mg/m^3
Absorption coefficient	0.649 mm^{-1}
F(000)	3200
Crystal size	0.20 x 0.20 x 0.15 mm
Theta range for data collection	3.87 to 27.55 °.
Index ranges	0<=h<=14; -29<=k<=29; -34<=l<=34
Reflections collected	117588
Independent reflections	7334 [R(int) = 0.0642]
Reflections observed (>2σ)	5897
Max. and min. transmission	0.9089 and 0.8811
Refinement method	Full-matrix least-squares on F^2
Data / restraints / parameters	7334 / 26 / 475
Goodness-of-fit on F^2	0.876
Final R indices [I>2σ (I)]	$R_1 = 0.0378$ $wR_2 = 0.0998$
R indices (all data)	$R_1 = 0.0527$ $wR_2 = 0.1121$
Largest diff. peak and hole	1.291 and -0.824 $e.Å^{-3}$

Bond lengths [Å] and angles [°] for **4b**.

Ru(1)-C(27)	1.836(3)	Ru(1)-O(2)	2.142(2)
Ru(1)-O(3)	2.186(2)	Ru(1)-O(4)	2.196(2)
Ru(1)-P(2)	2.2780(8)	Ru(1)-P(1)	2.2876(8)
P(1)-C(1)	1.812(3)	P(1)-C(7)	1.815(3)
P(1)-C(13)	1.838(3)	P(2)-C(15)	1.818(3)
P(2)-C(21)	1.827(3)	P(2)-C(14)	1.827(3)
O(1)-C(27)	1.144(4)	B(1)-F(3A)	1.249(8)
B(1)-F(4)	1.319(7)	B(1)-F(2)	1.342(5)
B(1)-F(1)	1.384(5)	B(1)-F(3)	1.536(8)
B(1)-F(4A)	1.582(9)	F(3)-F(3A)	1.090(12)
F(3A)-F(4)	1.251(14)	F(4)-F(4A)	1.156(9)
B(2)-F(7)	1.339(5)	B(2)-F(8)	1.348(5)
B(2)-F(5)	1.370(5)	B(2)-F(6)	1.402(6)
C(1)-C(2)	1.391(5)	C(1)-C(6)	1.401(5)
C(2)-C(3)	1.391(5)	C(3)-C(4)	1.379(6)
C(4)-C(5)	1.373(6)	C(5)-C(6)	1.396(6)
C(7)-C(8)	1.389(5)	C(7)-C(12)	1.396(5)
C(8)-C(9)	1.388(6)	C(9)-C(10)	1.363(7)
C(10)-C(11)	1.383(7)	C(11)-C(12)	1.385(5)
C(13)-C(14)	1.519(5)	C(15)-C(16)	1.385(5)
C(15)-C(20)	1.387(5)	C(16)-C(17)	1.390(6)
C(17)-C(18)	1.388(6)	C(18)-C(19)	1.371(6)
C(19)-C(20)	1.385(5)	C(21)-C(26)	1.378(5)
C(21)-C(22)	1.390(5)	C(22)-C(23)	1.388(6)
C(23)-C(24)	1.350(7)	C(24)-C(25)	1.362(7)
C(25)-C(26)	1.387(5)		

C(27)-Ru(1)-O(2)	176.80(11)	C(27)-Ru(1)-O(3)	95.92(11)
O(2)-Ru(1)-O(3)	81.18(9)	C(27)-Ru(1)-O(4)	96.40(12)
O(2)-Ru(1)-O(4)	81.76(9)	O(3)-Ru(1)-O(4)	78.69(9)
C(27)-Ru(1)-P(2)	85.56(10)	O(2)-Ru(1)-P(2)	96.24(7)
O(3)-Ru(1)-P(2)	100.46(7)	O(4)-Ru(1)-P(2)	177.92(7)

C(27)-Ru(1)-P(1)	88.09(10)	O(2)-Ru(1)-P(1)	94.69(7)
O(3)-Ru(1)-P(1)	173.47(7)	O(4)-Ru(1)-P(1)	95.77(7)
P(2)-Ru(1)-P(1)	84.95(3)	C(1)-P(1)-C(7)	104.24(15)
C(1)-P(1)-C(13)	104.42(15)	C(7)-P(1)-C(13)	107.39(16)
C(1)-P(1)-Ru(1)	117.97(11)	C(7)-P(1)-Ru(1)	113.03(10)
C(13)-P(1)-Ru(1)	109.00(11)	C(15)-P(2)-C(21)	105.30(15)
C(15)-P(2)-C(14)	107.88(16)	C(21)-P(2)-C(14)	102.86(16)
C(15)-P(2)-Ru(1)	113.99(11)	C(21)-P(2)-Ru(1)	117.32(11)
C(14)-P(2)-Ru(1)	108.62(11)	F(3A)-B(1)-F(4)	58.2(7)
F(3A)-B(1)-F(2)	119.0(6)	F(4)-B(1)-F(2)	124.3(6)
F(3A)-B(1)-F(1)	121.8(6)	F(4)-B(1)-F(1)	111.5(4)
F(2)-B(1)-F(1)	112.2(4)	F(3A)-B(1)-F(3)	44.6(6)
F(4)-B(1)-F(3)	102.3(6)	F(2)-B(1)-F(3)	100.9(4)
F(1)-B(1)-F(3)	101.6(5)	F(3A)-B(1)-F(4A)	102.1(7)
F(4)-B(1)-F(4A)	45.9(4)	F(2)-B(1)-F(4A)	93.1(4)
F(1)-B(1)-F(4A)	100.8(4)	F(3)-B(1)-F(4A)	146.5(6)
F(3A)-F(3)-B(1)	53.6(5)	F(3)-F(3A)-B(1)	81.8(7)
F(3)-F(3A)-F(4)	144.2(8)	B(1)-F(3A)-F(4)	63.7(6)
F(4A)-F(4)-F(3A)	133.4(8)	F(4A)-F(4)-B(1)	79.2(6)
F(3A)-F(4)-B(1)	58.1(5)	F(4)-F(4A)-B(1)	55.0(5)
F(7)-B(2)-F(8)	114.4(4)	F(7)-B(2)-F(5)	111.2(4)
F(8)-B(2)-F(5)	110.0(4)	F(7)-B(2)-F(6)	106.4(4)
F(8)-B(2)-F(6)	109.5(4)	F(5)-B(2)-F(6)	104.8(4)
C(2)-C(1)-C(6)	119.1(3)	C(2)-C(1)-P(1)	121.5(3)
C(6)-C(1)-P(1)	119.3(3)	C(3)-C(2)-C(1)	120.1(3)
C(4)-C(3)-C(2)	120.6(4)	C(5)-C(4)-C(3)	119.8(4)
C(4)-C(5)-C(6)	120.8(4)	C(5)-C(6)-C(1)	119.6(4)
C(8)-C(7)-C(12)	119.2(3)	C(8)-C(7)-P(1)	122.4(3)
C(12)-C(7)-P(1)	118.3(3)	C(9)-C(8)-C(7)	119.9(4)
C(10)-C(9)-C(8)	120.5(4)	C(9)-C(10)-C(11)	120.4(4)
C(10)-C(11)-C(12)	119.9(4)	C(11)-C(12)-C(7)	120.0(4)
C(14)-C(13)-P(1)	110.0(2)	C(13)-C(14)-P(2)	110.3(2)
C(16)-C(15)-C(20)	119.7(3)	C(16)-C(15)-P(2)	118.5(3)
C(20)-C(15)-P(2)	121.7(3)	C(15)-C(16)-C(17)	120.2(4)
C(18)-C(17)-C(16)	119.5(4)	C(19)-C(18)-C(17)	120.4(4)

C(18)-C(19)-C(20)	120.3(4)	C(19)-C(20)-C(15)	119.9(4)
C(26)-C(21)-C(22)	117.9(3)	C(26)-C(21)-P(2)	122.2(3)
C(22)-C(21)-P(2)	119.9(3)	C(23)-C(22)-C(21)	120.1(4)
C(24)-C(23)-C(22)	120.9(4)	C(23)-C(24)-C(25)	120.0(4)
C(24)-C(25)-C(26)	120.0(4)	C(21)-C(26)-C(25)	121.1(4)
O(1)-C(27)-Ru(1)	177.9(3)		

Appendix 5: *Crystallographic data for compound* ***4c****.*

Crystal data and structure refinement for **4c**.

Identification code	k01mkw11
Empirical formula	C28 H38 Cl2 F12 O7 P2 Ru Sb2
Formula weight	1191.99
Temperature	150(2) K
Wavelength	0.71073 Å
Crystal system	Monoclinic
Space group	$P2_1/n$
Unit cell dimensions	a = 14.9330(2)Å α= 90°
	b = 13.8810(2)Å β = 91.8860(10)°
	c = 19.8660(3)Å γ = 90°
Volume	4115.69(10) $Å^3$
Z	4
Density (calculated)	1.924 Mg/m^3
Absorption coefficient	1.968 mm^{-1}
F(000)	2320
Crystal size	0.50 x 0.40 x 0.20 mm
Theta range for data collection	3.71 to 27.47°
Index ranges	-16<=h<=19; -18<=k<=17; -25<=l<=25
Reflections collected	55835
Independent reflections	9400 [R(int) = 0.0585]
Reflections observed (>2σ)	7637
Data Completeness	0.996
Refinement method	Full-matrix least-squares on F^2
Data / restraints / parameters	9400 / 50 / 662
Goodness-of-fit on F^2	0.980
Final R indices [I>2σ (I)]	R_1 = 0.0379 wR_2 = 0.0922
R indices (all data)	R_1 = 0.0517 wR_2 = 0.1010
Largest diff. peak and hole	1.283 and -1.513 $eÅ^{-3}$

Bond lengths [Å] and angles [°] for **4c**.

Sb(1)-F(5A)	1.70(3)	Sb(1)-F(2A)	1.73(2)
Sb(1)-F(4)	1.817(6)	Sb(1)-F(6)	1.859(4)
Sb(1)-F(5)	1.866(6)	Sb(1)-F(1)	1.869(3)
Sb(1)-F(3)	1.874(3)	Sb(1)-F(2)	1.906(4)
Sb(1)-F(4A)	1.97(2)	Sb(1)-F(6A)	1.976(16)
Sb(2)-F(11)	1.817(7)	Sb(2)-F(9)	1.846(8)
Sb(2)-F(7)	1.849(13)	Sb(2)-F(8)	1.851(10)
Sb(2)-F(12)	1.859(10)	Sb(2)-F(10)	1.869(8)
Sb(2A)-F(9A)	1.822(12)	Sb(2A)-F(10A)	1.824(8)
Sb(2A)-F(7A)	1.831(11)	Sb(2A)-F(12A)	1.842(9)
Sb(2A)-F(11A)	1.849(9)	Sb(2A)-F(8A)	1.850(9)
Ru(1)-C(1)	1.843(4)	Ru(1)-O(3)	2.163(3)
Ru(1)-O(2)	2.173(3)	Ru(1)-O(4)	2.182(3)
Ru(1)-P(2)	2.2860(9)	Ru(1)-P(1)	2.3046(9)
Cl(1)-C(4)	1.733(8)	Cl(2)-C(4)	1.759(8)
P(1)-C(21)	1.819(4)	P(1)-C(11)	1.823(4)
P(1)-C(2)	1.832(4)	P(2)-C(41)	1.813(4)
P(2)-C(31)	1.817(4)	P(2)-C(3)	1.831(4)
O(1)-C(1)	1.146(5)	C(2)-C(3)	1.533(5)
C(11)-C(16)	1.387(6)	C(11)-C(12)	1.398(6)
C(12)-C(13)	1.394(6)	C(13)-C(14)	1.369(8)
C(14)-C(15)	1.369(8)	C(15)-C(16)	1.398(6)
C(21)-C(22)	1.388(5)	C(21)-C(26)	1.393(5)
C(22)-C(23)	1.398(6)	C(23)-C(24)	1.384(6)
C(24)-C(25)	1.370(7)	C(25)-C(26)	1.388(6)
C(31)-C(36)	1.391(5)	C(31)-C(32)	1.393(5)
C(32)-C(33)	1.395(5)	C(33)-C(34)	1.387(6)
C(34)-C(35)	1.384(6)	C(35)-C(36)	1.390(5)
C(41)-C(42)	1.386(5)	C(41)-C(46)	1.396(5)
C(42)-C(43)	1.392(6)	C(43)-C(44)	1.374(7)
C(44)-C(45)	1.385(7)	C(45)-C(46)	1.381(6)
F(5A)-Sb(1)-F(2A)	98.4(19)	F(5A)-Sb(1)-F(4)	116.3(16)

F(2A)-Sb(1)-F(4)	143.9(11)	F(5A)-Sb(1)-F(6)	150.6(16)
F(2A)-Sb(1)-F(6)	52.1(12)	F(4)-Sb(1)-F(6)	92.6(3)
F(5A)-Sb(1)-F(5)	23.7(16)	F(2A)-Sb(1)-F(5)	122.2(12)
F(4)-Sb(1)-F(5)	93.0(3)	F(6)-Sb(1)-F(5)	174.3(3)
F(5A)-Sb(1)-F(1)	93.1(11)	F(2A)-Sb(1)-F(1)	97.0(9)
F(4)-Sb(1)-F(1)	90.9(2)	F(6)-Sb(1)-F(1)	91.67(16)
F(5)-Sb(1)-F(1)	89.4(2)	F(5A)-Sb(1)-F(3)	85.8(11)
F(2A)-Sb(1)-F(3)	83.1(9)	F(4)-Sb(1)-F(3)	89.6(2)
F(6)-Sb(1)-F(3)	89.29(16)	F(5)-Sb(1)-F(3)	89.6(2)
F(1)-Sb(1)-F(3)	178.89(13)	F(5A)-Sb(1)-F(2)	63.8(15)
F(2A)-Sb(1)-F(2)	36.2(10)	F(4)-Sb(1)-F(2)	179.4(3)
F(6)-Sb(1)-F(2)	87.3(2)	F(5)-Sb(1)-F(2)	87.1(3)
F(1)-Sb(1)-F(2)	88.52(16)	F(3)-Sb(1)-F(2)	90.95(17)
F(5A)-Sb(1)-F(4A)	92.8(18)	F(2A)-Sb(1)-F(4A)	167.9(13)
F(4)-Sb(1)-F(4A)	24.1(7)	F(6)-Sb(1)-F(4A)	116.5(8)
F(5)-Sb(1)-F(4A)	69.2(9)	F(1)-Sb(1)-F(4A)	86.8(7)
F(3)-Sb(1)-F(4A)	93.3(7)	F(2)-Sb(1)-F(4A)	155.9(8)
F(5A)-Sb(1)-F(6A)	176.6(16)	F(2A)-Sb(1)-F(6A)	84.4(14)
F(4)-Sb(1)-F(6A)	60.6(8)	F(6)-Sb(1)-F(6A)	32.3(7)
F(5)-Sb(1)-F(6A)	153.4(8)	F(1)-Sb(1)-F(6A)	88.5(5)
F(3)-Sb(1)-F(6A)	92.6(5)	F(2)-Sb(1)-F(6A)	119.3(8)
F(4A)-Sb(1)-F(6A)	84.3(11)	F(11)-Sb(2)-F(9)	90.7(5)
F(11)-Sb(2)-F(7)	92.8(9)	F(9)-Sb(2)-F(7)	175.6(10)
F(11)-Sb(2)-F(8)	91.6(6)	F(9)-Sb(2)-F(8)	89.5(7)
F(7)-Sb(2)-F(8)	87.8(11)	F(11)-Sb(2)-F(12)	178.5(7)
F(9)-Sb(2)-F(12)	89.8(5)	F(7)-Sb(2)-F(12)	86.8(10)
F(8)-Sb(2)-F(12)	89.8(7)	F(11)-Sb(2)-F(10)	89.1(5)
F(9)-Sb(2)-F(10)	91.0(6)	F(7)-Sb(2)-F(10)	91.6(10)
F(8)-Sb(2)-F(10)	179.1(7)	F(12)-Sb(2)-F(10)	89.5(6)
F(9A)-Sb(2A)-F(10A)	92.5(9)	F(9A)-Sb(2A)-F(7A)	175.5(9)
F(10A)-Sb(2A)-F(7A)	83.1(7)	F(9A)-Sb(2A)-F(12A)	89.1(9)
F(10A)-Sb(2A)-F(12A)	93.7(8)	F(7A)-Sb(2A)-F(12A)	90.6(7)
F(9A)-Sb(2A)-F(11A)	92.6(9)	F(10A)-Sb(2A)-F(11A)	92.0(7)
F(7A)-Sb(2A)-F(11A)	88.1(7)	F(12A)-Sb(2A)-F(11A)	174.0(7)
F(9A)-Sb(2A)-F(8A)	87.8(9)	F(10A)-Sb(2A)-F(8A)	178.3(7)

F(7A)-Sb(2A)-F(8A)	96.6(7)	F(12A)-Sb(2A)-F(8A)	88.0(6)
F(11A)-Sb(2A)-F(8A)	86.3(5)	C(1)-Ru(1)-O(3)	179.55(14)
C(1)-Ru(1)-O(2)	96.62(14)	O(3)-Ru(1)-O(2)	83.48(11)
C(1)-Ru(1)-O(4)	95.04(14)	O(3)-Ru(1)-O(4)	85.40(11)
O(2)-Ru(1)-O(4)	83.91(11)	C(1)-Ru(1)-P(2)	86.36(12)
O(3)-Ru(1)-P(2)	93.54(7)	O(2)-Ru(1)-P(2)	176.93(9)
O(4)-Ru(1)-P(2)	95.11(8)	C(1)-Ru(1)-P(1)	91.66(12)
O(3)-Ru(1)-P(1)	87.89(8)	O(2)-Ru(1)-P(1)	95.69(9)
O(4)-Ru(1)-P(1)	173.29(9)	P(2)-Ru(1)-P(1)	84.94(3)
C(21)-P(1)-C(11)	106.20(17)	C(21)-P(1)-C(2)	106.80(18)
C(11)-P(1)-C(2)	105.84(18)	C(21)-P(1)-Ru(1)	117.17(12)
C(11)-P(1)-Ru(1)	113.38(12)	C(2)-P(1)-Ru(1)	106.73(12)
C(41)-P(2)-C(31)	103.80(16)	C(41)-P(2)-C(3)	105.65(17)
C(31)-P(2)-C(3)	107.02(17)	C(41)-P(2)-Ru(1)	118.20(12)
C(31)-P(2)-Ru(1)	113.13(11)	C(3)-P(2)-Ru(1)	108.30(12)
O(1)-C(1)-Ru(1)	178.3(4)	C(3)-C(2)-P(1)	108.7(2)
C(2)-C(3)-P(2)	108.2(3)	Cl(1)-C(4)-Cl(2)	113.3(4)
C(16)-C(11)-C(12)	119.2(4)	C(16)-C(11)-P(1)	121.9(3)
C(12)-C(11)-P(1)	118.7(3)	C(13)-C(12)-C(11)	119.3(5)
C(14)-C(13)-C(12)	120.9(5)	C(15)-C(14)-C(13)	120.2(4)
C(14)-C(15)-C(16)	120.1(5)	C(11)-C(16)-C(15)	120.2(4)
C(22)-C(21)-C(26)	118.9(4)	C(22)-C(21)-P(1)	119.8(3)
C(26)-C(21)-P(1)	121.2(3)	C(21)-C(22)-C(23)	120.3(4)
C(24)-C(23)-C(22)	119.9(4)	C(25)-C(24)-C(23)	120.0(4)
C(24)-C(25)-C(26)	120.6(4)	C(25)-C(26)-C(21)	120.3(4)
C(36)-C(31)-C(32)	119.2(3)	C(36)-C(31)-P(2)	117.3(3)
C(32)-C(31)-P(2)	123.5(3)	C(31)-C(32)-C(33)	120.2(4)
C(34)-C(33)-C(32)	120.0(4)	C(35)-C(34)-C(33)	120.0(4)
C(34)-C(35)-C(36)	120.1(4)	C(31)-C(36)-C(35)	120.5(4)
C(42)-C(41)-C(46)	119.6(4)	C(42)-C(41)-P(2)	119.6(3)
C(46)-C(41)-P(2)	120.7(3)	C(41)-C(42)-C(43)	119.7(4)
C(44)-C(43)-C(42)	120.4(4)	C(43)-C(44)-C(45)	120.1(4)
C(46)-C(45)-C(44)	120.1(4)	C(45)-C(46)-C(41)	120.1(4)

Appendix 6: *Crystallographic data for compound* ***5a****.*

Crystal data and structure refinement for **5a**.

Identification code	k00mkw2
Empirical formula	C37 H35 Cl6 F6 N3 O7 P2 Ru S2
Formula weight	1187.51
Temperature	170(2) K
Wavelength	0.71073 Å
Crystal system	Monoclinic
Space group	$P2_1/n$
Unit cell dimensions	a = 12.2606(3)Å α= 90°
	b = 13.8259(3)Å β = 99.5870(10)°
	c = 29.5038(5)Å γ = 90°
Volume	4931.45(18) $Å^3$
Z	4
Density (calculated)	1.599 Mg/m^3
Absorption coefficient	0.863 mm^{-1}
F(000)	2384
Crystal size	0.37 x 0.20 x 0.13 mm
Theta range for data collection	1.71 to 26.37 °.
Index ranges	-15<=h<=15; -16<=k<=17; -32<=l<=34
Reflections collected	20389
Independent reflections	9648 [R(int) = 0.0329]
Reflections observed (>2σ)	7901
Absorption correction	Multiscan
Max. and min. transmission	0.8998 and 0.7408
Refinement method	Full-matrix least-squares on F^2
Data / restraints / parameters	9648 / 15 / 609
Goodness-of-fit on F^2	1.039
Final R indices [I>2σ (I)]	R^1 = 0.0420 wR_2 = 0.1220
R indices (all data)	R^1 = 0.0577 wR_2 = 0.1430
Largest diff. peak and hole	0.783 and -0.682 $e.Å^{-3}$

Bond lengths [Å] and angles [°] for **5a**.

Ru(1)-C(33)	1.870(3)	Cl(4)-C(37)	1.734(5)
Ru(1)-N(2)	2.095(3)	Cl(5)-C(37)	1.707(4)
Ru(1)-N(1)	2.107(3)	Cl(6)-C(37)	1.835(5)
Ru(1)-N(3)	2.116(3)	C(1)-C(6)	1.391(5)
Ru(1)-P(1)	2.3098(8)	C(1)-C(2)	1.394(4)
Ru(1)-P(2)	2.3115(9)	C(2)-C(3)	1.389(5)
P(1)-C(1)	1.817(3)	C(3)-C(4)	1.389(6)
P(1)-C(7)	1.818(3)	C(4)-C(5)	1.360(5)
P(1)-C(13)	1.831(3)	C(5)-C(6)	1.389(5)
P(2)-C(21)	1.820(3)	C(7)-C(8)	1.392(5)
P(2)-C(15)	1.825(3)	C(7)-C(12)	1.392(4)
P(2)-C(14)	1.838(3)	C(8)-C(9)	1.374(5)
S(1)-O(3)	1.431(3)	C(9)-C(10)	1.382(6)
S(1)-O(2)	1.438(3)	C(10)-C(11)	1.374(5)
S(1)-O(4)	1.438(3)	C(11)-C(12)	1.381(4)
S(1)-C(34)	1.824(4)	C(13)-C(14)	1.546(5)
S(2)-O(7)	1.417(3)	C(15)-C(16)	1.402(5)
S(2)-O(5)	1.434(3)	C(15)-C(20)	1.403(5)
S(2)-O(6)	1.438(3)	C(16)-C(17)	1.394(5)
S(2)-C(35)	1.789(5)	C(17)-C(18)	1.383(5)
N(2)-C(29)	1.131(4)	C(18)-C(19)	1.383(5)
O(1)-C(33)	1.135(4)	C(19)-C(20)	1.376(5)
N(1)-C(27)	1.127(4)	C(21)-C(22)	1.392(5)
N(3)-C(31)	1.136(4)	C(21)-C(26)	1.393(5)
F(1)-C(35)	1.324(6)	C(22)-C(23)	1.390(5)
F(2)-C(35)	1.340(6)	C(23)-C(24)	1.363(6)
F(3)-C(35)	1.339(6)	C(24)-C(25)	1.388(6)
F(4)-C(34)	1.339(4)	C(25)-C(26)	1.382(5)
F(5)-C(34)	1.344(4)	C(27)-C(28)	1.460(5)
F(6)-C(34)	1.319(4)	C(29)-C(30)	1.461(5)
Cl(1)-C(36)	1.753(4)	C(31)-C(32)	1.459(5)
Cl(2)-C(36)	1.744(4)	Cl(3)-C(36)	1.755(4)

N(2)-Ru(1)-N(1)	83.10(10)	O(7)-S(2)-C(35)	103.2(2)
C(33)-Ru(1)-N(2)	176.18(12)	O(5)-S(2)-C(35)	103.5(2)
C(33)-Ru(1)-N(1)	93.59(12)	O(6)-S(2)-C(35)	103.3(2)
C(33)-Ru(1)-N(3)	90.04(11)	C(29)-N(2)-Ru(1)	169.6(3)
N(2)-Ru(1)-N(3)	88.06(10)	C(27)-N(1)-Ru(1)	177.4(3)
N(1)-Ru(1)-N(3)	89.70(10)	C(31)-N(3)-Ru(1)	170.1(3)
C(33)-Ru(1)-P(1)	90.92(9)	C(6)-C(1)-C(2)	119.2(3)
N(2)-Ru(1)-P(1)	91.14(7)	C(6)-C(1)-P(1)	118.5(2)
N(1)-Ru(1)-P(1)	93.03(7)	C(2)-C(1)-P(1)	122.2(3)
N(3)-Ru(1)-P(1)	177.05(8)	C(3)-C(2)-C(1)	120.0(3)
C(33)-Ru(1)-P(2)	86.11(10)	C(2)-C(3)-C(4)	120.2(3)
N(2)-Ru(1)-P(2)	97.28(8)	C(5)-C(4)-C(3)	119.6(3)
N(1)-Ru(1)-P(2)	177.49(7)	C(4)-C(5)-C(6)	121.2(4)
N(3)-Ru(1)-P(2)	92.79(8)	C(5)-C(6)-C(1)	119.7(3)
P(1)-Ru(1)-P(2)	84.49(3)	C(8)-C(7)-C(12)	118.5(3)
C(1)-P(1)-C(7)	103.13(14)	C(8)-C(7)-P(1)	119.6(3)
C(1)-P(1)-C(13)	107.32(15)	C(12)-C(7)-P(1)	121.8(2)
C(7)-P(1)-C(13)	106.43(15)	C(9)-C(8)-C(7)	120.5(3)
C(1)-P(1)-Ru(1)	114.08(10)	C(8)-C(9)-C(10)	120.3(4)
C(7)-P(1)-Ru(1)	117.18(11)	C(11)-C(10)-C(9)	119.9(3)
C(13)-P(1)-Ru(1)	108.08(11)	C(10)-C(11)-C(12)	120.0(3)
C(21)-P(2)-C(15)	105.75(15)	C(11)-C(12)-C(7)	120.7(3)
C(21)-P(2)-C(14)	108.95(16)	C(14)-C(13)-P(1)	108.4(2)
C(15)-P(2)-C(14)	105.27(15)	C(13)-C(14)-P(2)	106.5(2)
C(21)-P(2)-Ru(1)	113.47(11)	C(16)-C(15)-C(20)	119.0(3)
C(15)-P(2)-Ru(1)	117.91(11)	C(16)-C(15)-P(2)	119.2(2)
C(14)-P(2)-Ru(1)	104.98(11)	C(20)-C(15)-P(2)	121.7(3)
O(3)-S(1)-O(2)	115.67(19)	C(17)-C(16)-C(15)	120.2(3)
O(3)-S(1)-O(4)	115.08(18)	C(18)-C(17)-C(16)	119.7(3)
O(2)-S(1)-O(4)	114.91(16)	C(19)-C(18)-C(17)	120.4(3)
O(3)-S(1)-C(34)	102.80(17)	C(20)-C(19)-C(18)	120.5(3)
O(2)-S(1)-C(34)	103.07(16)	C(19)-C(20)-C(15)	120.2(3)
O(4)-S(1)-C(34)	102.60(17)	C(22)-C(21)-C(26)	119.5(3)
O(7)-S(2)-O(5)	116.19(18)	C(22)-C(21)-P(2)	121.1(3)
O(7)-S(2)-O(6)	114.30(19)	C(26)-C(21)-P(2)	119.0(3)

O(5)-S(2)-O(6)	113.98(18)	F(4)-C(34)-S(1)	112.1(3)
C(23)-C(22)-C(21)	119.8(4)	F(5)-C(34)-S(1)	111.2(2)
C(24)-C(23)-C(22)	120.3(4)	F(1)-C(35)-F(3)	107.2(5)
C(23)-C(24)-C(25)	120.5(4)	F(1)-C(35)-F(2)	105.2(4)
C(26)-C(25)-C(24)	120.0(4)	F(3)-C(35)-F(2)	109.4(5)
C(25)-C(26)-C(21)	119.9(4)	F(1)-C(35)-S(2)	112.9(4)
N(1)-C(27)-C(28)	178.7(4)	F(3)-C(35)-S(2)	110.3(3)
N(2)-C(29)-C(30)	179.3(4)	F(2)-C(35)-S(2)	111.6(4)
N(3)-C(31)-C(32)	177.9(4)	Cl(2)-C(36)-Cl(1)	110.7(2)
O(1)-C(33)-Ru(1)	178.2(3)	Cl(2)-C(36)-Cl(3)	111.0(2)
F(6)-C(34)-F(4)	107.0(3)	Cl(1)-C(36)-Cl(3)	110.1(2)
F(6)-C(34)-F(5)	107.3(3)	Cl(5)-C(37)-Cl(4)	114.6(3)
F(4)-C(34)-F(5)	106.7(3)	Cl(5)-C(37)-Cl(6)	107.3(3)
F(6)-C(34)-S(1)	112.2(2)	Cl(4)-C(37)-Cl(6)	106.5(3)

Appendix 7: *Crystallographic data for compound* ***5b****.*

Crystal data and structure refinement for **5b**.

Identification code	k02mkw8
Empirical formula	C34 H34.50 B2 F8 N3.50 O P2 Ru
Formula weight	844.78
Temperature	173(2) K
Wavelength	0.71073 Å
Crystal system	Monoclinic
Space group	$P2_1/c$
Unit cell dimensions	a = 16.34100(10)Å $\alpha = 90^\circ$
	b = 12.87300(10)Å $\beta = 130.58^\circ$
	c = 24.0470(2)Å $\gamma = 90^\circ$
Volume	3842.13(5) $Å^3$
Z	4
Density (calculated)	1.460 Mg/m^3
Absorption coefficient	0.562 mm^{-1}
F(000)	1708
Crystal size	0.25 x 0.25 x 0.25 mm
Theta range for data collection	3.57 to 30.03°
Index ranges	-21<=h<=23; -18<=k<=17; -33<=l<=33
Reflections collected	87651
Independent reflections	11215 [R(int) = 0.0631]
Reflections observed (>2σ)	9518
Data Completeness	0.997
Refinement method	Full-matrix least-squares on F^2
Data / restraints / parameters	11215 / 0 / 499
Goodness-of-fit on F^2	1.029
Final R indices [I>2σ (I)]	$R_1 = 0.0432$ $wR_2 = 0.1157$
R indices (all data)	$R_1 = 0.0529$ $wR_2 = 0.1231$
Largest diff. peak and hole	1.530 and -0.858 $eÅ^{-3}$

Bond lengths [Å] and angles [°] for **5b**.

Ru(1)-C(1)	1.864(2)	Ru(1)-N(1)	2.085(5)
Ru(1)-N(2)	2.111(2)	Ru(1)-N(3)	2.115(2)
Ru(1)-N(1A)	2.18(3)	Ru(1)-P(1)	2.3175(6)
Ru(1)-P(2)	2.3195(6)	P(1)-C(16)	1.819(2)
P(1)-C(10)	1.819(2)	P(1)-C(9)	1.827(2)
P(2)-C(28)	1.811(2)	P(2)-C(22)	1.823(2)
P(2)-C(8)	1.834(2)	F(1)-B(1)	1.415(5)
F(2)-B(1)	1.376(5)	F(3)-B(1)	1.375(6)
F(4)-B(1)	1.365(5)	F(5)-B(2)	1.376(5)
F(6)-B(2)	1.387(5)	F(7)-B(2)	1.368(5)
F(8)-B(2)	1.388(5)	O(1)-C(1)	1.130(3)
N(1)-C(2)	1.140(7)	N(2)-C(4)	1.135(3)
N(3)-C(6)	1.132(3)	N(4)-C(34)	1.156(15)
C(2)-C(3)	1.458(7)	C(4)-C(5)	1.457(4)
C(6)-C(7)	1.462(4)	C(8)-C(9)	1.532(3)
C(10)-C(11)	1.384(4)	C(10)-C(15)	1.396(4)
C(11)-C(12)	1.398(4)	C(12)-C(13)	1.380(5)
C(13)-C(14)	1.380(5)	C(14)-C(15)	1.392(4)
C(16)-C(21)	1.399(4)	C(16)-C(17)	1.403(4)
C(17)-C(18)	1.391(4)	C(18)-C(19)	1.389(4)
C(19)-C(20)	1.382(4)	C(20)-C(21)	1.392(4)
C(22)-C(23)	1.388(4)	C(22)-C(27)	1.390(4)
C(23)-C(24)	1.397(5)	C(24)-C(25)	1.363(6)
C(25)-C(26)	1.371(5)	C(26)-C(27)	1.388(4)
C(28)-C(33)	1.390(4)	C(28)-C(29)	1.390(4)
C(29)-C(30)	1.399(5)	C(30)-C(31)	1.374(6)
C(31)-C(32)	1.355(5)	C(32)-C(33)	1.393(4)
C(34)-C(35)	1.275(18)	C(2A)-N(1A)	1.02(3)
C(2A)-C(3A)	1.45(3)		

C(1)-Ru(1)-N(1)	177.75(13)	C(1)-Ru(1)-N(2)	95.24(10)
N(1)-Ru(1)-N(2)	86.46(10)	C(1)-Ru(1)-N(3)	94.04(9)

N(1)-Ru(1)-N(3)	87.54(15)	N(2)-Ru(1)-N(3)	85.55(8)
C(1)-Ru(1)-N(1A)	172.5(5)	N(1)-Ru(1)-N(1A)	9.2(5)
N(2)-Ru(1)-N(1A)	77.3(5)	N(3)-Ru(1)-N(1A)	85.9(7)
C(1)-Ru(1)-P(1)	92.09(8)	N(1)-Ru(1)-P(1)	86.21(8)
N(2)-Ru(1)-P(1)	172.67(6)	N(3)-Ru(1)-P(1)	94.07(6)
N(1A)-Ru(1)-P(1)	95.4(5)	C(1)-Ru(1)-P(2)	86.96(8)
N(1)-Ru(1)-P(2)	91.44(14)	N(2)-Ru(1)-P(2)	95.32(6)
N(3)-Ru(1)-P(2)	178.61(6)	N(1A)-Ru(1)-P(2)	93.2(7)
P(1)-Ru(1)-P(2)	84.92(2)	C(16)-P(1)-C(10)	104.97(11)
C(16)-P(1)-C(9)	106.56(12)	C(10)-P(1)-C(9)	107.08(11)
C(16)-P(1)-Ru(1)	117.72(8)	C(10)-P(1)-Ru(1)	114.46(8)
C(9)-P(1)-Ru(1)	105.39(8)	C(28)-P(2)-C(22)	105.23(11)
C(28)-P(2)-C(8)	106.08(12)	C(22)-P(2)-C(8)	106.13(12)
C(28)-P(2)-Ru(1)	116.97(9)	C(22)-P(2)-Ru(1)	114.62(7)
C(8)-P(2)-Ru(1)	107.04(8)	C(2)-N(1)-Ru(1)	178.1(4)
C(4)-N(2)-Ru(1)	170.1(2)	C(6)-N(3)-Ru(1)	175.9(2)
O(1)-C(1)-Ru(1)	177.9(2)	N(1)-C(2)-C(3)	176.6(7)
N(2)-C(4)-C(5)	179.4(3)	N(3)-C(6)-C(7)	178.9(3)
C(9)-C(8)-P(2)	108.22(16)	C(8)-C(9)-P(1)	107.98(16)
C(11)-C(10)-C(15)	119.2(2)	C(11)-C(10)-P(1)	121.7(2)
C(15)-C(10)-P(1)	119.12(19)	C(10)-C(11)-C(12)	120.1(3)
C(13)-C(12)-C(11)	120.2(3)	C(14)-C(13)-C(12)	120.1(3)
C(13)-C(14)-C(15)	119.8(3)	C(14)-C(15)-C(10)	120.5(3)
C(21)-C(16)-C(17)	119.5(2)	C(21)-C(16)-P(1)	119.74(19)
C(17)-C(16)-P(1)	120.71(19)	C(18)-C(17)-C(16)	119.8(3)
C(19)-C(18)-C(17)	120.2(3)	C(20)-C(19)-C(18)	120.3(3)
C(19)-C(20)-C(21)	120.2(3)	C(20)-C(21)-C(16)	119.9(2)
C(23)-C(22)-C(27)	118.4(2)	C(23)-C(22)-P(2)	123.3(2)
C(27)-C(22)-P(2)	118.24(19)	C(22)-C(23)-C(24)	119.7(3)
C(25)-C(24)-C(23)	121.1(3)	C(24)-C(25)-C(26)	119.7(3)
C(25)-C(26)-C(27)	120.1(3)	C(26)-C(27)-C(22)	120.9(3)
C(33)-C(28)-C(29)	118.9(3)	C(33)-C(28)-P(2)	120.4(2)
C(29)-C(28)-P(2)	120.6(2)	C(28)-C(29)-C(30)	119.1(3)
C(31)-C(30)-C(29)	120.8(3)	C(32)-C(31)-C(30)	120.5(3)
C(31)-C(32)-C(33)	119.8(3)	C(28)-C(33)-C(32)	120.9(3)

N(4)-C(34)-C(35)	177.4(12)	F(4)-B(1)-F(3)	111.7(4)
F(4)-B(1)-F(2)	110.6(3)	F(3)-B(1)-F(2)	107.4(4)
F(4)-B(1)-F(1)	108.6(4)	F(3)-B(1)-F(1)	109.4(3)
F(2)-B(1)-F(1)	109.2(4)	F(7)-B(2)-F(5)	107.6(3)
F(7)-B(2)-F(6)	109.6(4)	F(5)-B(2)-F(6)	110.5(3)
F(7)-B(2)-F(8)	111.7(4)	F(5)-B(2)-F(8)	107.7(4)
F(6)-B(2)-F(8)	109.8(3)	N(1A)-C(2A)-C(3A)	172(3)
C(2A)-N(1A)-Ru(1)	168(2)		

Appendix 8: *Crystallographic data for compound* ***6a****.*

Crystal data and structure refinement for **6a**.

Identification code	k01mkw8
Empirical formula	C38 H48 F6 O11 P2 Ru S5
Formula weight	1118.07
Temperature	150(2) K
Wavelength	0.71070 Å
Crystal system	Orthorhombic
Space group	$P2_12_12_1$
Unit cell dimensions	a = 11.53960(10)Å $\alpha = 90^\circ$
	b = 20.25930(10)Å $\beta = 90^\circ$
	c = 20.42650(10)Å $\gamma = 90^\circ$
Volume	4775.39(5) $Å^3$
Z	4
Density (calculated)	1.555 Mg/m^3
Absorption coefficient	0.691 mm^{-1}
F(000)	2288
Crystal size	0.28 x 0.25 x 0.25 mm
Theta range for data collection	4.60 to 30.03 °.
Index ranges	-15<=h<=16; -28<=k<=27; -28<=l<=28
Reflections collected	92137
Independent reflections	13879 [R(int) = 0.0377]
Reflections observed (>2σ)	13626
Data Completeness	0.992
Max. and min. transmission	0.8462 and 0.8300
Refinement method	Full-matrix least-squares on F^2
Data / restraints / parameters	13879 / 0 / 596
Goodness-of-fit on F^2	1.037
Final R indices [I>2σ (I)]	$R_1 = 0.0339$ $wR_2 = 0.0762$
R indices (all data)	$R_1 = 0.0350$ $wR_2 = 0.0767$
Absolute structure parameter	-0.018(17)

Largest diff. peak and hole 0.819 and -0.816 e.Å^{-3}

Bond lengths [Å] and angles [°] for **6a**.

Ru(1)-C(1)	1.831(2)	Ru(1)-O(3)	2.1351(16)
Ru(1)-O(4)	2.1520(17)	Ru(1)-O(2)	2.1808(17)
Ru(1)-P(2)	2.2865(5)	Ru(1)-P(1)	2.2941(6)
S(1)-O(2)	1.5307(18)	S(1)-C(29)	1.776(4)
S(1)-C(28)	1.798(4)	S(2)-O(3)	1.5446(16)
S(2)-C(31)	1.774(3)	S(2)-C(30)	1.774(3)
S(3)-O(4)	1.5346(18)	S(3)-C(32)	1.777(4)
S(3)-C(33)	1.782(4)	S(4)-O(7)	1.430(3)
S(4)-O(6)	1.433(2)	S(4)-O(5)	1.434(3)
S(4)-C(34)	1.813(3)	S(5)-O(8)	1.432(2)
S(5)-O(10)	1.440(2)	S(5)-O(9)	1.4423(19)
S(5)-C(35)	1.821(3)	F(1)-C(34)	1.338(4)
F(2)-C(34)	1.327(4)	F(3)-C(34)	1.333(4)
F(4)-C(35)	1.340(3)	F(5)-C(35)	1.341(3)
F(6)-C(35)	1.330(3)	P(1)-C(2)	1.8168(13)
P(1)-C(8)	1.8204(16)	P(1)-C(14)	1.827(2)
P(1)-C(2A)	1.8510(13)	P(2)-C(16)	1.815(2)
P(2)-C(22)	1.824(2)	P(2)-C(15)	1.828(2)
C(1)-O(1)	1.148(3)	C(2)-C(3)	1.3900
C(2)-C(7)	1.3900	C(3)-C(4)	1.3900
C(4)-C(5)	1.3900	C(5)-C(6)	1.3900
C(6)-C(7)	1.3900	C(2A)-C(3A)	1.3901
C(2A)-C(7A)	1.4054	C(3A)-C(4A)	1.3769
C(4A)-C(5A)	1.3703	C(5A)-C(6A)	1.3618
C(6A)-C(7A)	1.3947	C(8)-C(9)	1.3897
C(8)-C(13)	1.391(3)	C(9)-C(10)	1.389(3)
C(10)-C(11)	1.373(4)	C(11)-C(12)	1.390(5)
C(12)-C(13)	1.402(4)	C(14)-C(15)	1.539(3)
C(16)-C(21)	1.389(4)	C(16)-C(17)	1.398(3)

C(17)-C(18)	1.393(3)	C(18)-C(19)	1.380(4)
C(19)-C(20)	1.383(4)	C(20)-C(21)	1.394(4)
C(22)-C(27)	1.389(3)	C(22)-C(23)	1.396(3)
C(23)-C(24)	1.393(4)	C(24)-C(25)	1.367(5)
C(25)-C(26)	1.389(5)	C(26)-C(27)	1.394(4)
C(57)-O(11)	1.198(6)	C(57)-C(63)	1.454(6)
C(57)-C(61)	1.465(6)		

C(1)-Ru(1)-O(3)	176.17(9)	C(1)-Ru(1)-O(4)	103.34(10)
O(3)-Ru(1)-O(4)	80.50(7)	C(1)-Ru(1)-O(2)	95.20(9)
O(3)-Ru(1)-O(2)	85.21(7)	O(4)-Ru(1)-O(2)	83.48(7)
C(1)-Ru(1)-P(2)	88.07(8)	O(3)-Ru(1)-P(2)	88.10(4)
O(4)-Ru(1)-P(2)	168.01(5)	O(2)-Ru(1)-P(2)	91.93(5)
C(1)-Ru(1)-P(1)	91.07(8)	O(3)-Ru(1)-P(1)	88.32(5)
O(4)-Ru(1)-P(1)	98.25(6)	O(2)-Ru(1)-P(1)	172.95(5)
P(2)-Ru(1)-P(1)	85.02(2)	O(2)-S(1)-C(29)	103.69(19)
O(2)-S(1)-C(28)	104.73(17)	C(29)-S(1)-C(28)	98.21(19)
O(3)-S(2)-C(31)	103.71(13)	O(3)-S(2)-C(30)	103.00(13)
C(31)-S(2)-C(30)	98.9(2)	O(4)-S(3)-C(32)	104.60(15)
O(4)-S(3)-C(33)	103.53(15)	C(32)-S(3)-C(33)	98.0(3)
O(7)-S(4)-O(6)	114.86(18)	O(7)-S(4)-O(5)	115.22(18)
O(6)-S(4)-O(5)	116.12(17)	O(7)-S(4)-C(34)	102.14(16)
O(6)-S(4)-C(34)	102.81(15)	O(5)-S(4)-C(34)	102.77(16)
O(8)-S(5)-O(10)	115.59(14)	O(8)-S(5)-O(9)	115.41(13)
O(10)-S(5)-O(9)	115.20(12)	O(8)-S(5)-C(35)	102.72(14)
O(10)-S(5)-C(35)	103.13(13)	O(9)-S(5)-C(35)	101.87(12)
C(2)-P(1)-C(8)	104.43(7)	C(2)-P(1)-C(14)	106.42(9)
C(8)-P(1)-C(14)	106.45(9)	C(2)-P(1)-C(2A)	7.0
C(8)-P(1)-C(2A)	100.66(7)	C(14)-P(1)-C(2A)	102.29(9)
C(2)-P(1)-Ru(1)	114.61(6)	C(8)-P(1)-Ru(1)	117.90(6)
C(14)-P(1)-Ru(1)	106.27(7)	C(2A)-P(1)-Ru(1)	121.50(6)
C(16)-P(2)-C(22)	102.57(10)	C(16)-P(2)-C(15)	106.16(10)
C(22)-P(2)-C(15)	106.06(11)	C(16)-P(2)-Ru(1)	118.09(8)
C(22)-P(2)-Ru(1)	114.49(7)	C(15)-P(2)-Ru(1)	108.54(7)
O(1)-C(1)-Ru(1)	176.8(2)	C(3)-C(2)-C(7)	120.0

C(3)-C(2)-P(1)	120.15(5)	C(7)-C(2)-P(1)	119.84(6)
C(2)-C(3)-C(4)	120.0	C(5)-C(4)-C(3)	120.0
C(4)-C(5)-C(6)	120.0	C(7)-C(6)-C(5)	120.0
C(6)-C(7)-C(2)	120.0	C(3A)-C(2A)-C(7A)	118.3
C(3A)-C(2A)-P(1)	119.5	C(7A)-C(2A)-P(1)	121.6
C(4A)-C(3A)-C(2A)	119.9	C(5A)-C(4A)-C(3A)	122.1
C(6A)-C(5A)-C(4A)	117.7	C(5A)-C(6A)-C(7A)	122.0
C(6A)-C(7A)-C(2A)	119.1	C(9)-C(8)-C(13)	118.87(17)
C(9)-C(8)-P(1)	119.43(10)	C(13)-C(8)-P(1)	121.48(15)
C(10)-C(9)-C(8)	120.94(19)	C(11)-C(10)-C(9)	120.1(2)
C(10)-C(11)-C(12)	120.0(2)	C(11)-C(12)-C(13)	119.9(3)
C(8)-C(13)-C(12)	120.1(3)	C(15)-C(14)-P(1)	108.31(15)
C(14)-C(15)-P(2)	108.51(14)	C(21)-C(16)-C(17)	119.5(2)
C(21)-C(16)-P(2)	119.72(18)	C(17)-C(16)-P(2)	120.65(18)
C(18)-C(17)-C(16)	119.3(2)	C(19)-C(18)-C(17)	120.9(2)
C(18)-C(19)-C(20)	119.8(2)	C(19)-C(20)-C(21)	119.9(3)
C(16)-C(21)-C(20)	120.5(3)	C(27)-C(22)-C(23)	119.2(2)
C(27)-C(22)-P(2)	119.26(18)	C(23)-C(22)-P(2)	121.48(18)
C(24)-C(23)-C(22)	120.1(3)	C(25)-C(24)-C(23)	120.6(3)
C(24)-C(25)-C(26)	119.8(2)	C(25)-C(26)-C(27)	120.3(3)
C(22)-C(27)-C(26)	119.9(3)	F(2)-C(34)-F(3)	107.8(3)
F(2)-C(34)-F(1)	106.3(3)	F(3)-C(34)-F(1)	106.2(3)
F(2)-C(34)-S(4)	112.3(2)	F(3)-C(34)-S(4)	111.2(2)
F(1)-C(34)-S(4)	112.7(2)	F(6)-C(35)-F(4)	106.9(2)
F(6)-C(35)-F(5)	107.1(2)	F(4)-C(35)-F(5)	106.9(2)
F(6)-C(35)-S(5)	112.2(2)	F(4)-C(35)-S(5)	111.60(19)
F(5)-C(35)-S(5)	111.92(19)	O(11)-C(57)-C(63)	119.9(5)
O(11)-C(57)-C(61)	121.1(5)	C(63)-C(57)-C(61)	119.0(5)
S(1)-O(2)-Ru(1)	121.74(10)	S(2)-O(3)-Ru(1)	118.46(10)
S(3)-O(4)-Ru(1)	131.37(11)		

Appendix 9: *Crystallographic data for compound* ***7a****.*

Crystal data and structure refinement for **7a**.

Identification code	k01mkw6
Empirical formula	C45.50 H54 F6 N3 O7.50 P2 Ru S2
Formula weight	1104.05
Temperature	150(2) K
Wavelength	0.7107 Å
Crystal system	Monoclinic
Space group	$P2_1/n$
Unit cell dimensions	a = 12.11030(10)Å $\alpha = 90^\circ$
	b = 21.97210(10)Å $\beta = 90.1040(3)^\circ$
	c = 19.6937(2)Å $\gamma = 90^\circ$
Volume	5240.26(7) $Å^3$
Z	4
Density (calculated)	1.399 Mg/m^3
Absorption coefficient	0.511 mm^{-1}
F(000)	2272
Crystal size	0.30 x 0.20 x 0.10 mm
Theta range for data collection	3.53 to 27.12°
Index ranges	-15<=h<=13; -27<=k<=28; -25<=l<=25
Reflections collected	82263
Independent reflections	11508 [R(int) = 0.0566]
Reflections observed (>2σ)	10152
Absorption correction	Semi-empirical from equivalents
Max. and min. transmission	1.055 and 0.944
Refinement method	Full-matrix least-squares on F^2
Data / restraints / parameters	11508 / 3 / 635
Goodness-of-fit on F^2	0.966
Final R indices [I>2σ (I)]	$R_1 = 0.0504$ $wR_2 = 0.1254$
R indices (all data)	$R_1 = 0.0580$ $wR_2 = 0.1312$
Largest diff. peak and hole	1.873 and -1.750 $eÅ^{-3}$

Bond lengths [Å] and angles [°] for **7a**.

Ru(1)-C(27)	1.937(3)	Ru(1)-C(33)	2.025(3)
Ru(1)-C(28)	2.030(3)	Ru(1)-C(38)	2.041(3)
Ru(1)-P(2)	2.3583(7)	Ru(1)-P(1)	2.3660(7)
S(1)-O(3)	1.433(3)	S(1)-O(2)	1.434(3)
S(1)-O(4)	1.438(3)	S(1)-C(43)	1.804(6)
S(2)-O(7)	1.375(5)	S(2)-O(6)	1.405(5)
S(2)-C(44)	1.601(14)	S(2)-O(5)	1.778(8)
P(1)-C(1)	1.821(3)	P(1)-C(7)	1.822(3)
P(1)-C(25)	1.834(3)	P(2)-C(19)	1.815(3)
P(2)-C(13)	1.820(3)	P(2)-C(26)	1.839(3)
O(1)-C(27)	1.121(4)	F(1)-C(43)	1.337(7)
F(2)-C(43)	1.328(7)	F(3)-C(43)	1.322(6)
F(4)-C(44)	1.415(10)	F(5)-C(44)	1.482(11)
F(6)-C(44)	1.332(8)	N(1)-C(28)	1.141(4)
N(1)-C(29)	1.474(4)	N(2)-C(33)	1.140(4)
N(2)-C(34)	1.471(4)	N(3)-C(38)	1.140(4)
N(3)-C(39)	1.471(4)	C(1)-C(6)	1.394(4)
C(1)-C(2)	1.402(4)	C(2)-C(3)	1.389(5)
C(3)-C(4)	1.383(5)	C(4)-C(5)	1.385(5)
C(5)-C(6)	1.390(5)	C(7)-C(8)	1.396(4)
C(7)-C(12)	1.397(4)	C(8)-C(9)	1.396(5)
C(9)-C(10)	1.374(6)	C(10)-C(11)	1.382(6)
C(11)-C(12)	1.398(5)	C(13)-C(14)	1.387(5)
C(13)-C(18)	1.400(4)	C(14)-C(15)	1.384(5)
C(15)-C(16)	1.385(5)	C(16)-C(17)	1.379(6)
C(17)-C(18)	1.382(5)	C(19)-C(24)	1.388(5)
C(19)-C(20)	1.400(5)	C(20)-C(21)	1.380(5)
C(21)-C(22)	1.386(7)	C(22)-C(23)	1.373(7)
C(23)-C(24)	1.400(6)	C(25)-C(26)	1.532(4)
C(29)-C(30)	1.509(6)	C(29)-C(31)	1.514(5)
C(29)-C(32)	1.516(6)	C(34)-C(37)	1.503(7)

C(34)-C(35)	1.512(6)	C(34)-C(36)	1.531(8)
C(39)-C(42)	1.519(6)	C(39)-C(41)	1.520(6)
C(39)-C(40)	1.521(5)	O(8)-C(46)	1.188(19)
C(45)-C(46)	1.56(2)	C(46)-C(47)	1.62(3)

C(27)-Ru(1)-C(33)	91.33(14)	C(27)-Ru(1)-C(28)	94.31(12)
C(33)-Ru(1)-C(28)	88.76(12)	C(27)-Ru(1)-C(38)	177.42(12)
C(33)-Ru(1)-C(38)	86.09(13)	C(28)-Ru(1)-C(38)	85.60(12)
C(27)-Ru(1)-P(2)	90.36(9)	C(33)-Ru(1)-P(2)	94.91(9)
C(28)-Ru(1)-P(2)	173.99(8)	C(38)-Ru(1)-P(2)	89.90(8)
C(27)-Ru(1)-P(1)	92.84(10)	C(33)-Ru(1)-P(1)	175.79(10)
C(28)-Ru(1)-P(1)	91.51(8)	C(38)-Ru(1)-P(1)	89.74(8)
P(2)-Ru(1)-P(1)	84.48(3)	O(3)-S(1)-O(2)	114.44(19)
O(3)-S(1)-O(4)	115.4(2)	O(2)-S(1)-O(4)	114.51(17)
O(3)-S(1)-C(43)	103.7(3)	O(2)-S(1)-C(43)	104.0(2)
O(4)-S(1)-C(43)	102.6(2)	O(7)-S(2)-O(6)	122.4(3)
O(7)-S(2)-C(44)	109.6(5)	O(6)-S(2)-C(44)	111.0(4)
O(7)-S(2)-O(5)	108.5(4)	O(6)-S(2)-O(5)	105.4(4)
C(44)-S(2)-O(5)	96.6(4)	C(1)-P(1)-C(7)	106.72(13)
C(1)-P(1)-C(25)	107.19(14)	C(7)-P(1)-C(25)	106.92(14)
C(1)-P(1)-Ru(1)	114.14(10)	C(7)-P(1)-Ru(1)	114.70(9)
C(25)-P(1)-Ru(1)	106.72(10)	C(19)-P(2)-C(13)	101.62(14)
C(19)-P(2)-C(26)	107.57(15)	C(13)-P(2)-C(26)	105.68(14)
C(19)-P(2)-Ru(1)	114.43(10)	C(13)-P(2)-Ru(1)	119.77(11)
C(26)-P(2)-Ru(1)	106.96(10)	C(28)-N(1)-C(29)	172.4(3)
C(33)-N(2)-C(34)	177.0(4)	C(38)-N(3)-C(39)	177.4(3)
C(6)-C(1)-C(2)	118.9(3)	C(6)-C(1)-P(1)	122.0(2)
C(2)-C(1)-P(1)	119.1(2)	C(3)-C(2)-C(1)	120.5(3)
C(4)-C(3)-C(2)	119.8(3)	C(3)-C(4)-C(5)	120.4(3)
C(4)-C(5)-C(6)	120.0(3)	C(5)-C(6)-C(1)	120.4(3)
C(8)-C(7)-C(12)	119.3(3)	C(8)-C(7)-P(1)	119.5(2)
C(12)-C(7)-P(1)	121.1(2)	C(9)-C(8)-C(7)	119.9(3)
C(10)-C(9)-C(8)	120.6(3)	C(9)-C(10)-C(11)	120.0(3)
C(10)-C(11)-C(12)	120.4(3)	C(7)-C(12)-C(11)	119.8(3)
C(14)-C(13)-C(18)	119.1(3)	C(14)-C(13)-P(2)	121.6(2)

C(18)-C(13)-P(2)	119.1(2)	C(15)-C(14)-C(13)	120.4(3)
C(14)-C(15)-C(16)	120.0(4)	C(17)-C(16)-C(15)	120.1(3)
C(16)-C(17)-C(18)	120.3(3)	C(17)-C(18)-C(13)	120.1(3)
C(24)-C(19)-C(20)	119.4(3)	C(24)-C(19)-P(2)	123.2(3)
C(20)-C(19)-P(2)	117.3(3)	C(21)-C(20)-C(19)	120.7(4)
C(20)-C(21)-C(22)	119.4(4)	C(23)-C(22)-C(21)	120.6(4)
C(22)-C(23)-C(24)	120.4(4)	C(19)-C(24)-C(23)	119.4(4)
C(26)-C(25)-P(1)	109.5(2)	C(25)-C(26)-P(2)	110.6(2)
O(1)-C(27)-Ru(1)	178.3(3)	N(1)-C(28)-Ru(1)	173.9(3)
N(1)-C(29)-C(30)	108.3(3)	N(1)-C(29)-C(31)	107.3(3)
C(30)-C(29)-C(31)	111.6(3)	N(1)-C(29)-C(32)	106.0(3)
C(30)-C(29)-C(32)	112.0(4)	C(31)-C(29)-C(32)	111.3(4)
N(2)-C(33)-Ru(1)	175.7(3)	N(2)-C(34)-C(37)	107.4(4)
N(2)-C(34)-C(35)	106.1(3)	C(37)-C(34)-C(35)	113.5(5)
N(2)-C(34)-C(36)	106.7(4)	C(37)-C(34)-C(36)	110.9(5)
C(35)-C(34)-C(36)	111.8(4)	N(3)-C(38)-Ru(1)	174.4(3)
N(3)-C(39)-C(42)	106.6(3)	N(3)-C(39)-C(41)	107.1(3)
C(42)-C(39)-C(41)	111.6(4)	N(3)-C(39)-C(40)	106.6(3)
C(42)-C(39)-C(40)	112.4(4)	C(41)-C(39)-C(40)	112.1(4)
F(3)-C(43)-F(2)	107.9(6)	F(3)-C(43)-F(1)	108.0(5)
F(2)-C(43)-F(1)	106.8(5)	F(3)-C(43)-S(1)	112.0(4)
F(2)-C(43)-S(1)	111.1(4)	F(1)-C(43)-S(1)	110.9(5)
F(6)-C(44)-F(4)	124.1(10)	F(6)-C(44)-F(5)	118.2(8)
F(4)-C(44)-F(5)	94.0(9)	F(6)-C(44)-S(2)	100.6(9)
F(4)-C(44)-S(2)	111.0(7)	F(5)-C(44)-S(2)	108.8(7)
O(8)-C(46)-C(45)	134.5(17)	O(8)-C(46)-C(47)	122.7(17)
C(45)-C(46)-C(47)	102.1(14)		

Appendix 10: Crystallographic data for compound **8a**.

Crystal data and structure refinement for **8a**.

Identification code	h02mkw2
Empirical formula	C39 H40 F6 N2 O11 P2 Ru S2
Formula weight	1053.86
Temperature	150(2) K
Wavelength	0.71073 Å
Crystal system	Monoclinic
Space group	P21/n
Unit cell dimensions	a = 15.8630(2)Å α= 90°
	b = 14.1260(2)Å β = 102.6350(10)°
	c = 20.1520(3)Å γ = 90°
Volume	4406.32(11) $Å^3$
Z	4
Density (calculated)	1.589 Mg/m^3
Absorption coefficient	0.609 mm^{-1}
F(000)	2144
Crystal size	0.40 x 0.25 x 0.05 mm
Theta range for data collection	4.31 to 27.50 °.
Index ranges	-20<=h<=20; -18<=k<=18; -26<=l<=26
Reflections collected	87279
Independent reflections	10006 [R(int) = 0.0677]
Reflections observed (>2σ)	7369
Data Completeness	0.989
Absorption correction	Semi-empirical from equivalents
Max. and min. transmission	0.97 and 0.85
Refinement method	Full-matrix least-squares on F^2
Data / restraints / parameters	10006 / 2 / 577
Goodness-of-fit on F^2	1.033
Final R indices [I>2σ (I)]	R_1 = 0.0636 wR_2 = 0.1672
R indices (all data)	R_1 = 0.0912 wR_2 = 0.1905
Largest diff. peak and hole	1.519 and -1.613 $e.Å^{-3}$

Bond lengths [Å] and angles [°] for **8a**.

Ru(1)-C(1)	1.838(5)	Ru(1)-O(2)	2.134(4)
Ru(1)-N(2)	2.177(4)	Ru(1)-N(1)	2.178(4)
Ru(1)-P(1)	2.3316(12)	Ru(1)-P(2)	2.3384(12)
S(1)-O(5)	1.382(6)	S(1)-O(3)	1.407(5)
S(1)-O(4)	1.466(7)	S(1)-C(38)	1.800(11)
S(2)-O(6)	1.384(7)	S(2)-O(7)	1.437(8)
S(2)-C(39)	1.697(15)	S(2)-O(8)	1.696(10)
P(1)-C(32)	1.817(5)	P(1)-C(25)	1.823(5)
P(1)-C(26)	1.821(5)	P(2)-C(12)	1.815(5)
P(2)-C(18)	1.817(5)	P(2)-C(24)	1.836(5)
F(1)-C(38)	1.275(9)	F(2)-C(38)	1.387(13)
F(3)-C(38)	1.286(11)	F(4)-C(39)	1.308(11)
F(5)-C(39)	1.467(15)	F(6)-C(39)	1.268(11)
O(1)-C(1)	1.143(6)	N(1)-C(2)	1.335(7)
N(1)-C(6)	1.352(7)	C(2)-C(3)	1.388(8)
N(2)-C(7)	1.341(6)	N(2)-C(11)	1.350(6)
C(3)-C(4)	1.362(9)	C(4)-C(5)	1.376(9)
C(5)-C(6)	1.386(7)	C(7)-C(8)	1.387(7)
C(8)-C(9)	1.362(9)	C(9)-C(10)	1.380(8)
C(10)-C(11)	1.374(7)	C(12)-C(13)	1.397(7)
C(12)-C(17)	1.400(7)	C(13)-C(14)	1.403(7)
C(14)-C(15)	1.370(9)	C(15)-C(16)	1.388(10)
C(16)-C(17)	1.384(8)	C(18)-C(23)	1.388(7)
C(18)-C(19)	1.402(7)	C(19)-C(20)	1.384(7)
C(20)-C(21)	1.391(8)	C(21)-C(22)	1.394(9)
C(22)-C(23)	1.382(8)	C(24)-C(25)	1.539(7)
C(26)-C(31)	1.391(7)	C(26)-C(27)	1.388(7)
C(27)-C(28)	1.396(7)	C(28)-C(29)	1.382(9)
C(29)-C(30)	1.357(9)	C(30)-C(31)	1.395(7)
C(32)-C(37)	1.381(7)	C(32)-C(33)	1.401(7)
C(33)-C(34)	1.391(8)	C(34)-C(35)	1.348(9)

C(35)-C(36)	1.391(9)	C(36)-C(37)	1.391(7)
C(1)-Ru(1)-O(2)	177.88(17)	C(1)-Ru(1)-N(2)	95.59(17)
O(2)-Ru(1)-N(2)	84.97(14)	C(1)-Ru(1)-N(1)	88.51(18)
O(2)-Ru(1)-N(1)	89.52(16)	N(2)-Ru(1)-N(1)	84.57(14)
C(1)-Ru(1)-P(1)	88.71(14)	O(2)-Ru(1)-P(1)	90.76(10)
N(2)-Ru(1)-P(1)	175.68(11)	N(1)-Ru(1)-P(1)	96.06(10)
C(1)-Ru(1)-P(2)	91.32(14)	O(2)-Ru(1)-P(2)	90.66(11)
N(2)-Ru(1)-P(2)	95.14(10)	N(1)-Ru(1)-P(2)	179.64(11)
P(1)-Ru(1)-P(2)	84.24(4)	O(5)-S(1)-O(3)	116.5(4)
O(5)-S(1)-O(4)	112.2(5)	O(3)-S(1)-O(4)	112.7(5)
O(5)-S(1)-C(38)	102.9(5)	O(3)-S(1)-C(38)	105.9(4)
O(4)-S(1)-C(38)	105.3(5)	O(6)-S(2)-O(7)	113.9(7)
O(6)-S(2)-C(39)	116.2(7)	O(7)-S(2)-C(39)	107.0(5)
O(6)-S(2)-O(8)	114.2(7)	O(7)-S(2)-O(8)	114.9(6)
C(39)-S(2)-O(8)	88.0(7)	C(32)-P(1)-C(25)	107.5(2)
C(32)-P(1)-C(26)	104.6(2)	C(25)-P(1)-C(26)	105.3(2)
C(32)-P(1)-Ru(1)	117.64(15)	C(25)-P(1)-Ru(1)	106.13(15)
C(26)-P(1)-Ru(1)	114.89(16)	C(12)-P(2)-C(18)	102.0(2)
C(12)-P(2)-C(24)	104.7(2)	C(18)-P(2)-C(24)	107.5(2)
C(12)-P(2)-Ru(1)	118.25(16)	C(18)-P(2)-Ru(1)	117.27(15)
C(24)-P(2)-Ru(1)	106.07(16)	O(1)-C(1)-Ru(1)	177.3(4)
C(2)-N(1)-C(6)	116.7(5)	C(2)-N(1)-Ru(1)	121.6(4)
C(6)-N(1)-Ru(1)	121.4(3)	N(1)-C(2)-C(3)	123.5(6)
C(7)-N(2)-C(11)	116.8(4)	C(7)-N(2)-Ru(1)	121.4(3)
C(11)-N(2)-Ru(1)	121.6(3)	C(4)-C(3)-C(2)	118.4(6)
C(3)-C(4)-C(5)	120.1(5)	C(4)-C(5)-C(6)	117.9(6)
N(1)-C(6)-C(5)	123.4(5)	N(2)-C(7)-C(8)	122.8(5)
C(9)-C(8)-C(7)	119.5(5)	C(8)-C(9)-C(10)	118.5(5)
C(11)-C(10)-C(9)	119.2(5)	N(2)-C(11)-C(10)	123.1(5)
C(13)-C(12)-C(17)	118.2(5)	C(13)-C(12)-P(2)	120.9(4)
C(17)-C(12)-P(2)	120.8(4)	C(12)-C(13)-C(14)	120.1(5)
C(15)-C(14)-C(13)	120.3(5)	C(14)-C(15)-C(16)	120.5(5)
C(17)-C(16)-C(15)	119.4(6)	C(16)-C(17)-C(12)	121.4(5)
C(23)-C(18)-C(19)	118.9(4)	C(23)-C(18)-P(2)	122.9(4)

C(19)-C(18)-P(2)	118.2(4)	C(20)-C(19)-C(18)	121.4(5)
C(19)-C(20)-C(21)	118.9(5)	C(22)-C(21)-C(20)	120.3(5)
C(23)-C(22)-C(21)	120.3(5)	C(18)-C(23)-C(22)	120.3(5)
C(25)-C(24)-P(2)	106.8(3)	C(24)-C(25)-P(1)	107.3(3)
C(31)-C(26)-C(27)	118.8(4)	C(31)-C(26)-P(1)	120.0(4)
C(27)-C(26)-P(1)	121.2(4)	C(26)-C(27)-C(28)	120.6(5)
C(29)-C(28)-C(27)	119.7(6)	C(30)-C(29)-C(28)	120.1(5)
C(29)-C(30)-C(31)	121.0(5)	C(26)-C(31)-C(30)	119.8(5)
C(37)-C(32)-C(33)	118.4(5)	C(37)-C(32)-P(1)	121.0(4)
C(33)-C(32)-P(1)	120.2(4)	C(34)-C(33)-C(32)	119.4(5)
C(35)-C(34)-C(33)	121.8(6)	C(34)-C(35)-C(36)	119.7(5)
C(35)-C(36)-C(37)	119.4(5)	C(32)-C(37)-C(36)	121.2(5)
F(1)-C(38)-F(3)	105.2(8)	F(1)-C(38)-F(2)	112.0(12)
F(3)-C(38)-F(2)	101.9(8)	F(1)-C(38)-S(1)	112.5(7)
F(3)-C(38)-S(1)	112.9(10)	F(2)-C(38)-S(1)	111.6(5)
F(6)-C(39)-F(4)	110.9(10)	F(6)-C(39)-F(5)	106.0(11)
F(4)-C(39)-F(5)	105.6(11)	F(6)-C(39)-S(2)	117.6(10)
F(4)-C(39)-S(2)	113.9(10)	F(5)-C(39)-S(2)	101.3(9)

*Appendix 11: Crystallographic data for compound **11a**.*

Crystal data and structure refinement for **11a**.

Identification code	k00mkw7
Empirical formula	$C_{41}H_{36}F_6N_2O_7P_2RuS_2$
Formula weight	1009.85
Temperature	170(2) K
Wavelength	0.71069 Å
Crystal system	Monoclinic
Space group	$P2_1/c$
Unit cell dimensions	a = 14.2643(2)Å α = 90°
	b = 13.7762(2)Å β = 108.1960(9)°
	c = 22.1901(4)Å γ = 90°
Volume	4143.5(1) $Å^3$
Z	4
Density (calculated)	1.619 Mg/m^3
Absorption coefficient	0.637 mm^{-1}
F(000)	2048
Crystal size	0.17 x 0.13 x 0.13 mm
Theta range for data collection	3.58 to 27.48 °.
Index ranges	0<=h<=18; -17<=k<=17; -28<=l<=27
Reflections collected	56381
Independent reflections	9467 [R(int) = 0.0468]
Reflections observed (>2σ)	8083
Max. and min. transmission	0.9247 and 0.8967
Refinement method	Full-matrix least-squares on F^2
Data / restraints / parameters	9467 / 0 / 551
Goodness-of-fit on F^2	0.978
Final R indices [I>2σ (I)]	R_1 = 0.0332 wR_2 = 0.0934
R indices (all data)	R_1 = 0.0428 wR_2 = 0.1006
Largest diff. peak and hole	0.484 and -0.541 $e.Å^{-3}$

Bond lengths [Å] and angles [°] for **11a**.

Ru(1)-C(27)	1.869(2)	C(2)-C(3)	1.378(4)
Ru(1)-N(1)	2.126(2)	C(3)-C(4)	1.391(4)
Ru(1)-N(2)	2.267(2)	C(4)-C(5)	1.376(5)
Ru(1)-O(2)	2.212(2)	C(5)-C(6)	1.398(4)
Ru(1)-P(2)	2.2826(6)	C(7)-C(12)	1.390(3)
Ru(1)-P(1)	2.3392(5)	C(7)-C(8)	1.393(3)
P(1)-C(1)	1.825(2)	C(8)-C(9)	1.395(3)
P(1)-C(7)	1.827(2)	C(9)-C(10)	1.376(4)
P(1)-C(13)	1.839(2)	C(10)-C(11)	1.385(4)
P(2)-C(15)	1.824(2)	C(11)-C(12)	1.381(3)
P(2)-C(14)	1.827(2)	C(13)-C(14)	1.528(3)
P(2)-C(21)	1.839(2)	C(15)-C(20)	1.388(3)
N(1)-C(28)	1.353(3)	C(15)-C(16)	1.399(3)
N(1)-C(33)	1.355(3)	C(16)-C(17)	1.382(3)
N(2)-C(39)	1.336(3)	C(17)-C(18)	1.380(4)
N(2)-C(34)	1.361(3)	C(18)-C(19)	1.385(4)
S(1)-O(4)	1.430(2)	C(19)-C(20)	1.393(4)
S(1)-O(3)	1.436(2)	C(21)-C(26)	1.393(3)
S(1)-O(2)	1.466(2)	C(21)-C(22)	1.396(3)
S(1)-C(41)	1.831(3)	C(22)-C(23)	1.395(3)
S(2)-O(7)	1.431(2)	C(23)-C(24)	1.376(4)
S(2)-O(6)	1.436(2)	C(24)-C(25)	1.391(4)
S(2)-O(5)	1.442(2)	C(25)-C(26)	1.395(3)
S(2)-C(40)	1.805(3)	C(28)-C(29)	1.370(3)
O(1)-C(27)	1.140(3)	C(29)-C(30)	1.390(3)
F(1)-C(40)	1.328(4)	C(30)-C(32)	1.388(3)
F(2)-C(40)	1.333(5)	C(30)-C(31)	1.506(3)
F(3)-C(40)	1.346(4)	C(32)-C(33)	1.395(3)
F(4)-C(41)	1.329(3)	C(33)-C(34)	1.474(3)
F(5)-C(41)	1.336(3)	C(34)-C(35)	1.391(3)
F(6)-C(41)	1.325(3)	C(35)-C(36)	1.390(3)
C(1)-C(6)	1.382(3)	C(36)-C(38)	1.390(3)

C(1)-C(2)	1.400(4)	C(36)-C(37)	1.503(3)
C(38)-C(39)	1.387(3)		
C(27)-Ru(1)-N(1)	96.25(8)	O(3)-S(1)-O(2)	113.0(1)
C(27)-Ru(1)-N(2)	171.96(8)	O(4)-S(1)-C(41)	106.1(1)
N(1)-Ru(1)-N(2)	76.73(7)	O(3)-S(1)-C(41)	103.9(1)
C(27)-Ru(1)-O(2)	99.48(8)	O(2)-S(1)-C(41)	101.4(1)
N(1)-Ru(1)-O(2)	85.26(6)	O(7)-S(2)-O(6)	125.9(1)
N(2)-Ru(1)-O(2)	84.00(6)	O(7)-S(2)-O(5)	115.3(1)
C(27)-Ru(1)-P(2)	90.50(7)	O(6)-S(2)-O(5)	114.4(1)
N(1)-Ru(1)-P(2)	95.60(5)	O(7)-S(2)-C(40)	104.6(1)
N(2)-Ru(1)-P(2)	86.35(5)	O(6)-S(2)-C(40)	104.9(2)
O(2)-Ru(1)-P(2)	169.85(5)	O(5)-S(2)-C(40)	103.7(2)
C(27)-Ru(1)-P(1)	84.33(7)	S(1)-O(2)-Ru(1)	131.6(1)
N(1)-Ru(1)-P(1)	179.11(5)	C(6)-C(1)-C(2)	120.0(2)
N(2)-Ru(1)-P(1)	102.74(5)	C(6)-C(1)-P(1)	124.5(2)
O(2)-Ru(1)-P(1)	93.98(4)	C(2)-C(1)-P(1)	127.6(2)
P(2)-Ru(1)-P(1)	85.17(2)	C(3)-C(2)-C(1)	119.9(2)
C(1)-P(1)-C(7)	102.1(1)	C(2)-C(3)-C(4)	120.4(3)
C(1)-P(1)-C(13)	119.7(1)	C(5)-C(4)-C(3)	119.6(3)
C(7)-P(1)-C(13)	104.1(1)	C(4)-C(5)-C(6)	120.7(3)
C(1)-P(1)-Ru(1)	117.21(7)	C(1)-C(6)-C(5)	119.4(3)
C(7)-P(1)-Ru(1)	116.73(8)	C(12)-C(7)-C(8)	119.0(2)
C(13)-P(1)-Ru(1)	107.10(7)	C(12)-C(7)-P(1)	119.7(2)
C(15)-P(2)-C(14)	118.0(1)	C(8)-C(7)-P(1)	121.3(2)
C(15)-P(2)-C(21)	104.3(1)	C(7)-C(8)-C(9)	119.5(2)
C(14)-P(2)-C(21)	115.7(1)	C(10)-C(9)-C(8)	120.7(2)
C(15)-P(2)-Ru(1)	116.30(7)	C(9)-C(10)-C(11)	120.2(2)
C(14)-P(2)-Ru(1)	106.81(7)	C(12)-C(11)-C(10)	119.3(2)
C(21)-P(2)-Ru(1)	116.07(7)	C(11)-C(12)-C(7)	121.4(2)
C(28)-N(1)-C(33)	118.8(2)	C(14)-C(13)-P(1)	108.2(2)
C(28)-N(1)-Ru(1)	124.1(1)	C(13)-C(14)-P(2)	110.7(2)
C(33)-N(1)-Ru(1)	116.8(1)	C(20)-C(15)-C(16)	119.5(2)
C(39)-N(2)-C(34)	117.9(2)	C(20)-C(15)-P(2)	122.5(2)
C(39)-N(2)-Ru(1)	126.6(1)	C(16)-C(15)-P(2)	117.9(2)
C(34)-N(2)-Ru(1)	114.3(1)	C(17)-C(16)-C(15)	120.3(2)

O(4)-S(1)-O(3)	117.4(1)	C(18)-C(17)-C(16)	120.0(2)
O(4)-S(1)-O(2)	114.8(1)	C(17)-C(18)-C(19)	120.2(2)
C(26)-C(21)-C(22)	119.3(2)	C(18)-C(19)-C(20)	120.2(2)
C(26)-C(21)-P(2)	120.7(2)	C(15)-C(20)-C(19)	119.7(2)
C(22)-C(21)-P(2)	121.1(2)	N(2)-C(34)-C(35)	121.3(2)
C(23)-C(22)-C(21)	120.2(2)	N(2)-C(34)-C(33)	126.9(2)
C(24)-C(23)-C(22)	120.2(2)	C(35)-C(34)-C(33)	122.8(2)
C(23)-C(24)-C(25)	120.3(2)	C(36)-C(35)-C(34)	120.7(2)
C(24)-C(25)-C(26)	119.9(2)	C(35)-C(36)-C(38)	117.1(2)
C(25)-C(26)-C(21)	120.2(2)	C(35)-C(36)-C(37)	121.4(2)
O(1)-C(27)-Ru(1)	178.5(2)	C(38)-C(36)-C(37)	121.5(2)
N(1)-C(28)-C(29)	121.9(2)	C(39)-C(38)-C(36)	119.6(2)
C(28)-C(29)-C(30)	120.5(2)	N(2)-C(39)-C(38)	123.2(2)
C(32)-C(30)-C(29)	117.6(2)	F(1)-C(40)-F(2)	106.7(3)
C(32)-C(30)-C(31)	122.1(2)	F(1)-C(40)-F(3)	108.1(3)
C(29)-C(30)-C(31)	120.3(2)	F(2)-C(40)-F(3)	106.1(3)
C(30)-C(32)-C(33)	120.0(2)	F(1)-C(40)-S(2)	112.2(3)
N(1)-C(33)-C(32)	121.1(2)	F(2)-C(40)-S(2)	112.6(3)
N(1)-C(33)-C(34)	125.0(2)	F(3)-C(40)-S(2)	110.8(2)
C(32)-C(33)-C(34)	123.9(2)	F(6)-C(41)-F(4)	108.4(2)
F(6)-C(41)-S(1)	110.7(2)	F(6)-C(41)-F(5)	107.7(2)
F(4)-C(41)-S(1)	111.9(2)	F(4)-C(41)-F(5)	107.3(2)
F(5)-C(41)-S(1)	110.6(2)		

*Appendix 12: Crystallographic data for compound **12a**.*

Crystal data and structure refinement for **12a**.

Identification code	k00mkw8
Empirical formula	$C_{67}H_{78}F_3O_6P_4Ru_2S_4$
Formula weight	1490.55
Temperature	170(2) K
Wavelength	0.71069 Å
Crystal system	Triclinic
Space group	P-1
Unit cell dimensions	a = 12.65510(10)Å α = 100.9820(5)°
	b = 12.99760(10)Å β = 92.9360(5)°
	c = 21.0650(2)Å γ = 103.1430(5)°
Volume	3296.11(5) $Å^3$
Z	2
Density (calculated)	1.502 Mg/m^3
Absorption coefficient	0.741 mm^{-1}
F(000)	1534
Crystal size	0.25 x 0.20 x 0.10 mm
Theta range for data collection	3.54 to 27.50 °.
Index ranges	0<=h<=16; -16<=k<=16; -27<=l<=27
Reflections collected	37510
Independent reflections	14940 [R(int) = 0.0297]
Reflections observed (>2σ)	13643
Absorption correction	Multiscan
Max. and min. transmission	0.9296 and 0.8364
Refinement method	Full-matrix least-squares on F^2
Data / restraints / parameters	14940 / 0 / 776
Goodness-of-fit on F^2	0.848
Final R indices [I>2σ (I)]	R_1 = 0.0312 wR_2 = 0.0850
R indices (all data)	R_1 = 0.0349 wR_2 = 0.0895
Largest diff. peak and hole	1.948 and -0.799 e.$Å^{-3}$

Bond lengths [Å] and angles [°] for **12a**.

Ru(1)-C(49)	1.852(2)	Ru(1)-P(1)	2.3329(5)
Ru(1)-P(2)	2.3530(5)	Ru(1)-S(2)	2.4385(5)
Ru(1)-S(1)	2.4661(5)	Ru(1)-S(4)	2.4962(5)
Ru(2)-C(50)	1.862(2)	Ru(2)-P(4)	2.3209(5)
Ru(2)-P(3)	2.3547(5)	Ru(2)-S(2)	2.4473(5)
Ru(2)-S(4)	2.4652(5)	Ru(2)-S(1)	2.4654(5)
S(1)-C(59)	1.855(3)	S(2)-C(55)	1.841(2)
S(3)-O(3)	1.434(2)	S(3)-O(5)	1.438(2)
S(3)-O(4)	1.445(3)	S(3)-C(58)	1.818(3)
S(4)-C(63)	1.827(2)	P(1)-C(6)	1.826(2)
P(1)-C(54)	1.839(2)	P(1)-C(12)	1.842(2)
P(2)-C(18)	1.827(2)	P(2)-C(24)	1.838(2)
P(2)-C(53)	1.844(2)	P(3)-C(30)	1.832(2)
P(3)-C(36)	1.835(2)	P(3)-C(52)	1.844(2)
P(4)-C(48)	1.824(2)	P(4)-C(42)	1.830(2)
P(4)-C(51)	1.843(2)	F(1)-C(58)	1.333(3)
F(2)-C(58)	1.335(3)	F(3)-C(58)	1.327(3)
O(1)-C(49)	1.150(3)	O(2)-C(50)	1.146(3)
O(6)-C(67)	1.204(3)	C(1)-C(2)	1.390(4)
C(1)-C(6)	1.395(3)	C(2)-C(3)	1.387(4)
C(3)-C(4)	1.384(5)	C(4)-C(5)	1.393(4)
C(5)-C(6)	1.393(3)	C(7)-C(12)	1.383(3)
C(7)-C(8)	1.391(3)	C(8)-C(9)	1.380(4)
C(9)-C(10)	1.383(4)	C(10)-C(11)	1.382(3)
C(11)-C(12)	1.392(3)	C(13)-C(14)	1.383(3)
C(13)-C(18)	1.397(3)	C(14)-C(15)	1.383(4)
C(15)-C(16)	1.377(5)	C(16)-C(17)	1.398(4)
C(17)-C(18)	1.391(3)	C(19)-C(20)	1.389(3)
C(19)-C(24)	1.396(3)	C(20)-C(21)	1.379(4)
C(21)-C(22)	1.383(4)	C(22)-C(23)	1.385(3)
C(23)-C(24)	1.391(3)	C(25)-C(26)	1.387(3)
C(25)-C(30)	1.397(3)	C(26)-C(27)	1.387(3)
C(27)-C(28)	1.384(3)	C(28)-C(29)	1.390(3)

C(29)-C(30)	1.400(3)	C(31)-C(32)	1.390(3)
C(31)-C(36)	1.396(3)	C(32)-C(33)	1.379(4)
C(33)-C(34)	1.382(4)	C(34)-C(35)	1.385(3)
C(35)-C(36)	1.399(3)	C(37)-C(38)	1.385(4)
C(37)-C(42)	1.393(3)	C(38)-C(39)	1.384(4)
C(39)-C(40)	1.379(4)	C(40)-C(41)	1.392(3)
C(41)-C(42)	1.389(3)	C(43)-C(48)	1.386(3)
C(43)-C(44)	1.391(3)	C(44)-C(45)	1.385(4)
C(45)-C(46)	1.386(4)	C(46)-C(47)	1.386(3)
C(47)-C(48)	1.397(3)	C(51)-C(52)	1.526(3)
C(53)-C(54)	1.529(3)	C(55)-C(56)	1.515(3)
C(56)-C(57)	1.526(4)	C(59)-C(60)	1.448(4)
C(60)-C(61)	1.384(7)	C(62)-C(64)	1.524(4)
C(62)-C(63)	1.523(3)	C(65)-C(67)	1.502(4)
C(67)-C(68)	1.482(4)		

C(49)-Ru(1)-P(1)	87.79(6)	C(49)-Ru(1)-P(2)	87.54(7)
P(1)-Ru(1)-P(2)	82.625(18)	C(49)-Ru(1)-S(2)	93.54(7)
P(1)-Ru(1)-S(2)	94.990(18)	P(2)-Ru(1)-S(2)	177.345(17)
C(49)-Ru(1)-S(1)	95.28(6)	P(1)-Ru(1)-S(1)	176.438(18)
P(2)-Ru(1)-S(1)	99.292(18)	S(2)-Ru(1)-S(1)	83.029(16)
C(49)-Ru(1)-S(4)	165.56(7)	P(1)-Ru(1)-S(4)	99.840(17)
P(2)-Ru(1)-S(4)	105.493(17)	S(2)-Ru(1)-S(4)	73.705(16)
S(1)-Ru(1)-S(4)	76.779(16)	C(50)-Ru(2)-P(4)	93.84(6)
C(50)-Ru(2)-P(3)	89.90(6)	P(4)-Ru(2)-P(3)	83.926(18)
C(50)-Ru(2)-S(2)	94.69(6)	P(4)-Ru(2)-S(2)	92.066(17)
P(3)-Ru(2)-S(2)	174.111(17)	C(50)-Ru(2)-S(4)	167.22(6)
P(4)-Ru(2)-S(4)	92.712(17)	P(3)-Ru(2)-S(4)	101.711(17)
S(2)-Ru(2)-S(4)	74.104(16)	C(50)-Ru(2)-S(1)	95.43(6)
P(4)-Ru(2)-S(1)	169.762(17)	P(3)-Ru(2)-S(1)	100.408(17)
S(2)-Ru(2)-S(1)	82.863(16)	S(4)-Ru(2)-S(1)	77.368(16)
C(59)-S(1)-Ru(2)	108.99(9)	C(59)-S(1)-Ru(1)	111.05(10)
Ru(2)-S(1)-Ru(1)	86.410(16)	C(55)-S(2)-Ru(1)	110.51(8)
C(55)-S(2)-Ru(2)	112.48(7)	Ru(1)-S(2)-Ru(2)	87.424(16)
O(3)-S(3)-O(5)	115.08(14)	O(3)-S(3)-O(4)	113.94(15)

O(5)-S(3)-O(4)	116.27(17)	O(3)-S(3)-C(58)	103.92(12)
O(5)-S(3)-C(58)	102.42(13)	O(4)-S(3)-C(58)	102.66(13)
C(63)-S(4)-Ru(2)	112.67(7)	C(63)-S(4)-Ru(1)	112.95(7)
Ru(2)-S(4)-Ru(1)	85.762(15)	C(6)-P(1)-C(54)	108.00(10)
C(6)-P(1)-C(12)	101.68(9)	C(54)-P(1)-C(12)	98.63(10)
C(6)-P(1)-Ru(1)	117.66(7)	C(54)-P(1)-Ru(1)	103.95(7)
C(12)-P(1)-Ru(1)	124.54(7)	C(18)-P(2)-C(24)	101.21(10)
C(18)-P(2)-C(53)	106.17(11)	C(24)-P(2)-C(53)	103.11(10)
C(18)-P(2)-Ru(1)	120.13(7)	C(24)-P(2)-Ru(1)	117.00(7)
C(53)-P(2)-Ru(1)	107.56(7)	C(30)-P(3)-C(36)	101.52(9)
C(30)-P(3)-C(52)	103.34(9)	C(36)-P(3)-C(52)	103.68(9)
C(30)-P(3)-Ru(2)	124.21(7)	C(36)-P(3)-Ru(2)	113.82(7)
C(52)-P(3)-Ru(2)	108.10(7)	C(48)-P(4)-C(42)	101.36(9)
C(48)-P(4)-C(51)	105.32(9)	C(42)-P(4)-C(51)	102.33(9)
C(48)-P(4)-Ru(2)	116.00(7)	C(42)-P(4)-Ru(2)	120.01(7)
C(51)-P(4)-Ru(2)	110.06(7)	C(2)-C(1)-C(6)	120.3(2)
C(3)-C(2)-C(1)	119.9(3)	C(4)-C(3)-C(2)	119.8(3)
C(3)-C(4)-C(5)	120.8(3)	C(4)-C(5)-C(6)	119.4(3)
C(5)-C(6)-C(1)	119.7(2)	C(5)-C(6)-P(1)	122.28(19)
C(1)-C(6)-P(1)	117.91(17)	C(12)-C(7)-C(8)	120.0(2)
C(9)-C(8)-C(7)	120.6(2)	C(8)-C(9)-C(10)	119.5(2)
C(11)-C(10)-C(9)	120.3(2)	C(10)-C(11)-C(12)	120.4(2)
C(7)-C(12)-C(11)	119.3(2)	C(7)-C(12)-P(1)	122.74(16)
C(11)-C(12)-P(1)	117.69(16)	C(14)-C(13)-C(18)	120.4(2)
C(15)-C(14)-C(13)	120.0(3)	C(16)-C(15)-C(14)	120.2(2)
C(15)-C(16)-C(17)	120.4(3)	C(18)-C(17)-C(16)	119.6(3)
C(17)-C(18)-C(13)	119.4(2)	C(17)-C(18)-P(2)	123.31(18)
C(13)-C(18)-P(2)	117.08(17)	C(20)-C(19)-C(24)	120.7(2)
C(21)-C(20)-C(19)	120.3(2)	C(20)-C(21)-C(22)	119.5(2)
C(21)-C(22)-C(23)	120.4(2)	C(22)-C(23)-C(24)	120.8(2)
C(23)-C(24)-C(19)	118.3(2)	C(23)-C(24)-P(2)	120.48(16)
C(19)-C(24)-P(2)	121.20(16)	C(26)-C(25)-C(30)	120.6(2)
C(25)-C(26)-C(27)	120.5(2)	C(28)-C(27)-C(26)	119.3(2)
C(27)-C(28)-C(29)	120.7(2)	C(28)-C(29)-C(30)	120.3(2)
C(25)-C(30)-C(29)	118.55(19)	C(25)-C(30)-P(3)	119.73(15)

C(29)-C(30)-P(3)	121.71(16)	C(32)-C(31)-C(36)	120.5(2)
C(33)-C(32)-C(31)	120.6(2)	C(32)-C(33)-C(34)	119.5(2)
C(33)-C(34)-C(35)	120.4(2)	C(34)-C(35)-C(36)	120.8(2)
C(31)-C(36)-C(35)	118.20(19)	C(31)-C(36)-P(3)	122.64(16)
C(35)-C(36)-P(3)	119.13(16)	C(38)-C(37)-C(42)	120.2(2)
C(37)-C(38)-C(39)	120.5(2)	C(40)-C(39)-C(38)	119.7(2)
C(39)-C(40)-C(41)	120.1(2)	C(42)-C(41)-C(40)	120.5(2)
C(41)-C(42)-C(37)	119.0(2)	C(41)-C(42)-P(4)	120.88(16)
C(37)-C(42)-P(4)	120.08(17)	C(48)-C(43)-C(44)	120.3(2)
C(45)-C(44)-C(43)	120.1(2)	C(44)-C(45)-C(46)	119.8(2)
C(45)-C(46)-C(47)	120.4(2)	C(46)-C(47)-C(48)	120.0(2)
C(43)-C(48)-C(47)	119.48(19)	C(43)-C(48)-P(4)	121.62(16)
C(47)-C(48)-P(4)	118.80(16)	O(1)-C(49)-Ru(1)	176.96(19)
O(2)-C(50)-Ru(2)	175.72(18)	C(52)-C(51)-P(4)	110.54(14)
C(51)-C(52)-P(3)	111.23(14)	C(54)-C(53)-P(2)	109.80(15)
C(53)-C(54)-P(1)	104.76(14)	C(56)-C(55)-S(2)	110.75(16)
C(55)-C(56)-C(57)	111.7(2)	F(3)-C(58)-F(1)	106.6(2)
F(3)-C(58)-F(2)	107.9(2)	F(1)-C(58)-F(2)	107.0(2)
F(3)-C(58)-S(3)	111.62(17)	F(1)-C(58)-S(3)	112.55(18)
F(2)-C(58)-S(3)	110.88(18)	C(60)-C(59)-S(1)	119.0(3)
C(61)-C(60)-C(59)	110.4(4)	C(64)-C(62)-C(63)	112.70(19)
C(62)-C(63)-S(4)	111.92(16)	O(6)-C(67)-C(68)	120.7(3)
O(6)-C(67)-C(65)	123.4(3)	C(68)-C(67)-C(65)	115.7(3)

Appendix 13: Crystallographic data for compound 14.

Crystal data and structure refinement for **14**.

Identification code	h02mkw2
Empirical formula	C15 H16 Cl F3 N2 O7 Ru S
Formula weight	561.88
Temperature	150(2) K
Wavelength	0.71073 Å
Crystal system	Triclinic
Space group	P-1
Unit cell dimensions	a = 8.2940(1)Å α = 96.431(1)°
	b = 10.1370(1)Å β = 94.382(1)°
	c = 12.8780(2)Å γ = 93.360(1)°
Volume	1070.31(2) $Å^3$
Z	2
Density (calculated)	1.743 Mg/m^3
Absorption coefficient	1.019 mm^{-1}
F(000)	560
Crystal size	0.25 x 0.25 x 0.20 mm
Theta range for data collection	3.58 to 33.22°
Index ranges	-12<=h<=12; -15<=k<=15; -19<=l<=19
Reflections collected	24350
Independent reflections	8140 [R(int) = 0.0455]
Reflections observed (>2σ)	7136
Data Completeness	0.990
Absorption correction	Semi-empirical from equivalents
Max. and min. transmission	0.79 and 0.70
Refinement method	Full-matrix least-squares on F^2
Data / restraints / parameters	8140 / 4 / 290
Goodness-of-fit on F^2	1.007
Final R indices [I>2σ (I)]	R_1 = 0.0307 wR_2 = 0.0683
R indices (all data)	R_1 = 0.0390 wR_2 = 0.0722

Largest diff. peak and hole 0.579 and -1.115 eÅ^{-3}

Bond lengths [Å] and angles [°] for **14**.

Ru(1)-C(2)	1.8856(17)	Ru(1)-C(1)	1.8994(17)
Ru(1)-N(1)	2.1115(13)	Ru(1)-O(3)	2.1104(12)
Ru(1)-N(2)	2.1136(13)	Ru(1)-Cl(1)	2.3569(4)
S(1)-O(5)	1.4368(13)	S(1)-O(7)	1.4412(13)
S(1)-O(6)	1.4458(13)	S(1)-C(15)	1.8234(19)
F(1)-C(15)	1.324(2)	F(2)-C(15)	1.317(2)
F(3)-C(15)	1.334(3)	O(1)-C(1)	1.127(2)
O(2)-C(2)	1.135(2)	N(1)-C(3)	1.346(2)
N(1)-C(7)	1.3548(19)	N(2)-C(12)	1.341(2)
N(2)-C(8)	1.3593(19)	C(3)-C(4)	1.381(2)
C(4)-C(5)	1.386(3)	C(5)-C(6)	1.390(2)
C(5)-C(13)	1.505(2)	C(6)-C(7)	1.392(2)
C(7)-C(8)	1.473(2)	C(8)-C(9)	1.391(2)
C(9)-C(10)	1.386(2)	C(10)-C(11)	1.393(3)
C(10)-C(14)	1.506(2)	C(11)-C(12)	1.385(2)

C(2)-Ru(1)-C(1)	89.36(7)	C(2)-Ru(1)-N(1)	96.96(6)
C(1)-Ru(1)-N(1)	172.20(6)	C(2)-Ru(1)-O(3)	93.30(7)
C(1)-Ru(1)-O(3)	96.55(6)	N(1)-Ru(1)-O(3)	87.68(5)
C(2)-Ru(1)-N(2)	174.13(6)	C(1)-Ru(1)-N(2)	96.19(6)
N(1)-Ru(1)-N(2)	77.36(5)	O(3)-Ru(1)-N(2)	87.99(5)
C(2)-Ru(1)-Cl(1)	88.67(6)	C(1)-Ru(1)-Cl(1)	87.85(5)
N(1)-Ru(1)-Cl(1)	87.73(4)	O(3)-Ru(1)-Cl(1)	175.19(4)
N(2)-Ru(1)-Cl(1)	89.61(4)	O(5)-S(1)-O(7)	115.72(9)
O(5)-S(1)-O(6)	114.33(8)	O(7)-S(1)-O(6)	113.57(8)
O(5)-S(1)-C(15)	104.00(9)	O(7)-S(1)-C(15)	103.08(9)
O(6)-S(1)-C(15)	104.15(9)	C(3)-N(1)-C(7)	118.10(14)
C(3)-N(1)-Ru(1)	126.13(11)	C(7)-N(1)-Ru(1)	115.54(10)
C(12)-N(2)-C(8)	117.97(14)	C(12)-N(2)-Ru(1)	126.33(11)
C(8)-N(2)-Ru(1)	115.68(10)	O(1)-C(1)-Ru(1)	174.33(15)

O(2)-C(2)-Ru(1)	176.14(16)	N(1)-C(3)-C(4)	122.98(16)
C(3)-C(4)-C(5)	119.70(16)	C(4)-C(5)-C(6)	117.41(15)
C(4)-C(5)-C(13)	121.80(17)	C(6)-C(5)-C(13)	120.79(17)
C(7)-C(6)-C(5)	120.55(16)	N(1)-C(7)-C(6)	121.23(14)
N(1)-C(7)-C(8)	115.82(13)	C(6)-C(7)-C(8)	122.95(14)
N(2)-C(8)-C(9)	121.55(14)	N(2)-C(8)-C(7)	115.16(13)
C(9)-C(8)-C(7)	123.28(14)	C(8)-C(9)-C(10)	120.33(15)
C(9)-C(10)-C(11)	117.60(15)	C(9)-C(10)-C(14)	121.22(16)
C(11)-C(10)-C(14)	121.17(16)	C(12)-C(11)-C(10)	119.42(16)
N(2)-C(12)-C(11)	123.06(16)	F(2)-C(15)-F(1)	108.04(19)
F(2)-C(15)-F(3)	107.70(17)	F(1)-C(15)-F(3)	108.02(17)
F(2)-C(15)-S(1)	112.23(14)	F(1)-C(15)-S(1)	110.20(14)
F(3)-C(15)-S(1)	110.51(15)		